KNARR VS COG: A SHIPSHAPE EVALUATION: Using modern naval architecture principles on 3D model reconstructions of a Nordic cargo ship and a Hanseatic ship to assess and compare their sailing performance

Hernandez Montfort, Jaume

Universiteit Leiden

KNARR VS COG:
A SHIPSHAPE EVALUATION

Using modern naval architecture principles on 3D model reconstructions of a Nordic cargo ship and a Hanseatic ship to assess and compare their sailing performance.

Jaume Hernandez Montfort

3D model of the Big Ship of Wismar and the Bremen cog used in the current thesis. Figure by Hernandez Montfort, using the 3D model of the Bremen cog by Tanner (2018) and the reconstructed model of the Big Ship of Wismar based on the visualization model by Ditta & Auer (in press). Rendered in Rhinoceros.

Knarr vs cog: a shipshape evaluation

Using modern naval architecture principles on 3D model reconstructions of a Nordic cargo ship and a Hanseatic ship to assess and compare their sailing performance.

Jaume Hernandez Montfort

Master Thesis MSc Archaeological Science, 1084VTSY

Supervisors: Dr. Lambers and Dr. Manders

Leiden University, Faculty of Archaeology

Wageningen, June 2023. Final version

Acknowledgements

I take this opportunity to express my gratitude to everyone who has supported and guided me throughout the completion of my master's thesis.

First and foremost, I am incredibly grateful to Jens Auer and Pat Tanner for sharing their 3D reconstruction models and the data of the Big Ship of Wismar and the Bremen cog. Without their generous contributions, this thesis would not have been possible. I also want to thank them, along with Massimiliano Ditta, for being so helpful and responsive whenever I had questions about the data and their work on the two ships.

Likewise, I would like to thank my two thesis supervisors Karsten Lambers and Martijn Manders for their guidance, support, and valuable feedback. I am truly fortunate to have had their mentorship throughout this journey.

I would also like to extend my gratitude to my employer, the Maritime Research Institute Netherlands, for allowing me to use their software and for their flexibility, which made it possible for me to balance work and studies.

I would also like to acknowledge the assistance provided by the student advisors, with a special mention to Rosemarijn de Ruiter, as well as the helpfulness of the librarians at Leiden University who allowed me to extend the loan period beyond the official maximum time until the completion of the thesis.

I am thankful to the University of Leiden, the professors I had the privilege of learning from, and my classmates for creating such a vibrant, stimulating, and enjoyable academic environment.

Last but certainly not least, I want to express my deep appreciation to my family and friends for their unconditional love, encouragement, and belief in my abilities. Their support and understanding during the ups and downs of this thesis journey have been a constant source of strength and motivation.

To all those who have played a role, big or small, in the completion of this master's thesis, I offer my sincere thanks.

Contents

List of Figures

List of Tables

List of Equations

I. Introduction

I.1 *Knarrs* and cogs: large seagoing cargo vessels in northern Europe

The 13th and 14th centuries were a period in which North European shipbuilding techniques and traditions experienced significant changes, from the Baltic Sea to the North Sea. The Viking Age had come to an end, and the Hanseatic League was rapidly expanding its trade network, which relied heavily on maritime transportation. Between 1000 and 1300, the Nordic or Scandinavian shipbuilding tradition, developed by the Vikings, was dominant in Northern Europe. Large Nordic cargo vessels, referred as *knarr* and characterized by their curved stems (Heide, 2014, p. 105), were involved in a professional long-distance Scandinavian merchant system connecting the Baltic and the North Sea (Englert, 2003, p. 277; Bill, 1997, p. 13). After 1300, however, the supremacy in the maritime trade in the region shifted to German merchants and the Hanseatic League, and the Nordic shipbuilding tradition disappeared. From that moment the cog became the most common cargo vessel in Northern Europe (Englert, 2003, p. 273; Haasum, 1995, p. 245).

The Nordic *knarr* and the cog had unique design features and belonged to two distinct shipbuilding traditions which emerged independently from each other from local small craft building traditions. Therefore, Crumlin-Pedersen (1991, p. 70) argues that the two building traditions are, in their early stages of development, easily recognizable in the archaeological record by their individual construction elements, the scantlings, and the different ways of using tools. It becomes however more difficult in later stages to differentiate the shipbuilding traditions based on these characteristics as both traditions adopted features from each other. Nevertheless, he points out that the large cargo vessels of this period evolved from very few basic types and thus some major construction features and even specific construction details, such as the use of square nails and staples or round shafted rivets, can be clearly attributed to one or the other tradition. The unique design features of the *knarr* and the cog were the result of the development processes needed to transform small coastal crafts into large seagoing vessels and had consequently a direct influence on their performance and capabilities.

The disappearance of the Nordic cargo ships and their replacement by cogs around 1300 was initially attributed to the cog having a better performance than the Nordic ships, by claiming that it was technically impossible to build large ships in the Nordic shipbuilding tradition. The archaeological and historical evidence show however that this statement is unfounded (Christensen, 2002, p. 92; Crumlin-Pedersen, 1991, p. 77; Englert, 2000, p. 41). As can be seen in Figure 1, the increase in size of Scandinavian cargo ships had already started before the 12th century and continued to increase

significantly up to the 13th century. The earliest cogs, such as the Kollerup (the oldest known seagoing cog), were smaller than their contemporary Nordic ships and, while cogs became considerably bigger in the following centuries, the massive size of the Bergen ship proves that size was not a technical limiting factor for ships built in the Nordic tradition. Estimating the cargo capacity of ships remains however a difficult task as very few wrecks are preserved sufficiently to create a complete hull reconstruction. Discrepancies are common between cargo capacity estimates made by different scholars or at different times. For instance, Christensen (1985, p. 208) specifies the cargo capacity of the Bergen ship to be 120 tons instead of the more than 150 tons shown by Crumlin-Pedersen in Figure 1. Crumlin-Pedersen (1999, p. Fig. 6) states that the cargo capacity of the Hedeby 3 is 60 tons instead of the 40 tons estimate shown in Figure 1.

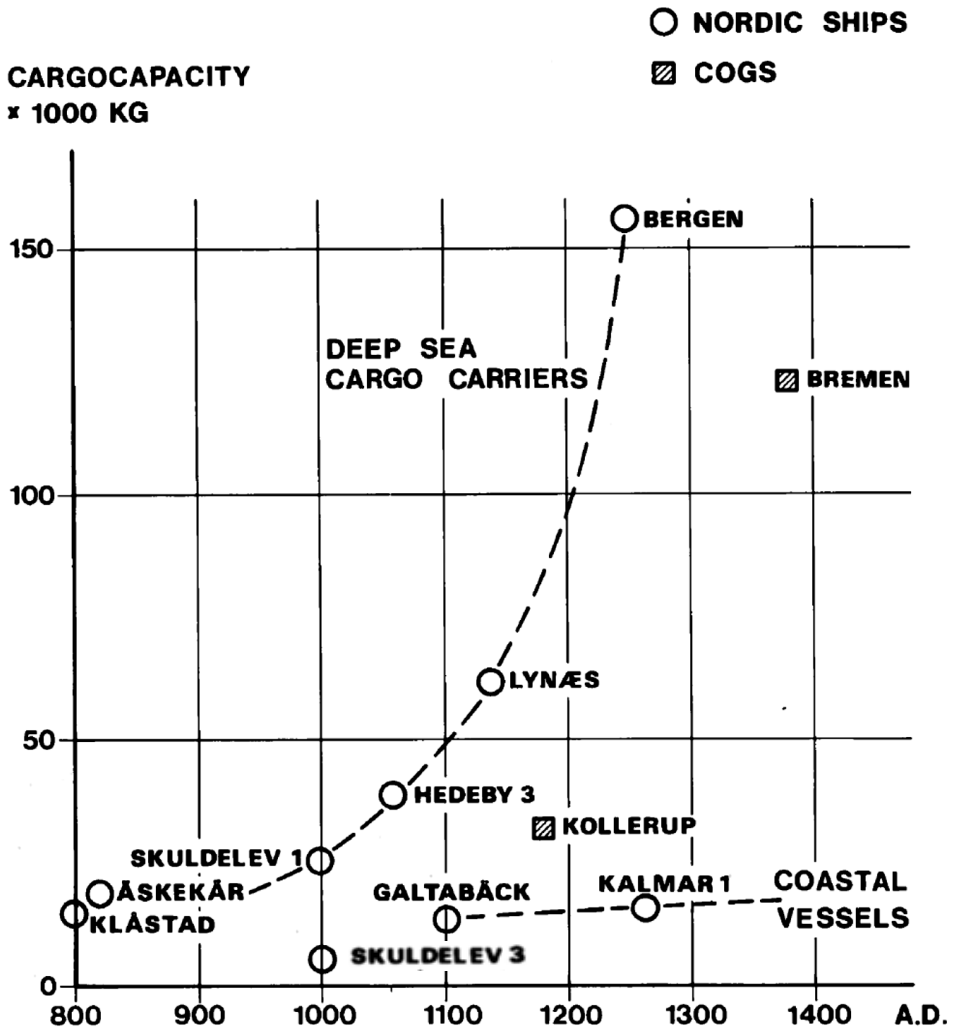

Figure 1 Cargo capacity of various Scandinavian ships and cogs. Cargo capacity considering a standard 40 % freeboard amidships. Capacities are calculated based on the reconstructed hull form and hull weight for the well-preserved ships (Askekarr, Skuldelev 1 and 3, Kalmar 1, Kollerup, and Bremen), and estimated based on the main dimensions and fullness of the midship section for the rest. (Crumlin-Pedersen, 1991, p. 79, Fig. 10).

For ships that are well preserved, and a complete reconstruction is possible, discrepancies in cargo capacity can also exist due to different estimates of the hull and ballast weights. For instance, while Crumlin-Pedersen (1991, p. 79) estimated the cargo capacity of the Bremen cog at 120 tons, Figure 1, the latest calculations by Tanner (2018; 2021) give a cargo capacity of 108 tons. Although when considering the 15 tons of ballast that were needed according to Tanner, the total capacity comes close to the initial estimate of 120 tons. In any case, the big ship of Bergen, which is bigger than all recorded contemporary cogs, proves that Nordic cargo ships could be built at least as big as and plausibly bigger than cogs, especially since new dendrochronological dating has shifted the age of the Bergen ship from 1248 to 1188 (Englert, 2000, p. 43; Christensen, 2002, p. 92). Hence, the disappearance of the Nordic shipbuilding tradition and the supremacy of the cog cannot be explained by the size of the vessels. Moreover, the archaeological finds, the historical records and the iconography in medieval city seals confirm that cogs and Nordic cargo ships sailed side by side for many years and that they even borrowed features from each other (Christensen, 2002, p. 92).

Scholars have therefore moved away from the discourse based on technical capabilities to explain the disappearance of large Nordic cargo vessels after the 13th century. As Christensen (1989, p. 20) stated: “It is now time to abandon shipbuilding technology as an explanation for Hanseatic supremacy, and look for the explanation elsewhere”. Three other main reasons have been suggested since. The first attempt to explain the transition from Nordic to cog-like shipbuilding traditions in Scandinavia from a societal perspective was made by Varenius (1992). In his work, Verarius claims that the religious and social changes associated with the Christianization of Northern Europe and the establishment of the medieval state made the symbolism of the Viking ship irrelevant and introduced a new economic and qualitative attitude towards shipbuilding (Bill, 1995, pp. 195-196). Other scholars have argued that the socio-economic changes that fuelled the transition were rather a direct consequence of the scarcity of high-quality timber and the need to build cheaper ships, which gave the cheaper-to-build and less complex cogs the upper hand in the maritime trade (Bill, 1995, p. 201; Crumlin-Pedersen, 1991, pp. 77-80; Dokkedal, 1996, pp. 61-62; Godal, 1995, p. 282). Finally, others point to the political and militaristic power of the Hanseatic League and its monopolistic trade organisation as main factors for the consolidation of the cog as the dominant vessel type in the region (Christensen, 2002, p. 92).

I.2 Statement of the Problem and Research Questions

As mentioned in the previous section, the discovery of large cargo ships in the Nordic tradition has disproved the first theory that stated that cogs replaced the Nordic shipbuilding tradition in Northern Europe because of their larger size and because of the technical limitations of building large ships in the Nordic tradition. Therefore, other reasons linked to social, economic, and religious aspects have been suggested to explain the changes in shipbuilding traditions in the 13th and 14th centuries, while technical reasons have been dismissed. However, shipbuilding technology does not only relate to the size of the vessels or their construction techniques but also to their performance in terms of stability, speed and sailing behaviour. Even if the aforementioned social, economic, and religious aspects were key factors in the disappearance of the large Nordic cargo vessels in Northern Europe, it is still worth checking how the performance of the two types of ships compared to each other. This has so far not been done. Besides the differences in building techniques, Nordic cargo ships and cogs had very distinct hull shapes, see Figure 2 to Figure 4, and thus differences in performance in terms of stability, speed and ship motions are to be expected even when comparing ships of the same size. Investigating the performance of the vessels, rather than just their size, would allow us to see whether the socio-economic reasons for the shift from Nordic ships to cogs went hand in hand with an improvement of the ships' performance as a result of their different hull shapes. This thesis aims to shed light on this topic by calculating and comparing the performance of a Nordic cargo ship and a cog of the same size.

Unfortunately, most wrecks are only partially preserved and while it is possible to study shipbuilding techniques and practices from fragmentary finds (Bill, 2009, p. 430), evaluating the cargo capacity, hydrostatics and sailing behaviour characteristics requires a complete reconstruction of the hull. Simple hull shape coefficients have been proposed as a way to assess the capabilities of ships (McGrail, 1987, pp. 195-198). However, besides the most basic coefficients, such as ratios length-to-beam or beam-to-depth, hull shape coefficients also require a complete hull geometry. Moreover, simple shape coefficients can only provide a rough indication of the potential behaviour of the ship, but it remains a very basic and inaccurate approach. They can be useful in comparing a series of contemporary and similar hull shapes in a qualitative way, but they do not provide quantitative information about their actual performance (Tanner, 2020, pp. 315-316). Furthermore, they only account for the overall shape of the hull while other parameters, such as local geometry features and the actual loading condition and weight distribution, can play a major role in a ships' behaviour. Estimating the loading condition of wrecks is also essential when exploring information from historical records because most of the records only mention the carrying capacity of ships (Bill, 1997,

p. 129). It remains however problematic that the definition of the medieval measuring unit last varies greatly from region to region (Crumlin-Pedersen, 1985, p. 85).

Another problematic aspect when comparing different ship types, especially when using historical records, is that the terms used to describe medieval vessels were used in very different ways depending on the region, time, and other circumstances. There is still an ongoing debate about the use of the term cog as a clearly defined ship type. Dhoop (2016, pp. 48-49) argues that a differentiation should be made between the archaeological and the historical records and that the term cog as a label to describe a shipbuilding tradition is an archaeological construct with little parallel in the historical record. Moreover, as Maarleveld (1995, p. 3) points out, hull shape, propulsion type, and construction techniques do not necessarily go hand in hand but are greatly influenced by local conditions such as the availability of materials or the proficiency and knowledge of the local builders. It makes sense therefore to study hull shape independently from construction techniques and materials.

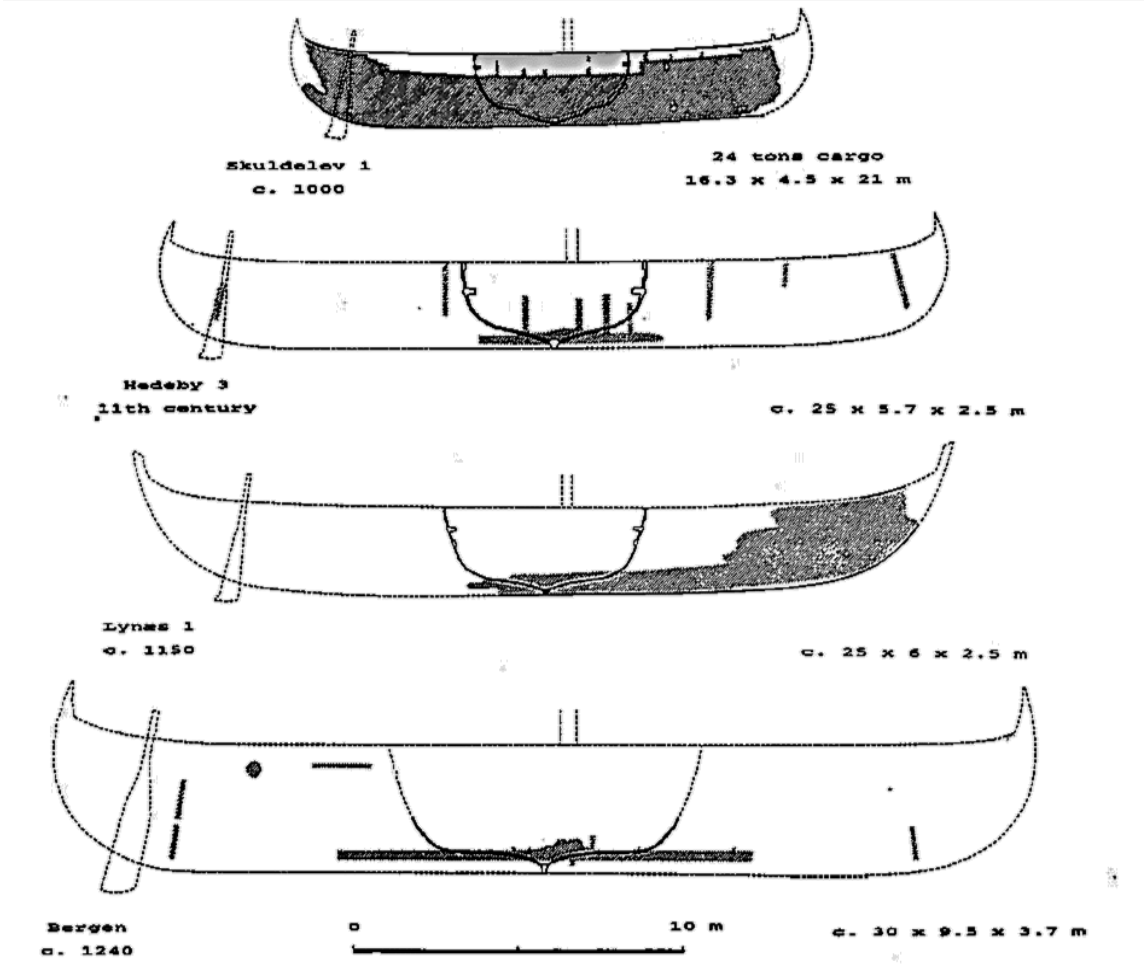

Figure 2 Profile and midsection view of large Nordic cargo ships. The date of the Bergen ship should be 1188 according to latest dendrochronological data, as already mentioned in section I.1. (Crumlin-Pedersen, 1991, p. 77, Fig. 8).

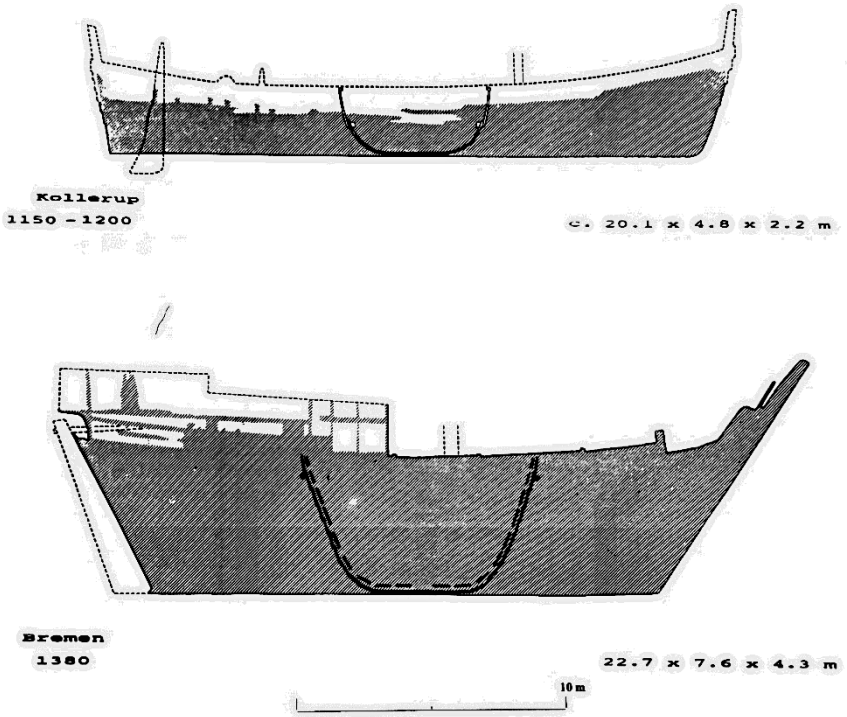

Figure 3 Profile and midsection view of cogs. (Crumlin-Pedersen, 1991, p. 80, Fig. 11).

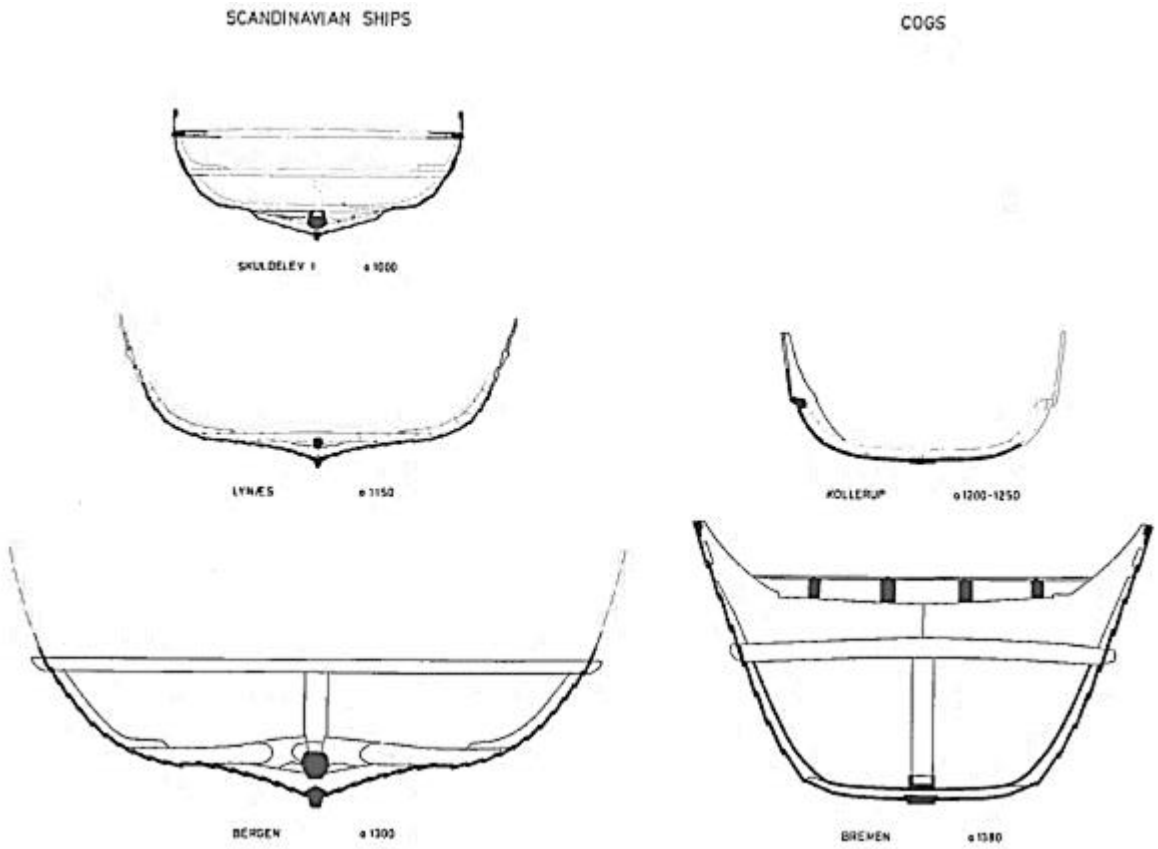

Figure 4 Cross section view of three Scandinavian cargo ships and two cogs. The date of the Bergen ship should be 1188 according to latest dendrochronological data. (Crumlin-Pedersen, 1985, p. 91, Fig. 14).

The 3D reconstruction of shipwrecks opens the door to estimating the carrying capacity, possible loading conditions and performance capabilities of ancient ships by means of mathematical evaluations of the hull's geometry, using modern naval engineering approaches that are systematically carried out on modern ships. While the construction of actual replicas would be ideal to study and reproduce the technical details of their construction, the way in which they were sailed, and their real-life sailing performance, digital calculations allow for a systematic evaluation and comparison of the behaviour of different hull shapes and loading configurations. This is especially valuable when different alternative reconstructions are to be investigated (McGrail, 1988, p. 35).

The aim of this thesis is thus to answer the following question:

> How can modern naval architecture methods be applied to the digital reconstruction models of ships, in particular a Nordic cargo ship and a Hanseatic cog, to assess and compare their sailing performance?

Besides the main research question, the following related sub-questions will also be investigated.

- What are the differences in sailing performance between Nordic cargo ships and cogs?
- Could these differences have played a role in the disappearance Nordic cargo ships and the dominance of cogs after 1300?
- Which ship geometric characteristics impacting the sailing performance of Nordic cargo ships and cogs would have been favoured at that time, considering the intended use of the vessels?
- What are the benefits and limitations of applying modern naval architecture design methods to past shipbuilding traditions?

I.3 Methodological approach

To compare the performance of Nordic cargo ships and cogs and to answer the research questions, it is first necessary to examine what defines these two ship types and their related shipbuilding traditions. For this purpose, a literature investigation is done in chapter II, focusing on the origins, development, and evolution of the two shipbuilding traditions as well as the influences they had on each other. The different theories for the transition from Nordic ships to cogs are also discussed in more detail in this chapter.

Next, it is necessary to define what performance means and how this is evaluated in archaeology. This is discussed in chapter III. Following the definition of by McGrail (1988, p. 35), the evaluation of the performance of the two ship types in the current thesis is done by assessing their cargo capacity, speed potential and stability. Additionally, the ship motions in the Baltic and North Sea will be calculated and compared.

Since the goal of the thesis is to assess and compare the differences in performance between Nordic cargo ships and cogs due to their different hull shape characteristics, modern naval architecture calculations are performed on 3D model reconstructions of a Nordic cargo ship and a cog of similar size. Length, beam, and displacement have a great effect on a ship's hydrodynamic behaviour and therefore it is important to compare ships of similar size when evaluating their hull shape and related performance. The Bremen cog is chosen because it represents the quintessential cog. The archaeological definition of what a cog should look like was based on its remains and it has therefore become the standard representation of this shipbuilding tradition (Zwick, 2014, p. 62). Moreover, a detailed 3D model reconstruction of the ship has already been made and hydrostatic and stability calculations have been carried out (Tanner, 2018; Tanner, 2020; Tanner & Belasus, 2021). The description of these analyses and the 3D model itself will be covered in chapter IV, which presents the two case studies and the data used in the current thesis. The main dimensions of the Bremen cog are 23.2 m in length and 7.7 m in width (Tanner, 2018, p. 27). These are equal to the main dimensions of the reconstructed Big Ship of Wismar: 23.3 m long and 7.6 m wide. The Big Ship of Wismar is a 12th century wreck discovered in 2017 and excavated in 2018, following the excavations of two 13th century ships found in 2016 in the harbour of Wismar, in Germany. The ship has characteristics typical of the Nordic shipbuilding tradition and its timber has been provenanced as coming from western Sweden (Ditta & Auer, in press). After the ship was excavated, its timbers were 3D scanned and the hull was reconstructed into a digital 3D model, mainly for visualization purposes. The process of recording the wreck and creating its 3D reconstruction model is documented in the papers by Ditta and Auer (in press; 2021) and Van Damme *et al.* (2020) and will be covered in more

detail in chapter IV as well. Some hydrodynamic coefficients were derived from its shape but no thorough displacement and cargo estimates, nor performance analyses have been done yet. The authors state however the importance of having seakeeping and stability calculations done on the vessel (Ditta & Auer, in press). This will be done in the current thesis.

Table 1 shows the different calculation tasks done on the 3D models of the Big Ship of Wismar and the Bremen cog to assess their performance, and whether these are covered in the current thesis or are already available from previous work.

A detailed description of the methodology used to complete these tasks and of the tools used to perform the different calculations is given in chapter V. A short summary is however presented here. As it can be seen in the table, most of the work done in the current thesis involves the model of the Big Ship of Wismar. The already available results for the Bremen cog regarding its loading conditions, stability and speed potential calculations are used as a comparison to the ones of the Big Ship of Wismar. In order to make a fair comparison, the same criteria and methodology as used on the Bremen cog is be applied to the Big Ship of Wismar.

Table 1
Tasks performed in the current thesis and previously available data for the two case studies.

Task	Big Ship of Wismar	Bremen cog
Creation of a detailed 3D model	Part of this thesis	Available
Loading conditions and weight calculation (Excluding inertia)	Part of this thesis	Available
Stability calculations	Part of this thesis	Available
Speed potential estimation	Part of this thesis	Available
Weight distribution including inertia	Part of this thesis	Part of this thesis
Seakeeping calculations	Part of this thesis	Part of this thesis

Because the 3D model of the Big Ship of Wismar was done mainly for visualization purposes, it consists basically of the 3D scanned mesh of the preserved timbers, the outer surface of the hull and few other structural elements not necessarily defined as closed volumes. Consequently, it is not immediately suitable for the performance of stability nor seakeeping calculations, as these require first to compute the weight of the vessel, for which a complete volumetric model of all the structural elements is needed. Therefore, the first task on the models was to generate a complete detailed 3D model for the Big Ship of Wismar using as basis the 3D scanned mesh of the preserved timbers, the 3D visualization model by Ditta & Auer, and the database containing the information of the individual preserved timbers. The detailed 3D model of the ship was created using the proprietary

software Rhinoceros. Once the 3D model was completed, I computed the mass of the hull and the corresponding centre of gravity by calculating the volume of each of the elements in the model in Rhinoceros and multiplying it by the density of the element's material. Next, I added the mass of the crew and equipment, and obtained the draft of the empty vessel by using Rhinoceros plug-in ORCA 3D. For the loading conditions including the weight of the cargo, the opposite approach was used: a draft was defined and the corresponding ship's weight including cargo was obtained. The fully loaded draft was taken as the one corresponding to the requirements found in the Icelandic Grågås codex, which is a collection of laws recorded in 1117 and in use until the 1280s (Ditta & Auer, in press). According to the codex, the freeboard of a cargo ship was supposed to be two fifths of the depth of the hull amidships (Morcken, 1980, p. 178). For the Big Ship of Wismar this results in a draft of 1.61 m which matches the lower end of the first wale, thus the water being in between the two wales (Ditta & Auer, in press). For the Bremen cog this results in a draft of 1.74 m (Tanner, 2018, p. 23). Other intermediate drafts between the empty and the fully loaded ship were also considered. Once the loading conditions were defined, I performed stability calculations with the ORCA 3D software following the same approach as for the Bremen cog, as documented in Tanner (2018) and discussed in more detail in chapter IV.

Speed estimations on the Big Ship of Wismar were performed in the same way as for the Bremen cog. This includes the use of the ORCA 3D software to estimate the calm water resistance of the hull at different speeds following the Holtrop method, and the estimate of the power generated by the sails at different wind speeds. The speed of the vessel is then found when resistance and propulsive power equal each other. The propulsive power generated by the sails was roughly estimated considering the area of the sail, different sail efficiency factors, and a basic relationship between wind speed and power for square sails given by (Gerr, 1995, p. 164). No evidence exists about the dimensions of the sail of the Big Ship of Wismar, and there is hardly any knowledge about the sail proportions of Viking ships as no sails have ever been preserved. Moreover, other sources of information such as historical references and iconographical representations do not match the limited archaeological evidence (Bischoff, 2017, p. 1). I estimated thus the sail area of the Big Ship of Wismar based on the sail proportions of the Skuldelev 3 vessel and the hull geometry of the Big Ship of Wismar. The sail reconstruction of the Skuldelev 3 was possible because both the position of the mast on the keelson and the holes for rigging at the hull sides were preserved (Bischoff, 2017, p. 10). Additionally, experiments on its full-scale replica showed that the ship performs well under sail, which according to Bischoff (2017, p. 22) is a good indicator that the sail reconstruction might be correct.

Seakeeping calculations were not available for the Bremen cog, and these were thus performed in the current thesis for both ships. Since seakeeping calculations require the mass moments of inertia of the vessel, these were computed for the Bremen cog as well, as they are not available from previous assessments. This is because stability calculations do not require modelling the mass moments of inertia of the vessel, as only the position of the centre of gravity is needed. I computed the mass moments of inertia by calculating the moments of volume at the model's origin coordinates of each of the elements in the 3D models with Rhinoceros and multiplying them by the density of the element's material. Moments of inertia were then translated to the centre of gravity of the ship using the parallel axis or Steiner's theorem. Seakeeping calculations were done using the proprietary software SHIPMO from the Maritime Research Institute Netherlands (MARIN), which is a strip-theory code in the frequency domain based on linear seakeeping theory. For these calculations, the geometry of the hulls is defined by a series of 2D sections along the length of the ship. As already mentioned, a more detailed description of the methodology and tools is given in chapter V.

The results of the calculations are presented in chapter VI and are discussed in chapter VII. Finally, the conclusions and answers to the research questions are presented in chapter VIII.

II. The Nordic and "cog-like" shipbuilding traditions

In this chapter a critical review of the different theories about the origins and development of both Nordic and cog-like traditions is made. The debates about the technological diffusion between the two traditions and the problems of mixing archaeological and historical concepts for the definition of the two shipbuilding traditions are also presented. Finally, a review of the theories explaining the disappearance of the Nordic tradition and the dominance of the cog after 1300 is made.

II.1 Changes in shipbuilding traditions

The 13th century marked a period of significant transformation in shipbuilding traditions across the North Sea and the Baltic Sea regions. Prior to the emergence of the cog and the decline of the Nordic shipbuilding tradition, each region had its distinct developments and contributions to maritime transportation.

II.1.1 The southern coasts of the North Sea

The archaeological record of the southern coasts of the North Sea (modern Germany, the Low Countries, and northeast France) shows a limited variety of ship types from ca. 750 to 1200, consisting of simple and expanded logboats, flat-bottomed barges, Utrecht-type ships (ships derived from expanded logboats), and ships with Scandinavian features (Van de Moortel, 2011, pp. 68, 73). A significantly greater diversity in ship types is seen both in the archaeological and historical records after 1200, fuelled by the growing urban economy and the related increase in waterborne trade (Van de Moortel, 2011, pp. 68, 101). Shifts in construction techniques, materials, and sizes are also noticeable in the 13th century. For instance, while treenails are the most common technique used to join overlapping planks in flat-bottomed barges in the region before 1300, iron nails become more common afterwards (Van de Moortel, 2011, p. 81). Similarly, iron edge-fasteners become more common than treenail edge-fasteners from 1200 (Van de Moortel, 2011, p. 89). Iconographic evidence suggests that the use of the saw became widespread in shipbuilding from the 13th century (Bill, 1994, p. 156). Moreover, an account from 1285/1286 referring to the construction of a cog-like ship contains two entries concerning saws but no mention to axes (Van de Moortel, 1991, p. 33). This could indicate a transition from split to sawn planks, which allowed shipbuilders to use lower quality timber. Van de Moortel (2011, pp. 73, 75, 94) argues that the scarcity of high-quality oak trees in the late Middle Ages would explain the reduction in size of the Utrecht-type ships and, likewise, why a significant number of logboats from the late Middle Ages were made from spiralling-grain oak trees while all the early Middle Age ones were made from straight-grain trees.

It is also in the 13th century that cogs appear in the archaeological record. The cog wrecks found in the region (2 in Belgium, 13 in the Netherlands and 1 in Germany) date from the late 13th to early 15th centuries (Van de Moortel, 2011, pp. 82, 84-86). The origin of the cog is still debated. Even though the provenance of only six cogs has undoubtedly been linked to the region south of the North Sea, most scholars agree that it originated in the Netherlands based on the high number of finds, its resemblance with the fluvial flat-bottomed shipbuilding tradition typical of this region, and on the fact that the earliest historical references to the term 'cog' appear in two mid-10th century documents from Utrecht (Van de Moortel, 2011, pp. 82, 87-88). As it has already been mentioned in the introduction, and will be further discussed in section II.2, the use of historical references to the term cog to infer about archaeological ship remains is however problematic and many scholars urge for a distinction between the archaeological definition of what a cog is and the historical references to the term cog (Dhoop, 2016, pp. 48-49; Englert, 2003, p. 46). From an archaeological perspective, Van Moortel (2011, p. 83) argues that both cogs and river barges share the following characteristics: a similar box-shaped hull with wide and thick planking, thick and close-set frames, a flat bottom, overlapping (side) planking, moss as caulking material, long flat scarfs, and double-clenched iron clamps (sintels) to join the planks, see Figure 5 and Figure 6.

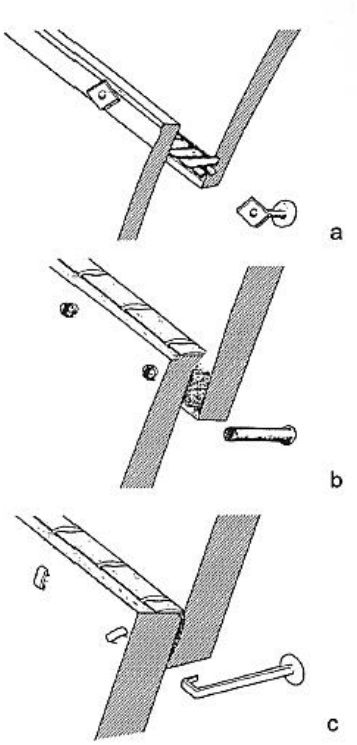

Typical joining method of the Nordic shipbuilding tradition, consisting of iron rivets and luting with animal hair

Typical joining method for barges and Utrecht-type ships consisting of wedged treenails and caulking with moss, mosslath, and widely spaced iron staples (*sintelnagels*)

Typical joining method of the earliest cogs, consisting of double-clenched iron nails and caulking with moss, mosslath, and widely spaced iron staples (*sintelnagels*). Later cogs use closely spaced butterfly-shaped iron staples instead, see Figure 6.

Figure 5 Techniques for joining and caulking overlapping planking. (After Crumlin-Pedersen, 1997, p. 29, Fig. 1.6).

Figure 6 The butterfly-shaped iron staple (*sintel* in Dutch) used in later cogs. (Reinders, 1985, fig. 8).

The differences between barges and cogs would be related to the fact that barges were made for inland transport while cogs were seagoing vessels. Therefore, barges have flat bottoms with hard chines (sharp change in angle between the sides and the bottom parts of the hull) and open extremities while cogs have a slightly curved bottom, round bilges, and closed extremities with a stem and stern post (Van de Moortel, 2011, p. 87), see Figure 7.

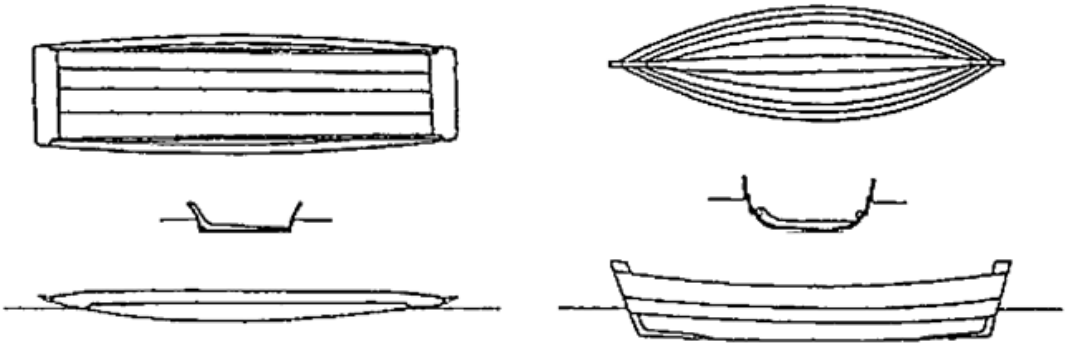

Figure 7 General hull shape differences between river barges (left) and cog-like ships (right). (Litwin, 1998, p. 89, Fig. 4).

Van de Moortel (2011, p. 87) argues that the need for a seagoing vessel fostered the change from low and slender barges to high and wider vessels. She mentions that indeed the oldest Kollerup cog has a slender body similar to river crafts as well as a mast step like seen in barges (Van de Moortel, 2011, p. 90). Additionally, she claims that the length to beam ratio reached an optimal value around the late 12th century and that from that moment on, the need for larger cargo capacities pushed the shipbuilders to increase the height of the freeboard (Van de Moortel, 2011, p. 88). Although no evidence of a ship linking the river crafts to the seagoing cogs has been found yet, and thus it remains unclear when, where, and from which ship type the seagoing cog actually developed, Van Moortel (2011, pp. 88-90) claims that the most likely precursors of the cog are the Romano-Celtic coastal and seagoing vessels. She points out that double-clenched nails were already used in the Romano-Celtic shipbuilding tradition to connect the planking to the frames, see Figure 8, and

second, overlapping planks, iron edge-fasteners, and long flat planking scarfs secured with double rows of fasteners as the ones used in cogs, were already used in local Romano-Celtic barges.

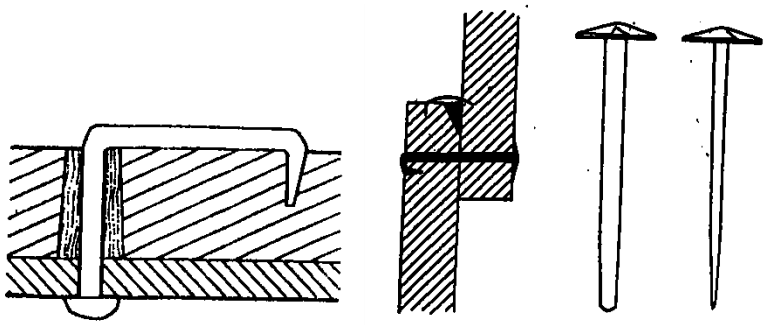

Figure 8 Methods of planking fastening using iron hooked nails. Left: Iron nail driven through a treenail and clenched by hooking to fasten the planking to the frames in Romano-Celtic boats. Right: Iron hooked nails used to fasten the planking in cogs. (McGrail, 2006, p. 38, fig. 27).

Moreover, the typical feature of mixing carvel bottom planking and clinker side planking was already widely used in the Roman provinces, and the use of a broad frame as mast step seen in the earliest cog, the Kollerup, was also found in Late Roman vessels (Weski, 1999, p. 371). Additionally, the mast step on the Kollerup cog was placed well forward of amidships, see Figure 9, which is a typical feature of Romano-Celtic vessels (McGrail, 1995, p. 140). Later cogs would have their masts closer to amidships (McGrail, 2006, p. 47). Other similarities between seagoing Romano-Celtic ships and cogs are the high bow and stern stems, plank keels, and the use of moss as caulking material (McGrail, 2006, p. 41).

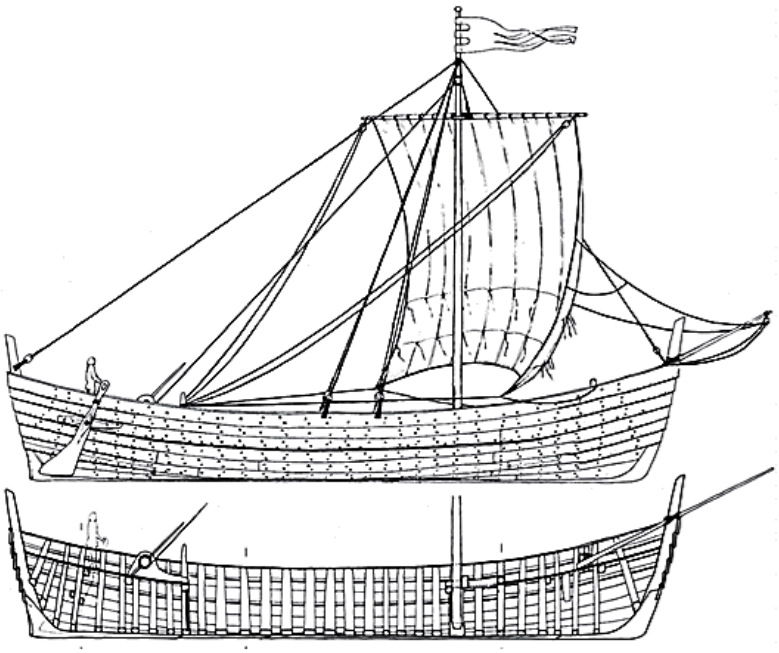

Figure 9 Reconstruction profile of the Kollerup cog. (Crumlin-Pedersen, 2000, p. 241, Fig. 9. After P. Kohrtz Andersen, 1983).

Romano-Celtic barges, Utrecht-type ships, and cogs belong to the same building tradition and represent most of the ship finds in the southern coasts of the North Sea. Clinker-built vessels with characteristic Nordic features, although widespread chronologically and geographically, are scarce, fragmentary, and limited to coastal and fluvial areas (Van de Moortel, 2011, p. 95; Bill, 1997, p. 153). The distinctive Nordic biti system is absent in the region (Bill, 1997, p. 151). The biti system consists of using cross beams in the framing structure, separating floor timbers and knees, rather than using continuous scarfed frames, see Figure 10.

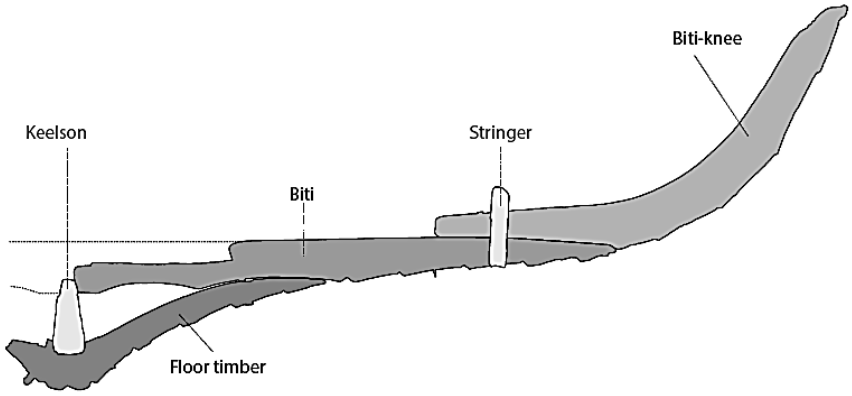

Figure 10 Cross-section of the Big Ship of Wismar showing the biti system. (Adapted from Auer & Ditta, 2019, p. 28, Fig. 23).

II.1.2 The Baltic Sea

Ship finds in the Southern and Eastern Baltic shores before 1000 are scarce (Bill, 1997, p. 155). The earliest textual evidence of medieval shipping in the Baltic Sea dates to the 9th century, when the first permanent coastal settlements were established by a number of nations, including the Scandinavians, the Western Slavs (or Wends), the Balts (Prussians and Ests), the Laps, and the Finns (Litwin, 1998, p. 88). The archaeological evidence until the early 13th century, before the German and Danish colonization, shows that the Scandinavians and the Slavs were the dominant shipbuilders in the area (Litwin, 1998, p. 88; Bill, 1997, p. 155).

The Slavic shipbuilding tradition evolved from the modification of logboats by extending their sides with overlapping planking and eventually transforming it into the keel of the ship, which by the end of the 9th century was also T-shaped like in Scandinavian ships (Litwin, 1998, p. 91). Although they were also made of oak, had a curved stem and stern, rivetted lapstrake planks, and a rudder blade attached to the starboard side like Scandinavian ships, they had a flatter bottom, moss as caulking material, and used pegs to fix structural elements instead of nails, see Figure 11 (Litwin, 1998, p. 91). This shipbuilding tradition reached its peak in the 11th and 12th centuries, when the Slav tribes

participated in trade and combat campaigns against the Vikings and other Baltic nations (Litwin, 1998, p. 91). However, the lack of central power would have hampered the development of a professional maritime trade and would explain why despite the discovery of Slavic wrecks, no archaeological evidence of large Slavic cargo ships has been found (Crumlin-Pedersen, 1999, p. 18). Due to this lack of central power, the Slavs suffered from their conflicts with the Danes and were soon occupied by the Germanic tribes, which also managed to conquer the Prussians and established a new and powerful state (Litwin, 1998, p. 88).

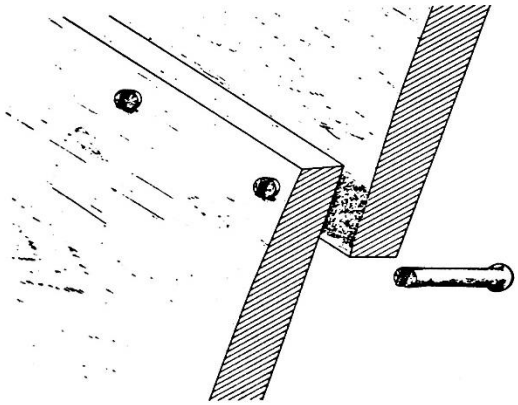

Figure 11 Slavic technique for joining and caulking overlapping planking. Planks are held together with treenails and sealed by means of moss or a mixture of moss and wool inserted in a groove. (Crumlin-Pedersen, 1991, p. 72, Fig. 4).

Several finds from Scandinavia, the Baltic and the British Isles show that a distinctive Scandinavian or Nordic shipbuilding tradition existed from the 4th century onwards (McGrail, 2006, p. 43). Scandinavian ships might have evolved from boats made of hides and skins by replacing these materials by oak timbers and substituting the traditional sewing technique to join the planks by the use of rivets after the introduction of iron smelting (Litwin, 1998, p. 89). Another view is that they could have evolved from simple logboats or rafts (Crumlin-Pedersen, 1972). The typical characteristics of the Scandinavian or Nordic shipbuilding tradition are summarised by Litwin (1998, pp. 90-91). These characteristics include rounded stem and stern posts fixed directly to the keel, which has a T-shaped section amidships and becomes hexagonal fore and aft, lapstrake planking caulked with animal hair and fastened with rivets, a rudder blade hinged usually on the starboard side near the stern, a mast step in the keelson, and the biti system, see Figure 12 and Figure 13.

Nordic ships were originally propelled by oars and the introduction of the sail occurred relatively late. The first archaeological evidence of a mast on a Nordic ship dates to the 8th century and the earliest ship known to have been sail-propelled, the Oseberg ship, Figure 14, dates from around 820 (McGrail, 2006, p. 43; Englert, 2000, p. 38; Werenskiold, 2011, p. 872). The archaeological evidence for Scandinavian Iron Age and Early Viking Age ships is however very limited and is mostly limited to burial and bog finds, which are not cargo vessels but small crafts and personnel carriers (Englert,

2000, p. 39). There is however iconographical evidence of sailing ships from the 6th century ship carvings on memorial stones in Gotland and sails were known in the region since Roman times (McGrail, 2006, pp. 43-44; Englert, 2000, pp. 37-38). It could be that rowed ships were better suited for the type of activities performed at sea, such as fishing and warfare, and that sails did not offer any substantial improvement (Englert, 2000, p. 39; Haywood, 1991, p. 72).

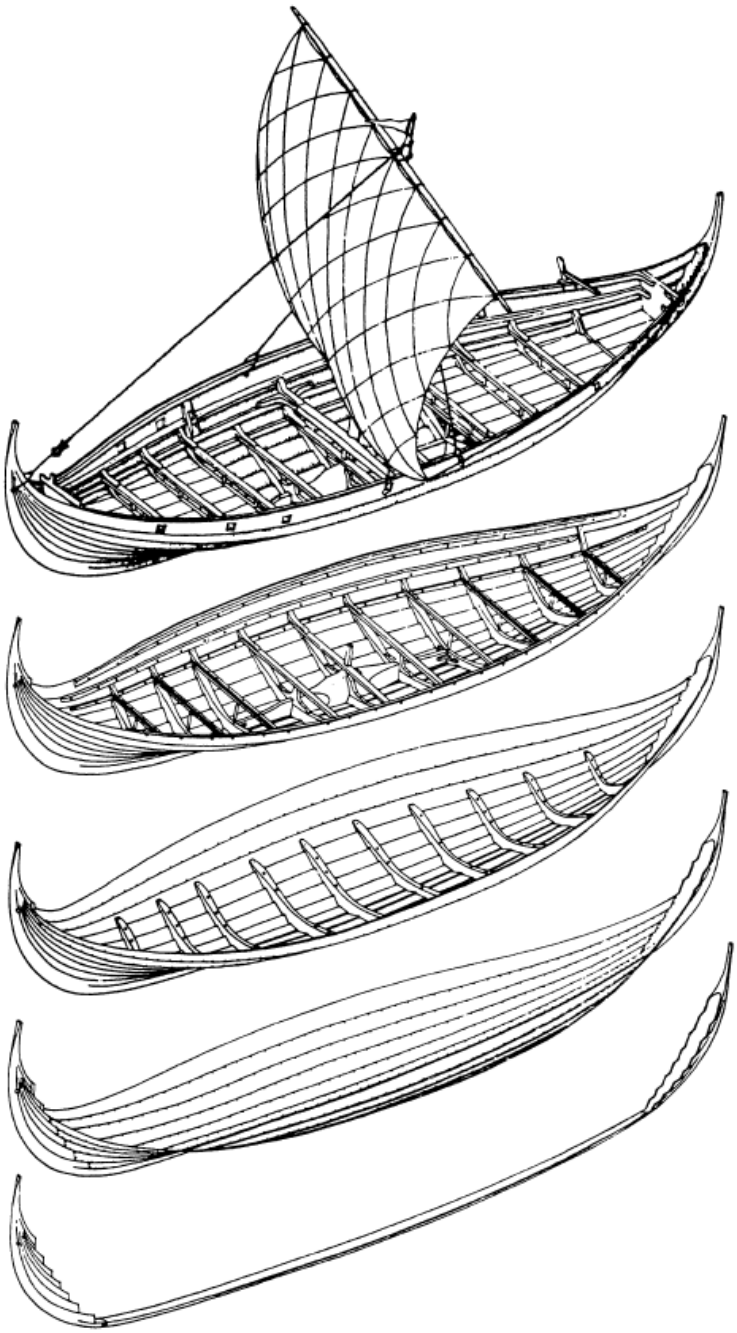

Figure 12 The construction steps of the Viking ship Skuldelev 3. From bottom to top: first the curved stems were attached to the keel. The hull was then built in the plank-first technique in which the outer planking provides the shape of the hull and is built before the installation of the frames. After the installation of the frames, the biti system is installed, followed by the upper beams, mast, rudder, sail, and rigging. (Bruun, 1997, p. 1285, Fig. 3a. Copyright: Rosendahl, E., 1993, Gyldendal Publishers, Copenhagen).

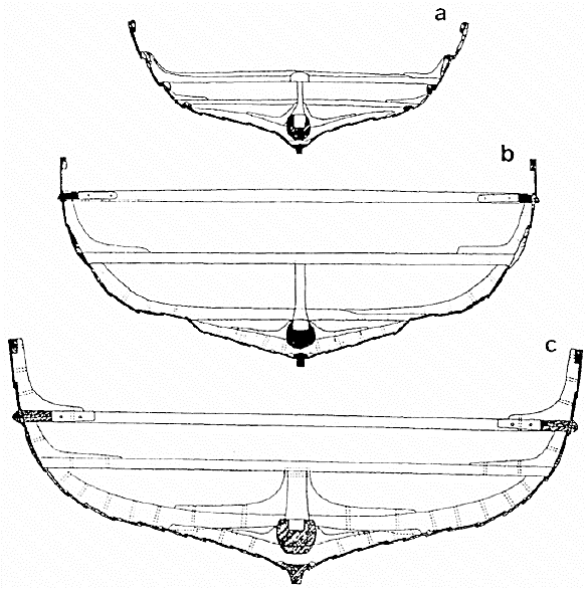

Figure 13 Cross section of Scandinavian cargo ships. a) the Skuldelev 3, b) the Skuldelev 1, c) the Hedeby 3. They all show the T shaped keel, the mast on the keelson and the biti system. (Litwin, 1998, p. 90, Fig. 5).

Figure 14 The Oseberg ship in the Viking Ship Museum in Oslo. (Werenskiold, 2011, pp. 872, fig.1).

It is in the 10th century, that a broad ship differentiation occurred within the Scandinavian or Nordic shipbuilding tradition including the introduction of genuine sailing vessels, as evinced archaeologically and by the information provided in the sagas (Litwin, 1998, p. 90; Englert, 2003, p. 274; Englert, 2000, p. 39). The types of ships included wind and oar propelled warships such as the

snakes (*snekkja*), the dragons (*drakkar*), and the longships (*langskip*), as well as merchant vessels of different sizes such as the *byrdingr*, the *skuta*, the *ferja*, and the larger *knarr* or *buza* (Litwin, 1998, p. 90; Crumlin-Pedersen, 2003, pp. 256-257), see Figure 15 for a few examples.

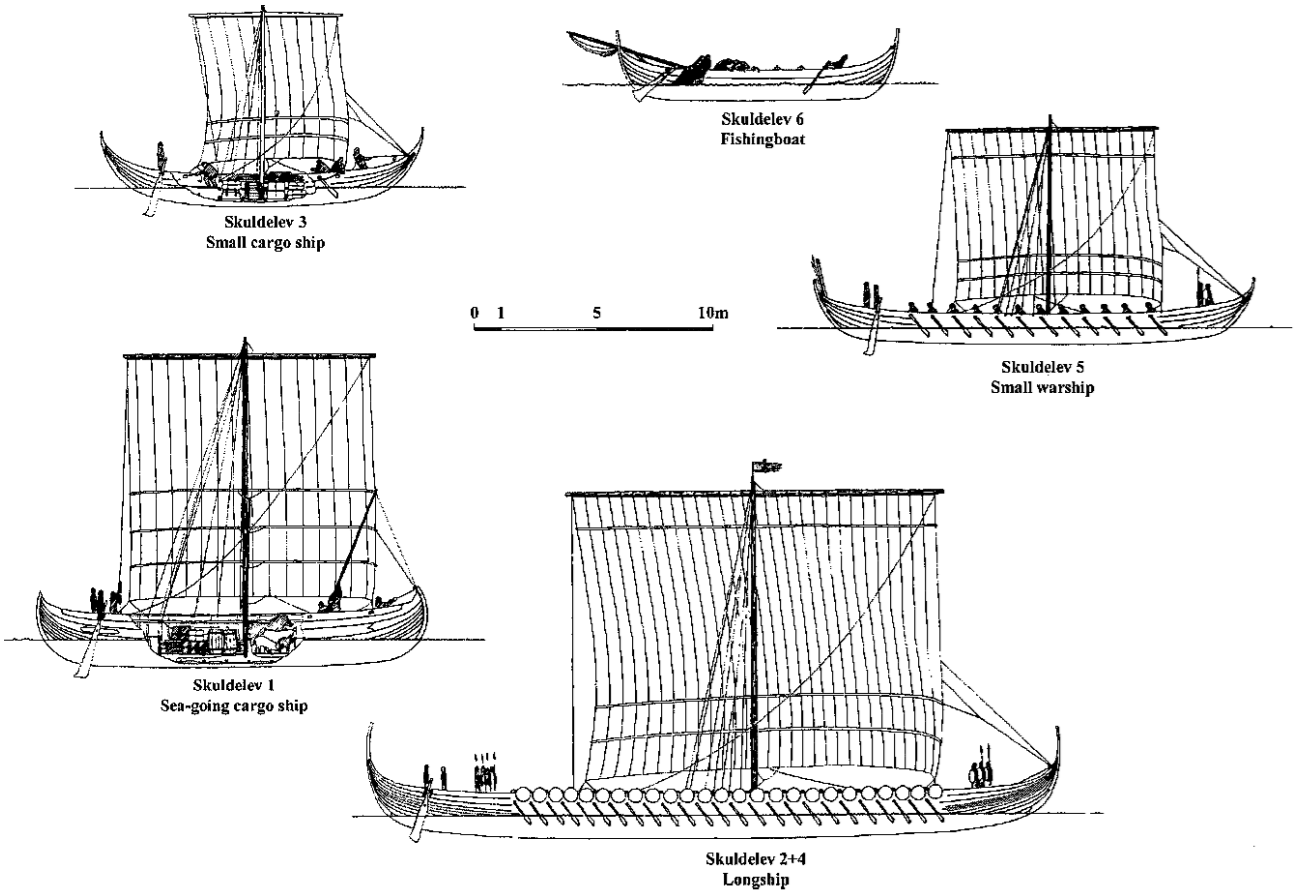

Figure 15 Reconstruction drawings of the Skuldelev ships. From top to bottom and left to right: a small fishing boat (*ferja*), a small sail propelled cargo vessel (*byrdingr* or *skuta*), a combined oar and sail propelled small warship (*snekkja*), a sea-going sail propelled cargo vessel (*knarr*), and a combined oar and sail longship (*langskip*). (Crumlin-Pedersen, 2003, p. 258, Fig. 38.5. Drawing by Morten Gothche).

Englert (2003, p. 274) points out that with the introduction of purely sailing merchant vessels, there was no need to accommodate oarsmen between frames and therefore the frame spacing reduced in favour of stronger hulls and larger cargo space. Moreover, these vessels are characterised by a cargo hold amidships without thwarts, deck beams nor deck, two fully decked platforms fore and aft of the ship, and heavy crossbeams near the mast and at the ends of the hold. After the 10th century a clear distinction between the slender oar and sail propelled personnel carriers and the wide sail propelled cargo vessels can be seen in the archaeological record when comparing the beam to length ratios, see Figure 16.

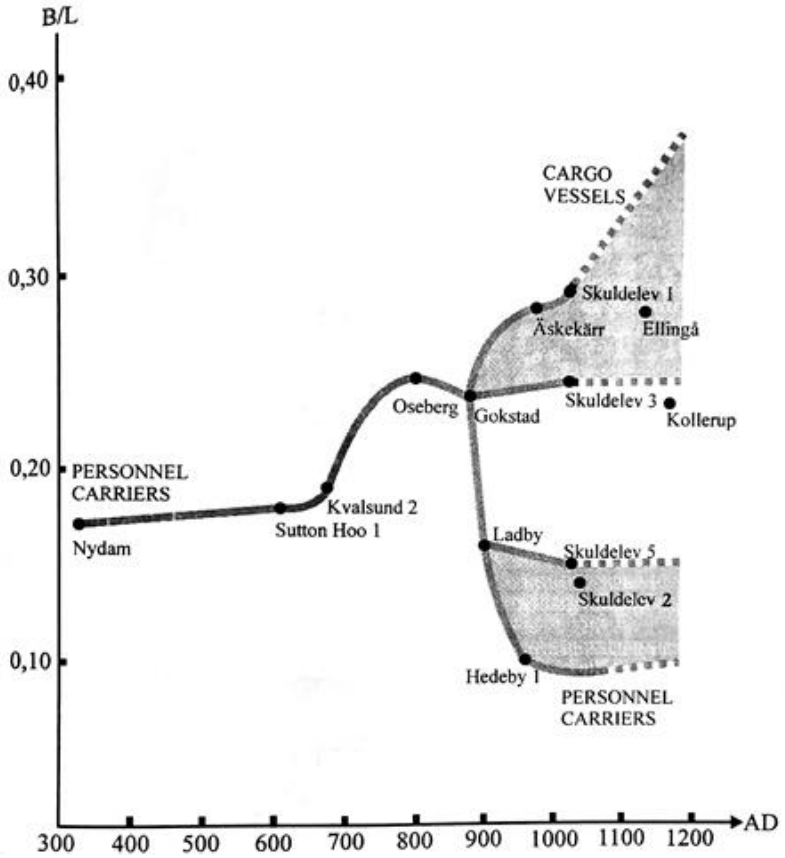

Figure 16 Beam to length ratio for North-European ship finds between 300-1200. Only ships with a length above 14 m are shown. (Crumlin-Pedersen, 1999, Fig. 5).

Contrarily to the trend seen with the cogs, Scandinavian shipbuilders did not extend the sides of the vessels to increase cargo capacity but just increased the overall size of the ships (Englert, 2003, p. 277). As already mentioned in the introduction, the archaeological record shows that up to the 13th century the size and cargo capacity of Scandinavian vessels was much larger than the size and capacity of contemporary cogs (Crumlin-Pedersen, 1991, pp. 76-79).

Evidence also indicates the existence of a professional long-distance Scandinavian merchant system connecting the Baltic and the North Sea until the 13th century, before the dominion of the Germanic merchants (Englert, 2003, p. 277). The archaeological finds, the iconography on city seals, and the historical sources show that ships from both shipbuilding traditions were used contemporarily for many years and that they even borrowed features from each other (Christensen, 2002, p. 92; Weski, 2003, pp. 282-283).

Denmark, as a transition zone between the North Sea and the Baltic, played a crucial role in the development of maritime technology and on the transfer of knowledge between the Nordic and the cog-like shipbuilding traditions (Westerdahl, 1995, pp. 222-223). Two ships built in a non-Nordic tradition appear in the archaeological record in the Jutland peninsula in Denmark as early as the

second half of the 12th century: the Kollerup, the oldest recorded cog dated around 1150, and the Skagen cog dated around 1193 (Englert, 2000, p. 44). According to Crumlin-Pedersen (2000, pp. 238-241) this indicates that the sea-going cog actually emerged in the Jutland peninsula rather than in the Netherlands, especially since no Dutch cog finds are dated before 1250 and their timber was not from the Netherlands. He argues that the development of seagoing cogs from local river crafts, including the lapstrake side planking and the longitudinal keelson, would have been inspired by the Nordic tradition. Crumlin-Pedersen (2000, p. 239) argues that the trigger to adapt river crafts into sea-going vessels could have been the closure of the western entrance to the Limfjord in northern Jutland around the 12th century, making it impossible for heavy cargo ships to be pulled overland across the sand and forcing them to travel around Skagen. The first textual reference of sailors travelling around Skagen is found in the Scania market privileges granted by King Abel of Denmark in 1251 (Westerdahl, 1995, p. 222). Van de Moortel (2011, p. 89) however points out that it is unlikely that the lapstrake technique would have been borrowed from the Nordic tradition without also borrowing the use of rivets, and thus the most likely origin of the cogs is in the Lowlands, where they developed from the Romano-Celtic river barges and seagoing ships, as explained in the previous section. The sea-going vessels of the Romano-Celtic tradition were however built in the frame-first technique instead of the plank-first technique like cogs and Nordic ships (McGrail, 2006, p. 42).

Regardless of the cog's origin, it is evident that this new shipbuilding tradition had a notable influence on the Nordic shipbuilding tradition. During the 13th century, many of the distinctive traditional constructive features of Late Viking Age ships were abandoned and replaced by new techniques typical of the cog-like construction. These borrowed features and techniques include the stern and stemposts connected to the keel with knee-shaped timbers, the long scarfs, the scarfed frames, and even in some cases the use of moss as caulking material (Bill, 1997, p. 156). A clear example is the small freighter from Gedesby in Denmark from ca. 1300 built in the Nordic tradition but with typical cog features such as the sternpost and the use of large knees on the crossbeams (Crumlin-Pedersen, 2000, p. 241).

The influence of the cog-like tradition was increased further with the expansion of the maritime trade by the new Germanic state, which resulted in the creation of the Hanseatic League and had a huge impact on the shipbuilding traditions of the region (Litwin, 1998, p. 88). The urban growth in Western Europe encouraged the trade between the Baltic and the North Sea, and large western European cargo ships started sailing into the Baltic Sea. The cog became the most common ship in the Baltic during the 13th and early 14th centuries. By the end of the 13th century, they were already being built locally in the Baltic shores and their representations used in numerous Baltic city seals (Litwin, 1998, p. 93). The influence of the cog was so big that the Nordic shipbuilding tradition, which

had dominated Northern Europe between 1000-1300, was essentially abandoned in the construction of large ships and survived only in boatbuilding practices after the 13th century, even in Scandinavia (Steen, 1934, p. 13). Also remarkable is the fact that at the beginning of the 13th century, the biti system suddenly disappeared even in clinker-built ships (Bill, 1997, p. 137).

II.2 Identification and classification issues

After the disappearance of the characteristic Nordic biti system and the decorative stem mouldings from clinker-built ships, the fundamental construction technology becomes uniform across all northern European ships despite their varying overall designs (Englert, 2000, p. 52). As Bill (1997, p. 156) points out: "the difference between an early cog find as the Kollerup cog and the almost contemporary Lynaes [Nordic] ship is much more marked than what is seen when comparing the [later] Bremen cog with a contemporary, clinker-built vessel". At this stage it becomes thus difficult to recognize whether one ship belongs to one or the other shipbuilding tradition, which could be the reason why in historical documentation different terms were used to describe the same ship (Crumlin-Pedersen, 1991, p. 70).

This poses an important problem to the definition of distinct shipbuilding traditions and the classification of ship types based on their construction techniques. With respect to the cog and the cog-like shipbuilding tradition the problem is fundamental, as written and iconographical sources were first used by Heinsius (1956) to define what a cog was, and archaeological evidence, especially from the Bremen cog, was afterwards matched and added to this definition (Dhoop, 2016, pp. 50-52; Weski, 2003, p. 281). With the discovery of more cog-like finds, it has become harder and harder to fit all their specific features into the list of characteristics deemed to be typical. Hence different groups of features have been made depending on whether they are considered as primary and unique or secondary and shared with other shipbuilding traditions (Dhoop, 2016, pp. 53-54). Dhoop (2016, p. 55) rightly questions whether some of the features are in fact related to the specific purpose of the vessel rather than a typical feature of a given shipbuilding tradition or ship type. He also argues that some features deemed typical of cogs, such as the sternpost rudder, were in fact so quickly adopted by other traditions that they can hardly be considered as a distinctive feature. Note that the oldest cog found, the Kollerug, still had a side rudder, Figure 9.

The problem with the actual definition of the typical cog is that it has been used together with the historical references of the term 'cog' to investigate the origins and evolution of a cog-like shipbuilding tradition, which is in fact a modern construct (Dhoop, 2016, p. 56). Medieval terms to describe ships were however fluid and subject to different dynamics including changes in popularity

and meaning (Englert, 2000, p. 45). Moreover, it is unclear whether technical construction details such as the use of sintels and double-clenched iron nails, which are considered to be characteristic features of the cog, would have been known or were of any importance for non-sailor medieval writers. Other factors such as the origin of the ship, the ethnicity of the crew, the type of cargo or the carrying capacity, seem to have played a bigger role in the names used to describe ships (Weski, 2003, p. 285). For instance, the city seal of Lübeck is described in a document from 1328 as having a cog in it, but the iconography on the seal suggests that it would have more likely been a ship built in the Scandinavian or Slavic tradition, see Figure 17 (Weski, 2003, p. 282; Crumlin-Pedersen, 2000, p. 233). The historical description of the seal of Stralsund from 1329 was one of the main reasons why the Bremen wreck of 1380 was identified as a cog. However, it could have been possible that the ship in that seal was built with rivets and a T-shaped keel instead of sintels and a flat bottom, just like the Kalmar II wreck which also resembles the ship on the seal (Weski, 2003, p. 283). Scholars therefore advocate for separating the archaeological definition of a cog from the historical classifications (Dhoop, 2016, p. 58; Weski, 2003, pp. 286-287).

Figure 17 City seals of Lübeck (left) and Stralsund (right). (Weski, 2003, p. 283, Fig. 42.1. After Ewe, 1972, n. 89, 91-93, 194).

The existence of a Nordic tradition has also been challenged by Bill (2009), who applied a multiple correspondence analysis on qualitative features from archaeological finds to identify shipbuilding traditions and investigate the relationships between them. His results show that the lapstrake technique considered to be characteristic of the Nordic tradition changed considerably over time and incorporated many features from other lapstrake traditions in northern Europe such as the cog-like ships and carvel-building traditions, especially in the southern parts of Scandinavia. According to him, the idea of a Nordic tradition is a modern construct from the 19th and 20th centuries which linked the archaeological finds with the shipbuilding practices of Northern Scandinavia, an area in

which high medieval shipbuilding practices remained in use due to the low urbanisation and the lack of exposure to other continental ships (Bill, 2009, p. 437).

Attempts of intermixing archaeological evidence with historical and iconographic sources have also been undertaken. Crumlin-Pedersen (2003) used the ship terms in the Norse sagas, contemporary English and continental texts, scaldic verses, and runic inscriptions to identify 20 ships from 950-1150, including the Skuldelev ships, see Figure 15. Although he argues that a good match can be made for most of the ships, he acknowledges that ship types evolved in shape and size and thus a name could refer to completely different ships depending on the period. He mentions for instance that, while 11th century longships were described in scaldic verses as fast, long and slender, they were described as large, high and wide in the 13th century sagas. Cargoes were defined with different terms depending on their size, seaworthiness, and shape. The term *knarr* was exclusively applied to cargo ships except in some early cases before the 10th century where it was also used to refer to warships (Crumlin-Pedersen, pp. 256-257; Heide, 2014, p. 107).

II.3 From *knarrs* to cogs

Despite the ongoing debates regarding the validity of the existence of two distinct and mutually exclusive shipbuilding traditions, it is evident that significant changes in shipbuilding techniques and designs took place during the 13th century. While some of the shipbuilding practices were broadly adopted, others were replaced and ultimately abandoned.

Varenius (1992, pp. 133,146) proposed that the disappearance of the characteristic features of the Nordic shipbuilding tradition was caused by the Christianisation of Northern Europe and the establishment of the medieval state, which made the religious and social symbolism of the Viking ship and its related shipbuilding tradition irrelevant. Basing his reasoning on the study of pictures and inscriptions on runestones, as well as ship iconography on early Scandinavian coins, he argues that Christianisation would have introduced or replaced societal values within the Viking society, which would have fostered the adoption of a more economic or quality-oriented approach to shipbuilding.

A significant shift to more economic solutions did occur in shipbuilding in the 12th-13th centuries. The evidence shows that elaborate and aesthetic designs are replaced by more economic options; mouldings disappear and flush scarfs, wing-shaped framing timbers, the biti system, and joggled stringers are replaced by lipped scarfs, parallel-sided frames, plank-shaped stringers, and protruding beams (Bill, 1997, p. 156). Likewise, the round cross-section rivets and short thin scarfs used in Scandinavian vessels shift to the less labour-demanding square cross-section rivets and long thick

scarfs during the 12th century (Bill, 1995, pp. 201-202). However, rather than being a direct effect of Christianization, which had occurred in Denmark two centuries prior, Bill (1995, p. 202) points to the rapid population and economic growth as well as the establishment of the feudal system in Denmark as the catalysts for these changes. He argues that the population and economic growth in Denmark would have required the transport of large quantities of food and goods, while the establishment of the feudal state and the implementation of taxes and tithes would have encouraged a more economic oriented approach to shipbuilding. The shipbuilding and seafaring activities experienced a shift from an elitist character towards a simpler, more economically driven approach in response to the demands of towns and landowners who owned the ships but relied on peasants to sail them (Bill, 1997, p. 161; Bill, 1995, p. 202).

Another important change in shipbuilding techniques relates to the production of planks and the introduction of the saw, which allowed for the use of sawn planks instead of split planks. Sawn planks were adopted by cogs from an early stage during the 13th century but Scandinavian boats continued using split planks, probably due to the lesser quality of sawn planks and the fact that, contrarily to cogs, ship flexibility and strength on Scandinavian ships relied strongly on the hull's planking (Bill, 1997, pp. 157-158). The need for high quality timber and the higher complexity of the Scandinavian ships' construction, would have facilitated the dominance of cogs. Scarcity of high-quality timber during the 11th and 12th centuries is revealed by the increased use of recycled shipbuilding materials and the reduction in plank size (Crumlin-Pedersen, 1991, pp. 78-79). The possibility of using sawn planks in the construction of cogs, which allowed to obtain more wood per tree, in combination to their lower production costs would have been key factors for the cog to become the preferred ships amongst German merchants (Dokkedal, 1996, pp. 61-62).

The argument of lower production costs does not explain however why the first German settlers and merchants in Denmark and in the Baltic continued to use Nordic or Slavic ships before the 13th century instead of introducing their own more cost-effective techniques (Englert, 2003, p. 279; Englert, 2000, p. 49; Weski, 1999, p. 362). Christensen (1989, p. 20; 2002, p. 92) argues that the rise of the cog in Northern Europe came with the expansion of the Hanseatic League. Even though Scandinavian merchants may have had ships that were just as large and capable, they could not compete with the Hanseatic League's political and militaristic power and their control over the lucrative trade of Baltic grain and salt from Lüneburg. Additionally, he argues that the devastating effects of the Black Death of 1349 had a significant impact on Norwegian society, including its shipbuilding and trade industries. As a result, German merchants were able to take advantage of the situation and seize control of a great part of the foreign trade from Bergen.

The socio-economic explanations proposed for the decline of the Nordic shipbuilding tradition and the replacement of large Nordic cargo ships by cogs emerged as alternative narratives when technical explanations became less prominent, especially after the discovery of large Nordic cargo ships like the Big Ship of Bergen, which demonstrated that large vessels could be built in the Nordic tradition. However, the capabilities of ships are not solely determined by their size or construction techniques. Factors such as hull shape, stability, sailing capabilities, and behaviour also play a significant role. Assessing the performance of these vessels, beyond their size, would shed light on whether the socio-economic factors behind the transition from Nordic ships to cogs were accompanied by an improvement in ship performance resulting from different hull designs. Unfortunately, most shipwrecks are only partially preserved, making it extremely challenging to evaluate ship performance based only on fragmentary remains without a complete hull. Furthermore, historical records provide limited information on ship performance, and establishing a direct connection between historical accounts and archaeological findings can be problematic, as discussed earlier. The following chapter will present the various approaches that are used in archaeology to assess ship performance.

III. Ship performance assessment in archaeology

The concept of ship performance and what it entails is very broad. According to Marchaj (1986, pp. 6-7), a modern non-racing boat should fulfil three main requirements. First, it must be seaworthy, which means that it must be built as a durable and strong construction able to survive in rough weather. Second, it must be sea-kind, which means that it should not experience rough motions even when sailing in rough weather. Third, it should be habitable, which means that it must provide a comfortable environment for the physical and intellectual activities of the crew.
McGrail (1988, p. 35) however focuses on the aspects related to the stability, speed potential and cargo capacity to define the performance of ancient ships. According to him, estimating maximum speeds and cargo capacities is more feasible than trying to assess aspects which are strongly dependent on the prevailing weather conditions and human behaviour such as the master's seamanship or the experience of the crew. Moreover, archaeological wreck finds are generally fragmentary and incomplete, with the upper parts of ships being rarely preserved. As a result, there is a scarcity of evidence regarding the rowing or sailing configurations of these vessels. Hull shapes and the structural and propulsive arrangements of ships need to be therefore theoretically reconstructed and estimated. The smaller the surviving proportion of a ship, the greater the likelihood of having multiple reconstructions compatible with the excavated remains (McGrail, 1987, p. 192). Once reconstruction models are available, McGrail (1987, pp. 192-193) suggests that the performance of an ancient ship can be evaluated using six main approaches with different levels of complexity. These six approaches will be presented in this chapter. McGrail (1987, p. 192) stresses that the validity and significance of the performance assessment will depend on the accuracy of the excavation documentation and post-excavation research, the authenticity of the theoretical reconstructions or models, the validity of the assigned values to different parameters (such as construction material and cargo density, safe freeboard, sail performance, etc.), and the relevance of modern naval architectural methods when analysing ships from earlier centuries.

III. 1 Using general sailing and shipbuilding knowledge and experience

The most basic approach to estimate the performance of ancient ships is to rely on the experience of sailors, shipbuilders, and naval architects who are familiar with a given shipbuilding tradition and hull form. This approach can provide a general qualitative insight on the performance of the vessel just by looking at the hull shape and lines. For instance, by looking at the hull lines, experienced sailors, shipbuilders, and naval architects would be able to assess whether the curves offer low

resistance and allow the ship to move smoothly through water (McGrail, 1987, p. 193). Other qualitative assessments include the reduced resistance by gentle underwater lines at the bow, the reduction of water embarkment by the presence of flare above the waterline, the increased stability provided by outward flare at the sides and beamer hull shapes, the reduced resistance and higher speeds achieved by longer hull shapes, the larger reserve stability provided by the freeboard, the increased leeway due to wind caused by large freeboard and superstructure, the flexibility or stiffness of the hull due to the nature of the planks and fastening arrangement, etc. (McGrail, 1987, pp. 193-194; Shaw, 2016, p. 16).

Drawing from his boatbuilder experience, Tanner (2018, p. 42) suggests that the shift from fully clinker-built ships to carvel (flush) bottom planking, as observed in cogs, could be attributed to the practical considerations involved in the building and repair activities. Because of the differences in the shaping and fitting of the hull strakes, Tanner claims that clinker construction is easier to build but more difficult to repair, whereas carvel construction is more complex to build but offers easier repairability. He explains that in carvel construction each plank requires meticulous shaping on both the bottom and top edges to ensure a tight seam that can be properly caulked, while clinker planking is more forgiving of minor mistakes and generally allows for quicker completion of the construction process. However, clinker planking would be more prone to damage when ships would ground as the planking and fastening is more vulnerable to erosion. Tanner hints that this might be the reason why carvel planking in cogs did not go further up above the turn of the bilge since the upper strakes would rarely touch the ground.

Hocker & Ward (2004, pp. 73-75) claim that the hollow waterlines observed at the bow of cogs, see Figure 18, contributed to enhanced speed and were thus intentionally incorporated into their design. This assumption is however questionable. As pointed out by Tanner (2018, p. 42), such design features are primarily a consequence of trying to maximise the width of the ship and therefore the cargo capacity, which cause these hollow lines in the transition of the planks to the vertical end posts.

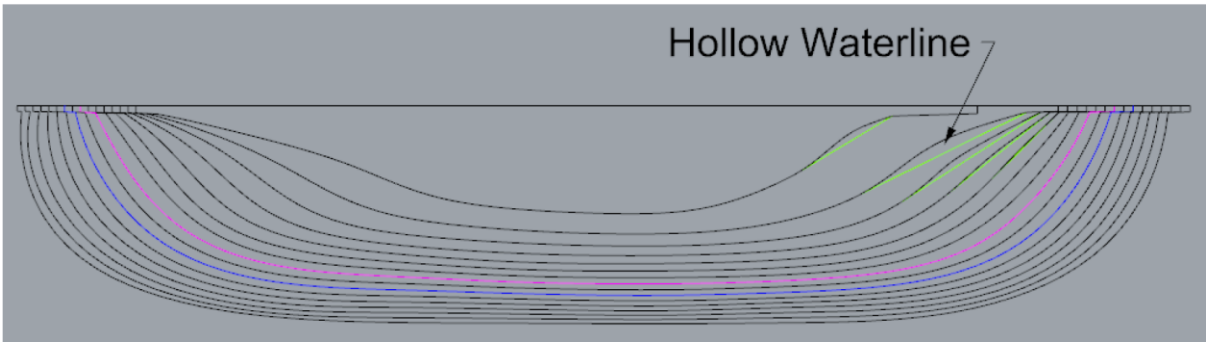

Figure 18 Hollow waterlines of the Bremen cog. (Tanner, 2018, pp. 41, Fig. 25).

According to Tanner (2018, p. 53) and based on his sailing experience, the full blunt bow of cogs such as the Bremen cog would offer increased buoyancy, which would reduce both the risk of broaching and the risk of pitchpoling, which is when the ship is sailing in waves coming from the stern and its bow buries into the back of the wave ahead while the wave behind lifts the aft section up. Marchaj (1964, p. 399) states that this would explain why squared rigged ships maintained the blunt bows for so long. Tanner (2018, p. 53) however points out that the hollow waterlines at the forefoot of cogs such as the Bremen cog would actually create a sharp edge that would dig into the waves and potentially increase the risk of broaching. Moreover, the flat bottom would be vulnerable to slamming (Tanner, 2018, p. 55).

Werenskiold (2011, pp. 871-879) states that Nordic ships would have been less vulnerable to slamming and their hull flexibility would allow to spread the bow impact forces, in the same way as experienced by sailors of traditional Norwegian clinker-built vessels. Hull flexibility of Nordic vessels is apparent by their construction technique of clinker planking and the larger spacing between rivets (Shaw, 2016, p. 18). Werenskiold (2011, pp. 871-879) also suggests that the hull flexibility would increase the sail performance in rough weather by dampening the mast movements and the fluctuations in the sail forces.

Experienced sailors would also be able to highlight that the low freeboard of Nordic ships would limit their positive hydrostatic stability range, requiring skilful handling by the helmsman and crew and the easy reduction of sail area, particularly when tacking, as a consequence of the high risk of waves washing over the gunwale and stern (Werenskiold, 2011, pp. 871-879).

Assessing ship performance through the examination of ship lines using general shipbuilding knowledge and sailing experience is a challenging skill to acquire. However, it is important to note that this approach lacks scientific reproducibility and does not offer measurable insights into ship performance (Ejstrud, et al., 2012, p. 4). Another way to evaluate and compare the performance of different ships in a more measurable way is to make use of simple hull geometry coefficients.

III. 2 Using simple hull geometry coefficients

Hull geometry coefficients are derived from the main dimensions of ships, for instance the ratios between length and beam or beam and draft, and these are then used to provide insights on the performance of ships. For instance, the ratio length over beam indicates the slenderness of the ship and consequently can provide some insights on the speed potential of a ship or its transverse stability. Slender hulls experience lower wave making resistance at forward speed and beamier hulls

possess higher transverse stability, when displacement is kept constant (McGrail, 1987, p. 194). Larger length over beam ratios also indicate higher directional stability and thus less manoeuvrability, while larger length over draft ratios indicate increased manoeuvrability (McGrail, 1987, pp. 194-195).

Hull geometry coefficients can also be used to make rough estimate of the speed potential of ships, although as McGrail (1987, p. 196) notes, reasonable estimates can only be done by means of numerical calculations, experimental tests with scaled models, or by the actual sea trial measurements on full-scale ships. McGrail indicates that for the speeds for which the ratio between speed and the square root of the length, $V/\sqrt{L}$, equals 0.6, a high slenderness ratio, $L/B > 0.5$, would indicate a good speed potential. Likewise, a midship coefficient below 0.85 or a block coefficient below 0.65 would indicate a good speed potential. The midship coefficient is a measure of a hull's fullness amidships and corresponds to the dimensionless ratio between the area of the midship section (A) and the product of the beam (B) and draft (T): $A/(BT)$, see Figure 19.

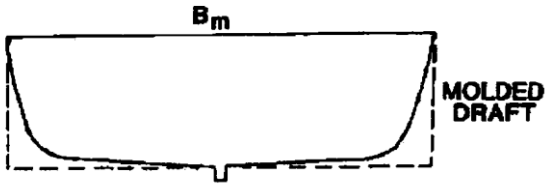

Figure 19 Definition of midship coefficient. (Steffy, 1994, p. 255)

The block coefficient is a measure of a hull's fullness and corresponds to the dimensionless ratio between the ship's volumetric displacement (∇) and the volume of a rectangular box with the size of its length at the waterline (L), beam, and draught: $\nabla/(\mathrm{LBT})$, see Figure 20.

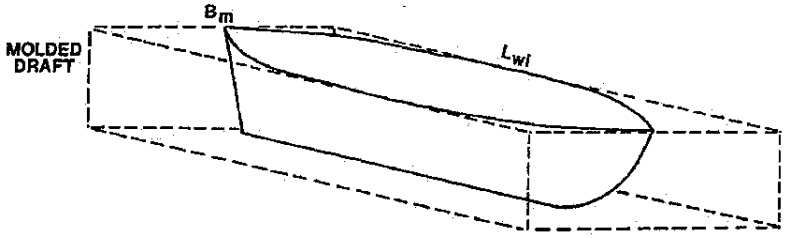

Figure 20 Definition of block coefficient. (Steffy, 1994, p. 255)

Tanner (2018, p. 6) evaluated the slenderness coefficient, midship coefficient, and block coefficient of the Bremen cog and concluded that the ship had a speed potential between below average and

good. However, he points out that this does not provide an accurate assessment of the potential speed of the vessel.

For higher speeds where $1.1 > V/\sqrt{L} > 0.6$, the prismatic coefficient can be used instead. Values below 0.55 would indicate good speed potential. The prismatic coefficient is the dimensionless ratio between the ship's volumetric displacement and the volume of the prism with length equal to the ship's length at the waterline and a transverse section equal to its midship section: $\nabla/(AL)$, see Figure 21.

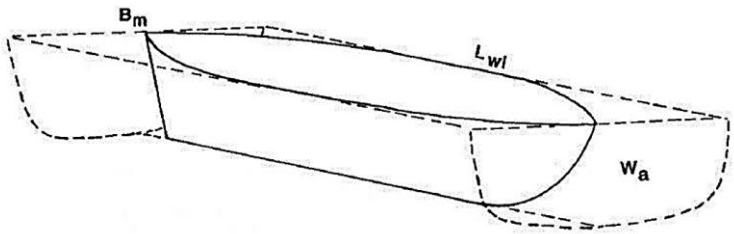

Figure 21 Definition of prismatic coefficient. (Steffy, 1994, p. 255)

Another coefficient that can be used to assess speed potential and resistance is the waterplane coefficient, which is the dimensionless ratio between the waterplane area and the product of the length and the beam of the vessel at the waterline, see Figure 22. Higher values indicate fuller ships and increased resistance. Cargo vessels have higher waterplane coefficient values than slender warships (Ejstrud, et al., 2012, p. 20).

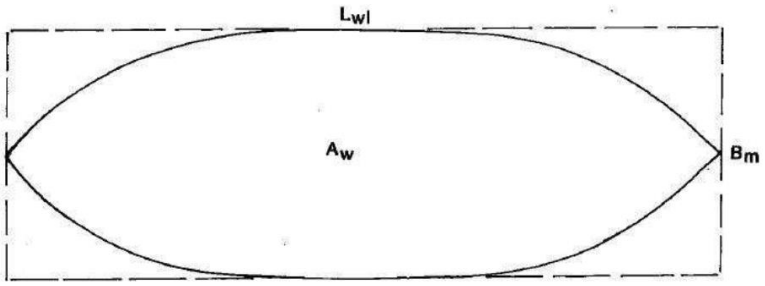

Figure 22 Definition of prismatic coefficient. (Steffy, 1994, p. 255)

McGrail (1987, p. 196; 1988, p. 38) notes that the theoretical maximum speed in knots for a displacement hull can roughly be estimated as $V_{max} = 1.4\sqrt{L_{wl}}$, which is the speed in which the ship will create a wave profile with a wavelength equal to its waterline length, with crests at the bow and stern and a trough amidships, dragging itself into that trough and drastically increasing the wave

making resistance, see Figure 23. McGrail indicates that ships sailing at higher speeds would require large propulsive mechanical power and would appear to be planing.

Based on this formula, McGrail (1987, p. 197) estimates the speed potential of the Skuldelev 1 and 3 ships to be 10 and 8.7 knots respectively.

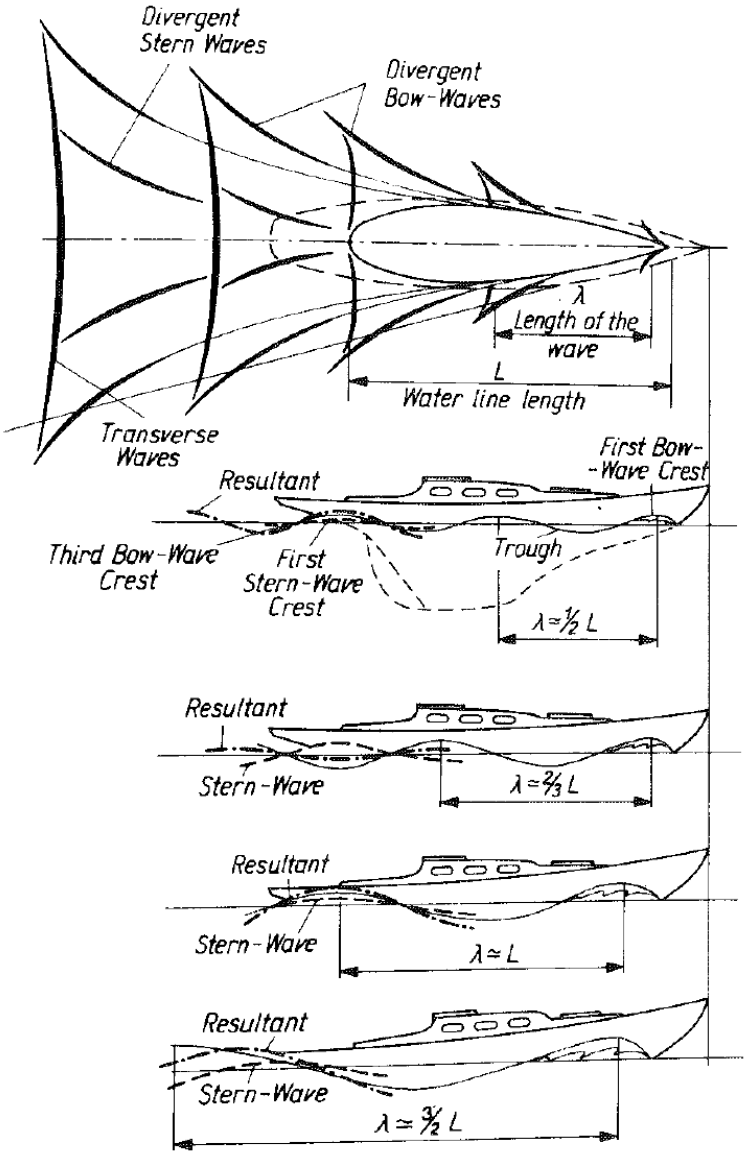

Figure 23 Drawing illustrating the relation between wave-making resistance, the ship's speed, and generated wavelength. (Marchaj, 1964, fig. 153).

It is important to acknowledge that the coefficients used to assess various aspects of ship performance, particularly the speed potential, have been determined based on a combination of experiments conducted on scale models and full-scale sea trials with modern ships. Such systematic evaluations have not been conducted yet on ancient ships, which possess very different shapes and

characteristics as compared to modern ships, and therefore their applicability to ancient vessels may be questionable (McGrail, 1987, pp. 196-197; Tanner & Belasus, 2021, p. 315).

III. 3 Using hydrostatic curves to estimate cargo capacity and transverse stability

The use of hydrostatic curves involves the definition of waterlines and the calculation of the underwater volume, the underwater sectional areas, the position of the centres of volume or area, and the equilibrium between gravitational and buoyant forces acting on the ship.
When a ship, or any other body, is partially immersed in a fluid, it will experience an upward buoyant force equal to the weight of the displaced volume. This is known as the Archimedes principle. The force will act on the ship at the centre of the displaced volume, referred to as the centre of buoyancy B. When the ship is floating in equilibrium, the buoyancy force will be equal to the weight of the body due to the downward gravitational forces, which will act on the body at its centre of gravity G, see Figure 24. The weight of the ship is therefore referred to as its displacement, which is the weight of the displaced water volume or the underwater volume of the ship. The displacement of the ship and the related centre of buoyancy can be calculated at different drafts, which creates a curve showing the relationship between draft and displacement or position of the centre of buoyancy. Freeboard can also be derived as it corresponds to the distance between the waterline and the top of the ship's deck. Other curves that can be derived are the trim curves, which show as a function of varying drafts, the changes in the longitudinal position of the centre of flotation CF, which is the centre of area of the waterplane, the longitudinal position of the centre of buoyancy, and the moments required to change the ship's trim by one inch or centimetre (McGrail, 1987, pp. 14-15).

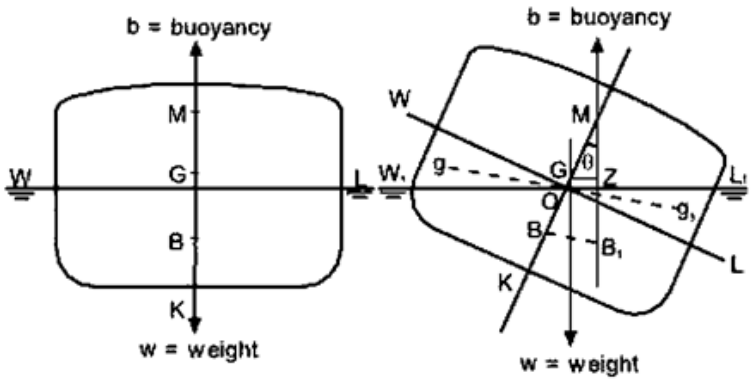

Figure 24 Drawing showing the forces and moments involved in the stable equilibrium of a ship and its static stability. (Derret & Barrass, 2001, p. 44).

If the weight of the ship in its empty condition is known, the cargo capacities can then be computed for different drafts. To obtain the weight of the ship in its empty condition, either a full-scale replica or a complete 3D model reconstruction are needed. In both cases the materials used in the original ship need to be known and in the case of a 3D model reconstruction the right material densities need to be chosen to obtain the weight of the ship based on the volume of its structural elements. In order to make valid comparisons between ships, it is crucial to use similar parameters and approaches for the estimation of weights, for instance, when defining the specific density of the wood at the moisture content relevant to the operational use, the average weight of the crew, the available cargo volume and related cargo densities, etc. (McGrail, 1987, pp. 13,200-201; McGrail, 1988, p. 37).

When trying to assess the cargo capacity of ancient ships, the challenge lies not only in the estimation of the ship's weight in its empty condition but also in establishing what would have been valid operational drafts (McGrail, 1987, pp. 13,199). The possible operational drafts can be estimated by considering the operational modes of the ships. For instance, operational drafts might be defined by the water depth in shallow water areas, by whether the ships transport heavy cargo or are used for the transport of people or warfare activities, by the minimum freeboard needed to ensure safety in terms of water embarkment, or by the requirements needed for a positive transverse stability (McGrail, 1987, p. 199). For Nordic cargo ships and cogs, the freeboard requirements found in the Icelandic Grågås codex are often used to establish the draft of the fully loaded ship.

The cargo capacities of some Nordic cargo vessels of the 11th to 12th centuries have been derived using different approaches. For most of them, including the Karschau ship (Englert, 2017, p. 278) and the Big Ship of Bergen (Christensen, 2002, p. 87), their capacities have only been roughly estimated without a complete hull reconstruction, and therefore without the use of hydrostatics nor the estimation of the weight of the empty ship. For the Skuldelev wrecks, hull reconstructions as well as full scale replicas have been made. For Lynaes 1, Englert (2000, p. 82) estimated the weight and resulting cargo capacity using the wetted surface of the hull and the average thickness of the planking, an estimate on the number of rivets, and assumptions on the weights of the mast and rigging, equipment, and crew, see Table 2. As seen in Table 2, Englert made a rough estimate of the inner timbers' mass by just using half the inner surface of the hull and an average timber height of 12 cm. The total mass of the ship in empty condition resulted in 18 tons and the cargo capacity at the Grågås condition 57 tons. He used a heterogeneous moisture content for the planking

considering a 35% moisture content for the planks above water and a moisture content of 50% for the planks in contact with water.

Table 2
Weight and cargo capacity estimates for the Lynaes 1 according to Englert (2000, pp. 82, Table 23).

Component		*Weight*
Immersed planking:		
	Wetted surface clinker hull x av. thickness x av. density waterlogged oak = 122.05 m² x 0.03 m x 1.0 t/m³ =	*3.662 t*
Freeboard planking:		
	Freeboard surface clinker hull x av. thickness x av. density oak = 72.35 m² x 0.03 m x 0.85 t/m³ =	*1.845 t*
Rivets:	*Rivets per metre x strakes x average strake length x rivet weight = 6/m x 2 x 18 x 26 m x 0.06 kg =*	*0.337 t*
Other timbers:	*Plain inner surface x av. moulded height x density oak = 178.71 m² x 0.5 x 0.12 m x 0.85 t/m³ =*	*9.114 t*
Hull weight:		14.958 t
Mast and rigging (estimated):		1.000 t
Ship's equipment (estimated):		1.000 t
Minimum crew and their personal equipment (estimated):	10 men of 100 kg each =	1.000 t
Total weight without cargo:		**17.958 t**
Cargo capacity:	**displacement - total weight without cargo =**	**57.032 t**
Displacement:		**74.990 t**

For cogs, a similar situation exists. For some, cargo capacities have only been estimated, e.g., the Kolding cog and the Almere cog (Englert, 2017, p. 278; Van de Moortel, 2011, pp. 84-86). For others, hull reconstructions have been employed, although a complete assessment of the weight of the empty ship and hydrostatic calculations derived from a complete 3D reconstruction model have only been done for few of them, including the Ijsselcog (Waldus, Verweij, & van der Velde, 2019) and the Bremen cog (Tanner, 2018). Tanner (2018) computed the weight of the Bremen cog by considering a 27% moisture content for all timber independently of whether they were located above or below water, unlike the approach followed by Englert (2000) for the Lynaes 1.

Calculating the displacement of the ship at a given draft and subtracting the weight of the empty vessel does not guarantee however that this loading condition would have been operational as the ship might have lacked the necessary transverse stability.

The transverse stability of a ship is its ability to return to its upright position after being subjected to heeling forces such as wind and waves. The transverse stability of a ship is, however, usually assessed in a static way assuming a calm water surface by looking at the balance of gravitational and buoyancy forces acting on the ship in a heeled position. When the ship heels, the underwater geometry of the ship changes and hence, the centre of buoyancy. The buoyancy force is consequently no longer aligned with the force due to the ship's weight acting at the centre of gravity, which remains unchanged, see right drawing in Figure 24. The mismatch between these two forces creates a righting or heeling moment depending on the vertical position of the centre of

gravity and the new position of the centre of buoyancy. When small heel angles are considered, the initial stability of the vessel is defined by the metacentric height GM, which is the vertical distance between the centre of gravity and the metacentre. The metacentre is the intersection point between the upright and inclined buoyancy forces, see Figure 24. The vertical distance between the centre of buoyancy and the metacentre (BM) is given by the ratio between the moment of inertia or second moment of area of the waterplane around the centreline axis (I) and the displacement volume (∇), $BM = I/\nabla$.

A negative initial stability, i.e., a negative GM value, occurs when the centre of gravity is at a higher position than the metacentre. This will cause a heeling moment, making the ship heel further instead of returning it at its upright position. In this case the ship is unstable and will heel until a new equilibrium is found or until the ship capsizes. A ship is initially stable when the GM value is positive. The larger the GM value is, the larger the righting moment will be. Likewise, the larger the transverse distance between the centre of gravity and the centre of buoyancy, which corresponds to the righting arm GZ, see Figure 24, the larger the righting moment will be. Large GM values make a ship very stable but consequently very stiff and uncomfortable while low GM values make the ship more comfortable by rolling softer but increase the risk of it becoming unstable at large heel angles.

The initial stability of a ship only provides information on the stability for small heel angles, when the metacentric height can be considered as fixed, and the righting arm can be computed as $GZ = GMsin\theta$ with θ being the heel angle. When heel angles become larger, the changes in the underwater volume cause the metacentre to shift and the initial GM value is no longer meaningful. The transverse stability at large heel angles is assessed by generating the GZ curve of the ship, which shows the value of the righting arm GZ for a wide range of heel angles, see Figure 25.
A lot of information on the transverse stability of a ship can be obtained from its GZ curve. The initial stability of the ship, its GM value, is given by the intersection of the tangent of the GZ curve at the origin with the ordinate of 1 radian or 57.3 degrees heel angle. A negative tangent means that the ship is initially unstable and that it will heel until reaching an equilibrium, referred to as angle of loll, if the GZ curve becomes positive at larger angles, or capsizing if the GZ curve remains negative. A positive tangent intersecting the origin such as in Figure 25 indicates a positive initial stability for the ship in its upright condition. The range of heel angles where the GZ value increases with increasing heel angles represents a safe range of operation as the ship will experience an increasing righting moment the more it heels.

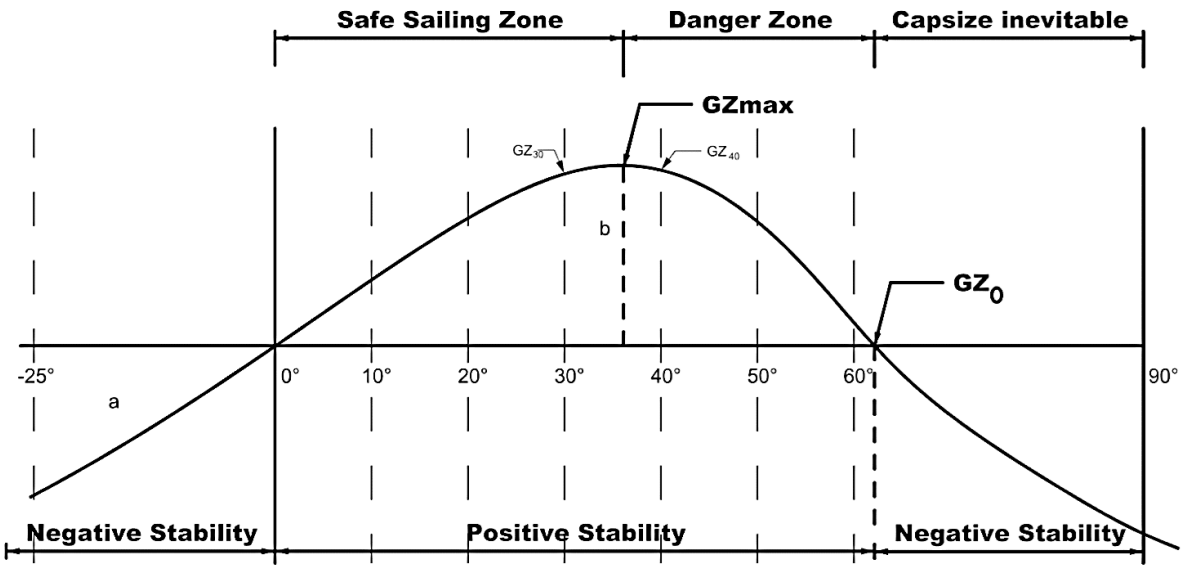

Figure 25 Example of GZ curve showing the complete transverse stability of a ship. (Tanner, 2020, p. 280, fig. 8-31)

Between the angle of maximum GZ value until the angle of vanishing stability GZ_0, although the ship still possesses a positive stability, the righting moment decreases with increasing heel angles. Under these conditions, the ship finds itself in a dangerous situation in which a small increase in the heeling forces from wind, waves, or changes in weight distribution on board, will produce a large increase of the heel angle of the ship, eventually reaching the angle of vanishing stability and causing the ship to capsize. Reducing the heeling forces by, for instance, easing or reefing the sails is crucial when the angle of maximum GZ is surpassed (Tanner, 2018, p. 28). Since the heeling or righting moments are given by the product of the heeling or righting arms and the displacement of the ship, the value of maximum GZ indicates the maximum heeling moment that the ship can face without risk of capsizing. The point of vanishing stability GZ_0 marks the angle at which the stability of the ship becomes negative, and the ship inevitably capsizes.

The area under the GZ curve represents the energy that the ship can absorb from external heeling forces such as wind, waves, and weight shifts. The larger the area under the GZ curve is, the larger are the heeling forces that the ship can withstand without capsizing. The area under the GZ curve can be computed up to a specific heel angle, for instance the angle of maximum GZ or the flooding angle.

The flooding angle is the angle at which the deck or the gunwale, i.e., upper edge of the ship's side, get submerged. Once the ship reaches this angle, water begins to embark, posing a significant risk of capsizing, particularly for open boats. Once the flooding angle is surpassed, the ship's stability

characteristics change too much, making the GZ curve irrelevant. This explains why modern safety regulations do not mandate the use of these curves for open boats (Ejstrud, et al., 2012, p. 27).

Examining the stability of archaeological reconstructions of ancient ships poses a challenge when it comes to determining which rules or criteria should be used as reference. It is unlikely that any specific stability rules were in place during the original construction of the vessels. Ancient boatbuilders may not have formulated their methods based on scientific principles but rather through an empirical approach based on common sense and trial and error processes to incorporate desirable qualities in their ships (Tanner, 2018, p. 28; McGrail, 1987, p. 12). For instance, negative initial stability would have been recognized in a ship which would heel and stabilize itself at an angle of loll instead of at its upright condition. This characteristic would have been avoided without the need to understand the concept of metacentric height (McGrail, 1987, p. 16). By examining the stability characteristics of ancient ships, archaeologists can infer the qualities that were considered desirable and those that were intentionally avoided by ancient shipbuilders (McGrail, 1987, p. 12). Although modern stability standards are based on modern ships and may not always be directly applicable to older ships, comparisons of the relative performance between ancient ships with regards to their stability can be made if the same modern standard calculations and underlying assumptions are used on different ships (Ejstrud, et al., 2012, p. 14; McGrail, 1987, p. 16).

Several modern rules exist to check the stability and safety of ships depending on their size, intended operational conditions and the country of the regulatory authorities. The International Maritime Organisation (IMO) is the United Nations agency responsible for developing international regulations and safety standards for ships. These regulations are then adopted and, in some cases, adapted by non-governmental organizations, known as classification societies, whose role is to certify that ships comply with the relevant safety standards. One of such classification societies is Bureau Veritas, a nowadays French company that was originally founded in Antwerp in 1828. The Bureau Veritas rules were used by Tanner (2018) to assess the transverse stability of the Bremen cog. This will be further described in chapter IV, where Tanner's work on the Bremen cog is presented. Modern safety standards, such as the ones defined by Bureau Veritas, the IMO, and other local regulatory authorities, specify requirements on the initial metacentric height, the values of the vanishing stability and flooding angles, the minimum freeboard, the value of maximum GZ value, and the areas below the GZ curve (Ejstrud, et al., 2012, pp. 10-14). Besides the requirements on the static stability in clam water, modern standards also specify rules to account for the effects of wind and waves on the stability of ships. To this purpose, the rules require that the reserve stability of a ship should be able to

absorb the energy from the wind and waves heeling forces acting on the ship in specific weather conditions (Bureau Veritas, 2022, pp. 78-82). This check is made by requiring that the area under the GZ curve up to the flooding angle after subtracting the area below the wind heeling arm, represented by the area "b" in Figure 26, is equal or larger than the area between the wind heeling arm and the GZ curve up to the heeling angle due to waves, represented by the area "a" in Figure 26.

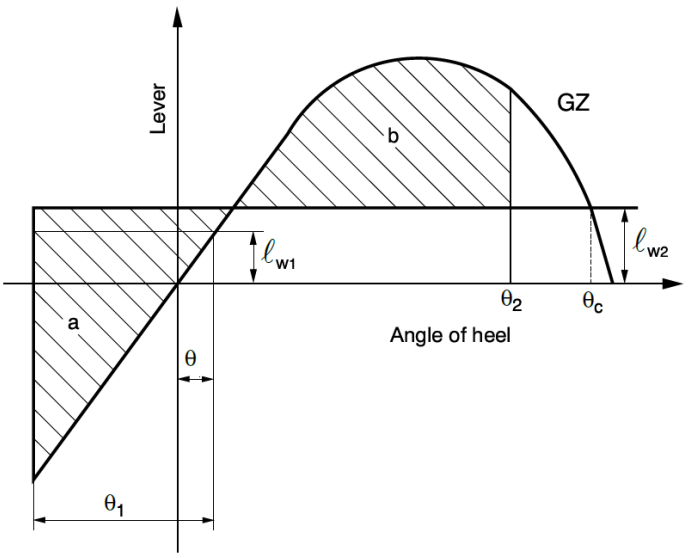

Figure 26 Weather criteria on the transverse stability of a ship as specified in modern safety standards. l_{w1} and l_{w2} represent the heeling arms due to the wind forces without and with gust respectively. θ is the heel angle caused by a steady wind, θ_1 is the heel angle caused by the effect of waves, θ_2 is the flooding angle, and θ_c is the second intersection angle between l_{w2} and the GZ curve. (Bureau Veritas, 2022, p. 79. Fig. 1).

The stability assessment of ancient ships is usually done by evaluating the initial metacentric height and freeboard. For instance, Waldus, Verweij, & van der Velde (2019) used a 3D model reconstruction of the Ijsselcog to determine its weight and initial metacentric height. They discovered that the ship had a negative metacentric height when empty, and subsequently calculated the required ballast weight to ensure a non-negative metacentric height. Ejstrud *et al*. (2012) performed 3D model reconstructions, hydrostatic and stability calculations on seven ancient boats, including the 6.5m long clinker-built boat known as Gokstad Faering which was found in the ninth century ship burial mound in Gokstad, Norway. The stability of the ships was evaluated by looking at the GM, freeboard, flooding angle, angle of vanishing stability, angle of maximum GZ, and a stability index defined as the ratio between the natural roll period and the ship's beam. According to this, a ship is considered as stiff when the stability index is below 1 and as tender when the index is above 1.5 (Ejstrud, et al., 2012, p. 30). Additionally, the effects of the weather were taken into

account by defining the critical wave height for which the wave induced excitation moment, derived from a formula using a given value for the wave slope and the natural roll period of the ship, equals the righting moment of the ship at the flooding angle, computed as $M = \Delta GMsin\theta_2$ (Ejstrud, et al., 2012, pp. 30-32).

A student from the Technical University of Berlin performed stability calculations on the hull shape of the Bremen cog, derived from photogrammetry measurements, and determined that the ship was unstable in its empty condition but stable when loaded or with 26 tons of ballast (Tanner & Belasus, 2021, p. 316). Full stability calculations applying modern standards as defined by Bureau Veritas were performed by Tanner for the Bremen cog (2018) and the 15th century clinker-built Newport merchant vessel (2013). The results from the Bremen cog will be discussed in chapter IV. Santos & Fonseca (2007) used, instead, the US Coast Guard criterion within the Code of Federal Regulations from 1983 to assess the stability of the late 16th century Portuguese Nau "Nossa Senhora dos Mártires", as they argue that the IMO regulations are not suitable for ships with extensive sail areas.

III. 4 Performing computer simulations

In real life conditions, the stability of a ship is affected by dynamic effects due to the changes in the underwater geometry as a result of the ship motions and the waves, especially in rough seas. This means that the stability of the ship in these conditions might differ significantly from the stability calculated using the GZ curves in static conditions and the ship might experience events leading to stability loss and capsize. To compute the dynamic stability of ships, time domain calculations are needed, where the actual underwater volume of the ship and the forces acting on it are computed for every time step. Time domain calculations are however complex and demand large computational requirements. Therefore, these calculations have not been applied to evaluate ancient ships yet (Ejstrud, et al., 2012, pp. 27-28; Tanner, 2020, p. 333).

As an alternative, Tanner (2020, pp. 332-334; Tanner & Belasus, 2021, pp. 321-322) used the game engine Unity 3D to model the behaviour of the Bremen cog when subjected to typical wave conditions of the Baltic Sea and the North Atlantic Ocean, see Figure 27. The gravitational forces acting on the hull were applied to the 3D model of the ship by the built-in physics engine of Unity 3D (Tanner, 2020, p. 333). The waves were generated using a third-party plug-in for Unity 3D in which the water surface is represented by a series of moving blocks and the predefined wave height and length were obtained by adjusting the wind forces acting on these blocks (Tanner & Belasus, 2021, p. 321). The outer hull surface was then defined as a grid of points and the Unity 3D physics engine applied the corresponding buoyancy forces on these points depending on whether they were

submerged or not at every time step (Tanner, 2020, p. 333). In these calculations, the wind does not act on the ship. Therefore, heeling angles and drift are not simulated and the ship speed is imposed on the ship model (Tanner, 2020, p. 333). These simulations only take into account the buoyancy forces, showing whether the ship remains afloat and whether there is water embarkment, although the effects of water embarkment are not modelled (Tanner, 2020, p. 334). While acknowledging that these simulations are primarily visual rather than physical, Tanner recognizes the significant potential of simulations on 3D model reconstructions.

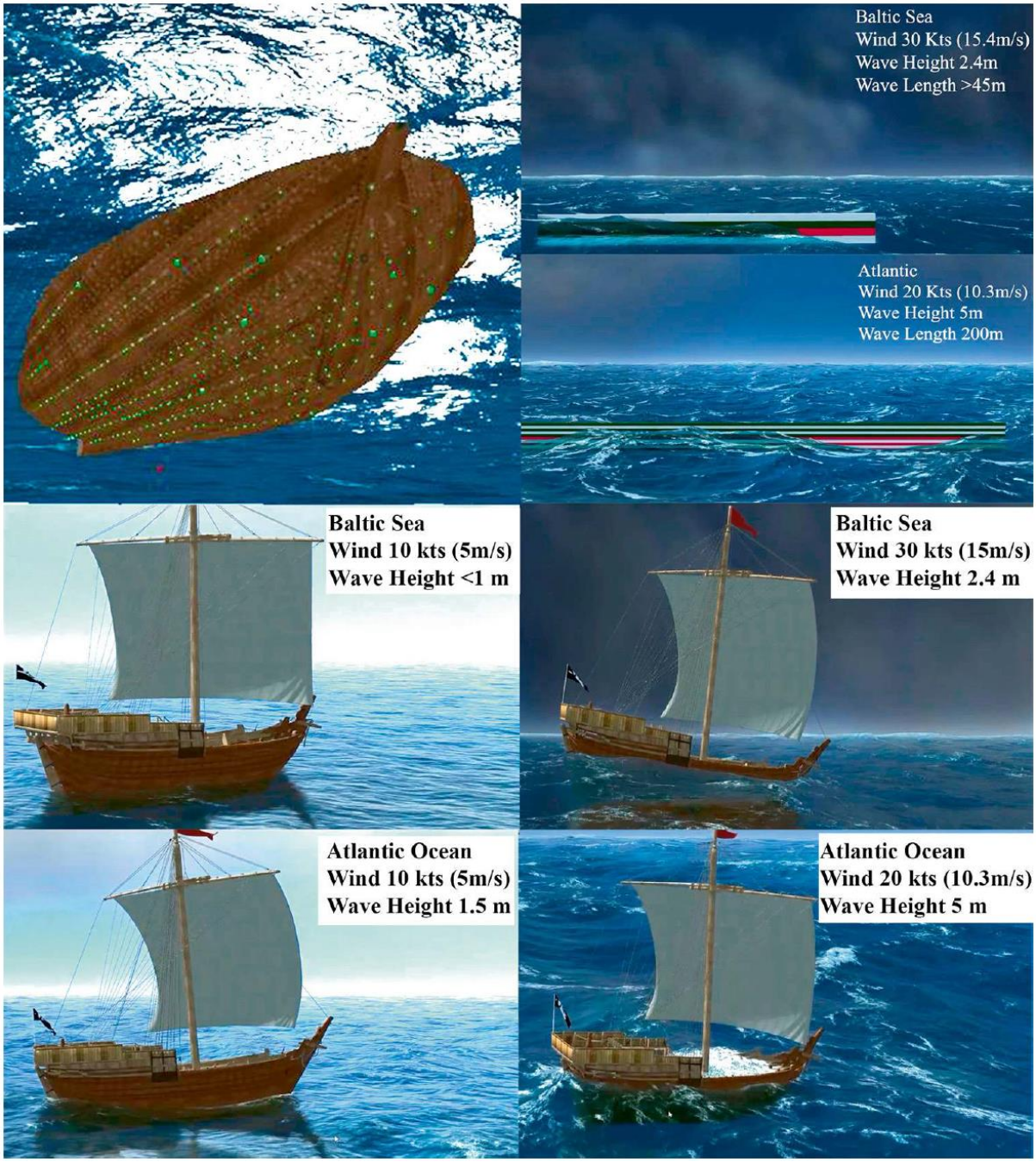

Figure 27 Screenshots of the simulations performed on the Bremen cog using the game engine Unity 3D. (Tanner & Belasus, 2021, pp. 322, fig. 4).

Numerical simulations can also be used to evaluate the performance of sails and rigging arrangements. For instance, Ciortan & Fonseca (2011) used computational fluid dynamics (CFD) calculations to evaluate the performance of the sails of the late 16th century Portuguese *Nau Nossa Senhora dos Mártires.* Werenskiold (2011) used the Wolfson Unit WinDesign velocity prediction program (VPP) to compute the sail performance and ship's speeds as a function of the wind angle and speed of the Oseberg ship, which is the earliest Nordic ship known to have been sail-propelled. Velocity prediction programs combine the hydrodynamic properties of the hull, the stability characteristics of the ship, and the aerodynamic properties of the rigging configuration to compute the ship's sailing performance. The aerodynamic coefficients were obtained from experimental wind tunnel tests with scaled models performed by the Wolfson Unit on similar single square rigged sail configurations and the hydrodynamic properties of the hull were obtained from experimental tests performed by MARINTEK (Norwegian Marine Technology Research Institute) with a scaled model of the ship in their towing tank.

III. 5 Performing experimental tests with scaled models

As shown for the Oseberg ship, experimental tests with scaled models in wind tunnel or towing tank facilities can provide valuable empirical data on the performance of ancient ships. The experimental testing with scaled models is a well-established technique in modern naval architecture and is commonly used in the shipbuilding industry to check the performance of a given design before the actual ship is built. The possibility of evaluating the performance of a full-scaled ship by experimenting on its scaled model relies on maintaining the laws of dimensional similitude which depend on the properties that want to be assessed. If the properties that need to be assessed are driven by gravitational forces, which is the case for the general ship motions which result from the effect of gravitational waves (Lloyd, 1989, p. 293), the scaling of the model needs to be done maintaining the similitude on the so-called Froude number $F_N = V/\sqrt{gL}$, where V is the flow velocity, g the acceleration of gravity and L the characteristic length. If, on the other hand, viscous forces are more important, for instance when assessing the performance of sails in wind tunnel tests (Jackson & Hawkins, 1998), then the model needs to be scaled maintaining the similitude on the so-called Reynolds number $R_N = \rho VL/\mu$, where ρ is the fluid density, V the flow velocity, L the characteristic length, and μ the dynamic viscosity of the fluid. These two laws of similitude cannot be maintained at the same time and thus the scale of the model will depend on what needs to be measured (Lloyd, 1989, p. 293). In both cases, geometric similarity remains the same and is defined by the scale ratio. For instance, for a scale ratio of 1:2 or λ=2, model scale distances will be half the

full-scale distances (λ), areas will be four times smaller (λ^2), and volumes will be eight times smaller (λ^3). Mass will also be eight times smaller. Rotation angles remain the same for both model scale and full scale. The differences between the two similitude laws occur when time and the associated responses such as speeds, accelerations, and forces, need to be scaled. For instance, when Froude scaling is applied, the time and speeds measured in model scale need to be $\sqrt{\lambda}$ smaller than what they would be in full-scale, but accelerations will be the same. In Reynolds scaling, the measured time in model scale will be four times (λ^2) shorter than what it would be in full scale, but speeds will need to be two times ($1/\lambda$) larger, and accelerations eight times larger ($1/\lambda^3$).

As already mentioned, wind tunnel tests were performed by the Wolfson Unit on the sail arrangement of the Oseberg ship and model tests were performed at MARINTEK to obtain the hydrodynamic resistance of the hull. For the latter, a 1:10 model of the ship was used, see Figure 28. The results of both tests, combined with the VPP calculations done by Wolfson Unit, showed that the ship experienced up to 10% loss of transverse stability when sailing at a speed causing a wave profile with the crests at the bow and stern and the trough amidships, which reduced the buoyancy in the midship section (Werenskiold, 2011, p. 876).

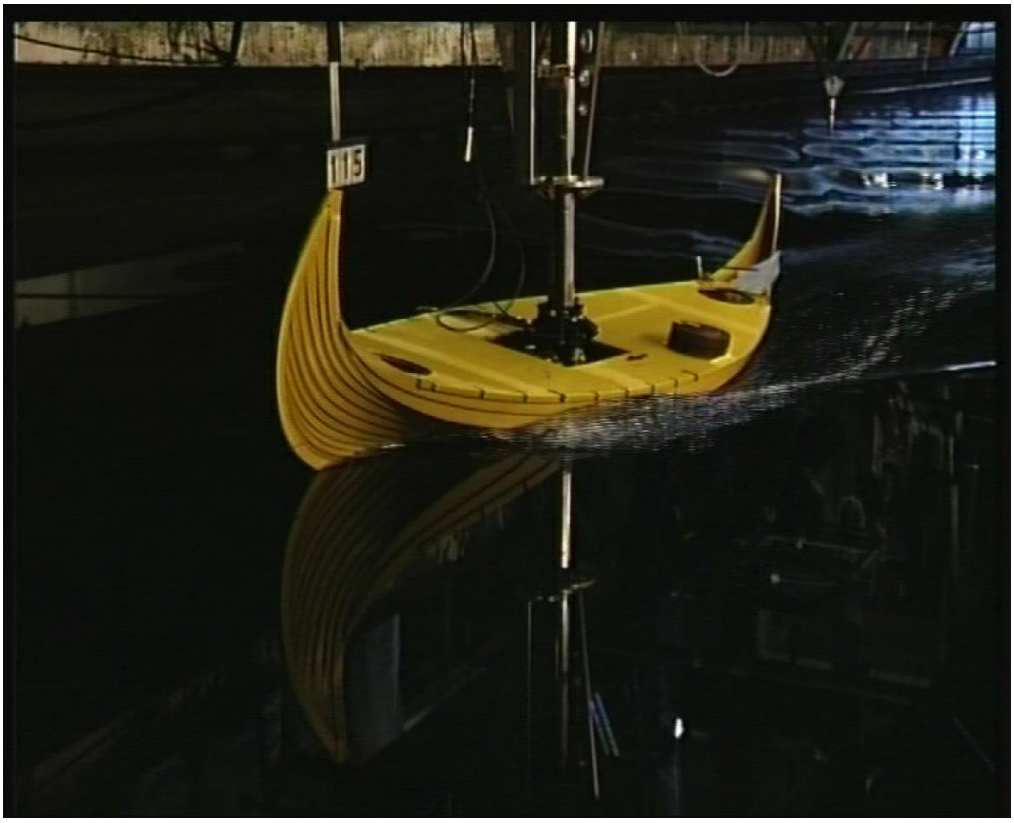

Figure 28 Calm water resistance tests performed by MARINTEK in 2008 on a 1:10 scale model of the Oseberg ship. (Werenskiold, 2011, fig. 8).

MARINTEK also performed tests on the model of the 23.4 m long Gokstad longship, Figure 29, found in the same burial mound as the Gokstad Faering boat and two other small boats. The tests were performed in MARINTEK's Ocean Basin facility, which is a tank facility able to model waves and wind, to assess the safety and sailing performance of the ship prior to the North Atlantic crossing done by Ragnar Thorseth in 1991 and 1992 on the Gokstad replica GAIA (Werenskiold, 2011). The tests showed that the ship was able to survive the 99.5 % percentile summer sea conditions and withstand breaking waves up to 11 m high and wind speeds up to 35 m/s. Additionally, torsion stiffness tests were also done (Werenskiold, 2011, pp. 871,879).

Figure 29 The Gokstad ship in the Viking Ship Museum in Oslo. (Bill, 2013, pp. 76, fig. 1).

Wind tunnel tests were also performed on a scaled model of the Bremen cog in 1991 by a ship engineering student at the University of Hamburg with the aim of assessing the rigging

reconstruction designed by Hoheisel, a naval architect and director of the German Maritime Museum (Tanner, 2018, p. 10; Tanner & Belasus, 2021, pp. 315-316). The results, which did not include the effects of waves, indicated that the ship could tack to windward (Tanner & Belasus, 2021, p. 316). Tank towing tests performed by professor Harro Postel of the Institute for Shipbuilding in Kiel showed however that the ship was unable to tack against the wind and could only sail downwind or at most with winds coming from the side in calm waters, if enough ballast was installed (Hoffmann & Hoffmann, 2009, pp. 287-289).

Tank tests in scientific testing facilities are however expensive and the costs can only be afforded by large commercial shipbuilding projects. They remain thus inaccessible for maritime archaeology research projects where budgets are very limited. As an alternative, Ejstrud, *et al.*, (2012) performed model tests in a lake in a public park nearby the University of Southern Denmark, see Figure 30. Tests were performed on seven ancient boats, including the Gokstad Faering boat, to study their sailing performance in terms of ship motions, water embarkment, and transverse stability. The results showed that the Gokstad Faering would not have been very safe in rough weather but that it had great speed capabilities thanks to its slenderness and light weight (Ejstrud, et al., 2012, pp. 99-100).

Figure 30 Model tests set-up in a lake. (Ejstrud, et al., 2012, pp. 36, fig.17).

While computer work and model scale tests have proven effective in estimating ship stability, cargo capacity, hull strength, and resistance, the assessment of actual sail performance, as well as the actual processes of sail making and tuning, continue to rely heavily on systematic trial and error experimentation on full-scale ships (Werenskiold, 2011; Coates, et al., 1995, p. 298).

III. 6 Experimental archaeology using full scale replicas

The exact dimensions and shape of sails and rigging of Viking ships remains however unknown because no complete archaeological remains have been found and the other sources of information such as iconography and historical records are contradictory (Bischoff, 2017, pp. 1,22). However, some evidence of the rigging arrangement has survived on the Skuldelev 3. This evidence includes the keelson, which indicates the position of the mast, three holes in each side at the foreship that would have been used to secure the tack, and one triangular hole in the aft that would have been used to insert the sheet (Andersen & Andersen, 1989, p. 147; Bischoff, 2017, p. 8). The width of the sail could be estimated because these holes represent the outermost points of fastening and, moreover, because there are two elongated holes through the bitis three frames aft and fore of the mast that have been interpreted as supports for the yard when lowered (Bischoff, 2017, p. 8). The mast height and therefore the sail height, were estimated based on experiments by the Viking Ship Museum in Denmark with the full-size replica of the ship, the Roar Ege, Figure 31. The results of these experiments showed that the ship could sail close-hauled with a 45 m^2 square sail, about 6.5 x 7 m, made of wool (Bischoff, 2017, p. 11), Figure 32. The ship reportedly reached up to 9 knots in a cross wind (Bruun, 1997, p. 1289).

Figure 31 The Roar Ege, full-scale replica of the Skuldelev 3 ship. (Vikingeskibs Museet, 2023).

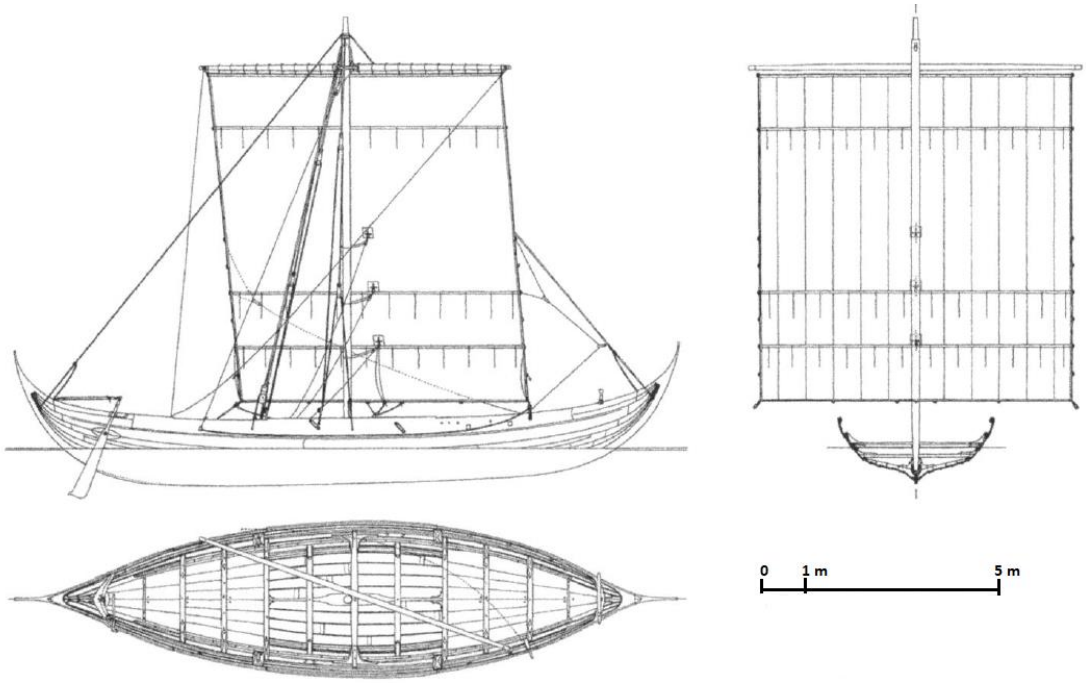

Figure 32 Reconstruction of the sail and rigging of the Skuldelev 3. (Bischoff, 2017, p. 10, Fig. 9).

Full scale replicas have been built by the Viking Ship Museum in Denmark for the five Skuldelev ships, Figure 33, and sailing experiments on them have provided substantial information on the performance of Nordic ships.

Figure 33 The full-scale replicas of the five Skuldelev ships. From front to back: Skuldelev 1, Skuldelev 2, Skuldelev 5, Skuldelev 3, and Skuldelev 6. (Vikingeskibsmuseet, 2023g).

The Saga Siglar, replica of Skuldelev 1 built in 1983, managed to handle rough weather in the North Atlantic and even hurricane-force storms with 35 m/s wind speeds and 12-14 m wave heights between Greenland and Newfoundland (Vinner, 1995, pp. 303-304). The ship managed to reach 14 knots in breaking waves above 15 m height, maintaining an average speed of 8.4 knots over a 4-hour period while the critical task of keeping the ship in alignment with the weather was accomplished using the spare steering oar (Werenskiold, 2011, p. 879). In other conditions, the ship reached 9 knots in wind speeds of 10-15 m/s and up to 10 knots in strong winds in the North Sea (Vinner, 1995, p. 292; Bruun, 1997, p. 1289). The ship unfortunately sank near Alicante, Spain, in 1992 while in a storm with wind speeds of 45 m/s and wave heights of 12 to 14 m (Vinner, 1995, pp. 303-304).

The Sea Stallion from Glendalough, replica of the Skuldelev 2 and the largest Viking longship replica with a length of 30 m, was launched in 2004. During initial trials, the ship was very sensitive to changes in ballast, centre of gravity, and trimming of the sail. Subsequent sailing experiments concluded that the ship would have sailed with ballast weight amidships to minimise its longitudinal inertia and pitching motions, which would have allowed tacking against the wind (Werenskiold, 2011, p. 875). During its voyage from Roskilde to Dublin in 2008, the ship reached speeds of 15 knots (Werenskiold, 2011, p. 875).

Experiments with the Skuldelev replicas have shown that these ships were able to sail against the wind up to 120 degrees from the stern, sailing at average speeds between 1.5 and 2 knots (Bruun, 1997, p. 1289).

Figure 34 The GAIA, replica of the Gokstad ship. (Werenskiold, 2011, fig. 3).

The replica of the Gokstad longship GAIA built in 1990, Figure 34, made Atlantic crossings in 1991 and 1992 reaching speeds of 12 knots with the wind on its side and maximum speeds of 17 knots (Werenskiold, 2011, p. 875).

Full scale replicas of cogs have also been built. In 1991, the Kieler Hansekogge, replica of the Bremen cog, was built, Figure 35. The rigging and sail dimensions were first obtained following the proportions found in the Timbotta manuscript from 1445, which states that the mast height should be 4 times the beam of the ship and the yard 4/5 times the height of the mast (Tanner, 2018, p. 10). This resulted in a mast height of 30.5 m and a yard of 24.6 m. Following the recommendations by the Viking Ship Museum in Denmark based on their experience with squared sails, the sail width was later reduced to 14.6 m, with a total area of 199 m^2 and the mast extending 24 m above deck (Hoffmann & Hoffmann, 2009, pp. 287-289). During the construction of the Kieler Hansekogge, it was determined, based on the weight of stones in the Vejby cog wreck found in Denmark, that a ballast weight of 24 tonnes was necessary for the ship to be stable (Hoffmann & Hoffmann, 2009, pp. 287-289). According to Hoheisel (Hoheisel, 1994, p. 259), the Kieler Hansekogge could sail at an angle with the wind of 70 degrees from the bow but with considerable drift angles of about 15 to 20 degrees. That means that the ship would hardly make any advance as the resultant course to windward would then be of 90 degrees or more (Tanner & Belasus, 2021, p. 318).

Figure 35 The Kieler Hansekogge, a replica of the Bremen cog. (Stein, 2023, photo: Ulrike Löptien).

Hoffmann & Hoffmann (2009, pp. 289-290) state that during the sea trials performed in summer 1992, with maximum wind speeds of 15 m/s, the Kieler Hansekogge was easily manoeuvred by a single individual in most conditions, but two helmsmen were required with higher wind speeds. The helmsman had to remain however vigilant as the ship would turn quickly. Hoffmann & Hoffmann (2009, pp. 289-290) also mention that the average speed of the ship, across various courses and wind conditions, was 5 knots and that the ship performed best when the wind was directly from behind or coming from the stern quarter. At wind speeds between 8 and 15 m/s, it was necessary to reef the sail or remove bonnets and the ship experienced excessive leeway, making it impossible to sail close to the wind, especially in the fully loaded condition (Brandt, Hoheisel, & Hochkirch, 1994, p. 65). During the sea trials, heavy pitching and rolling were experienced, with heel angles of about 15 degrees (Weski, 1999, p. 374; Hoffmann & Hoffmann, 2009, pp. 289-290).

As the Kieler Hansekogge was being built in Kiel, a second replica of the Bremen cog, the Ubena von Bremen, Figure 36, was built in Bremerhaven. The sail of the Ubena was made 4 m wider than the one of the Kieler Hansekogge in order to follow the Timbotta manuscript more closely (Tanner, 2018, p. 10).

Figure 36 The Ubena von Bremen, a replica of the Bremen cog. (Bremerhaven, 2023, photo: Juregen Teute).

The experiences by its captain are summarised by Tanner (2018, p. 45). According to the captain, the ship was able to take wind speeds up to 20 m/s under full sail but not directly from the aft as the ship would lose stability at the wave crests. The captain also reported that although being a dry ship, the Ubena rolled heavily causing seasickness for everyone on board. In wind speeds up to 6 m/s the ship would merely drift while speeds of 5 knots could be achieved in winds blowing from 100 degrees from the stern with speeds between 8 and 14 m/s. The leeway was however too large for the ship to make any headway. The ship was unable to sail against the wind, and while it could stay off the coast with an onshore wind, it could not sail away from the coast. Moreover, the large windage area from the ship's superstructure caused the ship to drift with speeds between 3 and 4 knots without sails.

A third replica of the Bremen cog, the Roland von Bremen, was built in 2000 with thicker hull planking and mast, and smaller rig and sail, which had an area of only 90 m^2. The ship sank in 2014 due to a faulty valve (Historischer Hafen Flensburg gGmbH, 2018). According to Hoffmann & Hoffmann (2009, p. 293), the ship was never really subjected to proper sailing sea trials and therefore there is hardly any information on its sailing performance.

Figure 37 Three replicas of cogs: the Kamper Kogge (top left), the Poeler Kogge (right), and the Pommernkogge Ucra (bottom left). (Feenstra, 2023; Förderverein "Poeler Kogge" e.V., 2023; Pommernkogge Ucra, 2023).

Besides the replicas of the Bremen cog, other cog replicas have been built: the Kamper Kogge, the Poeler Kogge, and the Pommernkogge Ucra, see Figure 37. The Kamper Kogge is reported to be able to sail against the wind up to an angle of 70 degrees, have an average speed of 5 knots and reach speeds roughly equal to the wind speed (Kamper Kogge, 2023). Stability calculations show that the ship requires 90 tons of ballast to be stable (Tempelman, 2003, p. 5).

Building full-scale replicas can provide valuable information about the building techniques and the sailing performance of ancient ships since real-life conditions and even the human element on the handling of the vessels are accounted for. However, the usefulness of full-scale replicas to evaluate performance in archaeology remains debatable. Coates, *et al.* (1995, p. 298) admit that there is "a belief by some […] that reconstructions are at worst a waste of time and money and at best a poor use of archaeological resources". Three main reasons could explain this.

First, building a replica is expensive and might not be the most cost-effective approach to test a relevant archaeological hypothesis, especially with the possibility of performing calculations and model tests. We cannot forget that archaeological remains are affected by distortion and fragmentation. In fact, for all the remains of Nordic ships and cogs discovered so far, the sail arrangement is missing and in most cases the superstructure and parts of the hull as well. Therefore, any ship reconstruction in archaeology is subject to assumptions and interpretations and no reconstruction can be considered as the truth. Computations and model tests are much more cost effective in evaluating different reconstruction alternatives.

Second, rigorous and measurable sea trial tests are very time consuming and extremely difficult as not only the ship responses but also the weather conditions need to be accurately measured. Most of the attempts that have been made have only been able to provide a general feeling of the performance of ships rather than actual empirical data (Coates, et al., 1995, p. 298). This makes the comparison between different ships an extremely difficult task.

Third, full-scale replicas usually include modern additions to fulfil modern safety standards and to increase comfort on board when the replicas are used for touristic purposes, as it is the case for all cog replicas. All cog replicas are equipped with engines and propeller arrangements with the related fuel tanks, as well as other modern elements such as electrical wiring, safety and navigation equipment, heating, and showers, watertight decks etc, making them not a trustworthy source of information with regards to the weight, capabilities nor the performance of real cogs (Tanner, 2018, pp. 10-12; Tanner & Belasus, 2021, p. 318). Nordic ship replicas are often also equipped with modern safety equipment, including engines and propellers. For instance, the Saga Siglar, replica of the Skuldelev 1, was fitted with a 22 HP diesel engine and a two-blade propeller which most likely affected the performance of the ship under sail (Vinner, 1995, p. 290).

Nonetheless, full-scale replicas have been proven to be very effective in generating social and educational interest in archaeology, which is crucial for attracting the necessary funding and support for archaeological research (Coates, et al., 1995, pp. 299-300).

Each of the six approaches to evaluate the performance of ships presented in this chapter has its own advantages and limitations. For the scope of the current thesis, which aims at comparing the performance of Nordic cargo vessels and cogs, computer calculations are performed on the 3D model reconstructions of a Nordic cargo ship and a cog of similar size. Following the definition by McGrail (1988, p. 35), the evaluation of the performance is done by assessing their cargo capacity, speed potential and stability. Additionally, their motion behaviour in the Baltic and North Sea will be calculated and compared as an evaluation of their seaworthiness.
As mentioned in the introduction, the two ships that are evaluated are the Big Ship of Wismar and the Bremen cog. These two case studies and the data that is used in the current thesis are described in the next chapter.

IV. Case studies and data

This chapter introduces the two ships used as case study for the performance calculations. It discusses the previous research conducted on the Big Ship of Wismar and the Bremen cog, and presents the data used for the calculations, including the 3D models.

IV.1 The Big Ship of Wismar

IV.1.1 Previous work

During excavations for the expansion of the harbour of Wismar in 2016, two 13th century medieval ships were found and, later in 2017, a third 12th century ship was found. This third ship, excavated end of 2017 and fully recorded in 2018, was named the Big Ship of Wismar and possesses typical characteristics of the Nordic shipbuilding tradition, such as riveted outer planking, animal hair as caulking material and the biti system (Ditta & Auer, in press). Dendrochronological analyses show that it was built from oak and pine from western Sweden around 1184-1190 and it was probably used for a short time before it sank in the early 13th century, as indicated by the good state of the planking, the lack of evidence of repairs, and the artefacts found in the sediment above the wreck (Ditta & Auer, 2021, pp. 193,195). The wreck was recorded using 3D photogrammetry, see Figure 38.

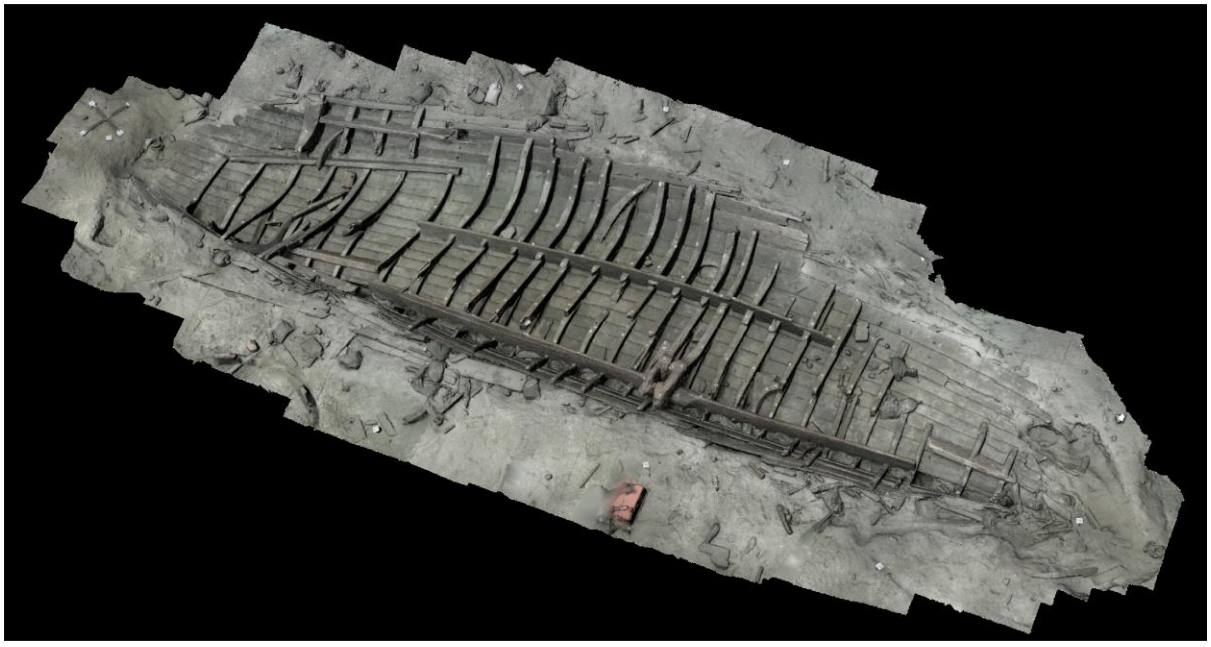

Figure 38 Photogrammetry 3D model of the wreck of the Big Ship of Wismar. (Ditta & Auer, in press).

During excavation, the timbers were removed in six phases following the reverse sequence of the ship's construction. These stages were also documented using 3D photogrammetry and each recovered timber was subsequently recorded using 3D laser scanners (Ditta & Auer, 2021, pp. 193-194). The 3D models of each timber were then annotated, used to create a complete 2D timber catalogue, and 3D printed at a scale of 1:20. The 3D printed timbers were then assembled with metal wires and screws and used to create a working model to be used as basis for the hull reconstruction (Ditta & Auer, in press; Van Damme, Auer, Ditta, Grabowski, & Couwenberg, 2020, pp. 13-14). Because of the absence of certain parts such as the keel, stem posts, and the whole starboard side, the 3D printed model had a significant longitudinal twist, which was greatly corrected, but not entirely suppressed, by mounting it on a frame. Thus, this model, Figure 39, does not represent the original vessel shape at the time of sinking nor its post-deposition shape, but an adjusted shape which still possesses some deformations due to its incompleteness and the deposition effects (Ditta & Auer, in press).

Figure 39 Assembled working model of the individually 3D printed timbers. Once assembled the 3D printed model was 3D scanned and is shown here on top of the photogrammetry model of the wreck. (Van Damme, Auer, Ditta, Grabowski, & Couwenberg, 2020, p. 14, Fig. 11).

The state of preservation of the wreck is described in Ditta and Auer (2021, pp. 194-196). A summary is given here as it will be important for the model reconstruction. The main mentioned elements are highlighted in Figure 40. The wreck was tilted at a 20 to 25 degree angle to the port side and had 17 preserved strakes of outer planking on that side while only four strakes were preserved on the starboard side. The keel and stemposts were missing, but 28 frame stations and associated timbers were preserved inside the wreck. The keel and posts were most likely deliberately removed when the ship was abandoned, as evinced by the surviving garboard strakes and the well-preserved aft

scarf on the aftmost outer planks. Most of the lapstrake outer planking was made of straight-grown oak trees, but some pine planks were used from the thirteenth strake upwards. Especially remarkable are the pine wales (large carved outer planks) in the fourteenth and fifteenth strakes which were probably installed for protection and to reinforce the ship longitudinally. The ship's oak planks ranged from 2.4 to 6.8 meters in length with a width of 30 cm on average in the midship area. The pine planks were longer and thicker than the oak ones. The planks in each strake were joined with short vertical scarf joints and sealed with sheep wool and tar. The strakes were riveted with round-shafted and round-headed iron nails and rectangular rove plates on the inside. They were sealed with hair from different animals and wood tar. An indication of the position of the waterline is given by the scarf joints. The openings of the scarf joints on the lower part of the vessel were facing aft as to prevent water ingress, while they were facing forward from strake 14 upwards.
The ship frames were spaced uniformly with an average distance of 51 cm. However, the spacing at the bow and stern was larger with an average distance of 86-87 cm. The open hold's length was defined by this frame spacing change. The floor timbers followed the shape of the hull and were made from oak crotches with rectangular section arms measuring 9 to 11 cm in moulded dimension. Contrarily, the bitis were made of straight-grown pine, while the biti knees were also made of oak. The bitis had rectangular sections ranging from 13.5 cm to 18 cm and were notched and fitted over the oak keelson along the centreline of the vessel. The bitis at the mast location were cut out to accommodate the mast and acted as an extension of the mast step. The frames and other internal timbers were fastened to the hull’s planks with 30 mm diameter pine treenails.
The hull had four types of stringers, which are the longitudinal strengthening internal timbers of a ship. The lowest stringers were short pine blocks, positioned on both sides of the vessel fore and aft of the keelson, serving as a continuation of the keelson but providing access to the top of the keel. Partially preserved on the port side on the eighth strake was an oak stringer running along the entire length of the keelson. Likewise on the sixteenth strake, above the height of the aft deck, there was an oak stringer probably running along the whole ship as well. Finally, a fourth oak stringer or inwale run was located on the inner upper edge of the last strake of the vessel.
Aft on the port side, the structure for a half-deck was provided by a beam shelf made of pine and several oak knees. The preserved structure also suggests that there was another deck at a higher position, probably the spot of the helmsman. Above that deck structure, a large wood knee acted as a support for the windlass. This structure has parallels on the Big Ship of Bergen and the Elling A ship. Also in the aft, a rectangular opening measuring 22 by 22 cm located in the sixteenth strake and a recess on the underside of the third stringer indicate the likely position of a protruding beam. Parallels of protruding beams are found in the Big Ship of Bergen and the Kalmar I wreck. Another

opening measuring 10 by 16 cm was probably the location of the bilge pump as indicated by its position above the aft deck and behind the end of the keelson. The Kalmar V wreck possesses a similar system.

Overall, the construction details of the Big Ship of Wismar show strong similarities with the Big Ship of Bergen and the Lynaes 1.

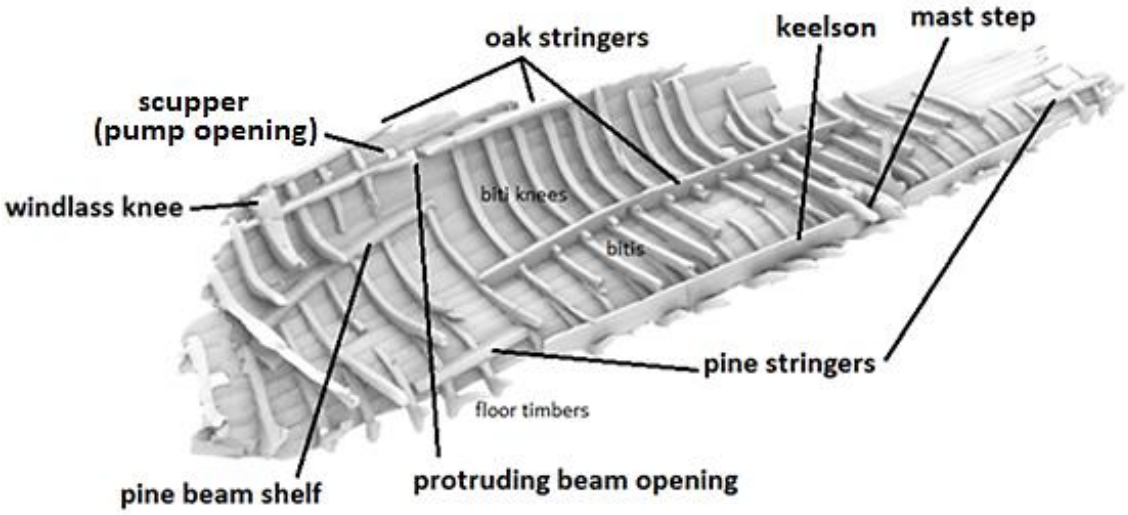

Figure 40 3D scanned model of the preserved timbers. (Figure by Hernandez Montfort after model by Ditta & Auer, in press).

The adjusted 3D model of preserved timbers shown in Figure 40 was used as basis for the hull reconstruction by Ditta and Auer (in press), which was done in Rhinoceros. The methodology followed by Ditta and Auer is here summarized. First, a watertight envelope representing the shape of the hull was made by creating a conventional lines plan of the outer hull and correcting the global distortions of the model. To this purpose, a series of arbitrary stations were created to avoid local distortions and then points were extracted for each edge of the outer strakes. Afterwards, the outer strakes were interpolated through these points and extended to the reconstructed stemposts, see Figure 41. The keel was reconstructed based on the curvature of the keelson, the foot of the floor timbers and the preserved keel of the Lynaes 1 while the stemposts were reconstructed symmetrically based on the shape of the stern post, which curvature is indicated by the end scarfs of the stern planking and the preserved timbers between the posts and the hull planking. The overall length was obtained by considering symmetry of the internal structural elements, which is suggested by the regular frame spacing, the symmetrical stringers and breaks aft and fore of the keelson.

The reconstructed hull, Figure 42, gives an overall length of 23.3 m, a maximum beam of 7.6 m and a depth amidships of 2.7 m for the Big Ship of Wismar (Ditta & Auer, in press).

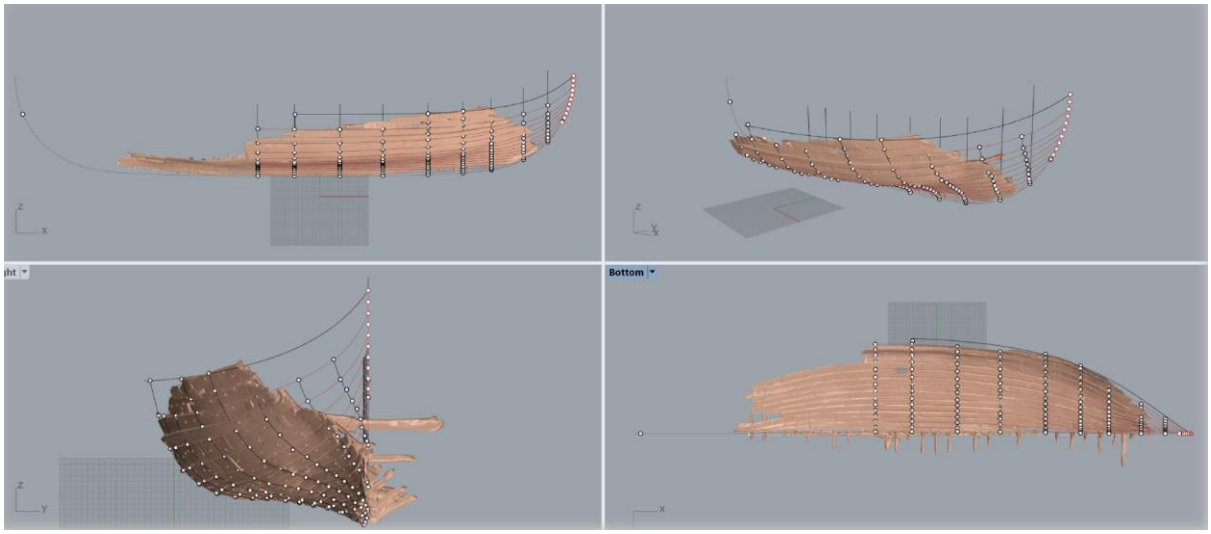

Figure 41 Hull reconstruction method on the Big Ship of Wismar. (Ditta & Auer, in press).

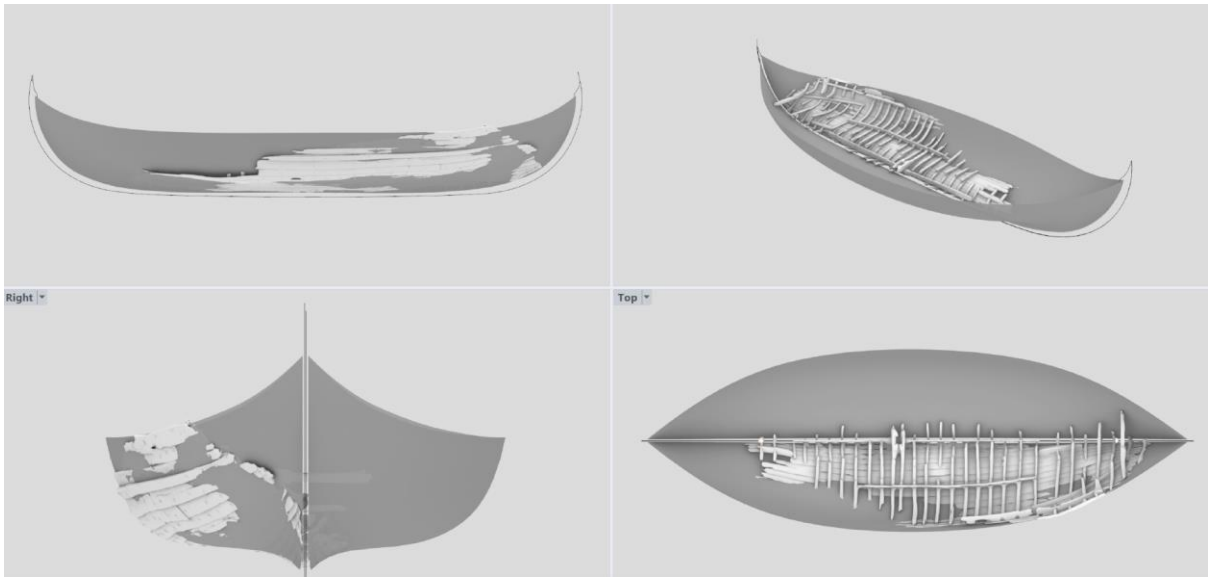

Figure 42 Reconstructed hull of the Big Ship of Wismar. (Ditta & Auer, in press).

Besides the reconstruction of the hull, Ditta and Auer (in press) also created a visual reconstruction of the ship with the aim of giving "an impression of the ship structures and arrangement resulting from the minimum hull shape reconstruction, the interpretation of the archaeological remains, and comparative sites", see Figure 43. To this purpose, elements not preserved were reconstructed based on archaeological parallels and on the preserved archaeological evidence. As already mentioned, the presence of aft decks is suggested by the preserved substructure, and it was assumed by Ditta and Auer that the same arrangement would have been found at the bow. The preserved windlass knee was also mirrored, and a windlass beam created between the two knees. The protruding beam at the aft was created based on the side opening previously mentioned. Two

other protruding beams were created based on the presence of notches in the upper stringer and on the iconography found in the 13th century seal of Winchelsea, Figure 44.

The bilge pump was created based on the evidence found on the 16th century Kalmar V ship. Finally, a side rudder was added based on the curvature of the stern, deemed unsuitable for a stern rudder, and longitudinal beams running between the protruding through beams were added based on the evidence from the Kalmar I wreck.

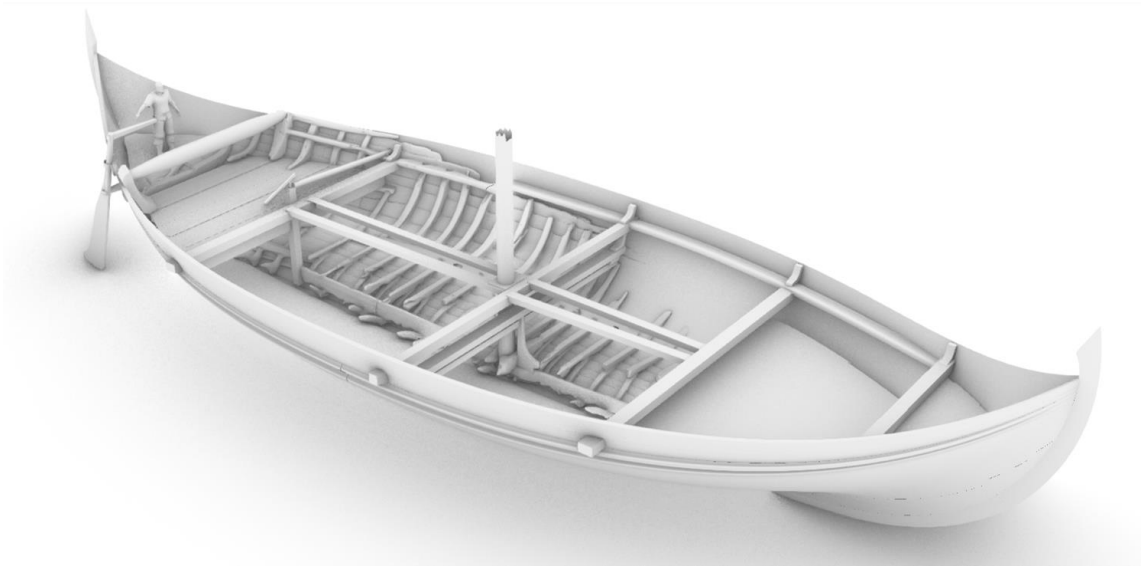

Figure 43 Visual reconstruction of the Big Ship of Wismar. Both the scanned model of the preserved timbers and the visualization model are shown here. (Figure by Hernandez Montfort, model by Ditta & Auer, in press).

Figure 44 City seal of Winchelsea showing a Nordic ship with three protruding beams. (Ditta & Auer, in press).

Finally, Ditta and Auer (in press) obtained basic volumetric values in Rhinoceros from the outer hull reconstruction shown in Figure 42. Using the freeboard law in the Icelandic Grågås codex, mentioned in the introduction, they obtained a ship displacement of 89.5 tons at a draft of 1.61 m.

They looked then at other basic geometric coefficients. They concluded that the length-to-beam ratio of 1:3 indicates the cargo-carrying nature of the vessel. They also suggested that hollow waterlines at the bow and the block coefficient of 0.4 indicate good speed potential while the prismatic coefficient of 0.6 indicates higher resistance. These two conclusions are however contradictory as higher resistance necessarily means lower speed. Using these coefficients in isolation is not a reliable way to gauge a ship's performance, and even if useful when comparing different hulls, they still provide only a very rough estimate of ship's performance. Ditta and Auer (in press) acknowledge however these limitations and express therefore their desire for stability and seakeeping analysis to be conducted on the Big Ship of Wismar.

IV.1.2 Data used in this thesis

The data used in this thesis was provided by Jens Auer (Landesamt für Kultur und Denkmalpflege Mecklenburg-Vorpommern) and consists of a Rhinoceros file with the reconstructed hull's envelope, Figure 42, the 3D model of the scanned adjusted model of the preserved timbers and the reconstructed visualization model made by Ditta & Auer (in press), Figure 43. Additionally, the full individual timber catalogue (Auer & Ditta, 2019) was provided, which includes all the 3D scanned models, 2D images, drawings, and descriptions for each individual timber.
Because the reconstructed ship model was created solely for the purpose of visualization, it was not immediately suitable for conducting calculations. For instance, the hull, keel, stems, and decks were modelled as surfaces instead of solids, hence unsuitable for calculating volumes and weights. Moreover, since the visualization model relied on being shown together with the 3D scanned mesh of the preserved timbers, the internal structural elements were not modelled or were only partially modelled such as the upper longitudinal stringer, see Figure 45.

The 3D mesh of the preserved timbers was likewise not suitable for calculations as it is modelled as a single mesh, thus it is impossible to separate the different elements to assign different materials and densities. Moreover, it still possessed deformations as previously mentioned and a great part of the elements were only partially preserved and needed thus to be fully modelled anyways.

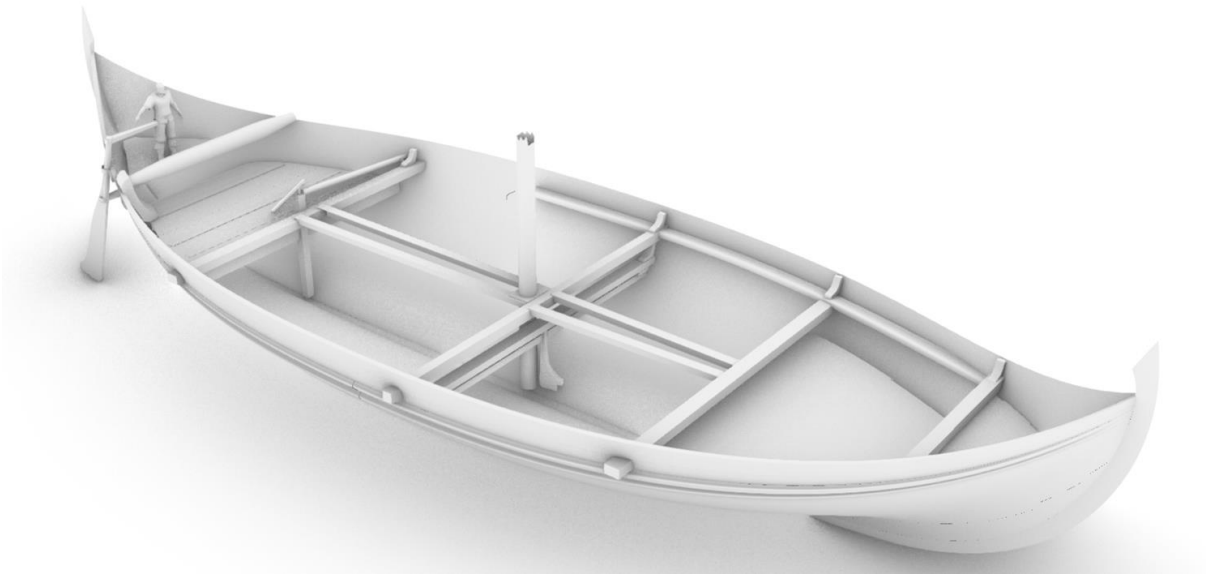

Figure 45 Visualization model of the Big Ship of Wismar without the mesh of preserved timbers. Notice the incomplete elements like the upper stringer or the mast and the lack of internal structural elements. (Figure by Hernandez Montfort, model by Ditta & Auer, in press).

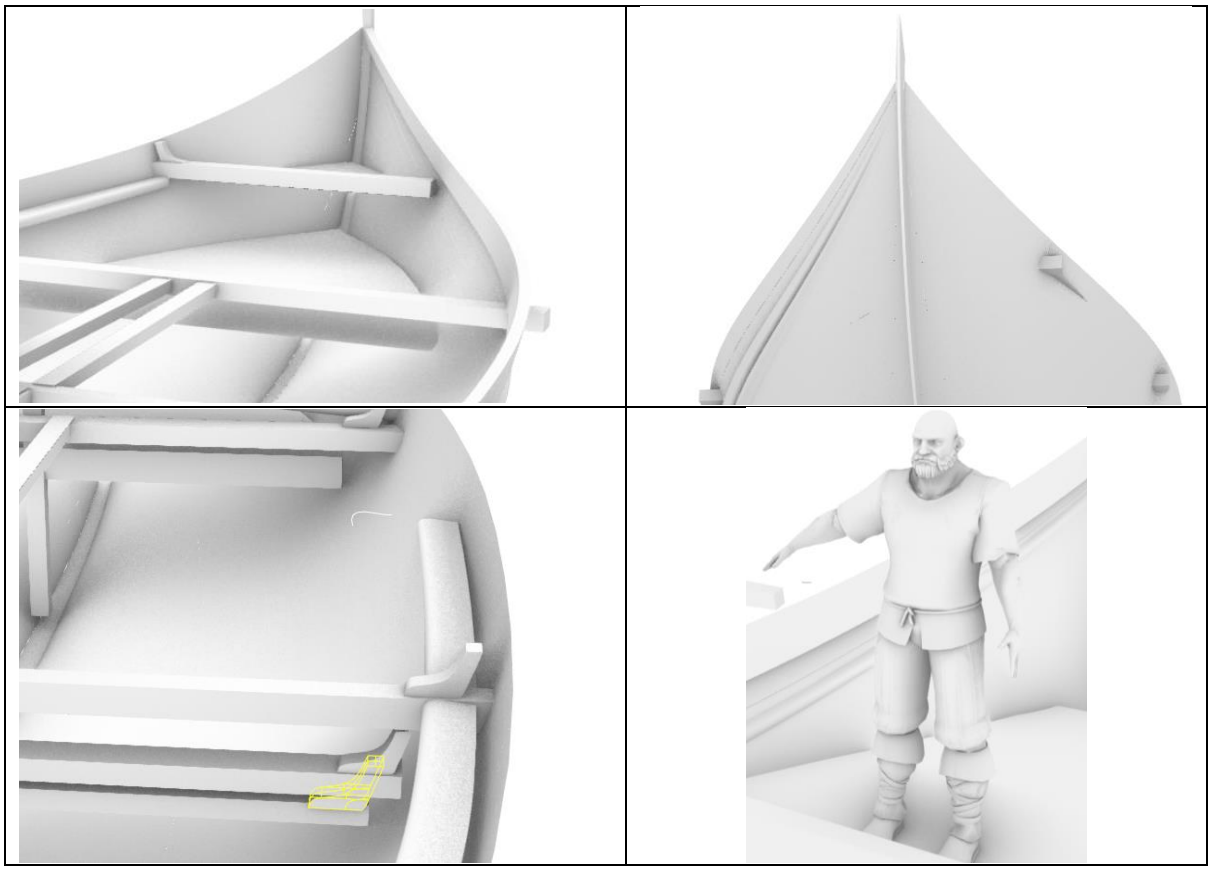

Figure 46 Detail views of the 3D visualization model. Upper left: View of the “hidden” side of the model where there is no support structure for the beams and deck. Also notice the exaggerated thickness of the last strake on the starboard side. Upper right: Notice the wales only on one side. The foremost beam protrudes on one side but not the other. All protruding beams are crossing the hull, but no openings are modelled on the hull. Bottom left: The oak knee highlighted in yellow intersects the upper beam and knee. Bottom right: The highly detailed model of the sailor. (Figure by Hernandez Montfort, model by Ditta & Auer, in press).

Some elements on the visualization model were only present on one side, the visible side, as the elements on the other side remained hidden and thus not relevant for the purpose of the model. For instance, the pine wales and several oak knees. The uppermost strake on the starboard side was given a thickness of 10.4 cm while the archaeological evidence shows an average thickness of 3 cm amidships, as mentioned earlier. Details like this or the fact that some elements defined as volumes were not completely closed or were intersecting with each other, are not relevant for visualization purposes but they are important when volumes and weights need to be calculated. In contrast, other elements had a very high level of detail, such as the model of the sailor, which is very valuable for visualization purposes but unnecessary for weight and volume calculations. Figure 46 shows a few detail views of the model.

Thus, one important task of the present thesis was to create a detailed 3D model of the vessel suitable for computing the weight and inertia of the vessel required for the stability and seakeeping calculations. A description on the methodology on how the different data was utilized for each of the tasks is presented in chapter V.

IV.2 The Bremen cog

IV.2.1 Previous work

The wreck was found in 1961 during dredging operations in the river of Weser in the harbour of Bremen. The ship sank shortly before it was completed and has been dendrochronologically dated to 1380 (Weski, 1999, p. 360). After a long conservation process, the Bremen cog was finally unveiled at the Deutsches Schiffahrtsmuseum in Bremerhaven in 2000, Figure 47 (Crumlin-Pedersen, 2000, p. 230).

Figure 47 The Bremen cog at the Deutsches Schiffahrtsmuseum in Bremerhaven. (Deutsches Schiffahrtsmuseum, 2023. Copyright: Annica Müllenberg).

As previously mentioned, the Bremen cog was used to define a shipbuilding tradition and as a blueprint for what the ships referred as cog in historical sources might have looked like. Since its discovery, a lot of research has been done. With regards to its performance and capabilities, previously conducted research includes the reconstruction of its hypothetical rigging arrangement and assessment of its related sailing performance with wind tunnel tests, weight and stability calculations, and scaled model tests in towing tank facilities (Tanner & Belasus, 2021, p. 316). Both weight and stability calculations from 3D models and model tests showed that the ship required ballast to be stable. There were however significant discrepancies between the different studies on the actual displacement, cargo capacity and required ballast, see Table 3.

Table 3
Weight and displacement values of different published versions of the Bremen cog. The versions in italic represent values from full scale replicas of the ship. (Taken from Tanner & Belasus, 2021, p. 316, Table 1).

Version by	Empty weight [ton]	Ballast [ton]	Cargo [ton]	Displacement [ton]	Draught [m]
Lahn, 1992	60	-	76-84	136-144	2.25
Hoheisel, 1994	55	26	-	81	1.53
Hoheisel, 1994	55	-	87	142	2.25
Jensen, 1999	-	-	-	139	2.25
Ubena von Bremen, 1991	40	35	-	75	2.25
Kieler Hansekogge, 1991	38	22	-	60	1.6
Roland von Bremen, 2000	100	20	-	120	2.25

Differences are also substantial between the full-scale replicas of the vessel despite that they should in principle all have the same hull shape. However, different mast heights and sail areas were used between them and for the Roland von Bremen a much thicker hull planking was used. Additionally, they are all equipped with different modern elements such as engines, propellers, fuel tanks, electrical wiring, safety and navigation equipment, heating, and showers, watertight decks etc. Hence the weight of the replicas cannot be considered to represent the real weight of the Bremen cog (Tanner, 2018, pp. 10-12; Tanner & Belasus, 2021, p. 318).

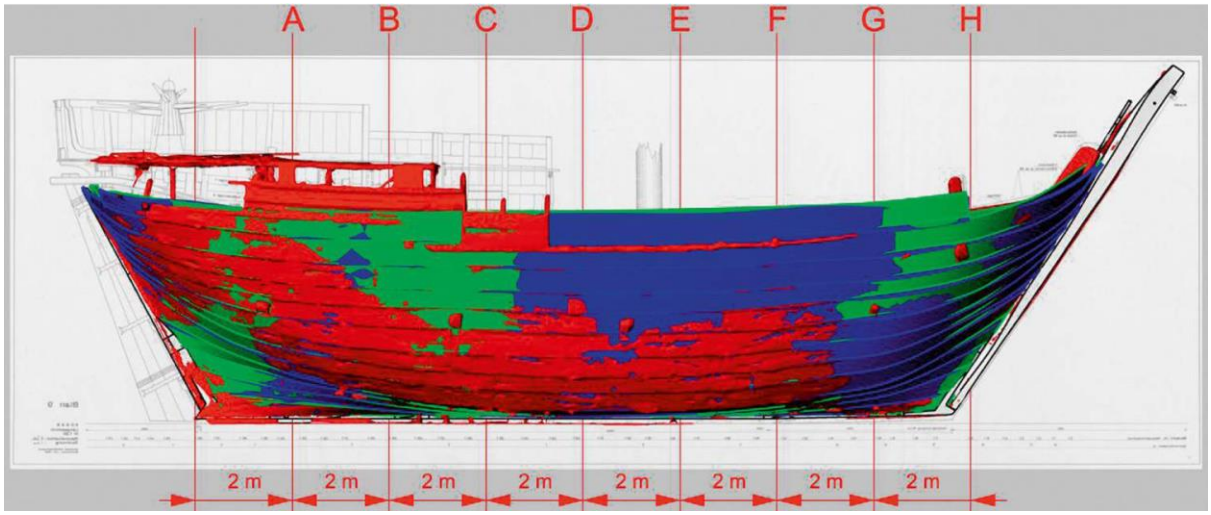

Figure 48 Geometry comparison of the hull shape between different datasets. Blue indicates the hull shape as created from Lahn's section drawings. Green indicates the geometry as generated from Lahn's lines plan drawings. Red indicates the geometry of the hull obtained by laser scanning by Pat Tanner in 2014. (Tanner & Belasus, 2021, p. 316, Fig. 1).

Tanner and Belasus (2021, p. 316) argue that variations in the reconstruction solutions are the cause of inconsistencies between the different hull versions. In fact, it remains difficult to know with absolute certainty which elements of the assembled ship are original timbers and which parts were just hypothetical reconstructed pieces incorporated to correct issues that arose during reassembly (Tanner, 2018, p. 3). Moreover, the hull shape as displayed in the museum is not an accurate representation of the real hull shape due to different distortion events (Tanner & Belasus, 2021, pp. 316-317). Hence the discrepancies when comparing 3D models of the hull shape produced by using different source materials or approaches, see Figure 48.

With the aim to reconcile the different hull versions with the archaeological evidence and have a valid hypothetical ship reconstruction that could be used for stability and hydrodynamic calculations, a complete revised digital reconstruction of the Bremen cog was done by Tanner. The process is documented in Tanner (2016) and Tanner & Belasus (2021). First, a series of fair curves to represent each strake were created and their curvature adjusted using Lahn's drawings and 3D scan data of the hull. Then digital 3D models of each surviving and missing elements were made, see Figure 49 and Figure 50. The new reconstruction resulted in a less full-bodied hull shape than Lahn's reconstruction, especially in the lower ends (Tanner & Belasus, 2021, pp. 317-318).

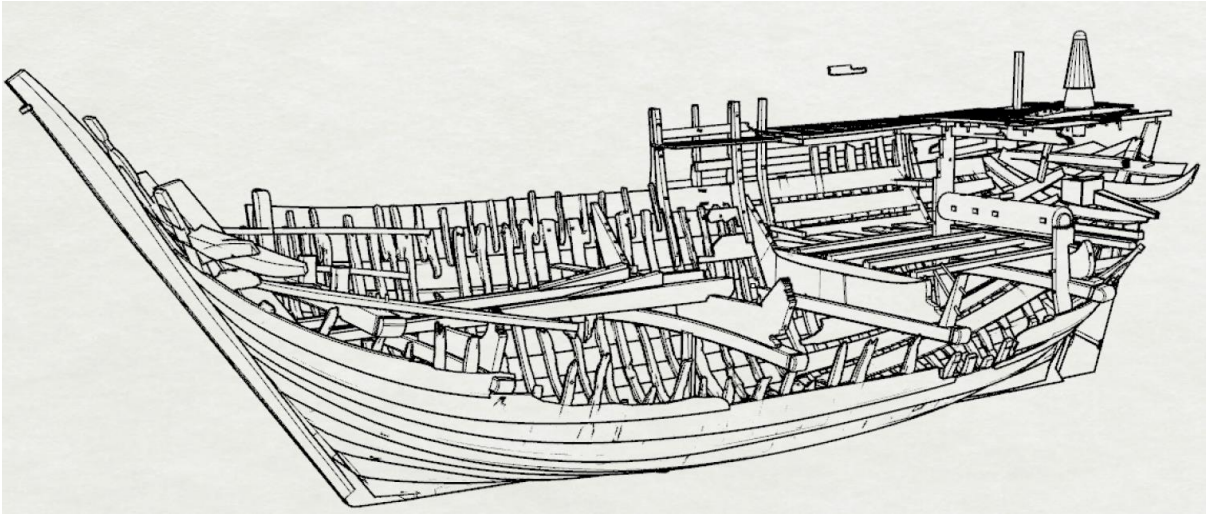

Figure 49 3D model of the preserved timbers of the Bremen cog. (Tanner, 2018, p. 3, Fig. 1).

Once the model was complete, different densities were applied to each element to compute the weight of the vessel. The total weight of the surviving timbers resulted in 25 tons when applying a density of 800 kg/m^3, which corresponds to the average density of oak with a 27% moisture content (Tanner & Belasus, 2021, p. 318). Treenails were not modelled as they possess the same density of the other wooden parts. Iron nails were not individually modelled but their weight was estimated at

700 kg by assuming a total of 3900 nails, based on an average nail spacing and an average weight of 0.18 kg per nail (Tanner, 2018, p. 9).

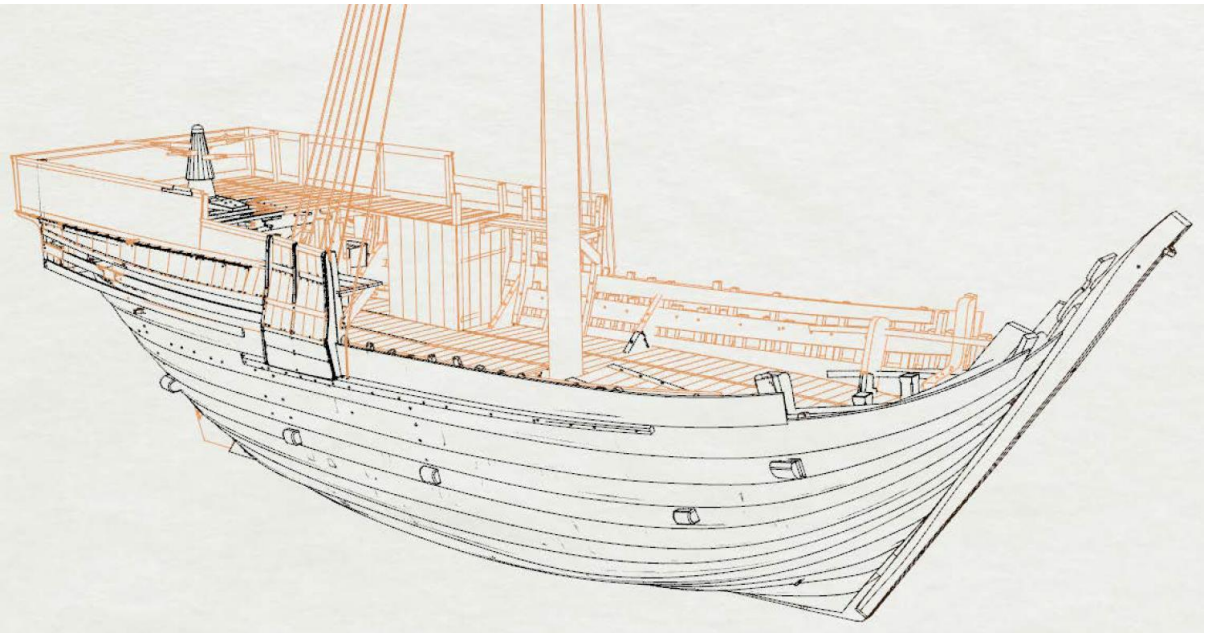

Figure 50 3D model of the reconstructed Bremen cog. Black lines indicate original recovered timber, orange lines indicate reconstructed extrapolated parts. (Tanner, 2018, p. 4, Fig. 2).

The total weight of the empty bare hull with superstructure but without mast nor rigging resulted in 43 tons. With the complete model, including weights, hydrostatic and stability calculations were performed with the ORCA 3D plug-in in Rhinoceros (www.orca3d.com). The stability calculations revealed that the ship had minimal reserve stability in an empty bare hull condition and would experience significant heeling due to wind or the addition of weight at the edge of its deck. Adding slightly more than 2 tons of weight at the deck edge would cause the ship to capsize. Tanner suggests that this limited reserve stability might be related to the ship sinking shortly before its completion (Tanner, 2018, p. 9).

The mast, sail area and rigging were reconstructed based on previous rigging and wind-tunnel tests research, the three replica ships and Tanner's own sailing experience. As a result, a 23.5 m high mast with a yard of 18 m, both made of spruce, and a sail area of 199 m^2 were chosen (Tanner, 2018, p. 12). The total weight of the rigging was modelled as 3861 kg with the centre of gravity at 10.46 m ahead and 10.48 m above the aft lower edge of the keel. Additionally, two anchors of 265 kg were added at the bow of the vessel, modelled in ORCA 3D as mass points. The weight of the complete empty ship resulted then in 47 tons (Tanner, 2018, p. 13). The results showed that the empty ship condition had a negative metacentric height (GM) of -0.292 m and overall negative stability and

would thus have capsized at any slight heeling moment (Tanner, 2018, p. 15). This confirms previous research indicating that the ship required ballast.

To determine the minimum ballast needed for the ship, Tanner (2018) performed stability calculations based on modern standard criteria set by the classification society Bureau Veritas (2022) and summarized in Table 4 and Table 5. For the weather criteria, different wind speeds were considered (5, 10, 15, and 20 knots) to compute the heeling moments and arms. This was done in ORCA 3D using the area of the sail (assuming the sail completely parallel to the ship's length), the lever arm, the wind speed, and a $\cos(\phi)^2$ distribution for the shape of the heeling arm, Figure 51. The angle of heel due to rolling waves was computed based on the formulation found in section 3.2.4 in Bureau Veritas' (2022) rules.

Table 4
Intact stability criteria. (After Bureau Veritas, 2022, pp. 78-79).

GM at free equilibrium >= 0.15
GZ at 30 degrees heel >= 0,2 m
Angle of GZmax >= 25 degrees
Area between 0 and 30 deg >= 3,151 mdeg
Area between 30 and 40 >= 1,1719 mdeg
Area between 0 and 40 >= 5,157 mdeg
Area between 0 and flooding angle >= 5,157 mdeg
Area between 30 and flooding angle >= 1,1719 mdeg

Table 5
Extra weather criteria. (After Bureau Veritas, 2022, pp. 80-82).

Angle at equilibrium <= 16 deg
Angle at equilibrium <= deck immersion * 0,8 deg
Angle at equilibrium < flooding angle
Area b >= area a
Angle at equilibrium + angle due to waves < flooding angle
Freeboard at equilibrium > 0,5 m

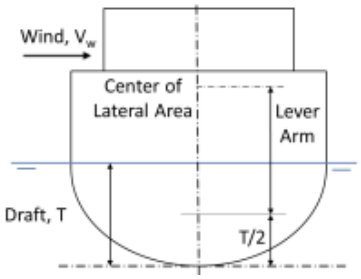

Figure 51 Definition of parameters to compute wind heeling arm. (Orca3D, 2021, p. 339, Fig. 14).

The amount of ballast required for the ship to be stable was 15 tons. At this condition, the ship fulfilled all stability criteria, including the effects of wind and rolling waves except for the wind speeds of 20 knots. In that speed the rolling wave criteria and maximum wind heel angle failed. However, it is assumed that in such high wind speeds the sail would have been reefed and then it did pass all criteria up to 20 knots wind speed. Moreover, one should note that the calculations were made for the worst case scenario in which the sail is completely perpendicular to the beam wind and that in reality sail sheets would be eased as wind increases to reduce the heel angle (Tanner, 2018, pp. 19-20).

The same stability criteria were applied to other loading conditions, including the fully loaded ship with a draft as defined in the Icelandic Grågås codex, an intermediate condition defined by a draft just below the protruding beams, and the bare hull with superstructure but no rigging nor mast. The obtained displacement, cargo capacity, and metacentric height for each of the conditions are summarized in Table 6.

Table 6
Loading conditions characteristics. (After data in Tanner & Belasus, 2021, p. 320, Table 4).

Condition	Weight [t]	Cargo [t]	Displacement [t]	Draft aft [m]	Freeboard [m]	Flooding angle [deg]	GM [m]
Unrigged	43	0	43	1.3	3.3	49.5	0.39
Unballasted rigged	47	0	47	unstable			-0.29
Ballasted empty	62	0	62	1.5	3.0	44.7	0.37
Beams not submerged	62	45	107	2.0	2.7	35.3	0.82
Grågås	62	108	170	2.8	1.7	24.1	1.10

Note. The GM values of the last two conditions are strongly dependent on the centre of gravity of the cargo in the hold. The GM for the Grågås condition appears as 1.30 m in Tanner, 2018, p. 27.

The ship in ballast empty condition and the ship in a condition with the beams not submerged fulfil all stability criteria. The ship at the Grågås draft condition fails to fulfil the criteria on sufficient area between 30 and the flooding angle since the latter is just 24.1 degrees. However, Tanner (2018, p. 28) points out that modern criteria aim to incorporate high stability and safety margins into vessel designs to prevent catastrophic failure due to inexperienced sailors and that criteria like GZ at 30 degrees angle are difficult to achieve for vessels over 25 meters, which would not even operate at such angles of heel. He therefore suggests an alternative set of criteria which he deems more relevant for this type of ship, Table 7. All three loading conditions (empty, beams above water and Grågås), fulfil the alternative criteria at any wind speed up to wind force 6 (25 knots), including a 50% increase in wind speed due to gusting (Tanner, 2018, p. 29). For the wind speeds of 20 and 25

knots, he assumed the sail to be reefed and so he considered an area of 100 m^2 instead of 199 m^2. The resulting heeling angles and freeboard due to the effects of wind are summarized in Table 8.

Table 7
Alternative stability criteria. (After Tanner, 2018, p. 28).

Criterion	Justification
Steady Equilibrium less than GZ0	Resultant heel angle due to wind not in negative stability zone
Steady Equilibrium less than Flooding angle	Caprail atop bulwark remains above water at resultant heel angle
Steady Equilibrium less than GZmax angle	Heel angle remains in safe positive stability zone
GZmax angle greater than Flooding angle	When caprail atop bulwark reaches water, clear visual warning of the ship heeling to GZmax angle, thus indicating need to reduce sail area
Steady Equilibrium + 9.58° (heel due to waves) less than Flooding angle	Caprail remains above water with ship heeled due to wind and waves

Table 8
Heeling angles and freeboard due to wind. (After data by Tanner, 2018, pp. 24, 25, 27, Tables 4, 6, 8)

Condition	Wind force	Wind speed [kn]	Heel angle [deg]	Freeboard [m]	Heel angle with gust [deg]	Freeboard with gust [m]
Ballast	3	9-10	8.0	2.4	15.7	1.9
	4	13-15	15.7	1.9	26.0	1.2
	5	19-21	15.8	1.9	16.1	1.2
	6	25-27	21.3	1.5	32.4	0.8
Water below beams	3	9-10	0.8*	1.5*	4.5	2.1
	4	13-15	4.5	2.1	9.7	1.8
	5	19-21	4.4	2.1	9.6	1.8
	6	25-27	6.8	1.9	14.2	1.5
Grågås	3	9-10	0.8	1.7	1.7	1.6
	4	13-15	1.7	1.6	3.9	1.5
	5	19-21	1.7	1.6	3.7	1.5
	6	25-27	2.6	1.6	5.7	1.7

Note. *These values seem to be wrong as the angle should be higher than for the Grågås condition and the freeboard should be greater than the one at higher wind forces and with gust.

Besides stability calculations, Tanner also performed potential speed estimates on the Bremen cog. To this purpose the ship's calm water resistance and required power were calculated for a range of speeds in ORCA 3D based on Holtrop & Mennen prediction technique, see Figure 52. Note that this only considers the bare hull and thus the drag due to appendages such as the rudder, and the drag due to wind and waves are not taken into account (Orca3D, 2021, p. 348). A formula by Gerr's (1995, p. 164) was then used to calculate the power provided by the sails as a function of the wind speed,

sail area, and sail efficiency, see Table 9. The resulting speed potential of the vessel is then found when resistance power and power provided by the sails match, Table 10. Speed values for different sail angles were also obtained using different values for the projected sail area at these angles (see Tanner, 2018, p. 30, Table 9).

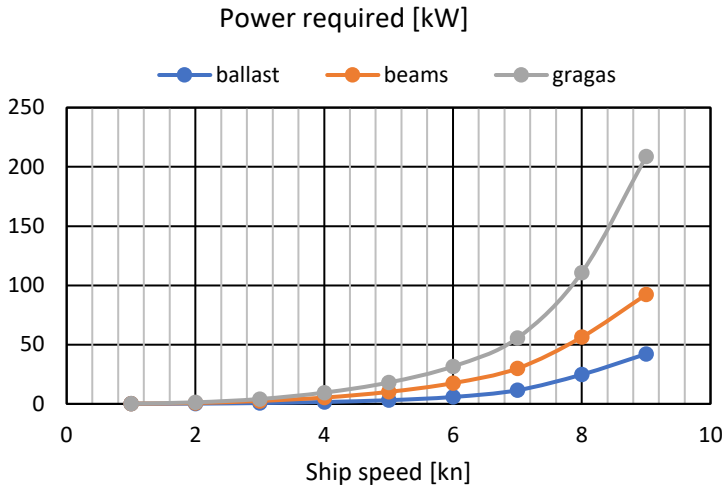

Figure 52 Power requirements for the Bremen cog. (Figure by Hernandez Montfort after data by Tanner, 2018, pp. 24, 25, 27, Tables 3, 5, 7).

Table 9
Power generated by square sail. (After data by Tanner, 2018, p. 23).

Wind force	Wind speed [kn]	Power per m^2 [kW/m^2]	Sail Area [m^2]	Power [kW]	Power with 70% efficiency [kW]	Power with 40% efficiency [kW]
3	9-10	0.118	199 (full)	23.48	16.44	9.39
4	13-15	0.161	199 (full)	32.04	22.43	12.82
5	19-21	0.312	100 (reefed)	31.20	21.84	12.48
6	25-27	0.559	100 (reefed)	55.90	39.13	22.36

Table 10
Speed potential, in knots, of the Bremen cog. (After data by Tanner, 2018, pp. 24, 25, 27, Tables 4, 6, 8).

		Ballasted		Water below beams		Grågås	
Wind force	Wind speed [kn]	Speed with 70% sail efficiency	Speed with 40% sail efficiency	Speed with 70% sail efficiency	Speed with 40% sail efficiency	Speed with 70% sail efficiency	Speed with 40% sail efficiency
3	9-10	7.5	6.8	5.9	4.9	4.9	4.0
4	13-15	7.9	7.2	6.5	5.5	5.4	4.5
5	19-21	7.8	7.1	6.4	5.4	5.4	4.4
6	25-27	8.9	7.8	7.4	6.4	6.4	5.4

IV.2.2 Data used in this thesis

The data used in this thesis was provided by Pat Tanner (University College Cork) and consists of the complete 3D model of the Bremen cog in Rhinoceros format, Figure 53. It is a model with a high level of detail containing every structural element of the ship's hull, superstructure, rigging (including not only ropes but even parrel beads, belay pins, etc..), crew and other equipment such as anchors, Figure 54.

Figure 53 The highly detailed 3D model of the Bremen cog. Dark timbers represent preserved timbers. Light brown timbers are reconstructed. (Figure by Hernandez Montfort after model by Tanner, 2018).

This model included the 3D geometric model of the ship, the position of the weights defined as points, the ship's lines plan, and drawings of the stability calculations results from ORCA 3D, such as the drafts and position of the centres of gravity and buoyancy and the metacentric height. Besides the 3D model of the ship, excel and pdf files containing the output results from the stability calculations were also provided by Tanner. These included the densities used to define each material, Table 11.

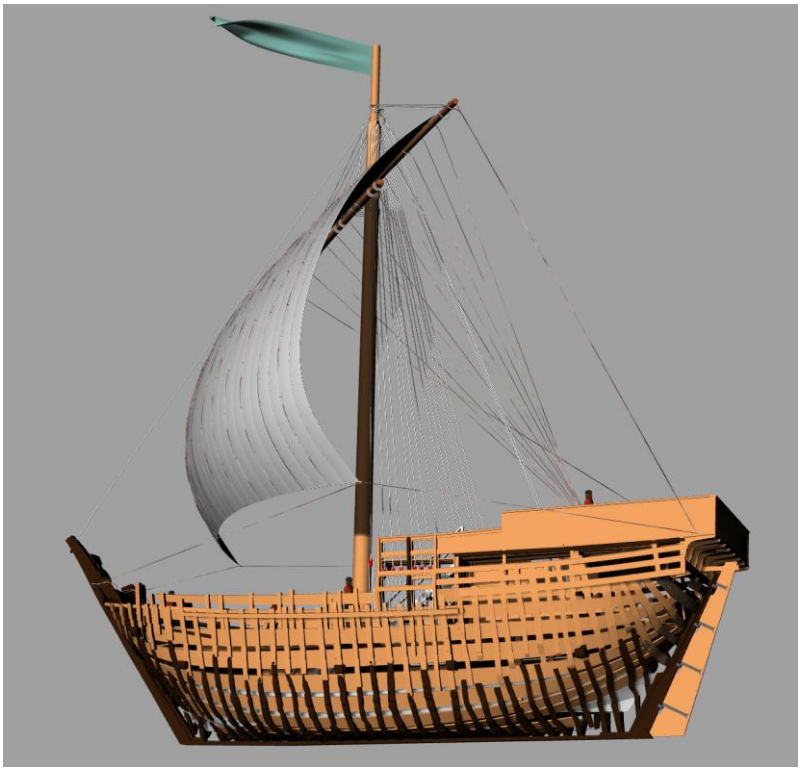

Figure 54 The internal timbers of the Bremen cog. Dark timbers represent preserved timbers. Light brown timbers are reconstructed. (Figure by Hernandez Montfort after model by Tanner, 2018).

Table 11
Materials and densities used in the Bremen cog model.

Material	Density	Used on
Iron	7850 [kg/m3]	Stem bolts, rudder hinges, anchors
Oak	800 [kg/m3]	Planks and timbers, anchor stocks, treenails
Spruce	450 [kg/m3]	Mast and yard
Hemp Rope	940 [kg/m3]	Rigging ropes
Lignum Vitae	1170 [kg/m3]	Rigging blocks, parrel beads
Stones	1600 [kg/m3]	Ballast
Sail canvas	0.45 kg/m^2	Sail, flag

Note. The density used for oak, spruce and lignum vitae corresponds to air seasoned wood with moisture content of about 27 %.

The weights in the 3D model were defined as points corresponding to the centre of gravity of the main parts (i.e., hull, rigging, superstructure, anchors, cargo, crew), Figure 55. Additionally, an excel file from the ORCA 3D calculations was provided, which contained the weight description (mass and position of the centre of gravity) for each of the 112 layers of the model and each element in them. While the weight definition as mass and centre of gravity position is enough for the performance of stability calculations, it is not enough for seakeeping calculations as the ship motions depend on how the weight is three-dimensionally distributed in the ship. To this purpose the moments of inertia needed to be computed for each element. This will be further explained in the next chapter where the calculation methods are described.

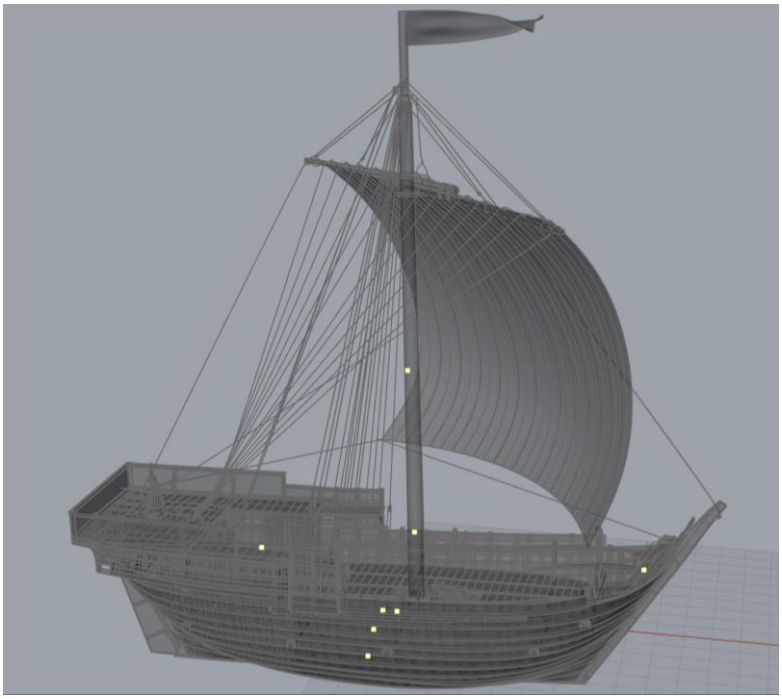

Figure 55 Weights in the Bremen cog defined as points. (Figure by Hernandez Montfort after model by Tanner, 2018).

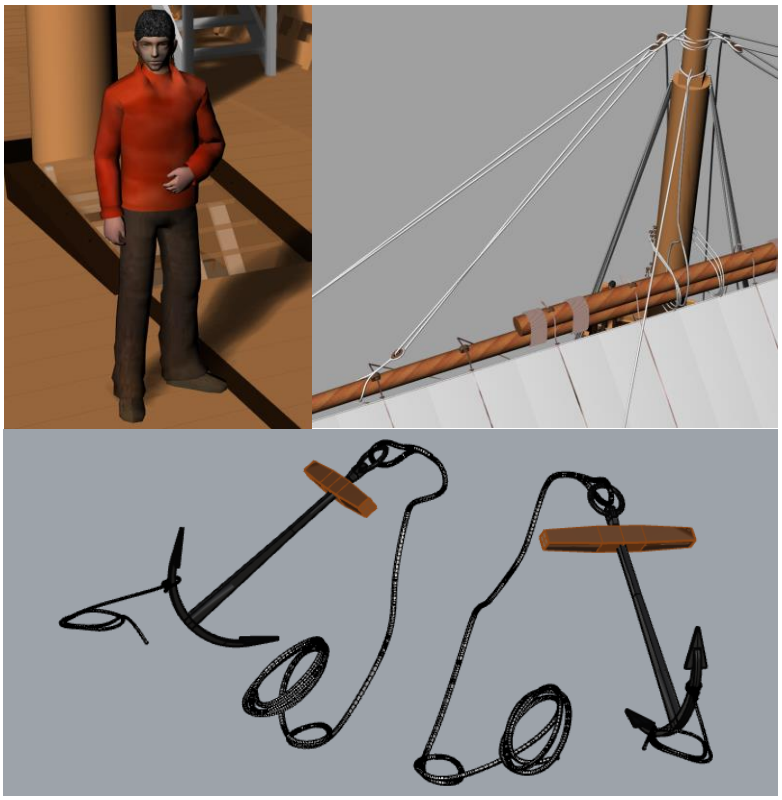

Figure 56 Extremely detailed elements on the Bremen cog model. The crew has a very high level of detail, including texture for clothing and facial features. The rigging includes not only the different ropes but also the parrel beads and blocks. The anchors were modelled including oak stocks and hemp ropes. (Figure by Hernandez Montfort after model by Tanner, 2018).

Because the 3D model of the Bremen cog was also fulfilling a visualization purpose besides the calculations one, some elements in the model, such as the rigging and the anchors, had a very high level of detail, see Figure 56. Such level of detail is valuable for visualization purposes, but it should be kept in mind that we cannot be sure of their accuracy since rigging and anchors have not been found. Considering their geometry and materials of the different parts (iron, oak for the stocks and hemp for the ropes) the anchors resulted in a weight of about 300 kg each.

The 3D model included 8 sailors. The weight did not however appear in the weight description from the ORCA 3D stability calculations. The sailing experiences by the full-scale replicas of the Bremen cog indicate that the ship would have needed a crew of between 12 and 15 people (Hoffmann & Hoffmann, 2009, pp. 289-290,292).

V. Calculation methods and tools

In this chapter the methodology I followed for each of the tasks shown in Table 1 is presented.

V.1 Creating the 3D model of the Big Ship of Wismar

As previously mentioned, the 3D model of the Bremen cog had a very high level of detail and had been used to make weight estimates and stability calculations. The 3D model of the Big Ship of Wismar needed however to be reconstructed to include all the structural elements of the hull and model them as solid objects ready to be used for weight calculations.

The first step consisted in modelling the hull as a solid with thickness instead of a surface, Figure 57. To this purpose I calculated the average thickness of the outer planking from the maximum thickness recorded for each plank in the catalogue of preserved timbers. This resulted in 3.5 cm for the oak planks and 9 cm for the pine wales. The strake surfaces were then offset half the thickness to both sides. The wales were mirrored to portside. The surfaces defining the keel were closed to form a solid. An opening on the outer planking was made to accommodate the protruding beams, Figure 58.

With the hull defined as a solid, the inner surface of the hull was extracted and used as basis for the reconstruction of the internal elements following the hull's shape, such as the frames and stringers. The scanned model of the preserved timbers was used as reference, Figure 59.

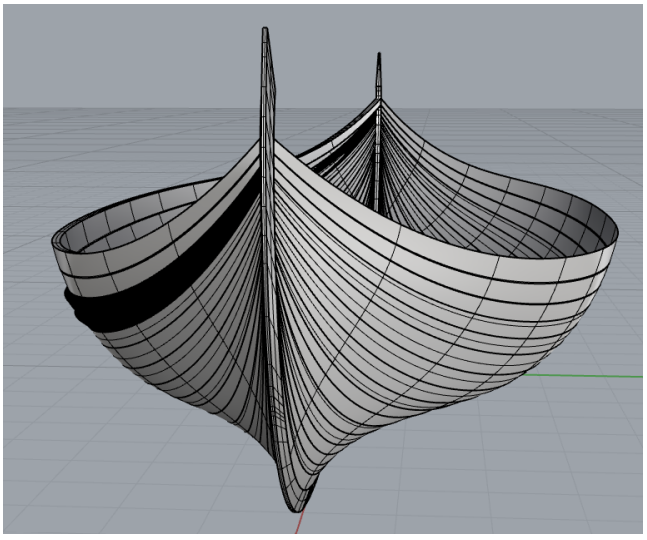

Figure 57 The hull of the visualization model of the Big Ship of Wismar as a surface. The different strakes of the hull and keel were defined as surfaces without thickness. The wales were only defined on the starboard side. The last strake on the starboard side was given an exaggerated thickness of 10.4 cm. No openings were modelled for the protruding beams. (Figure by Hernandez Montfort after model by Ditta & Auer, in press).

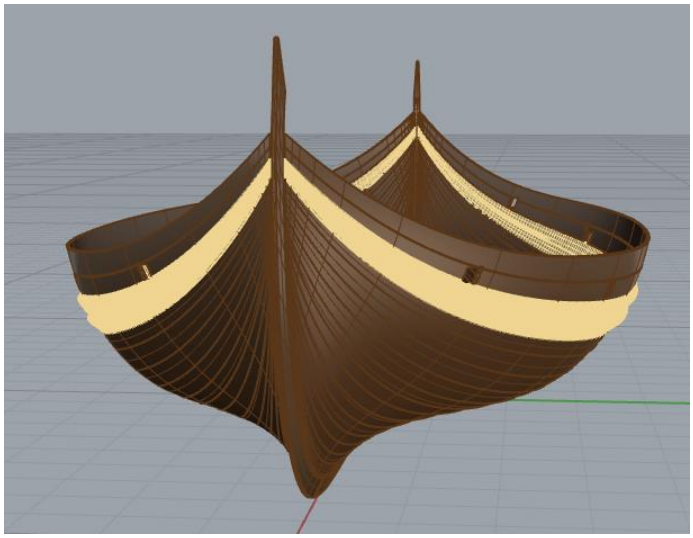

Figure 58 The hull of the Big Ship of Wismar as a solid. Oak is represented in brown. Pine is represented in sand colour. (Figure by Hernandez Montfort based on model by Ditta & Auer, in press).

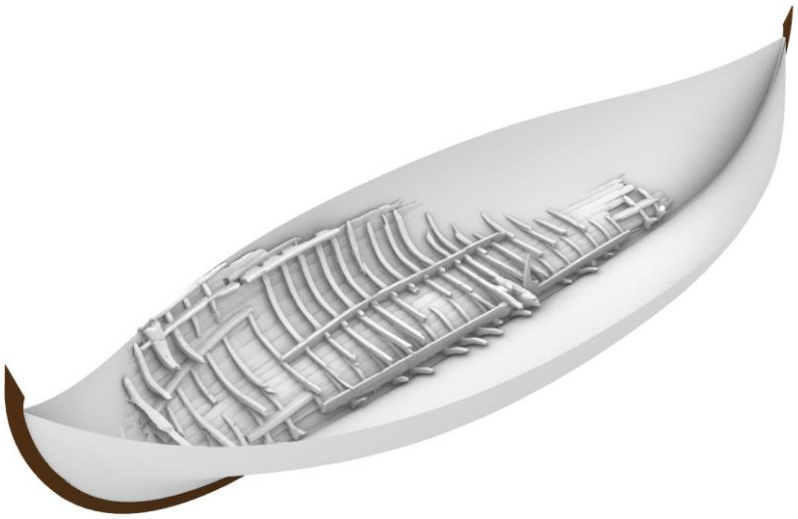

Figure 59 Base elements for the inner timbers' reconstruction. (Figure by Hernandez Montfort based on model by Ditta & Auer, in press).

The frames were modelled by defining vertical planes fitting the location of the frames on the scanned model and extrapolated to the bow and aft parts with no material remains, Figure 60. The intersection of these planes with the inner surface of the hull defined the position and the outer surface of the frames, Figure 61. The geometric boundaries of the frames were then obtained by offsetting these intersection lines by the thickness of the floor timbers, Figure 62. The thickness was established to fit as accurately as possible the dimensions of the floor timbers to the ones on the scanned model. The same thickness was applied to every floor timber. The upper limit of the floor timbers was defined by creating a vertical plane at the height of the bitis, Figure 63. The scanned model of preserved timbers showed that the bitis were placed at different heights depending on

their position along the ship, and thus floor timbers at the bow and aft parts of the ship were higher, see Figure 64. The scanned model also showed that the floor timbers at the aftmost and foremost positions were not vertical but had an inclination following the curvature of the keel. Therefore, I remade these frames with inclined planes instead of vertical ones, as visible in Figure 64.

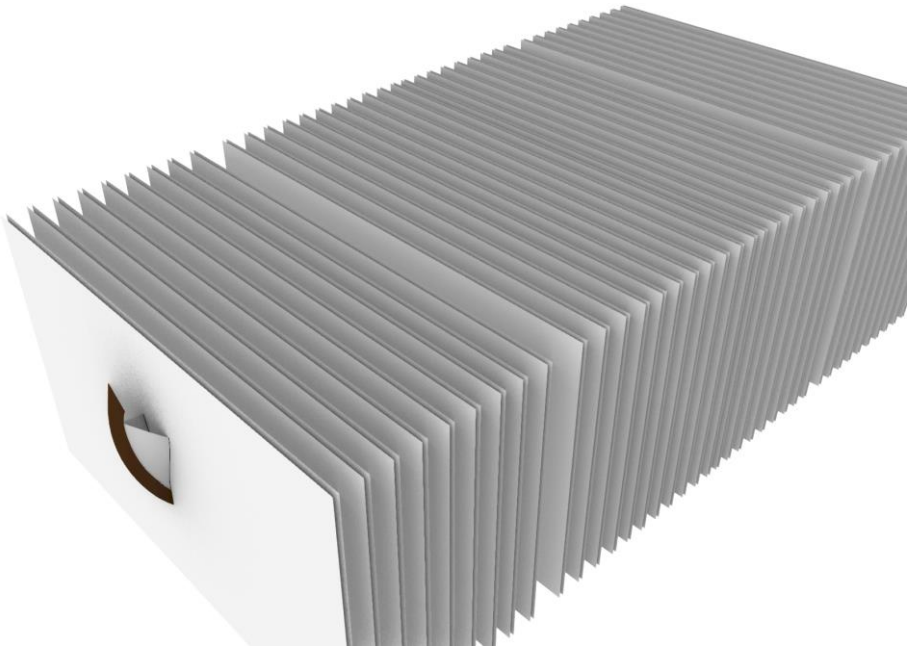

Figure 60 Vertical planes defining the location of the frames. The two different frame spacings defining the length of the hold are clearly visible. (Figure by Hernandez Montfort based on model by Ditta & Auer, in press).

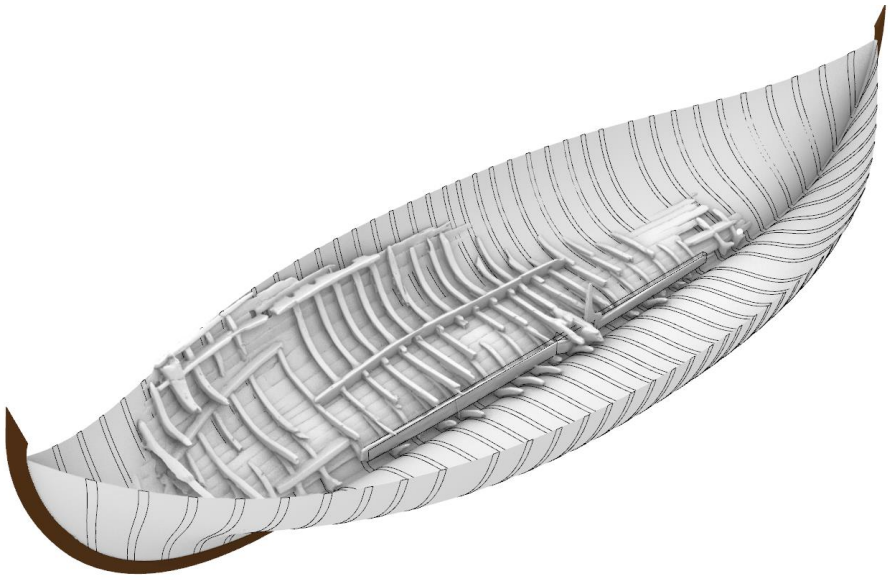

Figure 61 Lines on the inner hull surface defining the frames position. (Figure by Hernandez Montfort based on model by Ditta & Auer, in press).

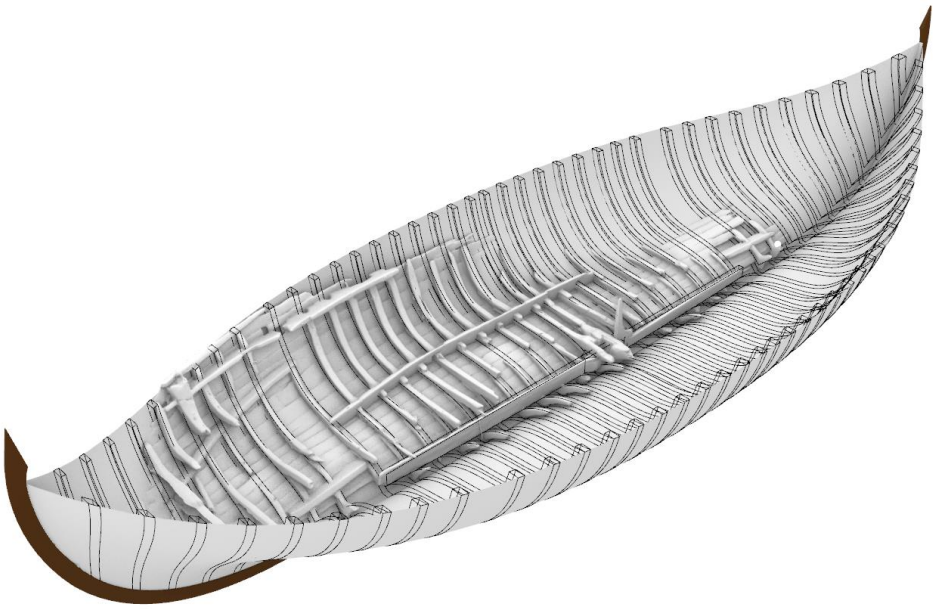

Figure 62 3D boundaries of frames defined by offsetting the lines to the floor timbers' thickness. (Figure by Hernandez Montfort based on model by Ditta & Auer, in press).

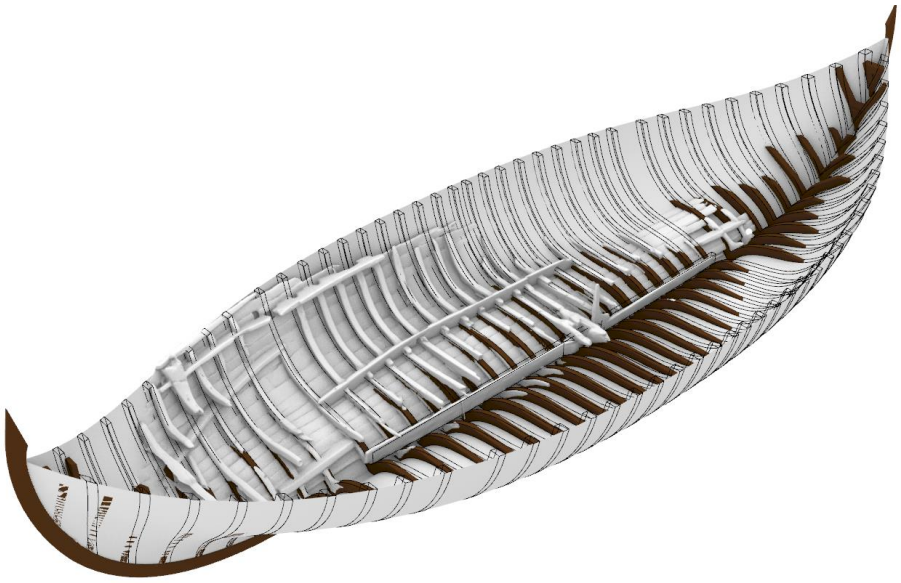

Figure 63 Floor timbers on the Big Ship of Wismar. (Figure by Hernandez Montfort based on model by Ditta & Auer, in press).

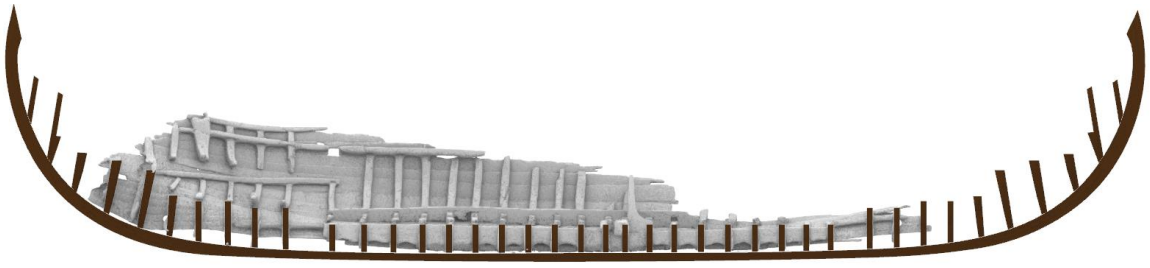

Figure 64 Profile view showing the position, height, and inclination of the floor timbers. (Figure by Hernandez Montfort based on model by Ditta & Auer, in press).

Next, the keelson, mast support piece, and the lower oak stringers were reconstructed based on the scanned model and the images in the timber catalogue, see Figure 65, Figure 66 and Figure 67.

Figure 65 The Keelson. Top: photography of the preserved keelson. (Taken from Auer & Ditta, 2019, timber number 211). Bottom: 3D model of the reconstructed keelson (Hernandez Montfort).

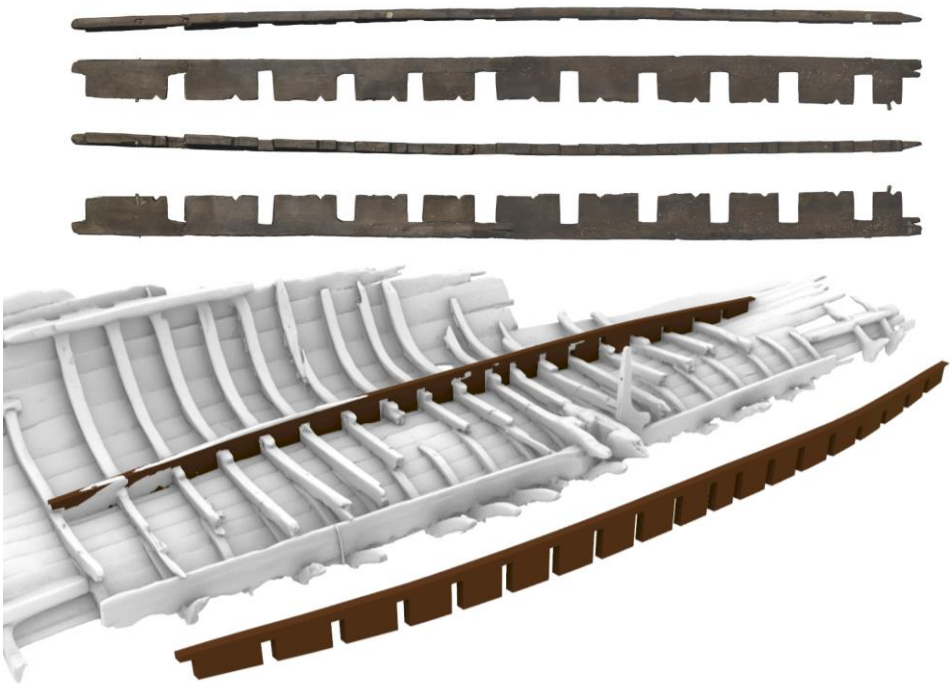

Figure 66 The lower oak stringers. Top: photography of the preserved lower oak stringer. (Taken from Auer & Ditta, 2019, timbers 215 and 295). Bottom: 3D model of the lower oak stringers at their position in the ship. (Hernandez Montfort based on the model by Ditta & Auer, in press).

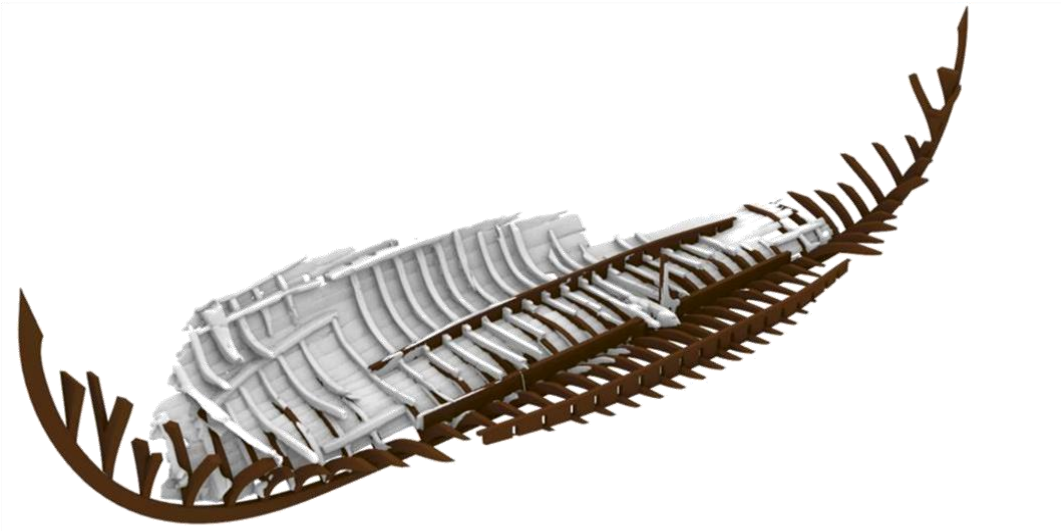

Figure 67 The model with keel, floor timbers, keelson, and lower oak stringers. (Hernandez Montfort based on the model by Ditta & Auer, in press).

I created then the bitis by defining horizontal planes at their lower and higher ends according to the scanned model. These planes, together with the vertical planes for the framing and the inner surface of the hull defined the boundary surfaces of the bitis. The two bitis at the mast location were modelled considering their special shape to accommodate the mast, see Figure 68 and Figure 69. The biti knees were then modelled on top of the bitis and following the shape of the hull, Figure 70 and Figure 71.

The pine stringers were modelled next. The lower pine stringers were cut out to fit the floor timbers, see Figure 72. The other stringers provide support to the deck beams and rest therefore on the floor timbers and/or bitis, Figure 73. Figure 74 shows the model including the biti knees and stringers.

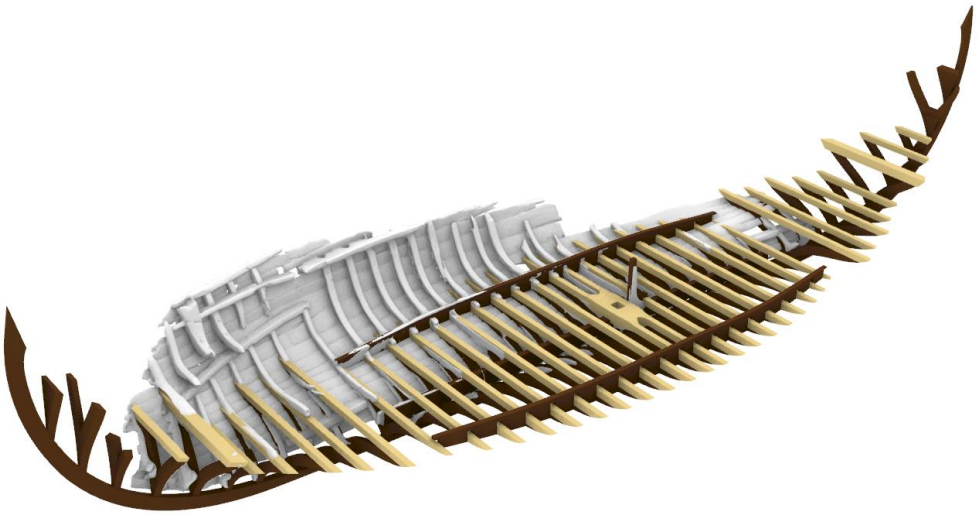

Figure 68 The model with the pine bitis. Notice the shape of the bitis at the mast location, acting as an extension of the mast step. Brown indicates oak, sand colour indicates pine. (Hernandez Montfort based on the model by Ditta & Auer, in press).

Figure 69 Photography of one of the bitis at the mast location. The curved part is the oak biti knee which is attached to the pine biti by means of treenails. (Taken from Auer & Ditta, 2019, timbers 251 (biti) and 300 (knee)).

Figure 70 Biti and biti knee connection. The oak biti knees rest on top of the pine bitis and are attached with treenails. (Taken from Auer & Ditta, 2019, timbers 203 (biti) and 303 (biti knee)).

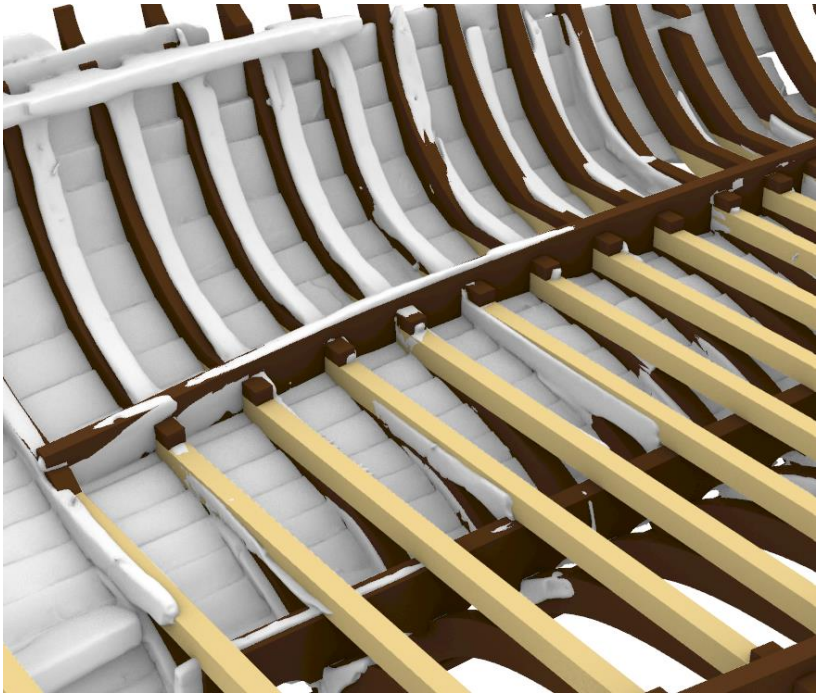

Figure 71 Close-up view of the biti construction. It can be seen how the keelson rests on the middle of the floor timbers and how the bitis rest on top of the floor timbers and the keelson. The biti knees rest on the bitis. The oak stringer has cuts to fit on the biti knees and bitis. The scanned model of the preserved timbers (in white) had distortions and thus does not match completely the shape of the reconstructed hull, hence the reconstructed biti knees do not match exactly the ones on the scanned model. Brown represents oak, sand colour represents pine. (Hernandez Montfort based on the model by Ditta & Auer, in press).

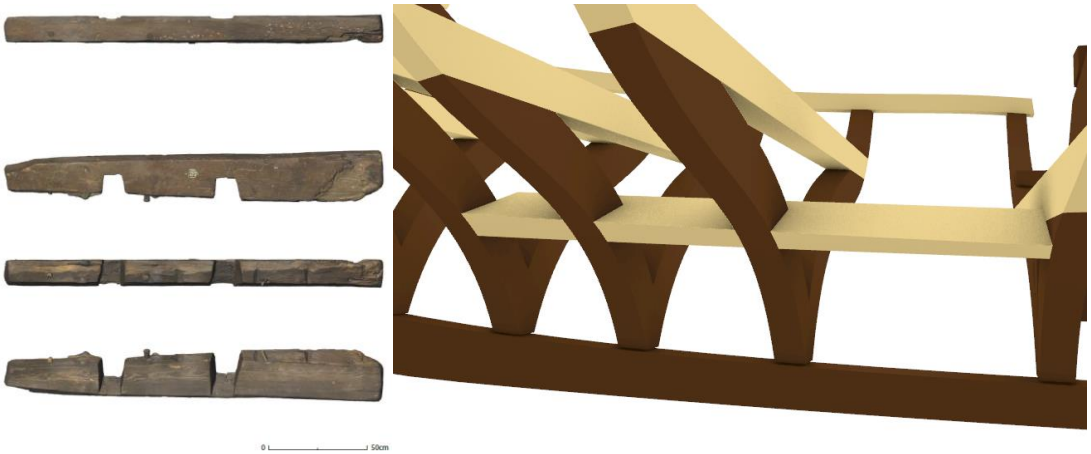

Figure 72 The lower pine stringer aft of the keelson. These pine stringers are cut out to fit the floor timbers and provide longitudinal strength as an extension of the keelson. Left: photography of a preserved lower stringer. Taken from Auer & Ditta, 2019, timber 221. Right: Reconstructed 3D model showing the position of the lower stringer. Brown indicates oak. Sand colour indicated pine. (Hernandez Montfort based on the model by Ditta & Auer, in press).

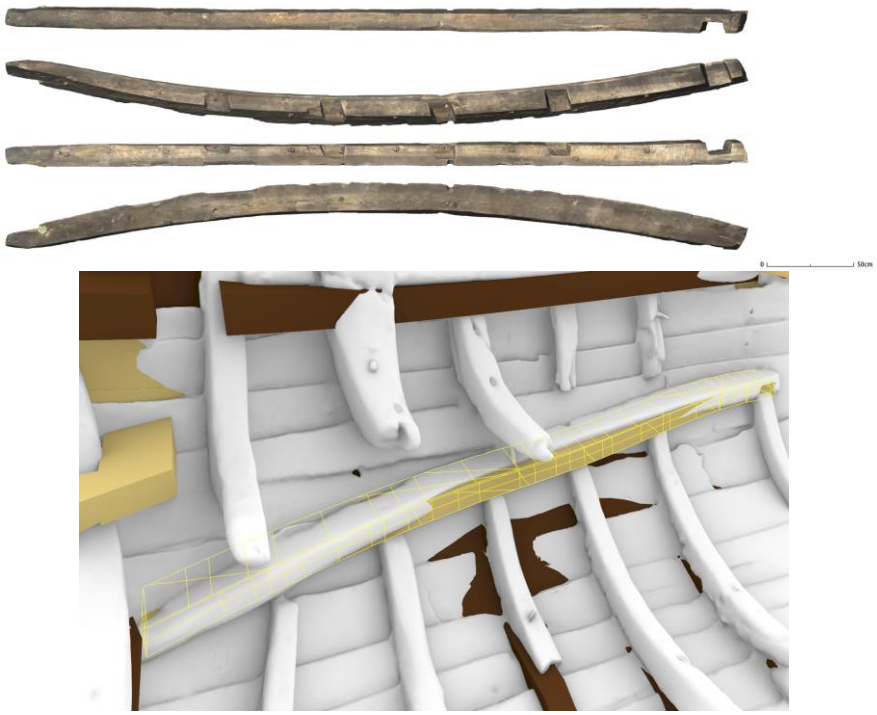

Figure 73 The upper pine stringer or deck beam shelf. These stringers had notches to fit the top of the biti knees. In the 3D reconstruction the notches are not modelled for the sake of simplification and the stringer just rests on top of the knees. Top: photography of the upper pine stringer. (Taken from Auer & Ditta, 2019, timber 324). Bottom: 3D model reconstruction. Brown indicates oak. Sand colour indicated pine. (Hernandez Montfort based on the model by Ditta & Auer, in press).

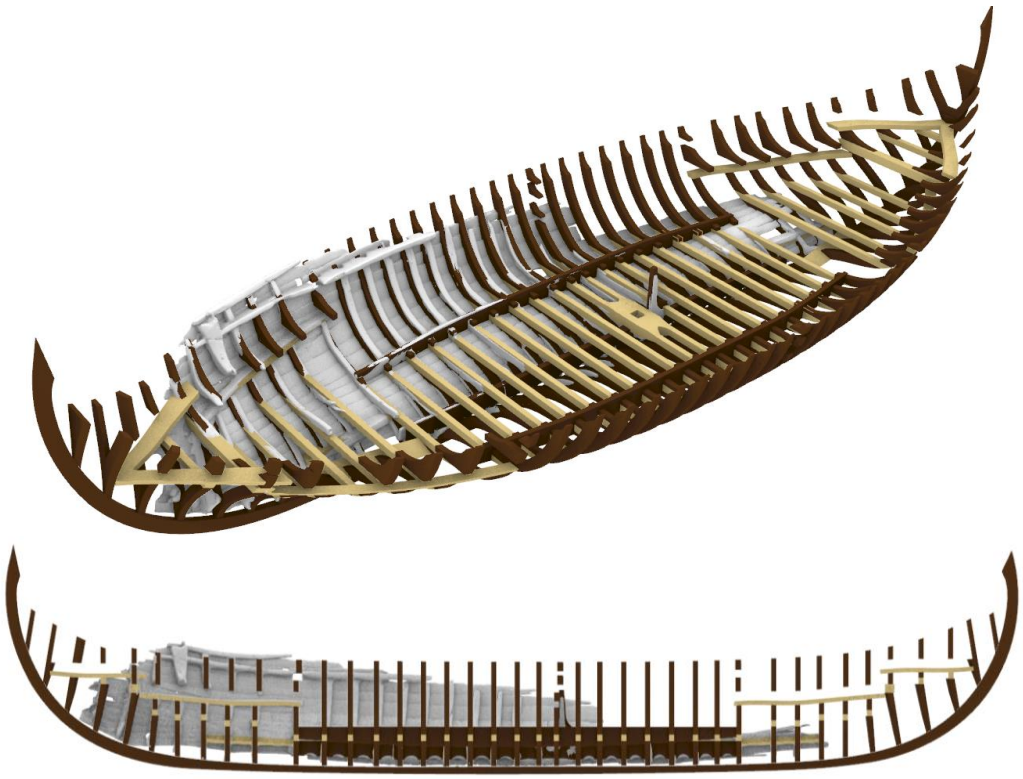

Figure 74 The position of the pine stringers in the Big Ship of Wismar. The pine stringers indicate the location of the deck structures. The gaps shown in some frames are the locations of the transverse beams. Brown indicates oak. Sand colour indicated pine. (Hernandez Montfort based on the model by Ditta & Auer, in press).

Next the transverse beams were added. These were not preserved so their rectangular shape is based on the opening found on the hull planks at the aft of the vessel, visible in Figure 74 and Figure 82, for the protruding beams, and on the thickness of the frames and distance to the deck for the deck beams. The foremost beam was protruding in the visualization model only in the portside. I decided to make both the foremost and aftmost beams also protruding on both sides, as they would have had a similar strengthening role than the other three beams in the mid-section. Figure 75 shows the model with the beams, including the windlass and the windlass knee. The windlass knee was made of elm tree while the windlass beam was assumed to be made of pine. The windlass knee and windlass geometry were taken from the visualization model, even if the windlass knee did not exactly match the geometry of the preserved element. As it represents just a relatively small element in the ship structure and no evidence exists for the geometry of the rest of the windlass, I deemed it unnecessary to model it with a higher level of detail, Figure 76.

Next the deck structures were added, Figure 77. A thickness of 4 cm was assumed for the deck planks.

Figure 75 The model of the Big Ship of Wismar including the transverse beams and windlass. Brown indicates oak. Sand colour indicated pine. Red indicates elm. (Hernandez Montfort based on the model by Ditta & Auer, in press).

Figure 76 Model of the windlass knee. The model of the windlass knee (red) against the scanned model of preserved timbers (white). (Hernandez Montfort, model by Ditta & Auer, in press).

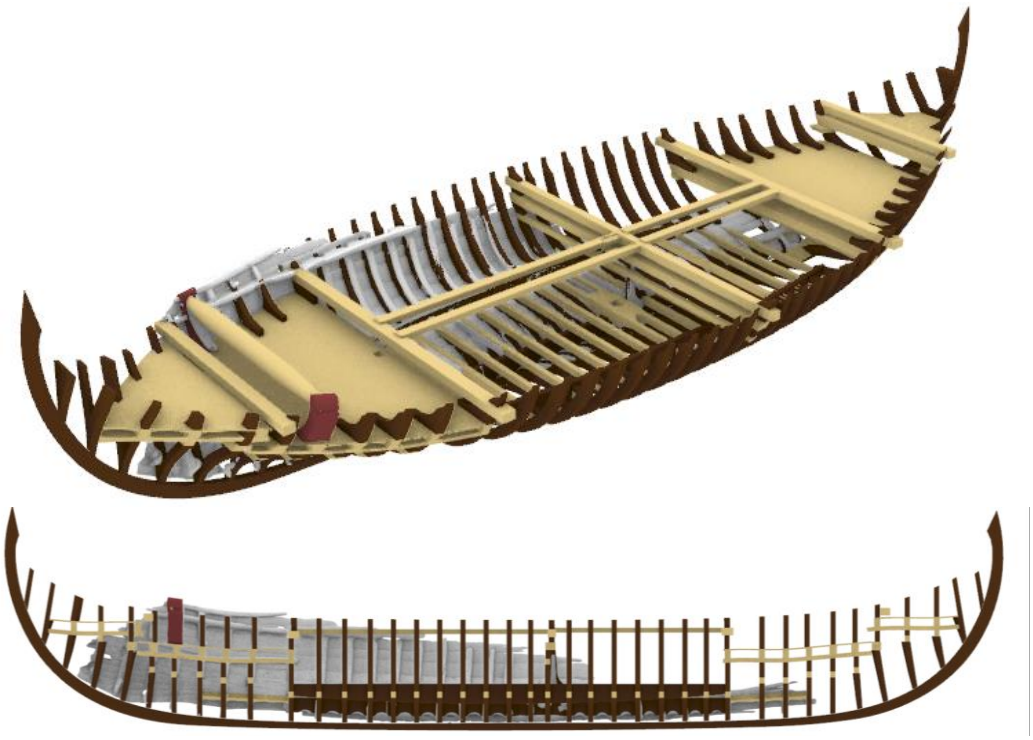

Figure 77 The model of the Big Ship of Wismar including aft and fore deck structures. Brown indicates oak. Sand colour indicated pine. Red indicates elm. (Hernandez Montfort based on the model by Ditta & Auer, in press).

Figure 78 Upper oak stringer. (Taken from Auer & Ditta, 2019, timber 214, 222).

Figure 79 Uppermost oak stringer. (Taken from Auer & Ditta, 2019, timber 362, 425).

The upper oak stringers were added next. These stringers would have run over the entire length of the vessel. The stringer above the deck level was cut out to fit the frames and the protruding beams and would have likely served as a waterway or clamp, Figure 78, while the uppermost stringer at the

edge of the hull was notched to fit on top of the frames, Figure 79. For the sake of simplification and since both stringer and frames were made of oak, the notches were not modelled. Figure 80 shows the reconstructed model including the upper oak stringers. The complete hull with outer planking but without mast, rigging, rudder, and pump is shown in Figure 81.

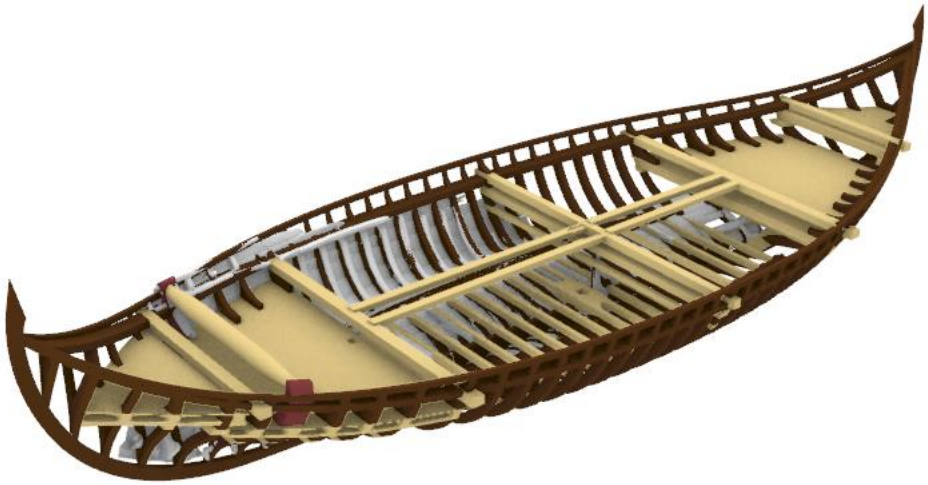

Figure 80 The model of the Big Ship of Wismar with the upper stringers. Brown indicates oak. Sand colour indicated pine. Red indicates elm. (Hernandez Montfort based on the model by Ditta & Auer, in press).

Figure 81 Model of the hull including outer planking. Brown indicates oak. Sand colour indicated pine. Red indicates elm. (Hernandez Montfort based on the model by Ditta & Auer, in press).

As already mentioned in chapter IV, the likely presence of a water pump was suggested by the opening in the outer planking at the starboard side above the position of the upper stringer and the small lower pine stringers that allowed access to the keel right aft of the keelson. A similar arrangement is seen in the Kalmar V wreck (Ditta & Auer, 2021, p. 195). I took the geometry of the pump directly from the visualization model by Ditta & Auer (in press), but I defined a thickness, modelled it as a solid object and made an actual opening on the outer planking, Figure 82.

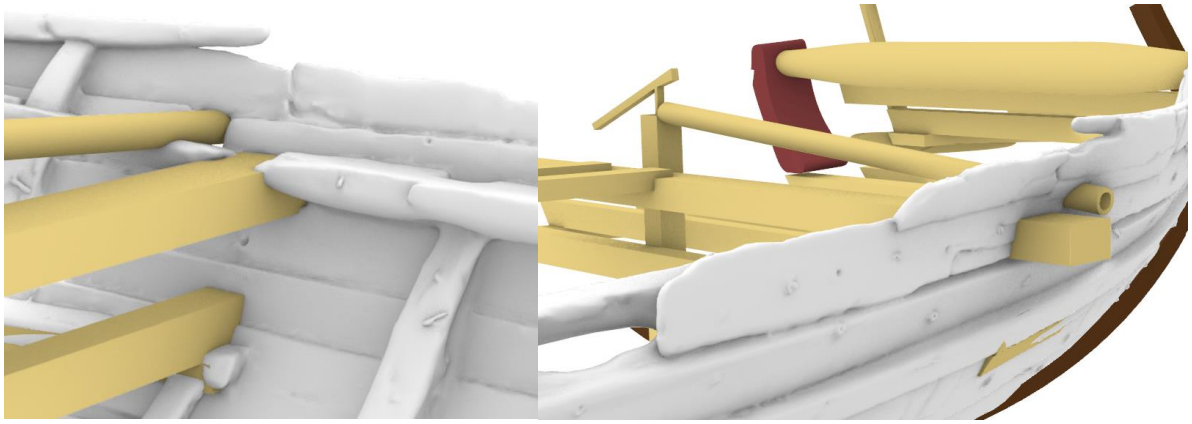

Figure 82 Model and position of the water pump. The circumference of the pump tube was defined based on the opening visible on the preserved outer planking. Also notice the opening just below for the protruding beam. Brown indicates oak. Sand colour indicated pine. Red indicates elm. (Hernandez Montfort, model by Ditta & Auer, in press).

I modelled the mast and rigging based on the Roar Ege, the replica of the Skuldelev 3, since it is the only ship for which actual rigging evidence has been found, as already discussed in section III.6. The sail of the Roar Ege is 45 m^2 and about 6.5 x 7 m. Since the Roar Ege has a length of 14 m and a width of 3.33 m (Vikingeskibsmuseet, 2023b) and the Big Ship of Wismar is 23.3 m long and 7.6 m wide, thus 1.7 times longer and 2.3 times wider, a sail about 2 times as wide and tall for the Big Ship of Wismar would seem appropriate. Furthermore, assuming that the aftmost fastening point would have been fore of the deck and pump, a sail width of about 12.5 m is found, Figure 83.

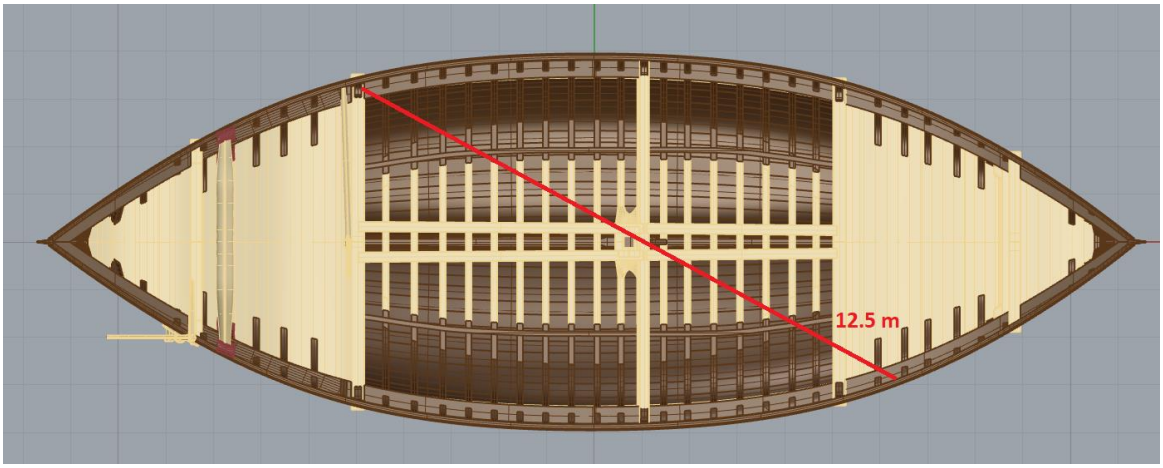

Figure 83 Hypothetical sail width. Brown indicates oak. Sand colour indicated pine. Red indicates elm. (Hernandez Montfort based on the model by Ditta & Auer, in press).

For the sake of simplicity, I assumed a sail of 150 m^2, 12 x 12.5 m, for the Big Ship of Wismar. The diameter of the mast was derived from a preserved timber piece interpreted as mast partner, which

was fitted around the mast and on the longitudinal supporting beams. I assumed the mast to be 14.5 m high.

The rudder geometry was directly taken from the visualization model by Ditta & Auer (in press). Figure 84, shows the model of the ship with all the aforementioned elements.

Figure 84 The model of the Big Ship of Wismar with mast, sail, rudder, and pump. Brown indicates oak. Sand colour indicated pine. Red indicates elm. (Hernandez Montfort based on the model by Ditta & Auer, in press).

The crew requirements for sailing these ships remain largely unknown, and there is limited information about crew organization and hierarchy onboard. Available written sources, such as 13th century sagas and Middle Age Norwegian laws, primarily focus on longships rather than *knarrs* (Ellmers, 1995, p. 237; Vikingeskibsmuseet, 2023c). Another source with limited information is the iconography found in the Bayeux tapestry, which depicts the invasion of England in 1066 by William the Conqueror (Ellmers, 1995, p. 235). Although most depictions are warships, a couple of trading vessels are depicted with a small crew of 4 persons, each performing a different task, see Figure 85. However, it is difficult to know the size of these vessels. A more reliable source of information on this topic is again the experiments performed with the full-scale replicas by the Viking Ship Museum in Denmark.

Figure 85 Ship depictions with their crew in the Bayeux Tapestry. The two merchant vessels have a crew of four men, each performing a specific task on board. (Ellmers, 1995, p. 236, Fig. 9).

Figure 86 The Ottar, full-scale replica of the Skuldelev 1. (Vikingeskibs Museet, 2023).

According to the Viking Ship Museum in Denmark, the crew of the Ottar, Figure 86, ranges between 6 and 15 men (Vikingeskibsmuseet, 2023a). The Ottar is the replica of the Skuldelev 1 ship, a seagoing *knarr* bigger than the Skuldelev 3. Englert (2000, p. 82) estimates a crew of 10 men for the Lynaes 1, with a weight of 100 kg each including their personal equipment. For the Big Ship of Wismar, I made the same assumption.

While it is not know with certainty what type of anchor these ships had, it is believed that they consisted either of rocks inside large walrus-hide bags with removable wooden or iron struts or large stones encased in a wooden structure in the style know as Killick anchors, Figure 87 (Morton Nance, 1921, p. 137; Shaw, 2016, pp. 20-21). I modelled the anchors for the Big Ship of Wismar as 0.4 m diameter spheres. Figure 88 shows the complete model of the Big Ship of Wismar. Rigging lines were added just for visualization purposes but were not modelled as solid objects.

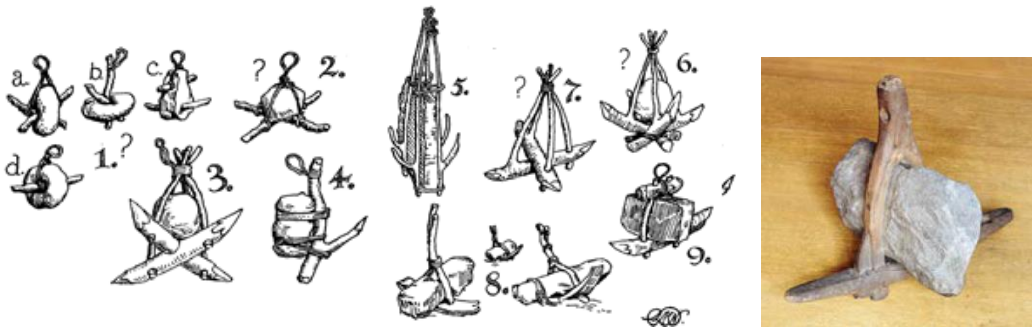

Figure 87 Examples of Killick anchors. (Drawings taken from Morton Nance, 1921, p. 138. Photograph taken from Shaw, 2016, p. 21).

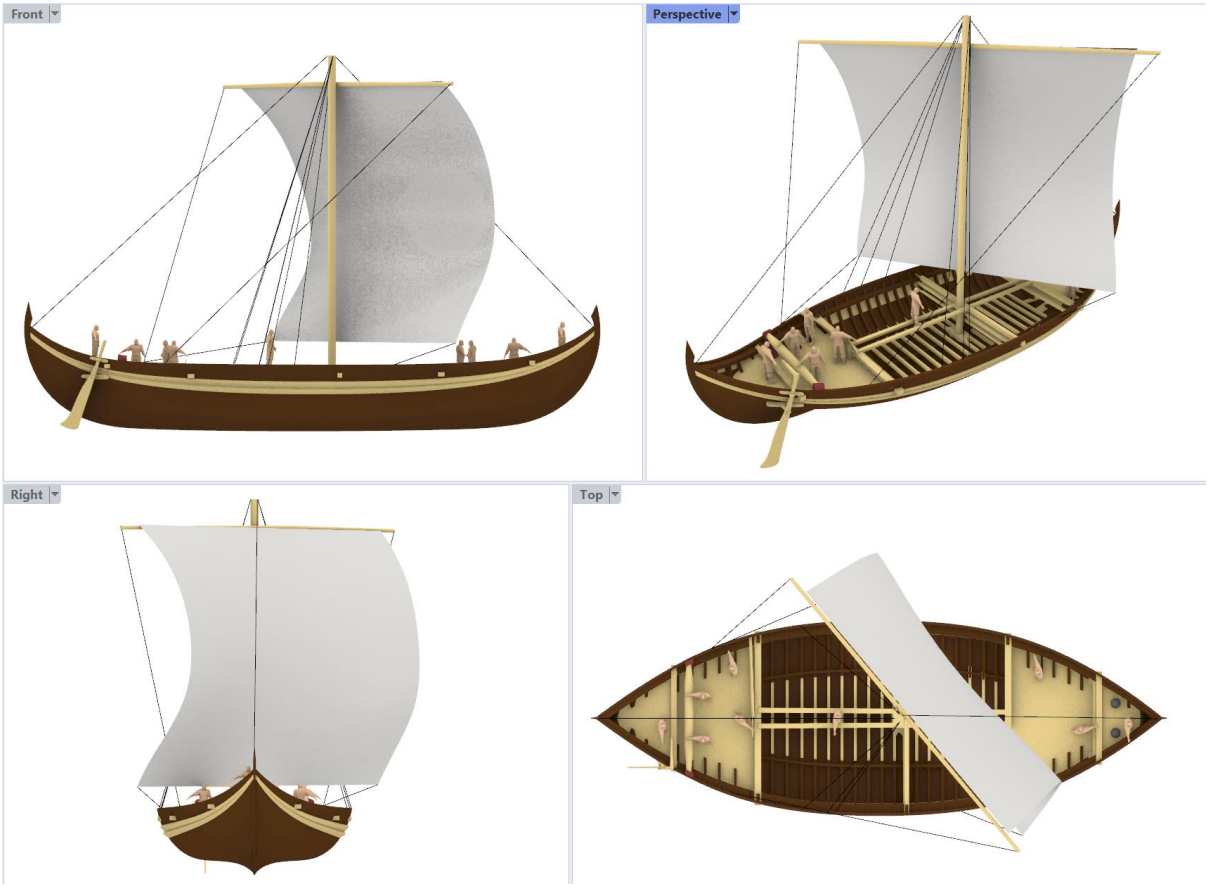

Figure 88 The complete 3D model reconstruction of the Big Ship of Wismar. Brown indicates oak. Sand colour indicated pine. Red indicates elm. Notice the anchors modelled as spheres at the bow of the ship. (Hernandez Montfort based on the model by Ditta & Auer, in press).

V.2 Weight and inertia calculations

V.2.1 General

Weight and inertia calculations were done by first calculating the volume, centres of volume and moments of volume in Rhinoceros for the different elements in the 3D models. The other calculations described here were done with an Excel spreadsheet.

The volumes and the moments of volume were multiplied by the density of the material of each element to obtain the mass and moments of inertia. The centre of gravity coincides with the centre of volume. To get the values at a proper coordinate reference, the models were translated and rotated to have their bow in the positive x direction and their centreline, baseline and aft at 0, 0, 0. The moments of inertia were computed at the origin point (0, 0, 0) for each element and added to each other to obtain the total moments of inertia for the ship with respect to the coordinate origin.

The centre of gravity of the ship is obtained by the summation of the mass products of each element (mass times distance to the origin in x, y, or z) divided by the summation of the masses, Equation 1.

Equation 1 Calculation of the centre of gravity of the ship

$$X_{COG} = \frac{\sum_i X_i m_i}{\sum_i m_i}; Y_{COG} = \frac{\sum_i Y_i m_i}{\sum_i m_i};\ Z_{COG} = \frac{\sum_i Z_i m_i}{\sum_i m_i}$$

Once the centre of gravity of the ship is known, the moments of inertia at the origin can be translated to the centre of gravity of the ship by applying the parallel axis or Steiner's theorem, that is, by subtracting to the moments of inertia at the origin the product of the ship's total mass and the distance from the origin to the parallel axis passing at the centre of gravity of the ship, Equation 2.

Equation 2 Steiner's theorem

$$I_{x_{COG}} = I_{x_0} - M(Y_{COG}^2 + Z_{COG}^2);\ I_{y_{COG}} = I_{y_0} - M(X_{COG}^2 + Z_{COG}^2);\ I_{z_{COG}} = I_{z_0} - M(X_{COG}^2 + Y_{COG}^2)$$

The radii of inertia (k_{xx}, k_{yy}, k_{zz}) are then obtained from Equation 3.

Equation 3 Relation between radii of inertia and moments of inertia

$$k_{xx} = \sqrt{\frac{I_{x_{COG}}}{M}};\ k_{yy} = \sqrt{\frac{I_{y_{COG}}}{M}};\ k_{zz} = \sqrt{\frac{I_{z_{COG}}}{M}}$$

For convenience when comparing different loading conditions and ships, the radii of inertia are commonly expressed as a percentage of the beam of the ship for the k_{xx}, and as a percentage of the length for the k_{yy} and k_{zz}.

Once the radii of inertia are known, the natural roll period of the ship is given by Equation 4, with g being the acceleration of gravity and f_{am} a factor representing the increase in radius of inertia due to the added mass of water around the hull. As a first estimate this factor can be taken as 1.2. The actual value of the increase due to the added mass can later be computed by means of seakeeping calculations.

Equation 4 Natural roll period of a ship

$$T_{roll} = \frac{2\pi k_{xx} f_{am}}{\sqrt{gGM}}$$

V.2.2 The Big Ship of Wismar

The iron rivets in the Big Ship of Wismar were not modelled in the 3D model. To take their weight into account, an estimate of the number of rivets and their impact on the density of the outer planking was made. The average distance between rivets was obtained from the timber catalogue as 17 cm. Likewise the average length (4,4 m) and width (30 cm) of completely preserved planks was obtained from the catalogue. In this way the number of rivets per plank was obtained by diving 440 cm by 17 cm and adding 4 extra rivets for the end scarfs. This results in about 30 rivets per plank. The density of the iron varies greatly. Unfortunately, little is known about the type of iron that was used for the rivets in the Viking ships. The full-scale replicas built by the Viking Ship Museum in Denmark have shown that the use of modern-day iron had a dreadful impact on the longevity of the ships, as rivets would corrode and create cracks on the timbers. The impact was so big that the new replicas are being built with copper rivets even if these were not used in the Viking ships (Vikingeskibsmuseet, 2020). The mass of the rivets was computed by assuming an iron density of 7750 kg/m^3. Their volume was computed by considering a cylindrical shape for the rivet with a radius of 0.4 cm and a length of 5 cm, a rivet head of 1.5 cm in radius and a height of 0.5 cm, and a square rove measuring 2.7 x 2.7 cm with a height of 0.5 cm, Equation 5. These dimensions correspond to the average dimensions found in the timber catalogue, measured from the holes and imprints on the timbers.

Equation 5 Volume of a rivet

$$Volume\ of\ a\ rivet\ [cm^3] = 0.4^2\pi * 5 + 1.5^2\pi * 0.5 + 2.7 * 2.7 * 0.5$$

The mass of a rivet is then 75 grams when multiplying the volume by the iron density. The mass of the rivets per plank is then equal to 2.2 kg. Since the volume per plank is given by 440 cm x 30 cm x 3.5 cm = 0.0462 m^3, the density of the planks can then be expressed as the density of the wood plus the extra density due to the rivets, which is the mass of rivets minus the mass of the wood of the holes divided by the volume of the plank. The resulting densities used for the outer riveted planks are shown in Table 12.

Two weight estimates were done for the Big Ship of Wismar. One considering a 27% moisture content for all wood, as done with the Bremen cog by Tanner (2018), and another considering a 35% moisture content for the timbers above water and a moisture content of 50% for the timbers in contact with water, as done for the Lynaes 1 ship by Englert (2000, p. 82). The below water density was applied to timbers below the pine wales.

Treenails were not modelled as they have the same density as the timbers.
The density of wool used for the sail canvas was derived to obtain a weight of 150 kg, in accordance with the weight of the woollen sail of the Ottar, which weighted 90 kg for 90 m^2 sail (Vikingeskibsmuseet, 2023d). The information about the sails being made of wool comes from the descriptions in the sagas (Shaw, 2016, p. 19). For the crew, the same assumption by Englert (2000, p. 82) was done, that is 100 kg per person including personal equipment. The anchors resulted in 56 kg each, with a density of 1600 kg/m^3 for the stones.

Table 12
Densities used in the Big Ship of Wismar

Material	Density [kg/m^3]	Used for	As in
Oak (27% MC)	800	Oak timbers	Bremen cog
Oak riveted planks (27% MC)	848	Outer hull planks	Bremen cog
Oak (35% MC)	850	Oak timbers	Lynaes 1
Oak riveted planks (35% MC)	898	Outer hull planks	Lynaes 1
Oak (50% MC)	1000	Wet keel	Lynaes 1
Oak riveted planks (50% MC)	1047	Wet outer hull planks	Lynaes 1
Pine (27% MC)	700	Pine timbers	Bremen cog
Riveted pine (27% MC)	748	Wales	Bremen cog
Elm (27% MC)	720	Windlass knee	Bremen cog
Pine (35% MC)	740	Pine timbers	Lynaes 1
Riveted pine (35% MC)	788	Wales	Lynaes 1
Elm (35% MC)	763	Windlass knee	Lynaes 1
Wool	350	Sail	Full scale replica
Stone	1600	Anchors	Bremen cog

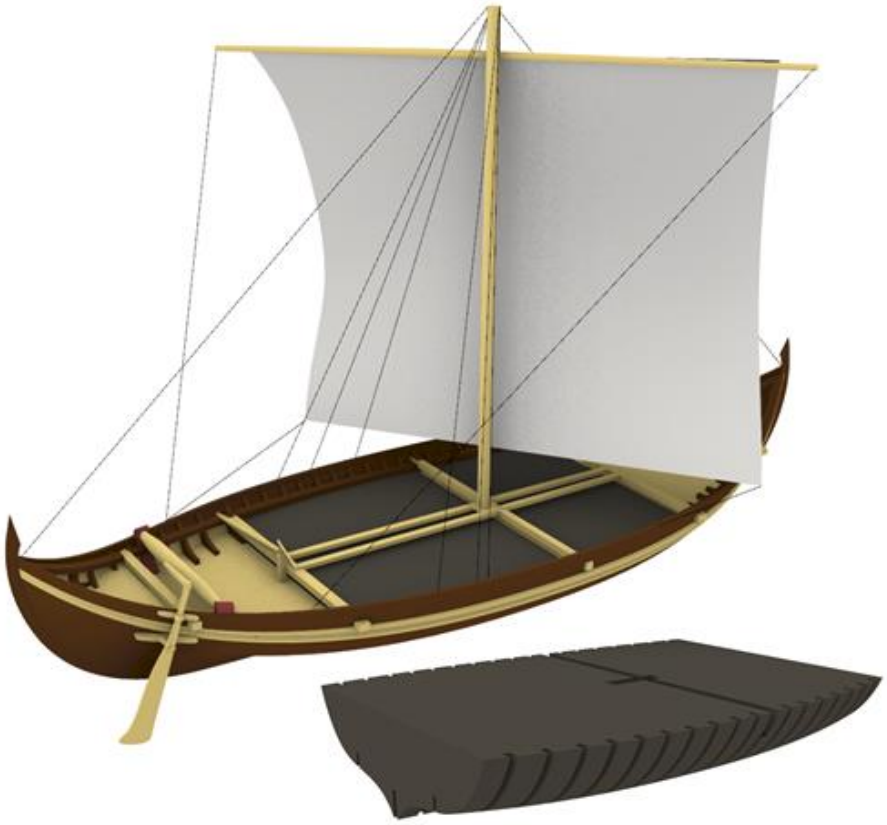

Figure 89 The cargo volume of the Big Ship of Wismar up to the waterway. (Hernandez Montfort based on the model by Ditta & Auer, in press).

Figure 90 The cargo volume of the Big Ship of Wismar up to the edge of the hull. (Hernandez Montfort based on the model by Ditta & Auer, in press).

The weight of the cargo was derived from the displacement of the ship at three different drafts, the Grågås codex draft of 1.6 m, the draft under the two wales of 1.3 m, and a draft of 1 m. The density of the cargo is given then by the volume of the hold. For the big ship of Wismar, the cargo volume was considered to reach up to the upper oak stringer that acts as a waterway, Figure 89. This is the same approach used by Englert (2000, p. 83) for the Lynaes 1. The cargo volume was then 83.7 m^3. As alternative a volume up to the edge of the hull was also considered, Figure 90, resulting in 119.3 m^3.

V.2.3 The Bremen cog

For the Bremen cog weight calculations had already been done by Tanner (2018). However, to compute the moments of inertia, the same procedure as done for the Big Ship of Wismar had to be done. Since the 3D model contained many layers and sublayers, weights defined as mass points, and two sail configurations (full and reefed), the first task consisted in figuring out which layers had to be used for the weight calculations. This was done by using the excel file with the weight calculations results for all elements from ORCA 3D and selecting the appropriate layers until the right ship displacement for each of the drafts was matched. Then I obtained the volume and moments of volume for each of the layers from Rhinoceros to compute the moments of inertia. In this process I found that few elements in the model were not defined as completely closed polysurfaces and thus no volume could be computed. Therefore, I remodelled these elements as closed polysurfaces. One of these elements was the keelson. Because ORCA 3D simply ignores the elements that are not closed for the calculation of volumes, the weight of the keelson considered was of only 43.9 kg. With the keelson remodelled the total mass of the keelson became 580.7 kg. The same occurred on three frames and two stanchions, their combined mass being 127 kg. The total extra mass, about 650 kg, was then removed from the ballast to keep the same displacement. Since the weight it is relatively small and mostly located at the bottom of the ship (keelson) it has no noticeable impact on the stability results by Tanner (2018).

The ballast had already been modelled as a volume in the 3D model by Tanner, Figure 91. The cargo was however defined as a mass point, thus a cargo volume had to be modelled to compute the moments of inertia, Figure 92. It was made in a way to match the centre of volume with the coordinates of the cargo mass point for the Grågås codex condition and the beams above water condition. The difference in vertical position of the centre of gravity of the cargo for both conditions was just 15 cm. The volumes resulted in 120 m^3 for the Grågås condition, which coincides with the estimate by Hocker (Hocker & Ward, 2004, p. 75) and 100 m^3 for the beams above water condition.

According to Waldus, Verweij, & van der Velde (2019, p. 488), the maximum cargo space of the Bremen cog would be of about 135 m^3.

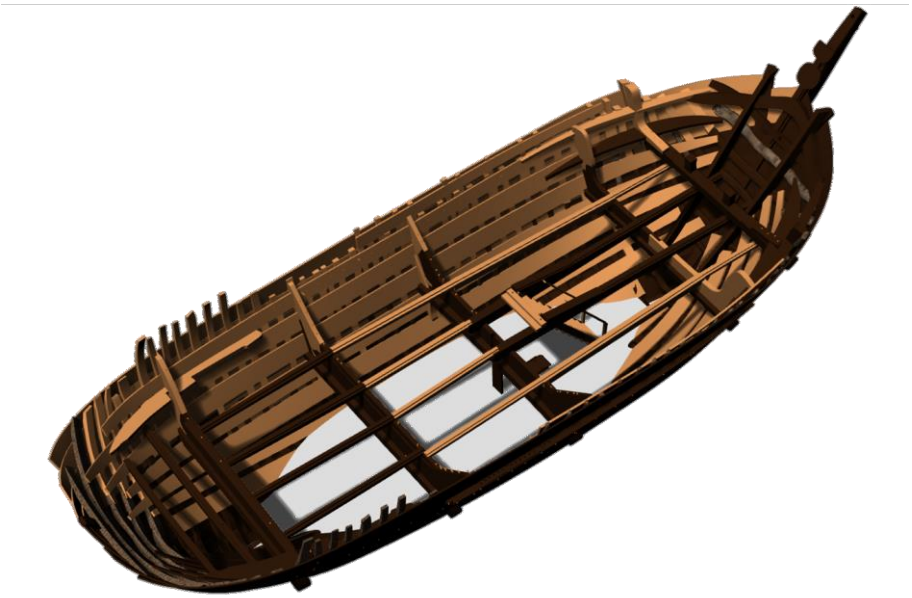

Figure 91 Space used for ballast in the Bremen cog. (Hernandez Montfort based on model by Tanner, 2018).

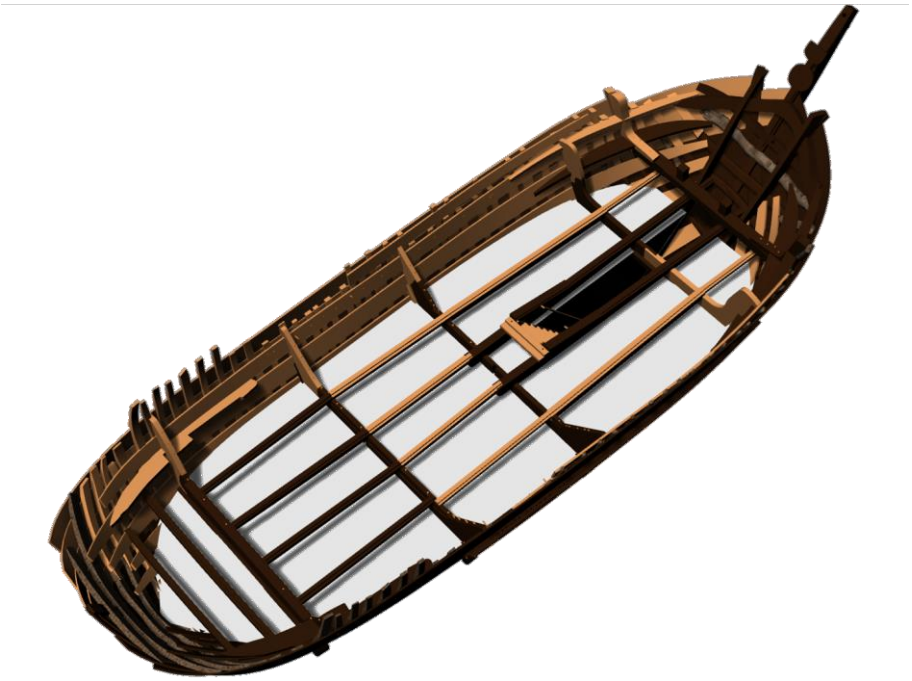

Figure 92 Cargo volume for the Bremen cog in the Grågås codex condition. (Hernandez Montfort based on model by Tanner, 2018).

V.3 Speed estimations

The estimation of the speed potential of the Big Ship of Wismar was done following the same procedure as for the Bremen cog and described in section IV.2.1. The calm water resistance was computed in ORCA 3D following the Holtrop & Mennen formulations from the faired outer surface of the hull, Figure 93. The Holtrop & Mennen approach computes the calm water resistance of ships using formulas obtained from regression analyses on model tests and sea trials results of modern ships. It uses the main dimensions of the hull, the displacement volume, and several hull form coefficients, such as the block coefficient, the prismatic coefficient, the waterplane area coefficient, the midship section area coefficient, and the position of the centre of buoyancy (Holtrop & Mennen, 1982). The method is based on formulations derived from empirical data of modern ships and therefore does not provide accurate results for the types of hulls studied here. However, the main goal of the current assessment is to compare the two hulls in terms of speed potential rather than obtaining an accurate value of their calm water resistance. Therefore, this method is acceptable.

The power provided by the sails was obtained from a very basic relationship between wind speed and power per square meter of sail suggested by Gerr's (1995, p. 164) for square sails. An efficiency factor is then applied to this value, as done by Tanner (2018, pp. 23-27) for the Bremen cog.

The resulting speed is found when the resistance power equals the power provided by the sails.

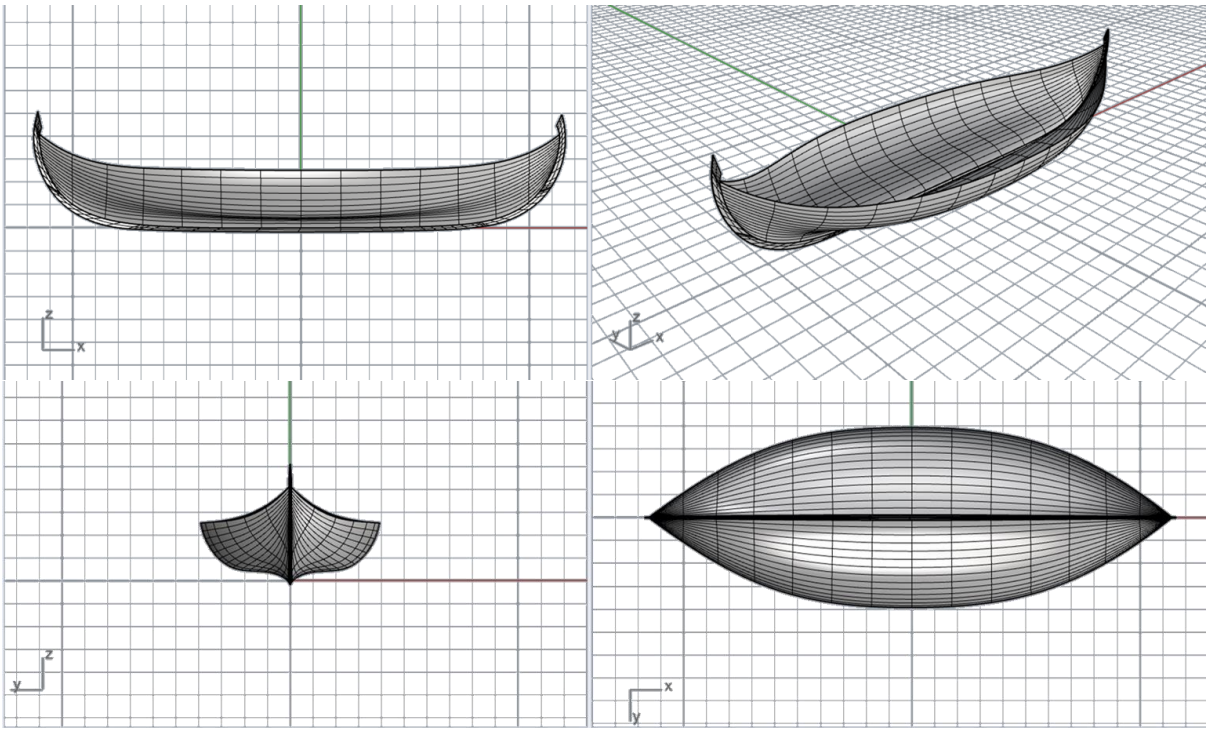

Figure 93 Faired outer surface of the Big Ship of Wismar used for calm water resistance calculations. (Hernandez Montfort based on the model by Ditta & Auer, in press).

V.4 Stability calculations

Stability calculations for the Big Ship of Wismar were done in ORCA 3D also using the faired surface of the outer hull as for the calm water resistance estimates. ORCA 3D computes the GZ curve of the vessel by calculating the GZ value for different heel angles, Figure 94. Different criteria on GZ values, heel angles, and areas below the GZ curve can be defined, as well as heeling moments due to wind. The same approach as for the Bremen cog by Tanner (2018) was followed and the same modern Bureau Veritas criteria as in Table 4 and Table 5 were applied. However, because of its low freeboard, the Big Ship of Wismar had a flooding angle below 25 degrees, which is the criterion on the maximum GZ value. The Bureau Veritas rules allow however for a more relaxed criterion, being that the angle of maximum GZ should be above 15 degrees instead of 25 degrees, under the condition that the area below the GZ curve up to the angle of maximum GZ is greater than the value given by 0.055 + 0.001 * (30° – angle of GZmax°), in meters*radians (Bureau Veritas, 2022, p. 79). This criterion was thus applied in the cases when the criterion of GZmax > 25 degrees was not fulfilled or when the flooding angle was less than 25 degrees. The complete list of criteria applied to the Big Ship of Wismar is shown in Table 13.

The heeling angle due to waves for the weather criterion is computed following Bureau Veritas rules from Equation 6.

Equation 6 Angle of heel due to waves

$$\theta_{waves} = 109kX_1X_2\sqrt{rs}; \qquad with\, r = 0.73 \pm \frac{0.6(OG)}{T_1}$$

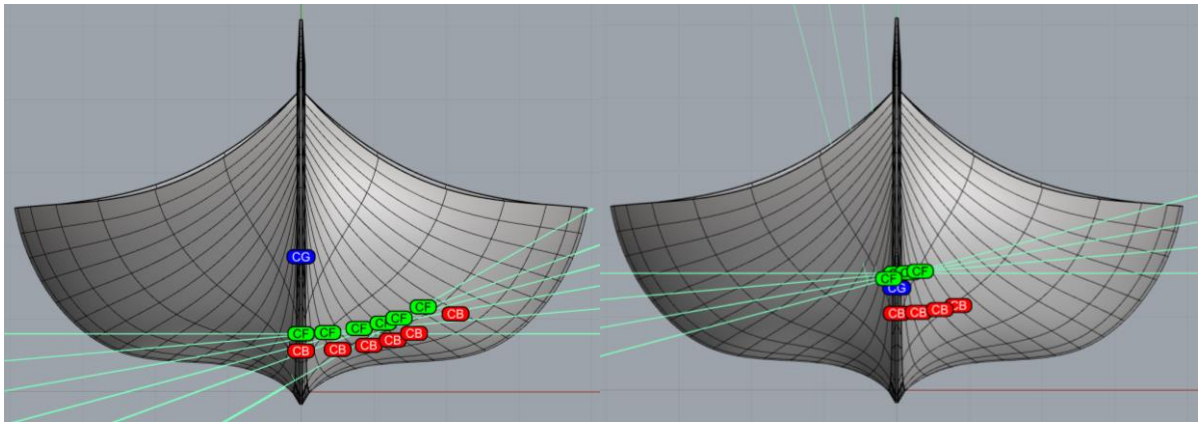

Figure 94 The Big Ship of Wismar under different heel angles. The position of the centre of gravity is shown in blue. The position of the centre of flotation, in green, and the position of the centre of buoyancy, in red, change as a function of the heeling angle. The green lines depict the waterlines at different heel angles. Left: the ship in empty condition and heel angles of 5, 10, 15, 120, and 30 degrees. Right: the ship in the Grågås codex condition and heel angles of 5, 10, and 15 degrees. (Hernandez Montfort based on the model by Ditta & Auer, in press).

Table 13
Stability criteria for the Big Ship of Wismar

Intact Stability
GM at free equilibrium >= 0.15
GZ at 30 degrees heel >= 0,2 m
Angle of GZmax >= 25 degrees
Area between 0 and 30 deg >= 3,151 m.deg
Area between 30 and 40 >= 1,1719 m.deg
Area between 0 and 40 >= 5,157 m.deg
Area between 0 and flooding angle >= 5,157 m.deg
Area between 30 and flooding angle >= 1,1719 m.deg
Angle of GZmax >= 15 degrees
Area between free equilibrium and angle GZmax >= 0.055+0.001(30-angleGZmax) m.rad
Weather criteria
Angle at equilibrium <= 16 deg
Angle at equilibrium <= deck immersion * 0,8 deg
Angle at equilibrium < flooding angle
Area b >= area a (accounting for wind and waves)
Angle at equilibrium + angle due to waves < flooding angle
Freeboard at equilibrium > 0,5 m

The values of k, X_1, X_2, and s are obtained from Table 14, Table 15, Table 16 and Table 17 respectively. OG is the distance between the centre of gravity of the ship and the waterline, being positive if the centre of gravity is above the waterline and negative if otherwise. T_1 is the mean draft of the ship. According to Bureau Veritas rules, the rolling period of the ship is given by Equation 7, where L_w is the length of the ship at the waterline.

Equation 7 Rolling period of the ship

$$T_R = \frac{2CB}{\sqrt{GM}}; \quad with\ C = 0.373 + 0.023\frac{B}{T_1} - 0.043\frac{L_w}{100}$$

Table 14
Values of k. (From Bureau Veritas, 2022, p. 82, Table 3).

$(A_k \times 100)/(L \times B)$	k
0.0	1.0
1.0	0.98
1.5	0.95
2.0	0.88
2.5	0.79
3.0	0.74
3.5	0.72
>= 4.0	0.7

Note. A_k is the lateral projected area of the keel. L the length of the ship and B the beam. Intermediate values are to be interpolated.

Table 15

Values of X_1 (From Bureau Veritas, 2022, p. 81, Table 1).

B/T_1	X_1
<= 2.4	1.00
2.5	0.98
2.6	0.96
2.7	0.95
2.8	0.93
2.9	0.91
3.0	0.90
3.1	0.88
3.2	0.86
3.4	0.82
>= 3.5	0.80

Note. Intermediate values are to be interpolated.

Table 16

Values of X_2 (From Bureau Veritas, 2022, p. 81, Table 2).

C_B	X_1
<= 2.4	1.00
2.5	0.98
2.6	0.96
2.7	0.95
2.8	0.93
2.9	0.91
3.0	0.90
3.1	0.88
3.2	0.86
3.4	0.82
>= 3.5	0.80

Note. C_B is the block coefficient of the hull. Intermediate values are to be interpolated.

Table 17

Values of s (From Bureau Veritas, 2022, p. 81, Table 2).

T_R	s
<= 6	0.100
7	0.098
8	0.093
12	0.065
14	0.053
16	0.044
18	0.038
>= 20	0.035

Note. T_R is the rolling period in s. Intermediate values are to be interpolated.

The resulting heel angles for each of the loading conditions considered are summarized in Table 18.

Table 18
Heel angle due to waves for stability calculations

Condition, draft	Empty	below wales	Grågås codex	1 m
Heel angle [deg]	21	15	14	18

The weather criteria were applied considering wind speeds of 5, 10, 15, and 20 knots. Additionally, they were applied to wind speeds equal to 150% the aforementioned speeds to take into account the effects of wind gust. This is the same approach followed by Tanner (2018) for the Bremen cog.

V.5 Seakeeping calculations

Seakeeping calculations were performed using the strip theory code SHIPMO from the Maritime Research Institute Netherlands (MARIN), which is a frequency domain code based on linear seakeeping theory. An information leaflet of SHIPMO can be found in Appendix D. One of the main requirements of strip theory is that the ship needs to be slender, that is, that the length is much greater than the beam or that the draught and beam are much smaller than the wavelength. The assumption of slenderness allows for solving the hydrodynamic problem in a two-dimensional strip-wise approach. To do so, the ship is divided in a series of strips or sections and the hydrodynamic forces are computed for each of them separately, Figure 95. The global forces on the ship are then obtained by means of integration along the length of the ship. For the Big Ship of Wismar and the Bremen cog, the hull geometry was defined by 40 equally spaced sections with 60 line-elements, see Figure 96, Figure 97, Figure 98 and Figure 99.

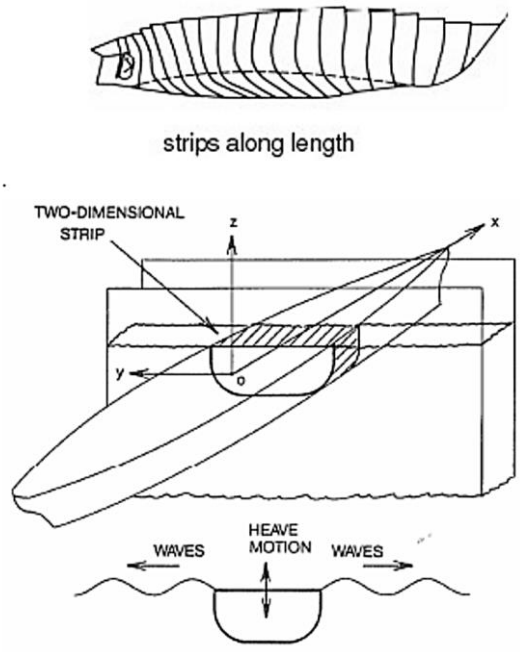

Figure 95 Strip theory method. (Lata & Thiagarajan, 2007, p. 1389, Fig. 2).

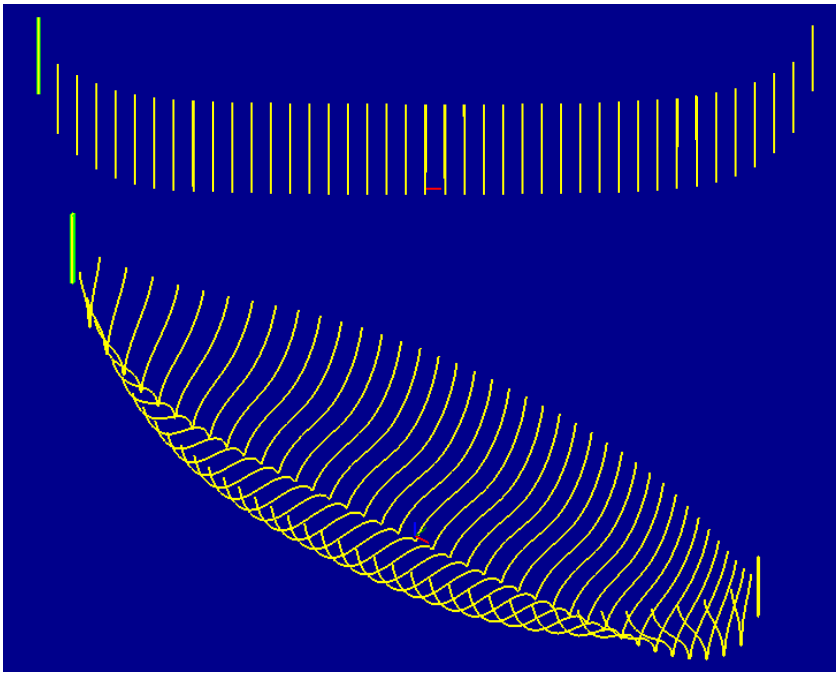

Figure 96 2D sections of the Big Ship of Wismar. Top: profile view. Bottom: 3D view. (Hernandez Montfort, generated with Rhinoceros and ConvertHullForm, https://converthullform.aerohydro.nl/)

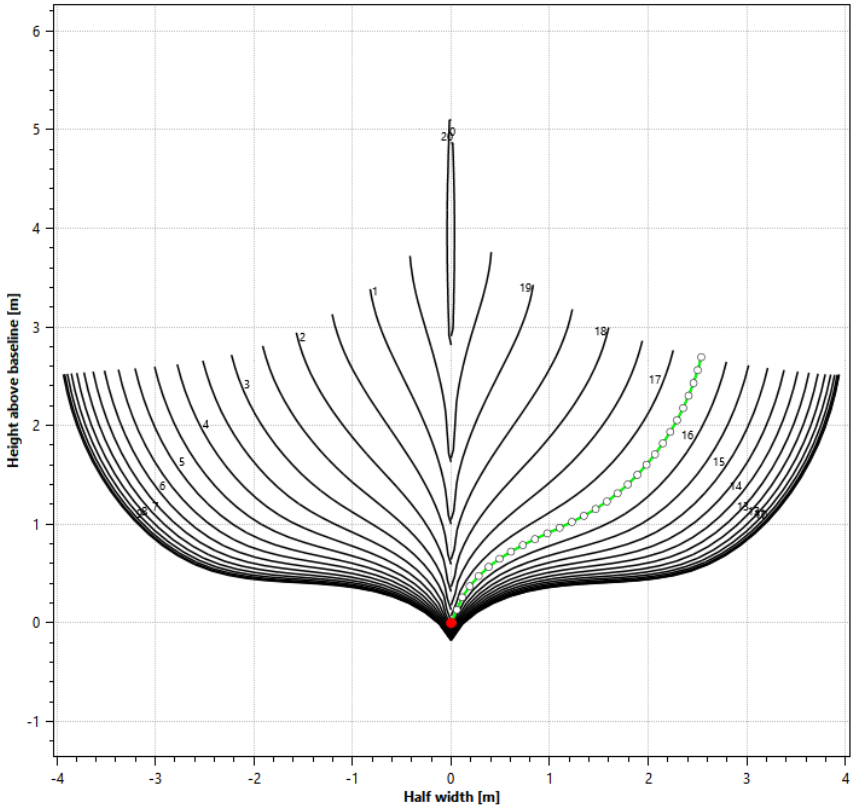

Figure 97 Body plan of the Big Ship of Wismar. The right half of the plot shows the foreside of the ship. The left half shows the aft side. The line elements are highlighted for one of the sections. (Hernandez Montfort, generated with Rhinoceros and ConvertHullForm, https://converthullform.aerohydro.nl/)

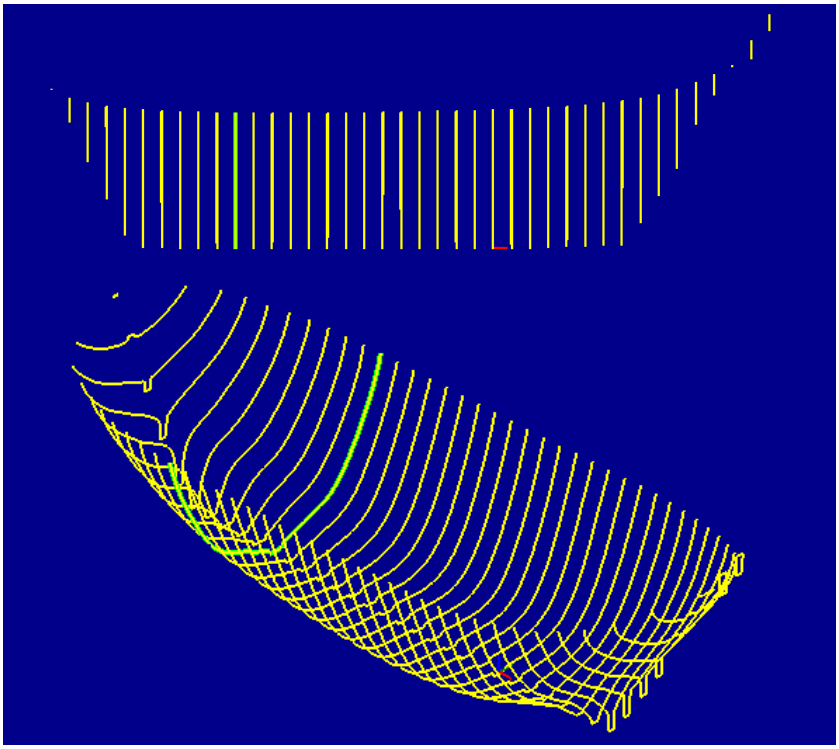

Figure 98 2D sections for the Bremen cog. Top: profile view. Bottom: 3D view. (Hernandez Montfort, generated with Rhinoceros and ConvertHullForm, https://converthullform.aerohydro.nl/)

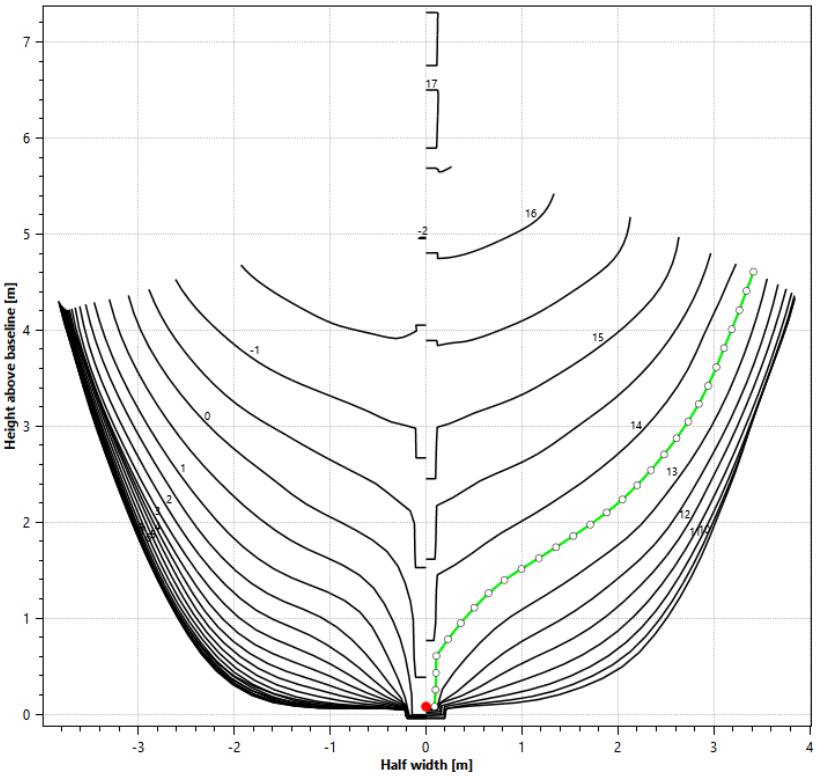

Figure 99 Body plan of the Bremen cog. The right half of the plot shows the foreside of the ship. The left half shows the aft side. The line elements are highlighted for one of the sections. (Hernandez Montfort, generated with Rhinoceros and ConvertHullForm, https://converthullform.aerohydro.nl/)

The hydrodynamic forces are assumed to be linear, which implies that the hydrodynamic problem can be defined as the superposition of two smaller problems: the diffraction and the radiation problem, Figure 100. Moreover, it is assumed that no interaction occurs between the different strips and so the hydrodynamic forces of each strip are equal to the ones that would be experienced by a section of an infinitely long cylinder with an identical cross-sectional geometry (Lloyd, 1989, p. 171), Figure 101. Once the hydrodynamic forces are obtained, the equations of motion are solved applying Newton's laws.

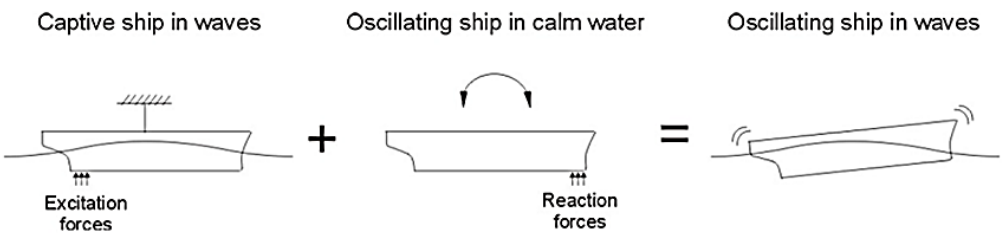

Figure 100 Superposition principle in linear seakeeping theory. (Reproduced with permission from the Maritime Research Institute Netherlands).

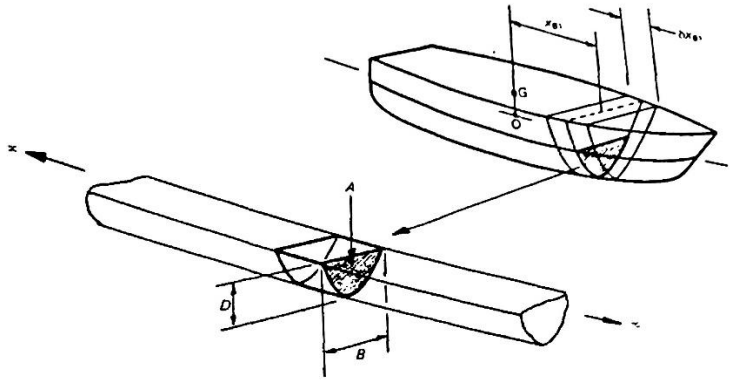

Figure 101 Representation of a hull's strip by an equivalent infinite cylinder. (Lloyd, 1989, p. 171, Fig. 9.1).

Other assumptions in strip theory are that the ship is rigid (it does not bend with the effects of the waves), that the speed is moderate (no planning effects), that the motions are small (no changes in wetted surface), the hull sections have vertical sides, the water depth is much greater than the draft (deep water approximations can be applied), and that the presence of the hull does not influence the waves (Froude-Krylov hypothesis) (Lloyd, 1989, p. 170).

Despite these theoretical limitations, strip theory is commonly used in the shipbuilding industry to assess the ship motions in moderate weather conditions and compare hull forms at early design stages.

Since strip theory calculations are done in the frequency domain, space and time can be separated and all forces and responses are treated as periodical entities defined by a sinusoid, with an amplitude, frequency, and phase, see Equation 8 and Equation 9.

Equation 8 Expression of the incoming wave

$$\zeta = \zeta_0 \sin(\omega_e t) \text{ in meters}$$

ζ_0 being the elevation at the origin; ω_e the encounter wave frequency; t the time

Equation 9 Expression of the resulting ship motions

$$x_i = x_{i0} \sin(\omega_e t + \delta_i) \text{ in meters for translations or radians for rotations}$$

x_i being the amplitude of the motion and δ_i its phase with respect to the wave, both being functions of the wave heading, wave frequency and ship's speed. With i=1 to 6 for the six degrees of freedom. The six degrees of freedom of a ship are the three translation motions, surge, sway, and heave, and the three rotation motions, roll, pitch, and yaw, see Figure 102.

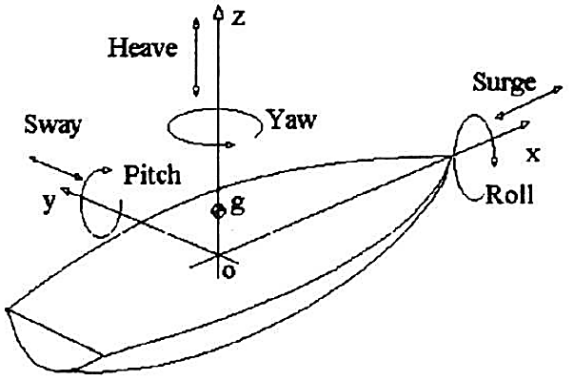

Figure 102 Definition of the six degrees of freedom of a ship. (Neves, Perez, & Valerio, 1999, p. 1392).

In frequency domain, the ship responses are evaluated in regular waves, and since linearity is assumed, the amplitudes of the responses are proportional to the wave amplitude. The results are therefore expressed as Response Amplitude Operators (RAO), which describes the amplitude of a given motion per meter regular wave amplitude as a function of the wave period or frequency, and the phase of the motion with respect to the incoming wave. The RAO of the translation motions heave, sway and surge are given thus in m/m while the rotation motions pitch, roll and yaw are given in deg/m, see Figure 103.

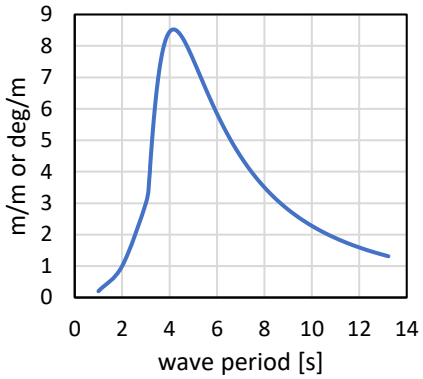

Figure 103 Example of RAO for a hypothetical motion. (Hernandez Montfort).

In seakeeping codes like SHIPMO, based on potential theory, motion damping is the result of the energy dissipated by the waves created by the moving hull. For motions such as pitch and heave this is the main source of damping. However, this is not the case for the roll motion for which other factors are more important, such as the creation of eddies at sharp corners of the bilge or appendages, the friction forces acting on the hull, and the hydrodynamic lift effects on the hull. These additional sources of energy dissipation are caused by viscosity, hydrodynamic lift effects, and flow separation, which are not considered in potential theory. These non-potential damping contributions were calculated in SHIPMO following the Ikeda and Tanaka semi-empirical method (Himeno, 1981). The roll damping from the sails was not accounted for.

Regular waves do not however occur in real life at sea. Instead, sea waves are of an irregular character. The irregular waves can however be approximated by the linear superposition of many sinusoidal waves with different amplitudes, frequencies, and phases. The relative importance of each sinusoidal component present in an irregular wave is expressed in the form of a wave amplitude energy density spectrum, also simply referred to as wave spectrum S_ζ (Lloyd, 1989, p. 99). Wave spectra are defined by the significant wave height (Hs) and the wave period. The wave period can be defined as the peak of the spectrum (peak period or Tp), the average period value of the spectrum (mean period or T_1), or the average time between two surface elevation zero up-crossings (zero up-crossing period or T_2), Figure 104. Several formulations exist to define the theoretical shape of wave spectra depending on whether they represent developing or fully developed seas. One of the most common theoretical wave spectra is the Joint North Sea Wave Observation Project (JONSWAP) spectrum. This wave spectrum is used in the current work to derive the ship motions in irregular waves. For a JONSWAP spectrum the peak period and zero up-crossing periods are related as $Tp = 1.285\ T_2$.

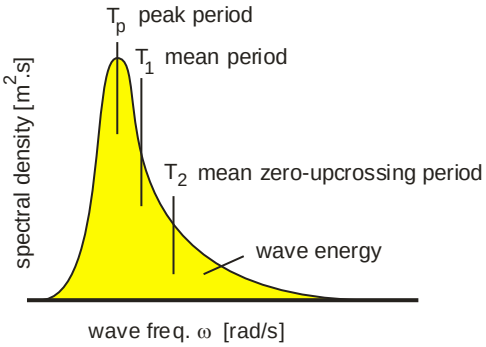

Figure 104 Wave spectrum definition. (Reproduced with permission from the Maritime Research Institute Netherlands).

The energy density spectra of the ship motions in irregular waves are obtained by means of spectral convolution, combining the wave spectra and the RAO of the ship motions, Equation 10.

Equation 10 The energy density spectra of the ship motions

$$S_{x_i}(\omega_e) = S_\zeta(\omega_e) RAO_{x_i}^2 \quad in \frac{m^2}{rad} \; or \frac{rad^2}{rad}$$

The root-mean-square (RMS or σ) of a ship motion in irregular waves is then obtained from the area under the energy density spectrum as shown in Equation 11.

Equation 11 RMS of ship motion from the energy density spectrum

$$\sigma_{x_i} = \sqrt{\int S_{x_i}(\omega_e) d\omega_e}$$

Since the values of the response of a ship's motion follow a normal or Gaussian distribution, the RMS value indicates the probability of occurrence of a given response value. As shown in Figure 105, 68.2 % of the time the response will be within +/- the RMS value with respect to the mean value (which is theoretically zero). 95.4 % of the time the response will be within +/- 2 times the RMS.

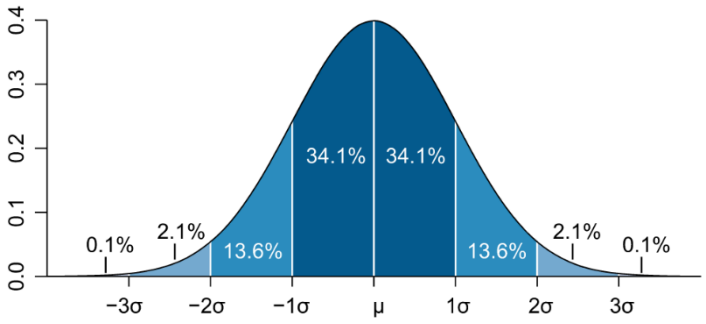

Figure 105 Relation between the RMS (σ) and the probability of occurrence of a response's value. (Reproduced with permission from the Maritime Research Institute Netherlands).

While the values of the ship motions follow a normal distribution, the values of the amplitudes follow a Rayleigh distribution as shown in Figure 106. The mean of the highest 1/3rd of the amplitudes, also referred to as Significant Single Amplitude or SSA, is equal to 2σ. The mean of the highest 1/3rd of the peak-to-trough values, the Significant Double Amplitude or SDA, is equal to 4σ.

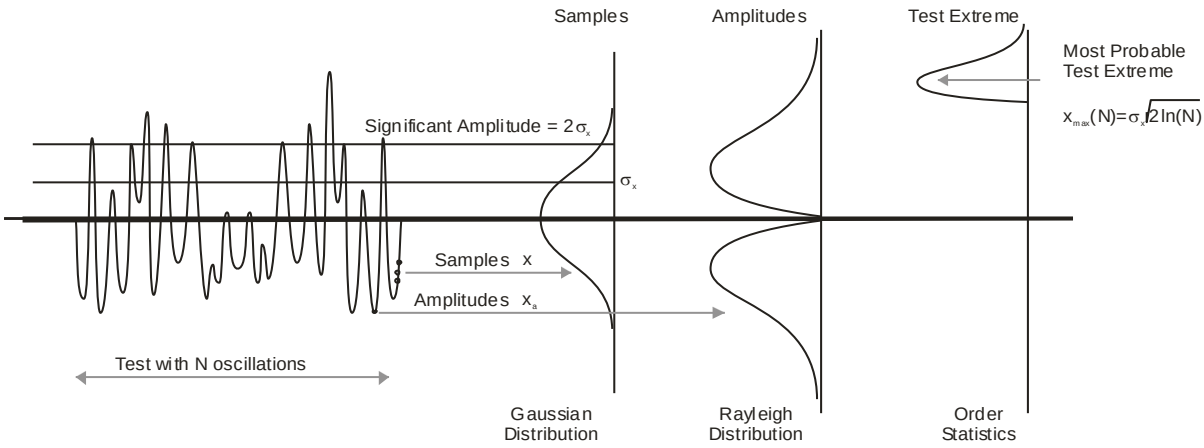

Figure 106 Distributions of samples, amplitudes, and extremes for a response in irregular waves. (Reproduced with permission from the Maritime Research Institute Netherlands).

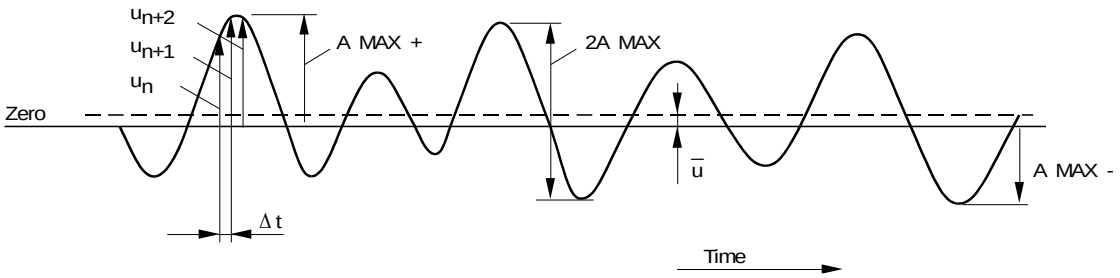

Figure 107 Definition of amplitudes for a response in irregular waves. A is the single amplitude, 2A the double amplitude, u the sample value and ū the mean value. (Reproduced with permission from the Maritime Research Institute Netherlands).

Figure 107 shows the definition of amplitudes for a response in irregular seas. For Rayleigh distributed values, the Most Probable Maximum (MPM) statistically relates to the Significant Double Amplitude as shown in Equation 12. As shown in the equation, the MPM depends on the exposure time. In the offshore industry, it is common to assume a MPM equal to the SDA, which would translate to about 3000 oscillations and about 8 hours of exposure for a motion with a period of 10 seconds.

Equation 12 Relation between SDA and MPM

$$MPM = \frac{SDA}{4}\sqrt{2\ln(N)} \qquad with\ N\ being\ the\ number\ of\ oscillations$$

As already mentioned, wave spectra are defined by the significant wave height and the wave period. The maximum significant wave height of a wave for a specific peak period before it breaks is governed by the average wave steepness defined in Equation 13. For wave peak periods below 8 seconds the largest average wave steepness is 0.104. For wave periods above 15 seconds the maximum average wave steepness is 0.062. For periods between these two values the value for the maximum average wave steepness can be interpolated (Det Norske Veritas, 2010, p. 33).

Equation 13 Wave steepness definition

$$Steepness = \frac{H_s}{T_p^2} \quad with\ Hs\ the\ significant\ wave\ height\ and\ Tp\ the\ peak\ period$$

The significant wave heights and periods that occur in real sea conditions depend on the geographical area. The occurrences of different wave heights and periods are commonly represented in the so-called wave scatter diagrams, which show the joint statistics of significant wave height and average zero up-crossing periods based on wave measurements (Olliver, Dacunha, & Hogben, 1986). The scatter diagrams for the North Sea and the Baltic Sea are shown in Figure 108 and Figure 109, respectively. They show the probability of occurrence for different significant wave heights and zero up-crossing periods expressed in per thousands. It should be noted that since scatter diagrams are based on zero up-crossing periods, they tend to emphasise short waves but underestimate the frequency of occurrence of long period swell underneath a local wind driven sea.

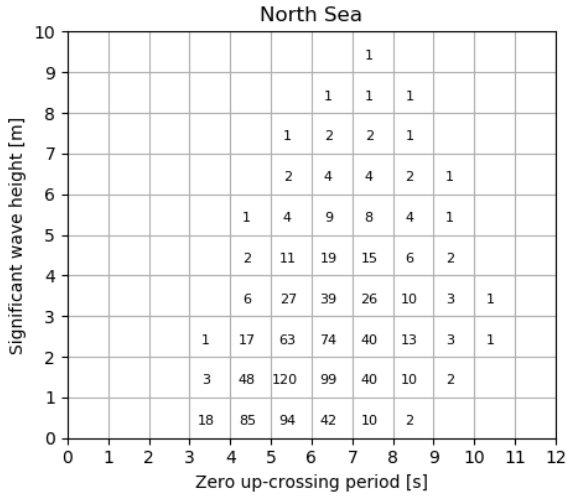

Figure 108 Scatter diagram for the North Sea. (Hernandez Montfort, after data by Olliver, Dacunha, & Hogben, 1986).

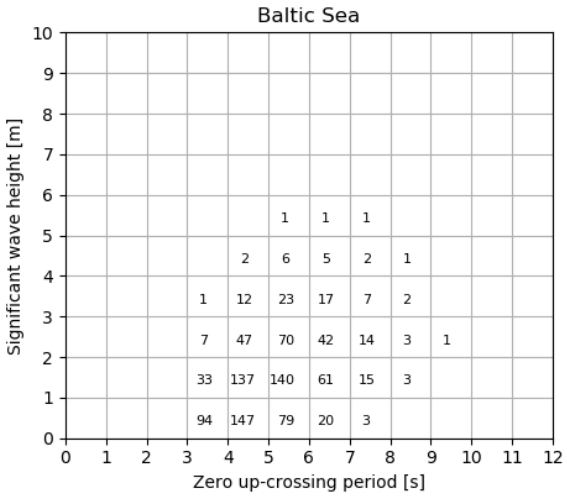

Figure 109 Scatter diagram for the Baltic Sea. (Hernandez Montfort, after data by Olliver, Dacunha, & Hogben, 1986).

By utilizing the data presented in the scatter diagrams, one can thus determine the likelihood of occurrence of various sea state conditions. This information, when combined with the ship motions at each sea state condition, can help determine the maximum wave heights and the frequency of exceedance (downtime) for a given criterion. For example, in Figure 110, the line shows the sea state conditions in which the MPM of roll equals 30 degrees. For all the sea state conditions above the line this criterion would be exceeded, which accounts for 45.4 % of the time for that given scatter diagram.

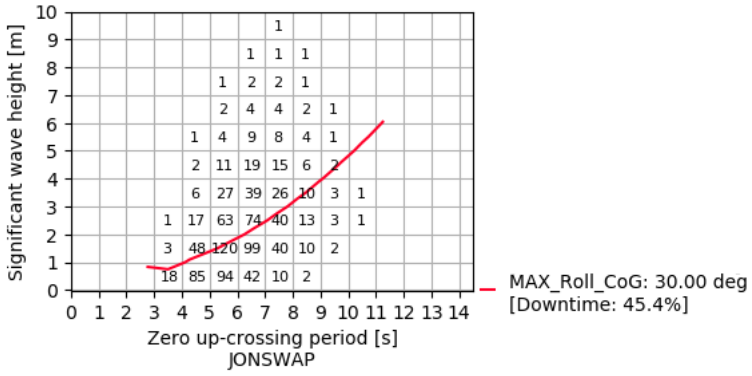

Figure 110 Example of ship motion plotted on a wave scatter diagram and related downtime. The downtime. (Hernandez Montfort).

For the Big Ship of Wismar and the Bremen cog, the most relevant criteria are related to flooding angles and the freeboard. Therefore, a criterion on the MPM of roll equal to the flooding angle is applied. An exposure time of 8 hours is chosen. The second criterion on the freeboard was set as the relative water elevation exceeding the freeboard height 30 times per hour, or once every two

minutes. The exposure time and the number of exceedances per hour used here are arbitrary values but they will serve as basis for comparison of the two vessels. The relative water elevation is governed by the incoming wave elevation and the ship motions.

Ships with squared sails without fore and aft sails such as jibs or spankers cannot sail against the wind and therefore both the Big Ship of Wismar and the Bremen cog would have been able to sail mostly with winds from the aft or from the stern quarter (Shaw, 2016, p. 20). Sailing experiments with full scale replicas show however that Nordic cargo ships such as the Big Ship of Wismar could in calm seas, sail up to 60 degrees against the wind at speeds of about 1.5 to 2 knots (Bruun, 1997, p. 1289). Experiments with replicas from the Bremen cog show that the ship could sail 67 to 75 degrees against the wind but with considerable leeway (Weski, 1999, p. 373). Because wind and wave direction are linked, the relevant ship motions from the seakeeping calculations are the ones with waves from the stern and up to about 60-70 degrees against the wind. Following the coordinate convention from SHIPMO, Figure 111, that means wave headings from 0 to 110-120 degrees.

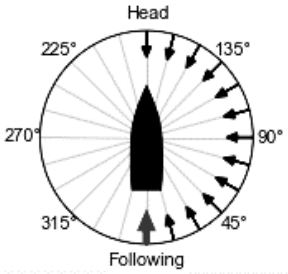

Figure 111 Wave heading convention used in seakeeping calculations. (Hernandez Montfort).

VI. Calculations results

In this chapter the results of the different calculations are presented. They will be discussed in the next chapter.

VI.1 Weight and inertia calculations

VI.1.1 The Big Ship of Wismar

As already mentioned in section V.2.2, two weight estimates were performed for the Big Ship of Wismar: one with an homogenous moisture content for the timbers following the approach by Tanner (2018) for the Bremen cog, and one with two different moisture content values for the timbers above and below water following the approach by Englert (2000) for the Lynaes 1.

For the approach using 27 % moisture content for all timbers, the results of mass and moments of inertia for the different elements in the ship are shown in Table 46 in Appendix A. The element ropes & other equipment was modelled as a mass point and thus no volume is shown. The density of the cargo is derived from its mass and volume. The results for the whole ship at the different loading conditions are presented in Table 19.

Table 19
Mass, inertia and roll period for the Big Ship of Wismar with homogeneous moisture content.

Draft [m]	Mass [kg]	Cargo [kg]	X_{COG} [m]	Y_{COG} [m]	Z_{COG} [m]	GM [m]	Ix_{COG} [kgm^2]	Iy_{COG} [kgm^2]	Iz_{COG} [kgm^2]	kxx [m]	Kyy [m]	kzz [m]	kxx [%B]	kyy [%L]	kzz [%L]	T_{roll} [s]
0.77	24219	0	11.47	0.00	1.74	4.86	217490	902755	877302	3.00	6.11	6.02	38%	28%	27%	3.3
1.60	101571	77352	11.55	0.00	1.40	3.09	471768	1521489	1722870	2.16	3.87	4.12	27%	18%	19%	2.9
1.30	70400	46181	11.54	0.00	1.47	3.46	366306	1272483	1382179	2.28	4.25	4.43	29%	19%	20%	3.0
1.00	42591	18372	11.51	0.00	1.61	4.05	269881	1046915	1075818	2.52	4.96	5.03	32%	23%	23%	3.0

Note. The moments of inertia are given at the centre of gravity of the ship.

The results for the condition using 35 % moisture content for the timbers above water and 50 % moisture content for the timbers below water are presented in Table 47 in Appendix A for the individual elements and in Table 20 for the whole ship.

Table 20
Mass, inertia and roll period for the Big Ship of Wismar with heterogeneous moisture content.

Draft [m]	Mass [kg]	Cargo [kg]	X_{COG} [m]	Y_{COG} [m]	Z_{COG} [m]	GM [m]	Ix_{COG} [kgm^2]	Iy_{COG} [kgm^2]	Iz_{COG} [kgm^2]	kxx [m]	Kyy [m]	kzz [m]	kxx [%B]	kyy [%L]	kzz [%L]	T_{roll} [s]
0.80	26162	0	11.46	0.00	1.85	4.62	218475	964440	942292	2.89	6.07	6.00	37%	28%	27%	3.2
1.60	101571	75409	11.55	0.00	1.40	3.09	478028	1571318	1766636	2.17	3.93	4.17	28%	18%	19%	3.0
1.30	70400	44238	11.53	0.00	1.47	3.46	372533	1322313	1425945	2.30	4.33	4.50	29%	20%	20%	3.0
1.00	42591	16429	11.51	0.00	1.62	4.04	276153	1096963	1119835	2.55	5.08	5.13	32%	23%	23%	3.0

VI.1.1 The Bremen cog

The results of mass and moments of inertia at the origin for the different elements in the ship are shown in Table 48 in Appendix A. The iron nails were modelled as a mass point and their contribution to the ship's inertia was disregarded. The density of some layers was adjusted to match the mass of the element as used in ORCA 3D for the stability calculations: the layer 'New' which included many elements of many sublayers with the same name, the layers 'Sail Area' and 'Flag', and the layer 'Anchors'. For the layer 'Min Ballast' the density was adjusted from 1600 to 1531 to take into account the 650 kg that were removed from the ballast and that correspond to elements that needed to be remodelled as closed polysurfaces (e.g. the keelson) as explained in section V.2.3. The density of the cargo is derived from its mass and volume.

The results for the whole ship at the different loading conditions are presented in Table 21. The same results but considering a moisture content of 35% for all oak timbers (850 kg/m^3) and 50% moisture content (1000 kg/m^3) for the hull planks up until the protruding beams, strakes 1 to 8, are presented in Table 22. The ship becomes then 3 tons heavier. The cargo is reduced to keep the drafts constant. For the Grågås condition the cargo would become 105 tons instead of 108 tons, for the beams above water condition the cargo would become 40 tons instead of 43 tons.

Table 21
Mass, inertia and roll period for the Bremen cog

Draft [m]	Mass [kg]	Cargo [kg]	X_{COG} [m]	Y_{COG} [m]	Z_{COG} [m]	GM [m]	Ix_{COG} [kgm^2]	Iy_{COG} [kgm^2]	Iz_{COG} [kgm^2]	kxx [m]	Kyy [m]	kzz [m]	kxx [%B]	kyy [%L]	kzz [%L]	T_{roll} [s]
Grågås	170356	108003	7,7	0,0	2,0	1.30	1295453	7050953	6848793	2,76	6,43	6,34	36%	28%	27%	5,8
Beams	105698	43345	7,6	0,0	2,2	0.83	905970	2855403	2575057	2,93	5,20	4,94	38%	22%	21%	7,8
Ballast	62353	0	7,5	0,0	2,7	0.37	774878	2188919	1860411	3,53	5,92	5,46	46%	26%	24%	13,9

Table 22
Mass, inertia and roll period for the Bremen cog with higher timber moisture content

Draft [m]	Mass [kg]	Cargo [kg]	X_{COG} [m]	Y_{COG} [m]	Z_{COG} [m]	GM [m]	Ix_{COG} [kgm^2]	Iy_{COG} [kgm^2]	Iz_{COG} [kgm^2]	kxx [m]	Kyy [m]	kzz [m]	kxx [%B]	kyy [%L]	kzz [%L]	T_{roll} [s]
Grågås	170356	105018	7,7	0,0	2,1	1.27	1319391	7295351	7101005	2,78	6,54	6,46	36%	28%	28%	5,9
Beams	105698	40360	7,7	0,0	2,3	0.77	912270	2866425	2599186	2,94	5,21	4,96	38%	22%	21%	8,0
Ballast	65339	0	7,7	0,0	2,7		786869	2243406	1934657	3,47	5,86	5,44	45%	25%	23%	

VI.2 Speed estimates for the Big Ship of Wismar

The required power to overcome the calm water resistance at different speeds for the Big Ship of Wismar according to the Holtrop & Mennen method is shown in Figure 112. In Table 23, the wetted surface of the hull is given. The power provided by the sails using Gerr's (1995) power per square meter estimates is presented in Table 24, while the speed potential is shown in Table 25.

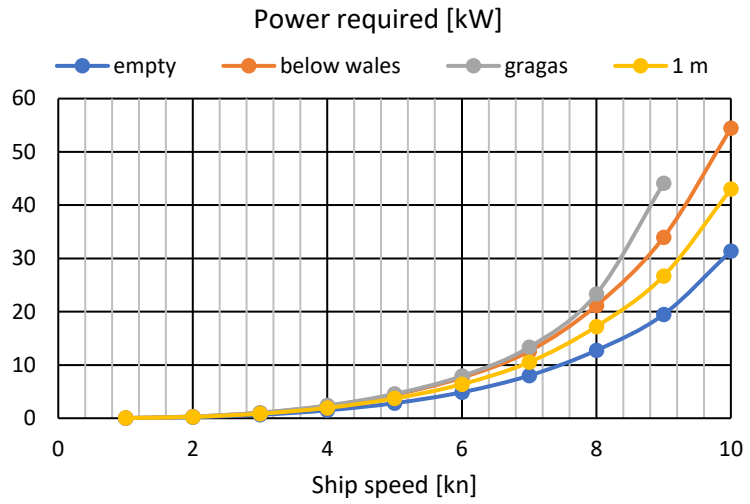

Figure 112 Power requirements for the Big Ship of Wismar. (Hernandez Montfort).

Table 23
Wetted surface for the Big Ship of Wismar

Condition	Empty	Draft below wales	Grågås	Draft 1 m
Wetted surface [m^2]	84.6	118.4	135.4	99.7

Table 24
Power generated by square sail for the Big Ship of Wismar

Wind force	Wind speed [kn]	Power per m^2 [kW/m^2]	Sail Area [m^2]	Power [kW]	Power with 70% efficiency [kW]	Power with 40% efficiency [kW]
3	9-10	0.118	150	17.7	12.4	7.1
4	13-15	0.161	150	24.2	16.9	9.7
5	19-21	0.312	150	46.8	32.8	18.7

Table 25
Speed potential, in knots, of the Big Ship of Wismar

		Speed [kn] with 70% sail efficiency				Speed [kn] with 40% sail efficiency			
Wind force	Wind speed [kn]	Empty	Below wales	Grågås	1 m draft	Empty	Below wales	Grågås	1 m draft
3	9-10	7.9	7.0	6.8	7.3	6.7	5.8	5.7	6.2
4	13-15	8.6	7.5	7.4	8.0	7.3	6.4	6.3	6.8
5	19-21	10.1	8.9	8.5	9.4	8.9	7.7	7.5	9.5

VI.3 Stability calculations for the Big Ship of Wismar

Stability calculations were performed for the ship in empty condition considering both a heterogeneous moisture content depending on whether the timbers were above or below water, and a homogeneous 27% moisture content for all timbers. Because the GM and displacement remain identical in both cases for all other conditions, see Table 19 and Table 20, the stability results are identical as well. For the empty condition, the difference in GM is just 5 cm and the difference in weight less than 2 tons. These differences have a very small impact on the stability of the vessel, especially for heeling angles below the flooding angle, the angle at which the edge of the hull goes underwater.

For the empty condition, the stability curve is shown in Figure 113. This includes the righting arm GZ for both weight estimate approaches and the heeling arms due to different wind speeds. The heeling angles due to wind and the distances from the water level to the pump and the edge of the hull (freeboard) for different wind speeds are shown in Table 26. The GM, maximum GZ, angle of maximum GZ, and flooding angle are given in Table 27.

For the condition with the waterline below the pine wales, the Grågås condition, and the condition with a draft of 1 m, the stability curves are shown in Figure 114, Figure 115, and Figure 116, respectively. The heeling angles due to wind and the distances from the water level to the pump and the edge of the hull for different wind speeds are shown in Table 28, Table 30 and Table 32. The GM, maximum GZ, angle of maximum GZ, and flooding angle are given in Table 29, Table 31 and Table 33.

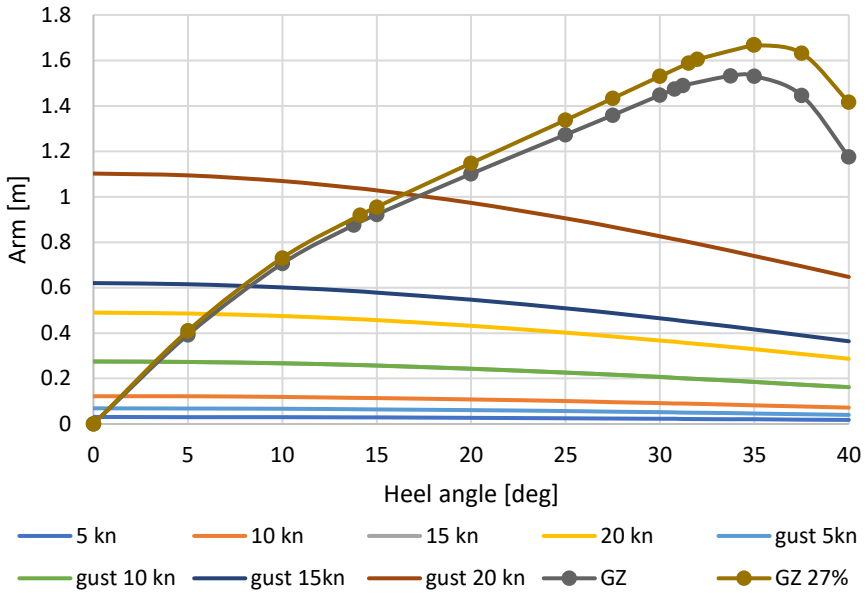

Figure 113 Stability curve for the empty condition. (Hernandez Montfort).

Table 26
Heeling angles and freeboards due to wind for empty condition.

	Heterogeneous MC			27 % MC		
Wind speed	Heel angle [deg]	Freeboard [m]	Pump above water [m]	Heel angle [deg]	Freeboard [m]	Pump above water [m]
No wind	0.00	1.72	1.35	0.00	1.75	1.38
5 kn	0.38	1.70	1.33	0.39	1.72	1.36
10 kn	1.52	1.62	1.26	1.57	1.64	1.29
15 kn	3.45	1.49	1.15	3.56	1.51	1.18
20 kn	6.30	1.31	1.0	6.56	1.32	1.02
5 kn + gust	0.85	1.67	1.30			
10 kn + gust	3.45	1.49	1.15			
15 kn +gust	8.22	1.19	0.90			
20 kn +gust	17.27	0.68	0.49			

Note. Because the differences do not impact the stability performance of the ship, the wind gust conditions were only computed for the case with heterogenous timber moisture content.

Table 27
Stability parameters for empty condition.

	Heterogeneous MC	27 % MC
GM [m]	4.62	4.86
GZmax [m]	1.53	1.67
Angle at GZmax [deg]	33.7	35.0
Flooding angle [deg]	31.2	32.0

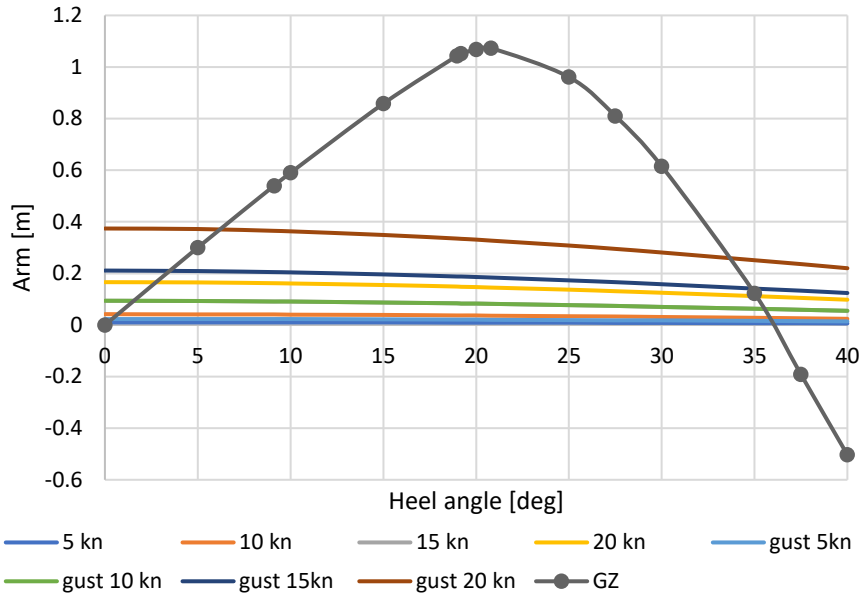

Figure 114 Stability curve for the water below wales condition. (Hernandez Montfort).

Table 28
Heeling angles and freeboards due to wind for the water below wales condition.

Wind speed	Heel angle [deg]	Freeboard [m]	Pump above water [m]
No wind	0.00	1.22	0.85
5 kn	0.17	1.20	0.84
10 kn	0.69	1.17	0.81
15 kn	1.55	1.11	0.76
20 kn	2.76	1.03	0.69
5 kn + gust	0.39	1.19	0.83
10 kn + gust	1.55	1.11	0.76
15 kn +gust	3.49	0.98	0.65
20 kn +gust	6.18	0.80	0.50

Table 29
Stability parameters for the water below wales condition.

GM [m]	3.46
GZmax [m]	1.07
Angle at GZmax [deg]	20.8
Flooding angle [deg]	19.2

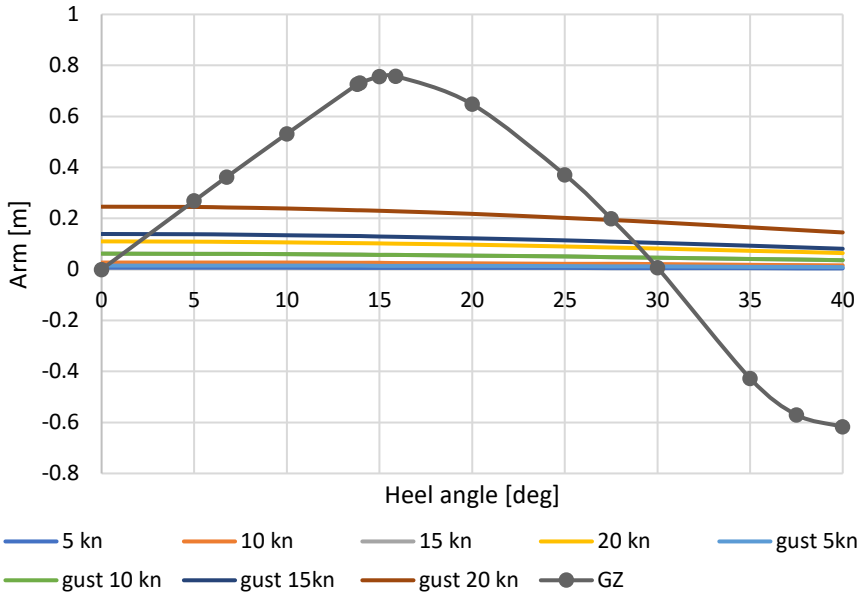

Figure 115 Stability curve for the Grågås condition. (Hernandez Montfort).

Table 30
Heeling angles and freeboards due to wind for the Grågås condition.

Wind speed	Heel angle [deg]	Freeboard [m]	Pump above water [m]
No wind	0.00	0.92	0.56
5 kn	0.13	0.91	0.55
10 kn	0.51	0.88	0.53
15 kn	1.14	0.84	0.49
20 kn	2.03	0.78	0.44
5 kn + gust	0.29	0.90	0.54
10 kn + gust	1.14	0.84	0.49
15 kn +gust	2.57	0.74	0.41
20 kn +gust	4.55	0.61	0.30

Table 31
Stability parameters for the Grågås condition.

GM [m]	3.09
GZmax [m]	0.76
Angle at GZmax [deg]	15.9
Flooding angle [deg]	13.9

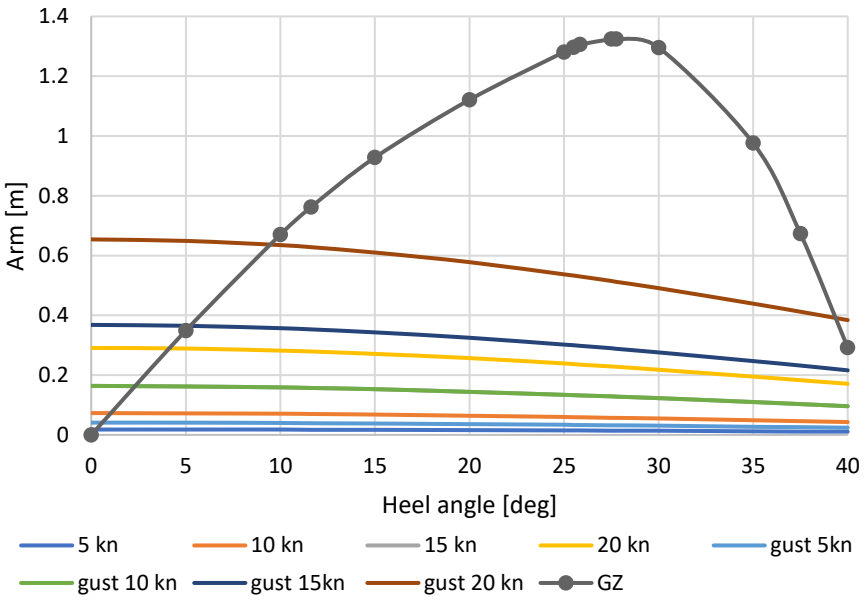

Figure 116 Stability curve for the 1 m draft condition. (Hernandez Montfort).

Table 32
Heeling angles and freeboards due to wind for the 1 m draft condition.

Wind speed	Heel angle [deg]	Freeboard [m]	Pump above water [m]
No wind	0.00	1.52	1.15
5 kn	0.26	1.50	1.13
10 kn	1.03	1.45	1.09
15 kn	2.32	1.36	1.02
20 kn	4.13	1.24	0.91
5 kn + gust	0.58	1.48	1.12
10 kn + gust	2.32	1.36	1.02
15 kn +gust	5.24	1.17	0.85
20 kn +gust	9.45	0.90	0.63

Table 33
Stability parameters for the 1 m draft condition.

GM [m]	4.04
GZmax [m]	1.32
Angle at GZmax [deg]	27.8
Flooding angle [deg]	25.8

The complete stability calculations results are documented in Appendix B. The following tables summarize the fulfilment of the criteria for the different loading conditions. An X is indicated if a criterion is not fulfilled. As shown in Table 34, the Grågås condition and the condition with the draft below the wales do not fulfil the criterion on the maximum GZ occurring at angles above 25, however they do fulfil the alternative criterion of it occurring at angles above 15 degrees and the criterion on the area below the curve. The criteria relating to angles above 30 degrees are also not fulfilled but these would not be applicable as the flooding angle is lower than 25 degrees and thus the ship would not operate in such large heeling angles. It can be concluded therefore that the ship fulfils the intact stability criteria for all conditions.

Table 34
Intact stability criteria fulfilment

	Empty	below wales	Grågås	1 m draft
GM at free equilibrium >= 0.15	Pass	Pass	Pass	Pass
GZ at 30 degrees heel >= 0,2 m	Pass	Pass	X	Pass
Angle of GZmax >= 25 degrees	Pass	X	X	Pass
Area between 0 and 30 deg >= 3,151 m.deg	Pass	Pass	Pass	Pass
Area between 30 and 40 >= 1,1719 m.deg	Pass	X	X	Pass
Area between 0 and 40 >= 5,157 m.deg	Pass	Pass	Pass	Pass
Area between 0 and flooding angle >= 5,157 m.deg	Pass	Pass	Pass	Pass
Area between 30 and flooding angle >= 1,1719 m.deg	Pass	X	X	X
Angle of GZmax >= 15 degrees	-	Pass	Pass	Pass
Area between free equilibrium and angle GZmax >= 0.055+0.001(30-angleGZmax) m.rad	-	Pass	Pass	Pass

Note. For the empty condition the last two criteria are not relevant because the other stricter ones are fulfilled.

Regarding the stability considering wind and waves, the conditions of 1 m draft and the draft below the wales would fulfil all criteria with winds up to 20 knots plus wind gust with a full sail, Table 38 and Table 36.

For the empty condition, Table 35, the criteria are fulfilled up to 20 knots winds or 15 knots plus extra wind gust. If the sail area would be reduced at the highest wind speeds the stability criteria would also be fulfilled. For the Grågås condition, Table 37, the criterion is not fulfilled even in the lowest wind speeds because a heel angle due to waves of 14 degrees is considered, which is equal to the flooding angle. Note that these criteria consider heel angles due to waves of 21 degrees for the empty condition, 15 degrees for the condition with the draft below wales, 18 degrees for the 1 m draft condition, and 14 degrees for the Grågås condition. The seakeeping calculations, covered in the next section, show that these values are quite extreme and most of the time the roll angles due to waves would be lower.

Table 35
Weather stability criteria fulfilment for the empty condition

	5 kn	10 kn	15 kn	20 kn	5 kn + gust	10 kn + gust	15 kn + gust	20 kn + gust
Angle at equilibrium <= 16 deg	Pass	Pass	Pass	Pass	Pass	Pass	Pass	X
Angle at equilibrium <= deck immersion * 0,8 deg	Pass	Pass	Pass	Pass	Pass	Pass	Pass	Pass
Angle at equilibrium < flooding angle	Pass	Pass	Pass	Pass	Pass	Pass	Pass	Pass
Area b >= area a	Pass	Pass	Pass	X	Pass	Pass	X	X
Angle at equilibrium + angle due to waves < flooding angle	Pass	Pass	Pass	Pass	Pass	Pass	Pass	X
Freeboard at equilibrium > 0,5 m	Pass	Pass	Pass	Pass	Pass	Pass	Pass	Pass

Table 36
Weather stability criteria fulfilment for the water below wales condition

	5 kn	10 kn	15 kn	20 kn	5 kn + gust	10 kn + gust	15 kn + gust	20 kn + gust
Angle at equilibrium <= 16 deg	Pass	Pass	Pass	Pass	Pass	Pass	Pass	Pass
Angle at equilibrium <= deck immersion * 0,8 deg	Pass	Pass	Pass	Pass	Pass	Pass	Pass	Pass
Angle at equilibrium < flooding angle	Pass	Pass	Pass	Pass	Pass	Pass	Pass	Pass
Area b >= area a	Pass	Pass	Pass	Pass	Pass	Pass	Pass	X
Angle at equilibrium + angle due to waves < flooding angle	Pass	Pass	Pass	Pass	Pass	Pass	Pass	X
Freeboard at equilibrium > 0,5 m	Pass	Pass	Pass	Pass	Pass	Pass	Pass	Pass

Table 37
Weather stability criteria fulfilment for the Grågås condition

	5 kn	10 kn	15 kn	20 kn	5 kn + gust	10 kn + gust	15 kn + gust	20 kn + gust
Angle at equilibrium <= 16 deg	Pass	Pass	Pass	Pass	Pass	Pass	Pass	Pass
Angle at equilibrium <= deck immersion * 0,8 deg	Pass	Pass	Pass	Pass	Pass	Pass	Pass	Pass
Angle at equilibrium < flooding angle	Pass	Pass	Pass	Pass	Pass	Pass	Pass	Pass
Area b >= area a	X	X	X	X	X	X	X	X
Angle at equilibrium + angle due to waves < flooding angle	X	X	X	X	X	X	X	X
Freeboard at equilibrium > 0,5 m	Pass	Pass	Pass	Pass	Pass	Pass	Pass	Pass

Table 38
Weather stability criteria fulfilment for the 1 m draft condition

	5 kn	10 kn	15 kn	20 kn	5 kn + gust	10 kn + gust	15 kn + gust	20 kn + gust
Angle at equilibrium <= 16 deg	Pass	Pass	Pass	Pass	Pass	Pass	Pass	Pass
Angle at equilibrium <= deck immersion * 0,8 deg	Pass	Pass	Pass	Pass	Pass	Pass	Pass	Pass
Angle at equilibrium < flooding angle	Pass	Pass	Pass	Pass	Pass	Pass	Pass	Pass
Area b >= area a	Pass	Pass	Pass	Pass	Pass	Pass	Pass	X
Angle at equilibrium + angle due to waves < flooding angle	Pass	Pass	Pass	Pass	Pass	Pass	Pass	X
Freeboard at equilibrium > 0,5 m	Pass	Pass	Pass	Pass	Pass	Pass	Pass	Pass

If the alternative criteria proposed by Tanner (2018) is applied, all conditions fulfil the criteria, without considering the effect of waves, in wind speeds up to 20 knots plus gust with a full sail. When the heeling angle due to waves is considered, the resulting angle from wind and waves exceeds the flooding angle for all conditions in wind speeds of 20 knots + gust, but the criterion is fulfilled for all other wind speeds. For the Grågås condition the criterion is exceeded for wind speeds above 15 knots without gust or speeds of 10 knots plus gust, see Table 39. With high wind speeds, the sail area would however be reduced.

Table 39
Fulfilment of alternative criteria

	Empty	Water below wales	Grågås	1 m draft
Steady Equilibrium less than GZ0	Pass	Pass	Pass	Pass
Steady Equilibrium less than Flooding angle	Pass	Pass	Pass	Pass
Steady Equilibrium less than GZmax angle	Pass	Pass	Pass	Pass
GZmax angle greater than Flooding angle	Pass	Pass	Pass	Pass
Steady Equilibrium + heel due to waves less than Flooding angle	Fail in 20 kn + gust	Fail in 20 kn + gust	Fail in 15 kn and 10 kn + gust	Fail in 20 kn + gust

VI.4 Seakeeping calculations

Seakeeping calculations were done considering a homogenous 27 % timber moisture content for both the Big Ship of Wismar and the Bremen cog. The seakeeping results show that for the Bremen cog, the ballast condition experiences the highest pitch motions, both in following (0 degrees heading) and stern quartering seas (45 degrees heading), followed by the Grågås condition and the condition with the draft below the protruding beams, Figure 117.

For the Big Ship of Wismar, the loading condition that experiences the highest pitch motions is also the empty condition and the pitch motions reduce with heavier conditions, being the Grågås condition the one experiencing the lowest pitch motions. As seen in Figure 117, pitch motions reduce with increasing ship's speed, and they are highest with waves directly from the stern and in wave peak periods around 4 seconds.

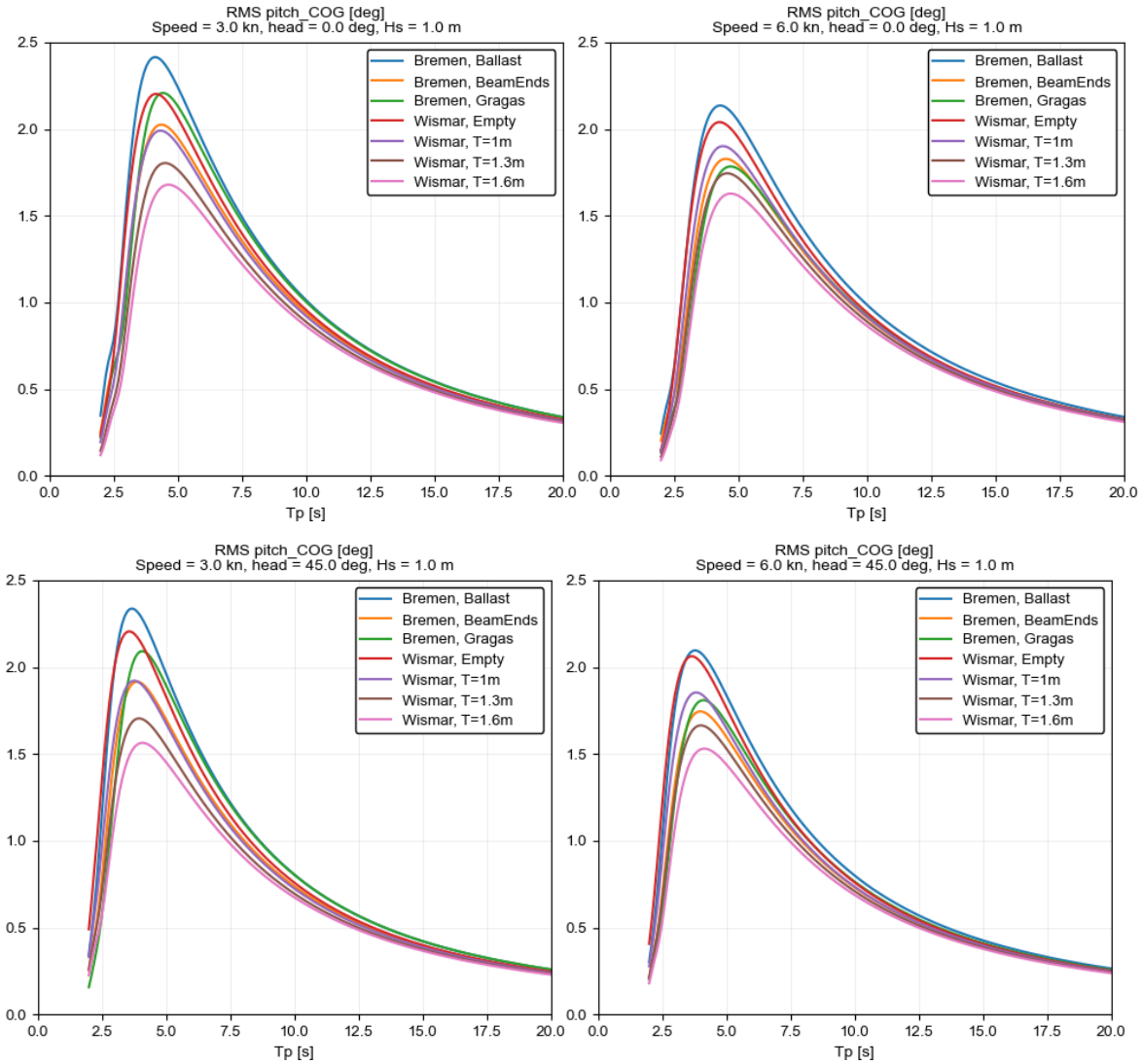

Figure 117 RMS value of pitch in degrees as a function of the wave peak period in seconds, for 1 m significant wave height in following seas (top) and stern quartering seas (bottom), 3 knots (left) and 6 knots (right). (Hernandez Montfort).

When comparing the two vessels in their Grågås condition, the Bremen cog experiences higher pitch motions especially in following waves. The same trend is seen when comparing the ballast condition of the Bremen cog and the empty condition of the Big Ship of Wismar, and the condition with the draft below the beams for the Bremen cog with the condition with the draft below the wales for the Big Ship of Wismar. The conditions of the 1 m draft for the Big Ship of Wismar and the draft below the beams for the Bremen cog experience similar pitch motions.

Figure 118 shows that the heave response of the vessels is very similar. The heavier loading conditions experience the lowest motions, and since the Big Ship of Wismar is lighter than the Bremen cog it experiences higher motions. However, the differences between the two ships and the different loading conditions are minimal.

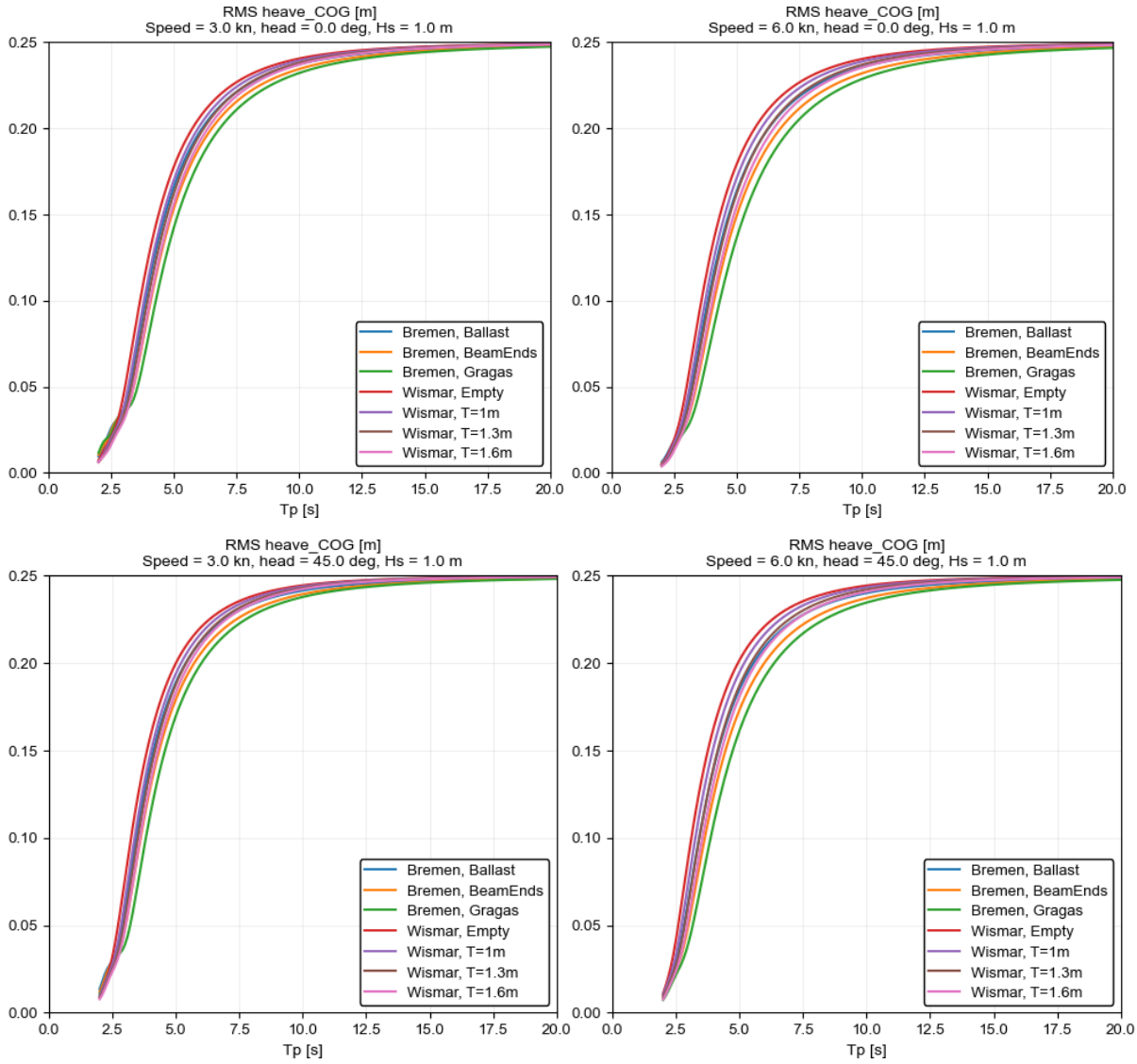

Figure 118 RMS value of heave in metres as a function of the wave peak period in seconds, for 1 m significant wave height in following seas (top) and stern quartering seas (bottom), 3 knots (left) and 6 knots (right). (Hernandez Montfort).

Regarding yaw motions, Figure 119, the Big Ship of Wismar experiences higher motions in its heavier conditions while for the Bremen cog the opposite trend is seen, with the highest motions experienced by the lightest conditions. The Bremen cog in the Grågås condition shows similar yaw response to the Big Ship of Wismar in the empty condition. It is important to acknowledge that the impact of rudders and sails were not considered, and hence any comparison of the two vessels regarding yaw motions needs to be approached with caution.

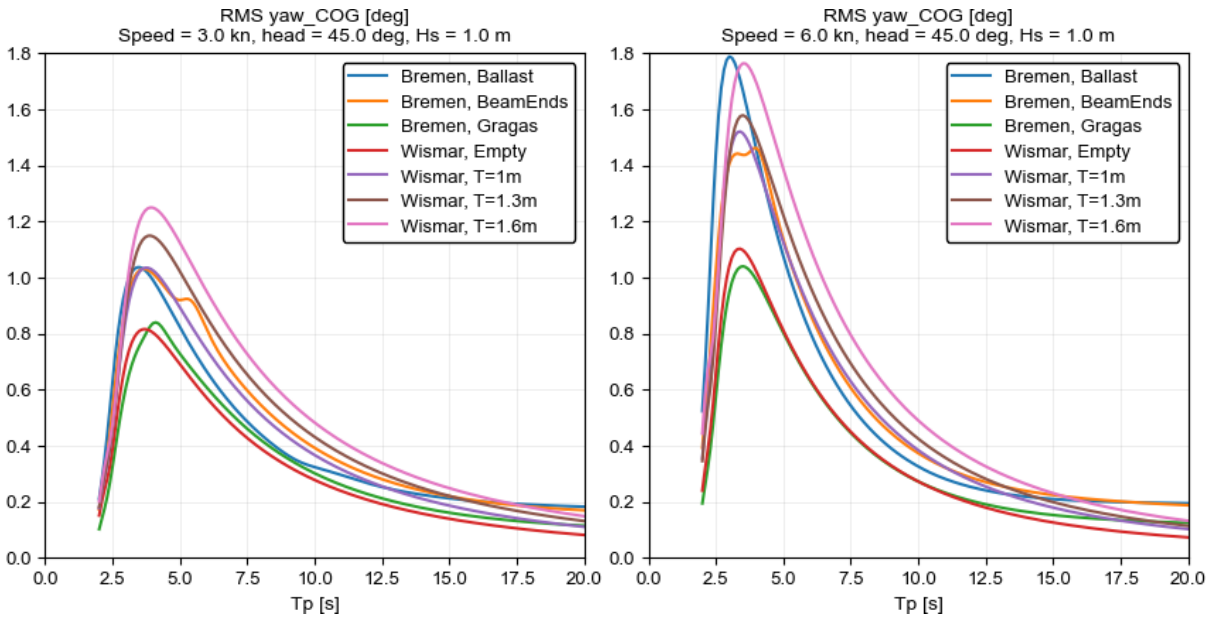

Figure 119 RMS value of yaw in degrees as a function of the wave peak period in seconds, for 1 m significant wave height in stern quartering seas, 3 knots (left) and 6 knots (right). (Hernandez Montfort).

Because of the differences in GM between both vessels and their loading conditions, the roll response varies greatly. The roll response significantly impacts the stability and seaworthiness of the ship, specifically in terms of the risk of water embarkment. Figure 120 shows the roll response of the vessels with waves from the beam (90 degrees) at zero speed and at a speed of 3 knots. The differences in natural roll periods between the two ships and their loading conditions is clearly visible. The natural period of roll is the period in which the roll response enters in resonance and thus where the peak of the roll response is in the plots. As already mentioned in section VI.1, for the Big Ship of Wismar, the natural roll period remains almost the same at around 3 seconds independently of the loading condition, due to a similar GM value between the loading conditions. For the Bremen cog, the GM is strongly affected by the different loading conditions and thus the natural roll period varies greatly from about 5 seconds for the Grågås condition to about 11 seconds

for the ballast condition. The natural roll periods computed by SHIPMO, taking into account the actual added mass of the ship, are shown in Table 40.

Table 40
Natural roll periods of the ships from seakeeping calculations.

Condition	Wismar empty	Wismar 1 m draft	Wismar below wales	Wismar Grågås	Bremen ballast	Bremen below beams	Bremen Grågås
Draft [m]	0.8	1.0	1.3	1.6	1.5	2.1	2.8
T_{roll} [s]	3.5	3.3	3.2	3.2	10.6	6.2	5.1

Note that the damping generated by the sail is not accounted for and thus the amplitudes of roll would in reality be lower. However, few trends are clear from Figure 120. The loading condition that experiences the highest roll motions for the Bremen cog is the condition with the draft below the protruding beams. For the Big Ship of Wismar, the lighter conditions roll more than the heavier ones. Except for the ballast condition, the Bremen cog rolls more than the Big Ship of Wismar.

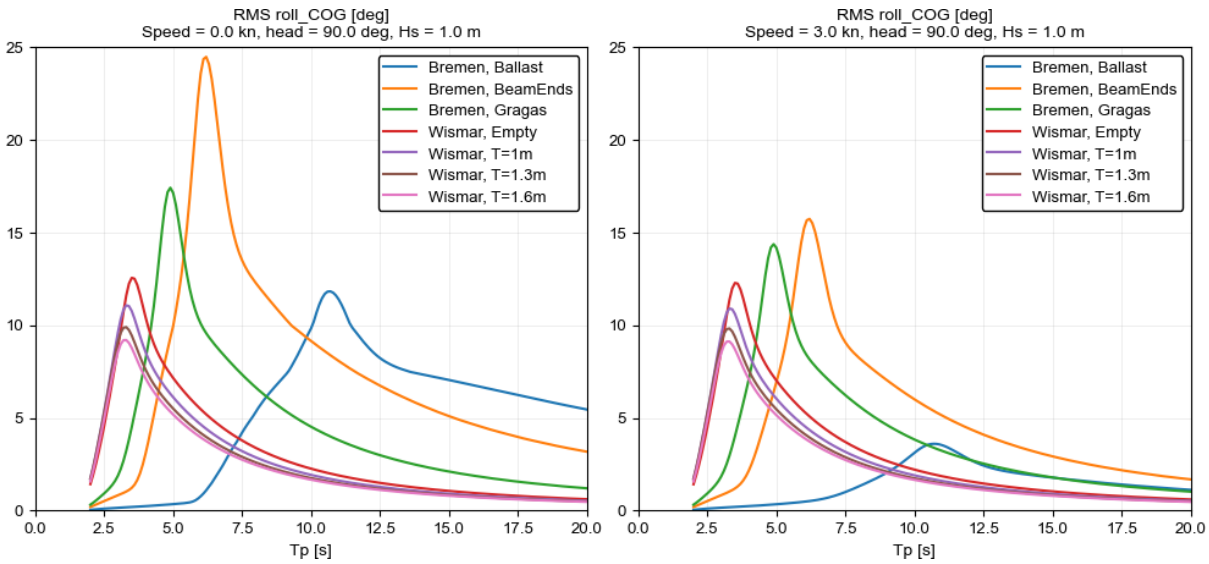

Figure 120 RMS value of roll in degrees as a function of the wave peak period in seconds, for 1 m significant wave height in beam seas, zero speed (left) and 3 knots (right). (Hernandez Montfort).

In stern quartering seas, the wave peak period in which the roll resonance occurs depends on the wave heading and the ship's speed because of the changes in the encounter wave period experienced by the ship. The ship enters in resonance when the encounter period matches the natural roll period. The relation between encounter wave period and wave peak period is given in Equation 14.

Equation 14 Relation between encounter wave period (T_e) and wave peak period (T_p) in deep water.

$$T_e = \frac{T_p}{1 - \frac{2\pi}{T_p g} V \cos\mu}$$

with V the ship's speed in m/s, μ the wave heading in radians, and g the acceleration of gravity.

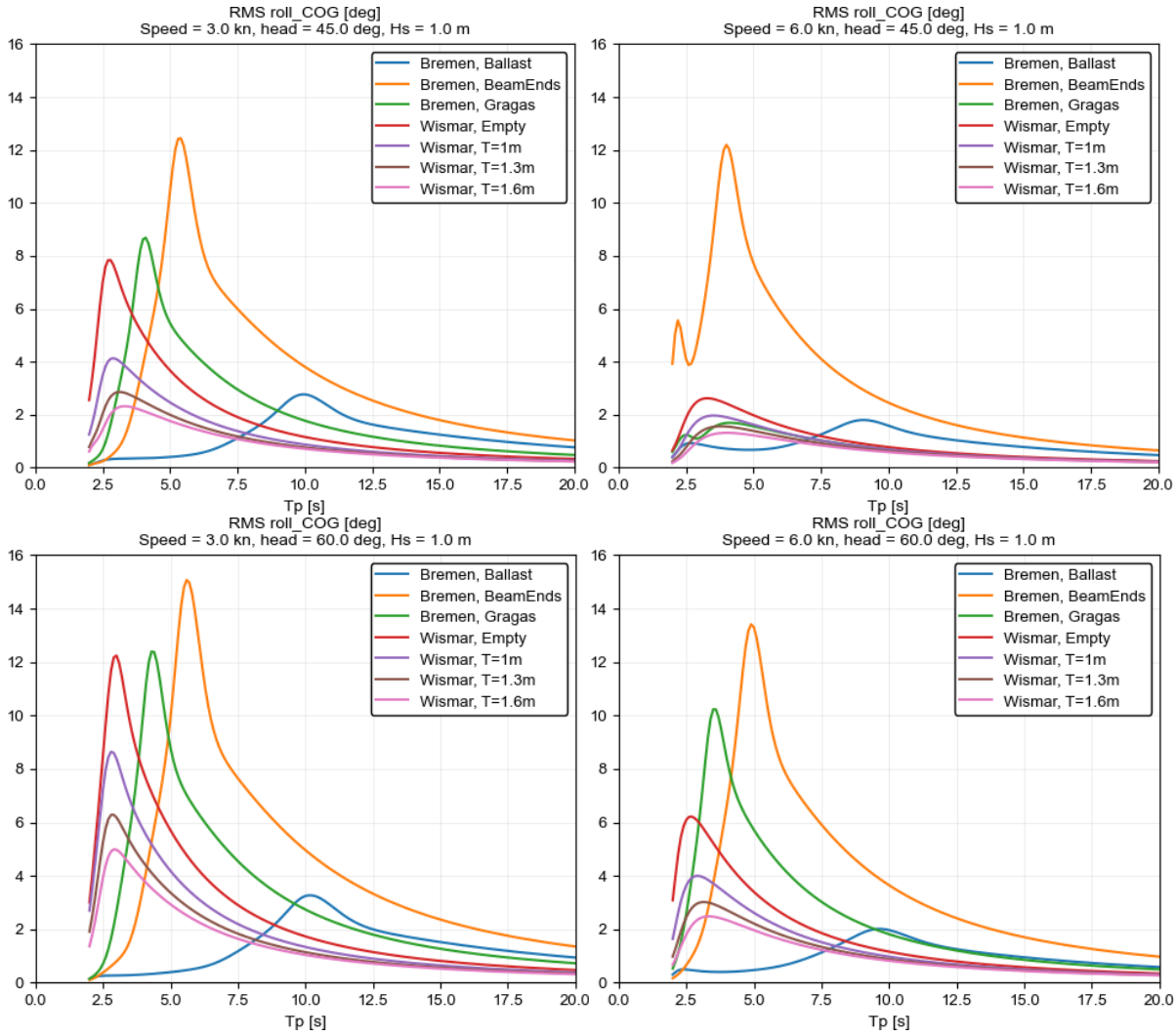

Figure 121 RMS value of roll in degrees as a function of the wave peak period in seconds, for 1 m significant wave height in stern quartering seas (45 degrees heading, top, and 60 degrees heading, bottom), 3 knots (left) and 6 knots (right). (Hernandez Montfort).

Figure 121 shows the RMS roll response in 1 m significant wave height and stern quartering seas for wave headings of 45 and 60 degrees, and 3 and 6 knots. Both the Bremen cog and the Big Ship of Wismar experience their highest roll motions in 60 degrees heading. The roll response is higher at lower speeds because the damping generated by the lift forces acting on the hull are smaller. The Bremen cog experiences higher roll motions than the Big Ship of Wismar except in the ballast

condition. That is because the roll excitation forces are higher at shorter wave periods and the ballast condition has a long natural roll period of about 11 seconds. The heavier loading conditions of the Big Ship of Wismar experience the lowest roll motions.

At 45 degrees wave heading, the roll response of the vessels is reduced, especially at higher speeds, because the encounter period moves away from the natural period of the vessels. This is however not the case for the Bremen cog in the condition with the draft below the protruding beams, which still experiences a high roll response in these conditions. This encounter period effect can clearly be seen in Figure 122. At 45 degrees wave heading and 6 knots, the encounter period matches the natural roll period at around 4 seconds for the draft below beams condition, while for the Grågås condition the encounter wave period does not match the natural roll period anymore.

This also occurs for the Big Ship of Wismar, for which plots can be found in Figure 136 in Appendix C.

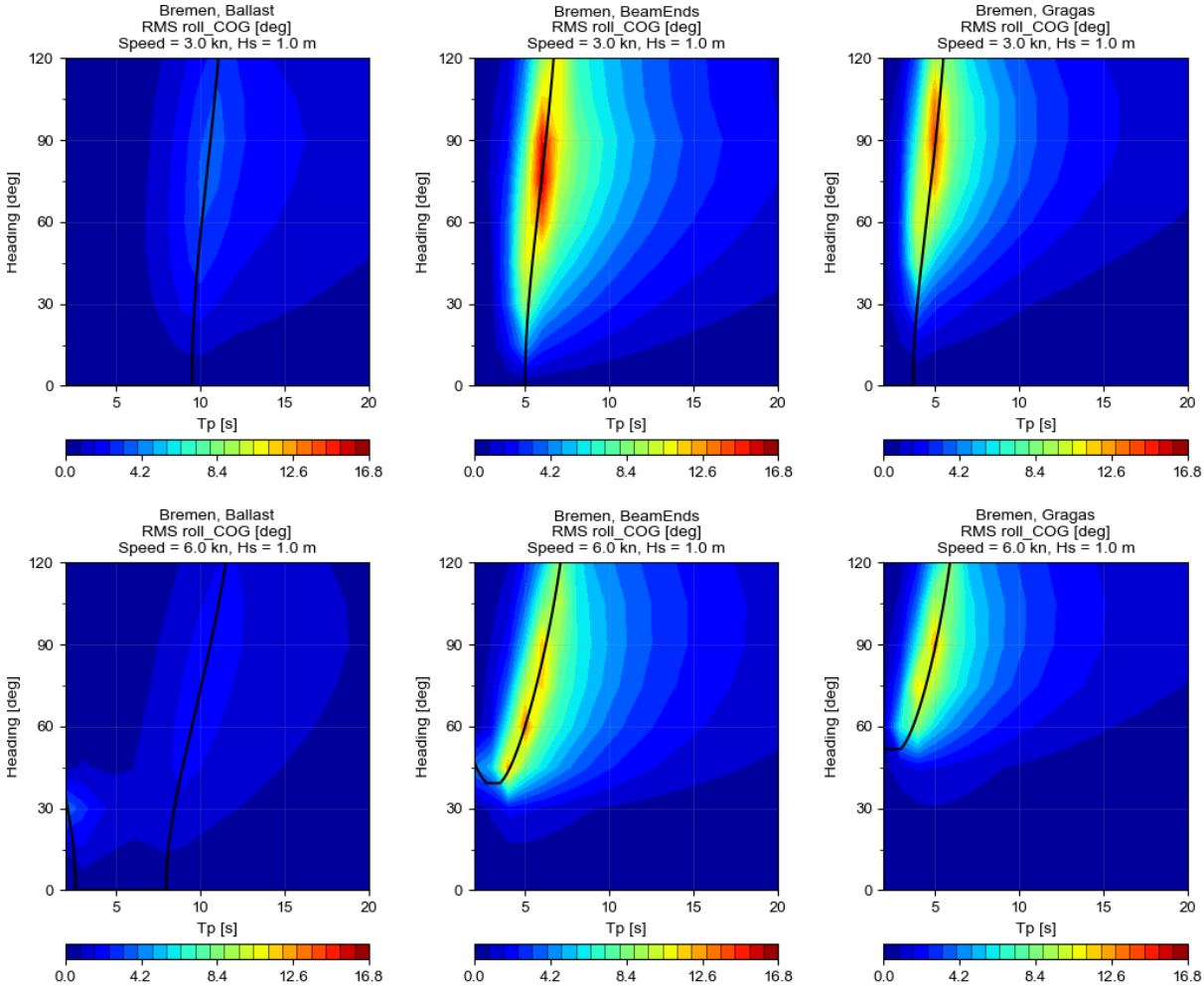

Figure 122 RMS roll for the Bremen cog in 1 m significant wave height as a function of the wave peak period and the wave heading, for 3 knots (top) and 6 knots (bottom). The black line indicates the conditions where wave peak period matches the natural roll period. (Hernandez Montfort).

For pitch, heave, and yaw motions, the contour plots of the RMS value in 1 m significant wave height as a function of the wave peak period and heading are shown in Figure 137 to Figure 142 in Appendix C.

The seaworthiness of the vessels in the Baltic Sea and the North Sea in terms of water embarkment and stability can be checked by applying the criterion of the Most Probable Maximum (MPM) of the roll motion being equal to the flooding angle for each loading condition. Figure 123 shows the sea state conditions in which this criterion would be exceeded in stern quartering seas in the North Sea for both the Big Ship of Wismar and the Bremen cog in the Grågås condition. The results show that even if the Big Ship of Wismar has a lower flooding angle value, the criterion is exceeded more often for the Bremen cog because it experiences higher roll motions. The differences are highest in 45 degrees wave heading when sailing at 3 knots and in 60 degrees wave heading when sailing at 6 knots, where the criterion is exceeded about twice as often for the Bremen cog than for the Big Ship of Wismar.

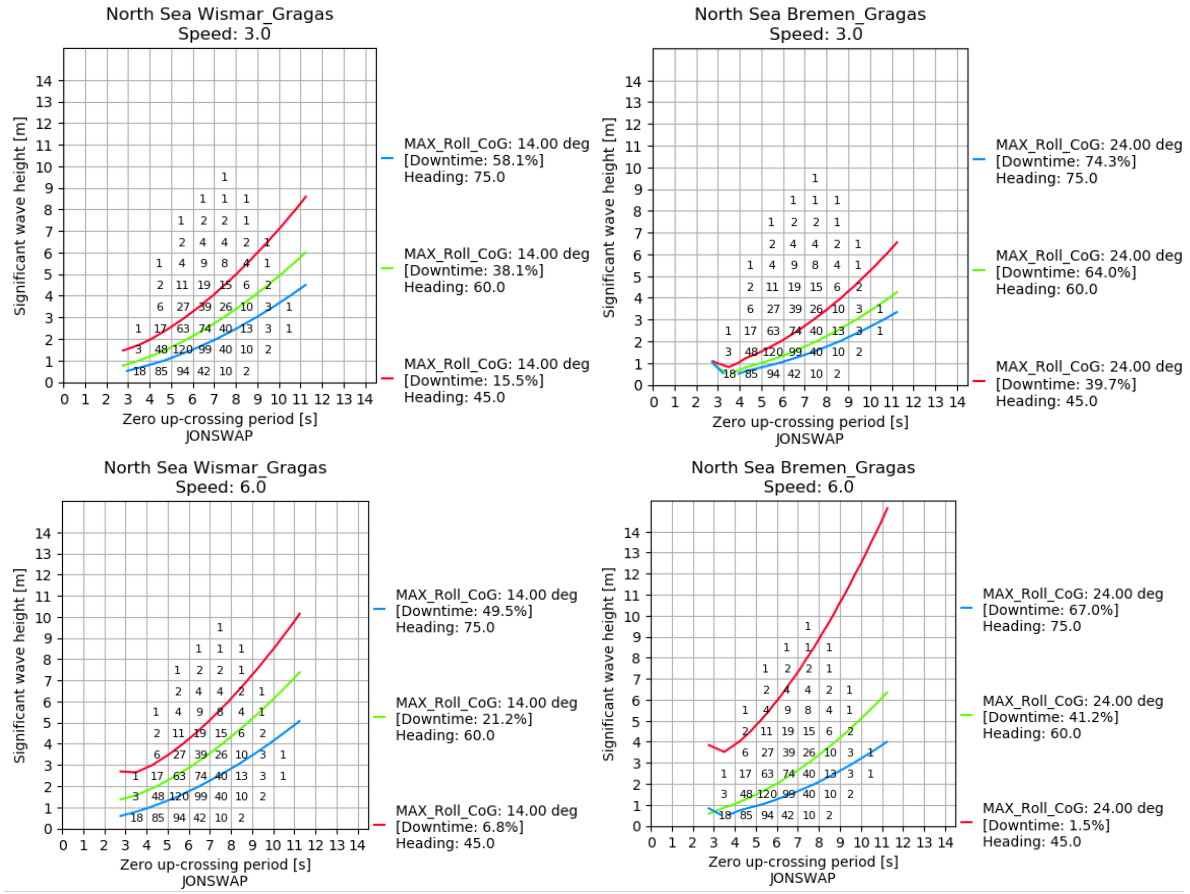

Figure 123 Downtime in the North Sea for an MPM of roll equal to the flooding angle for the Big Ship of Wismar (left) and the Bremen cog (right) in the Grågås condition, for 3 knots (top) and 6 knots (bottom). Each colour represents one wave heading. (Hernandez Montfort).

Figure 124 shows the occurrence of exceedance for the criterion of MPM of roll equal to the flooding angle for the Baltic Sea. Similarly as for the North Sea, the Bremen cog experiences higher occurrences of exceedance despite having a larger flooding angle than the Big Ship of Wismar. The differences are also highest in 45 degrees wave heading when sailing at 3 knots and 60 degrees wave heading when sailing at 6 knots.

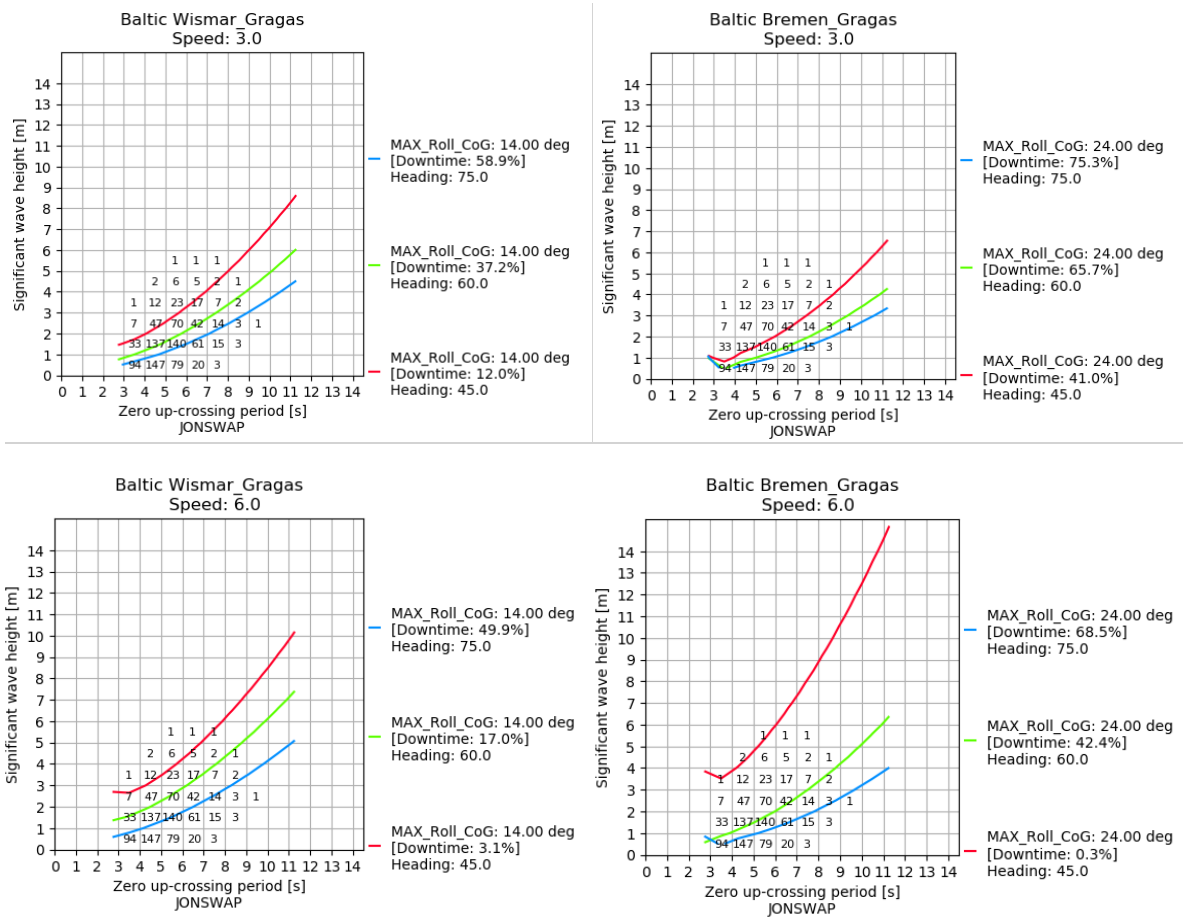

Figure 124 Downtime in the Baltic Sea for an MPM of roll equal to the flooding angle for the Big Ship of Wismar (left) and the Bremen cog (right) in the Grågås condition, for 3 knots (top) and 6 knots (bottom). Each colour represents one wave heading. (Hernandez Montfort).

A summary of the exceedances for the Grågås condition of both vessels is shown in Figure 125.

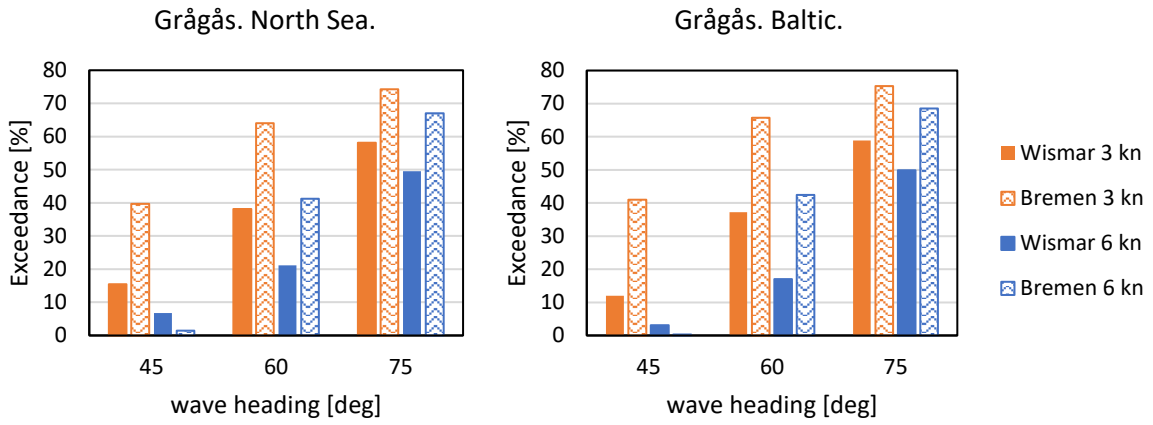

Figure 125 Summary of the exceedance for the criterion on roll MPM equal to the flooding angle for the North Sea (left) and Baltic (right) for the Big Ship of Wismar and the Bremen cog in the Grågås condition. (Hernandez Montfort).

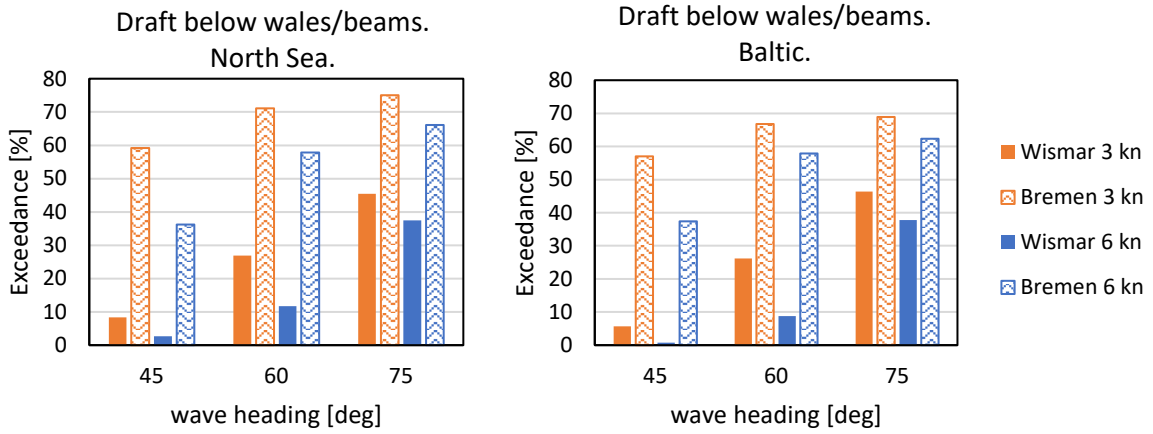

Figure 126 Summary of the exceedance for the criterion on roll MPM equal to the flooding angle for the North Sea (left) and Baltic (right) for the Big Ship of Wismar in the draft below wales condition and the Bremen cog in the draft below beams condition. (Hernandez Montfort).

When comparing the condition with the draft below the wales for the Big Ship of Wismar and the draft below the protruding beams for the Bremen cog, both with a cargo capacity around 45 tons, the differences between the two vessels are larger. As seen in Figure 126, the criterion is exceeded 7 times more often for the Bremen cog when sailing in the North Sea in 45 degrees wave heading and 3 knots, about 5 times more often in 60 degrees wave heading and 6 knots, and about 13 times more often in 45 degrees wave heading and 6 knots. In the Baltic, the differences are even larger. The criterion is exceeded 10 times more often for the Bremen cog in comparison to the Big Ship of Wismar in 45 degrees wave heading and 3 knots, 7 times more often in 60 degrees and 6 knots, and about 45 times more often in 45 degrees wave heading and 6 knots. That is because the natural roll period of the vessel of 6 seconds falls within the most common wave peak periods in the North Sea

and the Baltic, between 4 to 5 seconds zero up-crossing period. This can clearly be seen in the scatter diagram plots, which are shown in Figure 143 and Figure 144 in Appendix C.

The exceedance for the Big Ship of Wismar in the empty condition is somewhat lower than for the other two conditions. For the Bremen cog, because of its long natural period, low roll response, and high freeboard, the criterion of MPM roll equal to the flooding angle is barely exceeded, especially in the Baltic. In the North Sea, the maximum exceedance is in the order of just 6 % when sailing in 75 or 60 degrees at 3 knots. The scatter diagram plots for the empty and ballast conditions are shown in Figure 145 and Figure 146 in Appendix C. A summary of the exceedances is shown in Figure 127.

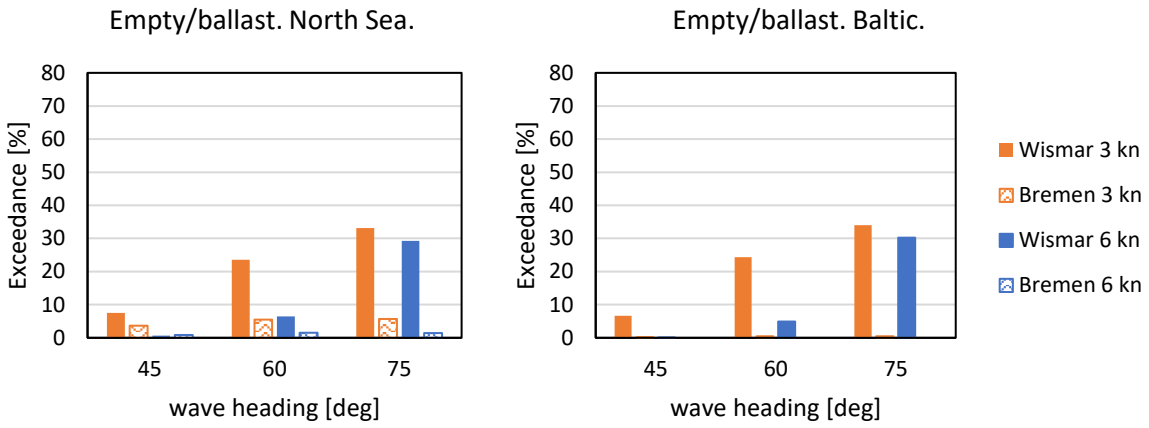

Figure 127 Summary of the exceedance for the criterion on roll MPM equal to the flooding angle for the North Sea (left) and Baltic (right) for the Big Ship of Wismar in the empty condition and the Bremen cog in the ballast condition. (Hernandez Montfort).

Another criterion related to the risk of water embarkment is the relative water elevation exceeding the freeboard of the vessel. Here not only the roll plays a role but also the other ship motions and the incoming wave elevation. However, the roll motion plays the most important role and thus similar trends as with the criterion on the roll angle can be seen. The freeboard is exceeded more often for the Bremen cog than for the Big Ship of Wismar both in the North Sea and the Baltic.

The scatter diagram plots for the Grågås condition are shown in Figure 147 and Figure 148 in Appendix C. Depending on the heading and speed, the freeboard is exceeded from 2 up to 14 times more often for the Bremen cog, see Figure 128.

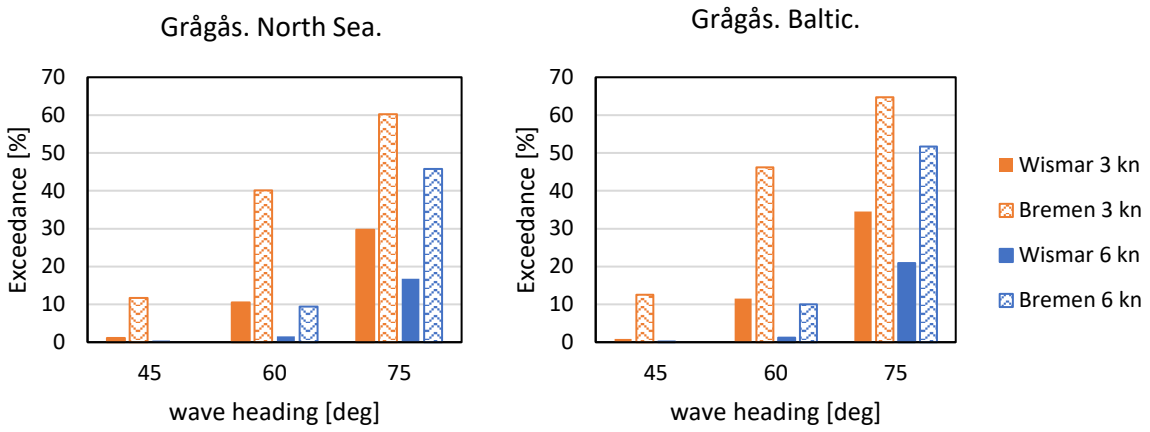

Figure 128 Summary of the exceedance for the criterion on the waves exceeding the edge of the hull for the North Sea (left) and Baltic (right) for the Big Ship of Wismar and the Bremen cog in the Grågås condition. (Hernandez Montfort).

As for the criterion on roll, the differences between the two ships are larger for the intermediate draft condition of the water below wales for the Big Ship of Wismar and the water below beams for the Bremen cog. In this condition, even in the conditions for which no exceedance occurs for the Big Ship of Wismar, the criterion is exceeded up to 30 % of the time for the Bremen cog, see Figure 129. The scatter diagram plots for this condition are shown in see Figure 149 and Figure 150 in Appendix C.

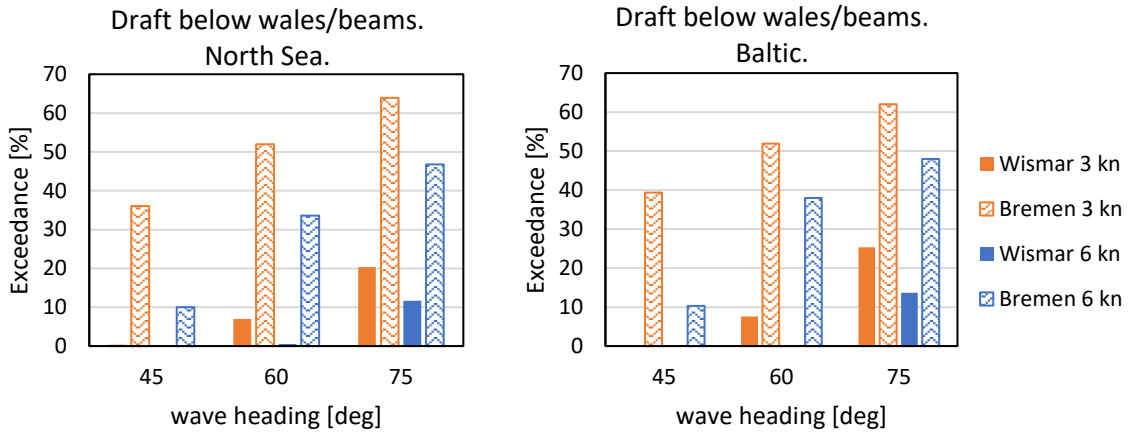

Figure 129 Summary of the exceedance for the criterion on the waves exceeding the edge of the hull for the North Sea (left) and Baltic (right) for the Big Ship of Wismar in the draft below wales condition and the Bremen cog in the draft below beams condition. (Hernandez Montfort).

In the empty or ballast condition, the criterion is barely exceeded for both the Big Ship of Wismar and the Bremen cog, Figure 130. The scatter diagram plots are shown in Figure 151 and Figure 152 in Appendix C.

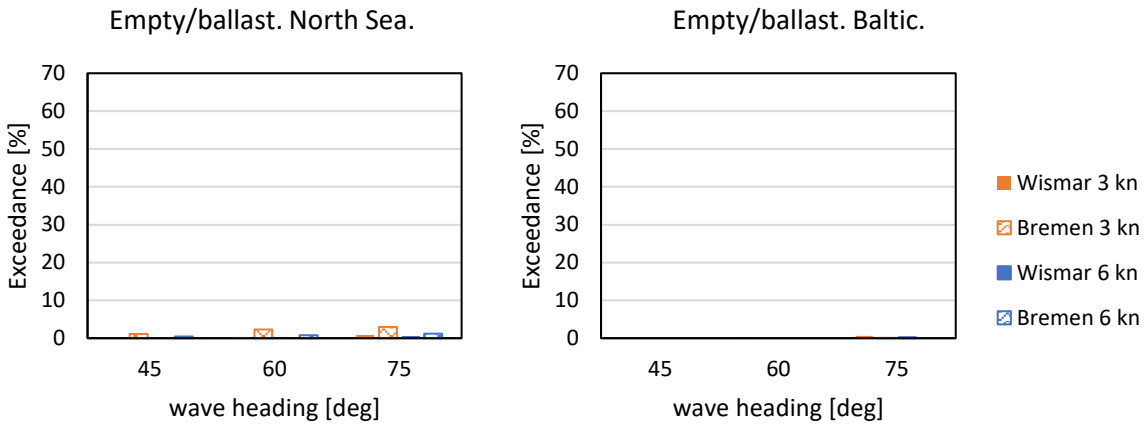

Figure 130 Summary of the exceedance for the criterion on the waves exceeding the edge of the hull for the North Sea (left) and Baltic (right) for the Big Ship of Wismar in the empty condition and the Bremen cog in the ballast condition. (Hernandez Montfort).

The results presented in this chapter show that the Big Ship of Wismar and the Bremen cog have significant differences in all the evaluated aspects: weight, cargo capacity, stability, speed potential, stability, and seaworthiness. Overall, the Big Ship of Wismar scores better than the Bremen cog in all aspects, besides the cargo capacity in the Grågås condition. The Big Ship of Wismar was lighter, more stable, faster, and experienced smaller motions in both the Baltic and the North Sea. In the next chapter these results are discussed and the performance of the two ships is evaluated by exploring the advantages and limitations of their characteristics within their historical contexts.

VII. Discussion

The results presented in the previous chapter demonstrate the usefulness of 3D reconstruction models in studying shipwrecks beyond their visual appeal. For the Bremen cog and the Big Ship of Wismar, the results from the weight, inertia, speed, stability, and seakeeping calculations show significant differences between them. In this chapter these results are discussed and the differences between the two ships are highlighted and interpreted.

The weight calculations have shown that Big Ship of Wismar was much lighter than then the Bremen cog. Table 41 summarises their draft, displacement, and cargo capacity.

Table 41
Summary of weight and cargo capacity

	Wismar				Bremen		
	Empty	1 m draft	Draft below wales	Grågås	Ballast	Draft below beams	Grågås
Draft [m]	0.8	1.0	1.3	1.6	1.5	2.0	2.8
Displacement [t]	24	43	70	102	62	107	170
Cargo [t]	0	18	46	77	0	45	108

At the empty condition, the Big Ship of Wismar weighted 24 tons while the Bremen cog weighted twice as much, 47 tons, in its unballasted condition. However, 15 tons of ballast were needed in the Bremen cog for it to be stable, being the total weight of its empty condition 62 tons, close to three times as heavy as the Big Ship of Wismar. Nordic ships were indeed built light by selecting high quality oak from which planks were split with an axe following the grain of the wood rather than by sawing them, which would produce weaker timbers (Bruun, 1997, p. 1283). This technique, together with the thin hull planks and the wide spacing between rivets made the ships extremely strong but flexible. This made them more likely to survive a storm as the ship would be able to bend and flex, dissipating the energy of the waves hitting the hull (Shaw, 2016, p. 18). The Big Ship of Wismar was built from a combination of oak and pine, the latter being lighter and more flexible but also weaker and more prone to worm infestation and weather deterioration (Shaw, 2016, pp. 16-17). The Big Ship of Bergen shares similarities with the Big Ship of Wismar, both in terms of its specific construction characteristics and the historical period. The preserved elements of the Bergen vessel, such as the keelson, mast bitis, through-beams, and windlass, closely resemble those found on the Wismar ship, indicating a strong connection between the two. However, it is noteworthy that the structural components recovered from the Bergen wreck are exclusively made of pine (Ditta & Auer, in press). The use of pine might be related to the increasing scarcity of high-quality oak in

Scandinavia from the Late Viking Age onwards, which forced Nordic shipbuilders to increase their use of pine (Shaw, 2016, p. 17).

Besides the mast and rigging elements, the Bremen cog was fully built from oak, see Table 48 in Appendix A. The oak timbers were however sawn rather than split and thus lower quality oak could be used in its construction as timbers did not need to follow the wood's natural grain. Planks and timbers were also thicker than the ones used in Nordic ships such as the Big Ship of Wismar. The planks used in the oldest recorded cog, the Kollerup, were however tangentially split and of much higher quality then the ones found in the Bremen cog. According to Crumlin-Pedersen (2000, p. 235), these variations should be understood as adjustments undertaken to meet distinct needs, incorporate evolving construction techniques, and address the availability or scarcity of resources that occurred over the two-century period separating the Kollerup and the Bremen cog. As covered in chapter II, a lot of changes in shipbuilding techniques indeed occurred between the 12th and 14th centuries. There was a marked shift to more economic construction techniques and evidence also points to a growing scarcity of high-quality timber. Furthermore, it appears that starting from 1200, there was a gradual process of exchange among the different local shipbuilding traditions, resulting in the adoption or abandonment of various construction techniques. This process, aimed to accommodate the evolving requirements of ship owners and users, ultimately lead to a standardization of shipbuilding practices across Northern Europe. However, localized traditions persisted in specific cases where they remained economically viable, or in isolated regions like northern Scandinavia where medieval techniques endured until modern times (Bill, 2009, p. 437; Englert, 2000, p. 52). A remarkable change in construction techniques is the abandonment of the biti system even in clinker-built ships (Bill, 1997, p. 137). As Bill (1997, p. 106) points out, there are three notable advantages in transitioning from a biti-system to a system without bitis. Firstly, the elimination of bitis allows for greater flexibility in the selection of materials for the scarfed frames, as symmetry in the floor-timbers is no longer a requirement. This simplifies the process of finding suitable materials for construction. Secondly, the removal of bitis can potentially reduce the overall workload involved in producing the framing system. In many vessels, the biti system is intricately integrated with the framing system, and by eliminating it, the construction process can be streamlined. Lastly, the absence of bitis results in a more uniform and regular hold space, particularly advantageous for cargo vessels. This improvement ensures better organization and arrangement of cargo within the hold.

In the Grågås condition, the Big Ship of Wismar would have had a cargo capacity of 77 tons while the Bremen cog would have had a cargo capacity of 108 tons, assuming a homogeneous 27 % moisture content for their timbers. However, the draft of the Bremen cog in the ballast condition, thus

without cargo capacity, roughly equals the draft of the Big Ship of Wismar in the full load Grågås condition. This means that the Big Ship of Wismar would have been able to sail in shallow waters and reach harbours inaccessible for the Bremen cog. As pointed out by Morcken (1988, p. 391), the coastal areas of Denmark, Germany, and The Netherlands along the North Sea primarily consist of sandy, low shores with a tidal range of approximately 3 meters. Therefore, harbours that dry out in low tides would have a maximum water depth of 3 meters during high tide and he states that the maximum draft for a ship to be able to use these harbours would be of about 1.5 m. Thus, these harbours would have been accessible for Nordic ships such as the Big Ship of Wismar but not for cogs like the Bremen cog, which would have needed the presence of quayside facilities with deep water depths (Ayers, 2013, p. 65) . The low-profile keel and wide bottom of the Big Ship of Wismar would in principle have allowed the ship to beach during the dry period between high tides, although a flat bottom such as the one in the Bremen cog would have been more suitable in these situations. In non-tidal waters, such as in the Baltic, beaching ships like the Big Ship of Wismar would have been avoided and the ship would have been anchored at some distance from the shore and loaded or unloaded by boats or using jetties (Englert, 2000, p. 84).

As mentioned in section IV.1.1, the Big Ship of Wismar shows strong similarities to the Lynaes 1 wreck. According to Englert's (2000, p. 79) reconstruction, the Lynaes 1 would have had an overall length of 24.7 m and a maximum width of 6.49 m. These values are indeed very similar to the ones obtained for the Big Ship of Wismar, although the Big Ship of Wismar is notably bulkier, with a length of 23.3 m and a width of 7.6 m. Applying the Grågås condition, the resulting draft for the Lynaes 1 would have been 1.51 m and the resulting length at the waterline 21.83 m. The reconstructed model of the Lynaes 1 was used to compute hydrostatics and geometry coefficients, however a detailed model of its internal elements to compute the weight in the same manner it has been done for the Bremen cog and the Big Ship of Wismar was not done. As already mentioned in chapter III, Englert (2000, p. 82) estimated the weight and resulting cargo capacity of the Lynaes 1 by considering the wetted surface of the hull, an average plank thickness, an estimated number of rivets and their mass, and assumptions regarding the weights of the mast, rigging, equipment, and crew.
The mass of the rivets of 60 grams used by Englert is close to the 75 grams I calculated for the Big Ship of Wismar considering the volume of the rivets. The assumption made by Englert for the mass of the mast, rigging, and equipment of 2 tons is also close to the 2.3 tons I estimated for the Big Ship of Wismar for the mast, sail, ropes and equipment, and anchors, see Table 47 in Appendix A. Englert considered a heterogeneous moisture content for the planking depending on whether the planks were below or above the draft. The mass of the ship in empty condition resulted in 18 tons and the cargo capacity at the Grågås condition 57 tons. Using the same assumptions of 50 % moisture

content for the oak planks below the water and 35 % moisture content for all the other timbers, the Big Ship of Wismar would have weighted 26 tons and had a cargo capacity of 75 tons in the Grågås condition.

In Table 42 a comparison is made between different 11-12th centuries Nordic cargo vessels with regards to their size and cargo capacities. It should be noted that for most ships the cargo capacities are estimates only and no actual calculations have been carried out. For the Skuldelev wrecks, hull reconstructions as well as full scale replicas have been made. For Lynaes 1 simple calculations were done by Englert (2000, p. 82). Only for the Big Ship of Wismar a detailed 3D model of the reconstructed ship has been used to calculate in detail the weight of the vessel.

Table 42
Cargo capacities for different 11-12th centuries Nordic cargo vessels. (Data taken from Englert, 2000, p. 83,98, Tables 24 and 28; Englert, 2017, p. 278, Table 1; Christensen, 2002, pp. 88-89).

Ship	Dated	Timber provenance	Length [m]	Beam [m]	Grågås draft [m]	Displacement [t]	Cargo capacity [t]	Cargo space [m^3]	Cargo density [t/m^3]
Big Ship of Wismar	1184-1190	Western Sweden	23.3	7.6	1.6	102	75	84 119	0.89 0.63
Big Ship of Wismar	1184-1190	Western Sweden	23.3	7.6	1.3 (below wales)	70	46	84 119	0.54 0.39
Skuldelev 3	ca. 1030s	Jutland?	14.1	3.3	0.84	8	4.5	12	0.38
Skuldelev 1	ca. 1030/1045	Western Norway	16.0	4.8	1.25	34	24	40	0.60
Lynaes 1	ca. 1140	Southwest Sweden	24.7	6.5	1.51	75	57	70-90	0.81-0.63
Lynaes 2	after 1140	South Jutland	25				ca. 50-60		
Roskilde 2	ca. 1185	Southwest Sweden	16.5	4.5			ca. 15		
Roskilde 4	1108/1113	Southwest Sweden	20.5	6.6	1.5		ca. 50		
Karschau	ca. 1145	Funen	26	6.8			ca. 60		
Big Ship of Bergen	1187/1188	Western Norway	27-30	9	2.5-2.7		ca. 120		

Note. References: Skuldelev 1 (Andersen, Crumlin-Pedersen, Vadstrup, & Vinner, 1997, pp. 268-269). Skuldelev 3 (Jensen, 1999, p. B 28). Lynaes 1 and Lynaes 2 (Crumlin-Pedersen, 1979a; Englert, 2000, p. 83; Bonde & Daly, Dendrokronologiske undersøgelser 1999, 2000, p. 331; Daly, Lynæs J.nr. 2526. Dendro.dk rapport 6, 2008). Roskilde 2 (Englert, 2000, p. 98). Roskilde 4 (Myrhoj & Gothche, 1997; Gothche, 2006; Bonde & Daly, 1998, p. 298). Karschau (Englert, 2017). Big Ship of Bergen (Christensen, 2002; Christensen, 1989)

As it can be seen in Table 42, the cargo capacity of the Big Ship of Wismar is larger than for the other ships in the Grågås condition, excepting the Big Ship of Bergen. When comparing the cargo densities,

both the Big Ship of Wismar and the Lynaes 1 show similar values in the Grågås condition. The smaller Skuldelev ships have lower cargo density values, with the smallest Skuldelev 1 having the lowest cargo density. The Big Ship of Wismar further confirms the idea by Crumlin-Pedersen (1985, p. 268) and Englert (2000, p. 83) that larger ships were better suited for transporting heavy cargo.

In the open sea, it is unlikely that the Big Ship of Wismar would have regularly sailed in the Grågås condition draft. The low freeboard of less than one meter would mean that a relatively small heeling angle of just 14 degrees would have resulted in water entering the ship. Moreover, as already mentioned in chapter IV, an indication of the design draft of the vessel is given by the openings of the scarf joints on the outer planking. These are facing aft in the lower part, preventing water ingress when the ship is advancing, while they face forward from strake 14 (the lowest wale) upwards to prevent water ingress due to the waves coming from the stern. Hence, it is highly probable that the Big Ship of Wismar would have sailed with a draft below both wales, at 1.3 meters. In the condition with the draft below wales, the Big Ship of Wismar had a capacity of 46 tons, like the cargo capacity of the Bremen cog with the draft below the beams.

In Table 43 a comparison is shown between different cogs for which cargo capacities have been estimated. Excluding the IJsselcog, the Bremen cog has the largest estimated cargo capacity. In its Grågås condition, the cargo density would be of about 0.9 t/m^3, similar the Big Ship of Wismar. In its draft below beams the cargo density would be of about 0.38 t/m^3 when considering the maximum cargo space of 120 m^3 and 0.45 t/m^3 when considering a cargo space of 100 m^3. These values are also comparable to the densities found for the Big Ship of Wismar with its draft below the wales. According to Ellmers (1994, p. 38) much larger cogs than the Bremen cog would have existed, based on a historical reference to a cog in 1241 with a capacity of 240 tons. Similarly, Hocker and Ward (2004, p. 75) argue that the cargo capacity of the Bremen cog, which was of 40 lasts or 120 m^3 and could accommodate 80 tons of rye, was relatively small compared to most other cogs described in historical records. These indicate that certain Hanseatic cogs surpassed 100 lasts, and by the 15th century, there were reports of 150 lasts cogs.
The definition of the unit "last" varied significantly across different regions and was even influenced by the specific type of cargo it referred to (Tanner, 2018, p. 34; Hocker & Ward, 2004, p. 89). Therefore, it is risky to employ it as a standardized measure for comparing ships (Crumlin-Pedersen, 1985, p. 85). Furthermore, as previously discussed in Chapter II of this thesis, the historical term "cog" exhibited considerable variation across different regions and could encompass ships based on factors other than their shipbuilding tradition or physical characteristics. As a result, the historical term "cog" may not necessarily align with the archaeological definition of what constitutes a cog.

Table 43
Cargo capacities for different cogs. (Data taken from Van de Moortel, 2011, pp. 84-86, Table 6; Englert, 2017, p. 278, Table 1; Waldus, Verweij, & van der Velde, 2019, pp. 483-488).

Ship	Dated	Timber provenance	Length [m]	Beam [m]	Grågås draft [m]	Displacement [t]	Cargo capacity [t]	Cargo space [m^3]	Cargo density [t/m^3]
Bremen	1378	Weser	23.2	7.7	2.8	170	108	135_{max} 120	0.80 0.90
Bremen	1378	Weser	23.2	7.7	2.0 (draft below beams)	107	45	135_{max} 120 100	0.33 0.38 0.45
Kollerup	1150	South Jutland	20.9	4.92	1.4	ca. 65	ca. 42		
Kolding	1189	Baltic coast of South Jutland	19.3	7.6	0.2	ca. 90	ca. 70		
NZ43 Spakenburg	1402-1414	Netherlands/ Westphalia	9 (keel)			17.8	9.8		
Almere	1410	unknown	12.7 (keel)			ca. 39.5	ca. 24.5		
IJsselcog	1415-1420		26	8.5	3.5	260	142	137	1.03
IJsselcog	1415-1420		26	8.5	2.5 (draft below beams)	178	60	137	0.43

Note. References: Bremen (Tanner, 2018; Daly, 2009). Kollerup (Hocker & Daly, 2006; Jensen, 1999; Kohrtz Andersen, 1983). Kolding (Daly, 2009; Hocker & Daly, Early cogs, Jutland boatbuilders, and the connection between East and West before AD 1250, 2006; Crumlin-Pedersen, 1979b; Crumlin-Pedersen, 2000; Daly, 2007). NZ43 Spakenburg (Daly, 2009; Van de Moortel, 1991). Almere (Daly, 2009; Hocker & Vlierman, 1996). IJsselcog (Waldus, Verweij, & van der Velde, 2019).

The largest cog from the archaeological record is the Ijsselcog. Its capacity in the Grågås condition is remarkably larger than the one of the Bremen cog, see Table 43. According to Waldus, Verweij, & van der Velde (2019, p. 484) this loading condition would however have been unrealistic for the ship, as cargo would have had to be stored above the main deck and the draft would have been too deep for the Ijssel River. Waldus, Verweij, & van der Velde (2019, p. 484) mention a cargo capacity of 350 tons at the Grågås draft of 3.51 m. However, this does not match their hydrostatic results which state a displacement of 258.5 tons for a draft of 3.44 m. It is impossible that an increase of 7 cm in draft would add 210 tons in displacement making a total of 468 tons (350 tons of cargo + 118 tons of the ballasted ship). A displacement of 350 tons is also unrealistic for a draft of 3.51 m. I assumed therefore a displacement of 260 tons and consequently a cargo capacity of 142 tons. These values, which translate to a cargo density above 1 ton/m^3, are still in line with their conclusion that it is unlikely that the Ijsselcog would have sailed in the Grågås draft. A more realistic draft would be a draft below the protruding beams at 2.45 m which would mean a cargo capacity of 60 tons on top of

the 40 tons of ballast required for the ship not to have a negative initial static stability (negative GM value). The use of stones as ballast is evinced by a small quantity of boulders found inside the hold of the wreck (Waldus, Verweij, & van der Velde, 2019, p. 483). Waldus, Verweij, & van der Velde (2019, pp. 483-484) mention that the ship could hence have transported about 108 tons of grain (791 kg/m^3) at a draft of 2.55 m or 67 tons of meat (591 kg/m^3) at a draft of 2.16 m. However, these values would mean that the 40 tons of ballast were used as cargo, which contradicts the fact that they considered the available cargo space of the ship with ballast. The Ijsselcog probably needed more than 40 tons of ballast to be stable, as a GM value of zero would not provide enough stability. However, full stability calculations as done by Tanner (2018) to find the minimum ballast for the Bremen cog have not been performed for the Ijsselcog. Moreover, it is unlikely that ballast stones in cogs would have been removed and replaced by cargo since in the process of loading and unloading the ships would become unstable and be prone to capsize.

It remains not completely clear whether the Bremen cog would have sailed in the Grågås condition or rather with the draft below the protruding beams. Tanner (2018, pp. 46-47) argues that the archaeological evidence proves that the protruding beams were built to be watertight and thus they could have been partially or fully submerged. Additionally, he argues that the stability of the vessel and its behaviour in waves improve for the ship in the Grågås draft. Indeed, the initial stability of the Bremen cog increases from a GM value of 0.82 m to 1.10 m, and the natural roll period of the ship shifts from 6.2 to 5.1 seconds, which translates to lower roll motions at sea as described in the previous chapter. However, the reserve stability of the ship at high heel angles is reduced for the ship in Grågås condition. Also, the flooding angle in the Grågås condition becomes 24.1 degrees instead of 35.3 degrees. Consequently, the criterion on the area below the GZ curve between 30 degrees and the flooding angle is not fulfilled for the Grågås condition but it is fulfilled for the ship in ballast condition and with the draft below the protruding beams. Besides the changes in stability and roll motions, the same arguments as for the Ijsselcog could be applied: that the draft of 2.8 m would be too large to access shallow waters and that the cargo capacity of 108 tons, which translates to a cargo capacity of 800-900 kg/m^3, seems unrealistically high. For reference, the density without considering barrels or any other container of wheat grain is of about 770 kg/m^3 and the density of wheat flour of about 600 kg/m^3. Barley, rye, and oats have a density of about 620 kg/m^3, 720 kg/m^3 and 420 kg/m^3, respectively (Engineering ToolBox, 2012). Coarse crushed salt has a density of about 800 kg/m^3 (Engineering ToolBox, 2010). Fish or whale oil have a density of about 920 kg/m^3 (Engineering ToolBox, 2003). Thus, it would mean that the total cargo space of the Bremen cog was filled with a material almost as dense as salt or oil, without any containers since then the density would become lower. Moreover, several city seals with cog iconography show the protruding beams

above the water, for instance the city seals of Harderwijk and Damme, Figure 131. Conversely, one could argue that for the city seals that show cogs without protruding beams such as the one of Stralsund in Figure 17, the beams could have been below water. However, by looking at the proportions of the hull and the draft, it is more likely that these cogs had no protruding beams, or that these were not represented. Furthermore, it makes little sense from a design point of view to have protruding beams below the waterline as they only add resistance to the hull. Probably the ship was designed to sail with a draft below the beams, although when carrying heavier cargoes such as wine or beer, about 1 ton/m^3, honey, 1.4 ton/m^3, or granulated salt, 1.2 ton/m^3 (Engineering ToolBox, 2012; Engineering ToolBox, 2003; Engineering ToolBox, 2010), the beams could have been partially or fully submerged although most likely at a lower draft than the Grågås condition.

Figure 131 City seals of Damme from around 1300 (left) and Harderwijk from 1263 (right) depicting a cog with protruding beams. (Hartemink, 2023; Hartemink, 2022).

The three full scale replicas of the Bremen cog all sail with their beams above the water and the measured heeling angles due to wind for the Ubena von Bremen and the Kieler Hansekogge confirm the stability results for the draft below beams condition (Tanner, 2018, pp. 44-46).

Table 44
Sample of the stability results

	Big Ship of Wismar				Bremen cog		
	Empty	1 m draft	Below wales	Grågås	Ballast	Below beams	Grågås
GM_0 [m]	4.86	4.05	3.46	3.09	0.37	0.82	1.10
GZmax [m]	1.67	1.32	1.07	0.76	0.35	0.51	0.38
GZmax angle [deg]	35.0	27.8	20.8	15.9	41.25	35.95	26.30
Flooding angle [deg]	32.0	25.8	19.2	13.9	44.7	35.3	24.1
Freeboard [m]	1.75	1.52	1.22	0.92	2.97	2.72	1.74
Angle at 15 kn wind [deg]	3.56	2.32	1.55	1.14	15.71	4.47	1.70
Freeboard at 15 kn wind [m]	1.51	1.36	1.11	0.84	1.92	2.05	1.63

The complete stability results for both the Bremen cog and the Big Ship of Wismar have already been presented. A small sample of the results is shown in Table 44 to illustrate the differences between the two ships. The Big Ship of Wismar has clearly a larger initial static stability with GM values between 3.5 and 4.9 m, while the GM values for the Bremen cog are between 0.37 and 1.1 m. The highest initial stability for the Big Ship of Wismar occurs at the empty condition and it reduces with the increasing cargo. The opposite occurs for the Bremen cog, for which the ballast condition has the lowest initial stability and the Grågås condition the highest. The GM values of the Big Ship of Wismar are relatively unaffected by variations in loading conditions. In contrast, for the Bremen cog, the weight distribution of the cargo would have played a more critical role, requiring sailors to exercise caution with its storage within the hold.

In terms of maximum righting arm (GZ), the Big Ship of Wismar also has a significantly higher reserve stability than the Bremen cog. This is also clear when comparing the stability curves in Figure 132, Figure 133, and Figure 134. The Big Ship of Wismar has a much larger area under the GZ curve for heeling angles below 25 to 30 degrees. This means that the Big Ship of Wismar would have had a much larger reserve stability to counteract the effects of wind and waves. Because of its larger stability, the heeling angles caused by wind are much smaller for the Big Ship of Wismar than for the Bremen cog. The differences are especially considerable in the empty/ballast conditions. As indicated in Table 44, a crosswind of 15 knots with a full sail would cause about 4 degrees heel to the Big Ship of Wismar in the empty condition while the heeling angle would reach about 16 degrees for the Bremen cog in the ballast condition. The difference would be even larger if the windage area of the hull above the water and the superstructure would be considered.

The flooding angle and the angle of maximum GZ are however larger for the Bremen cog due to its larger freeboard. Nevertheless, the Big Ship of Wismar heels less and thus would not reach as high heel angles as the Bremen cog. For all conditions except the Bremen cog in ballast condition, the GZmax occurs at an angle higher than the flooding angle. As pointed out by (Tanner, 2018, p. 29), the water reaching the edge of the hull would be a clear visual warning to reduce the sail area in order to remain in the safe stability zone. This means that for the Bremen cog in ballast condition the warning would occur past the maximum righting arm of the ship and thus the ship could find itself in a dangerous situation.

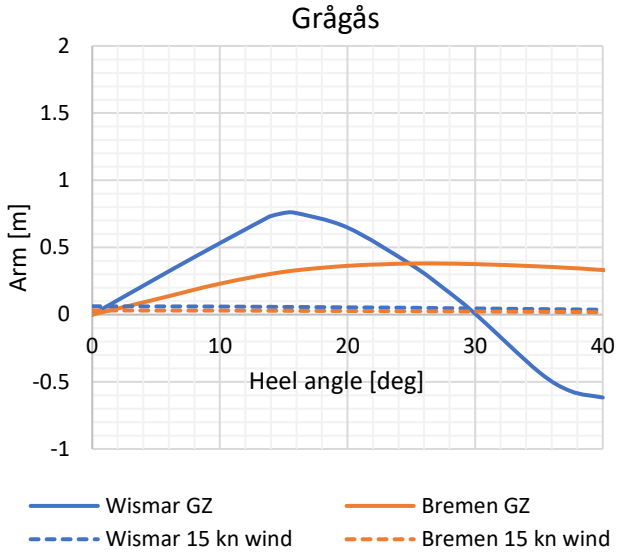

Figure 132 Stability curves for the Big Ship of Wismar and the Bremen cog in the Grågås condition.

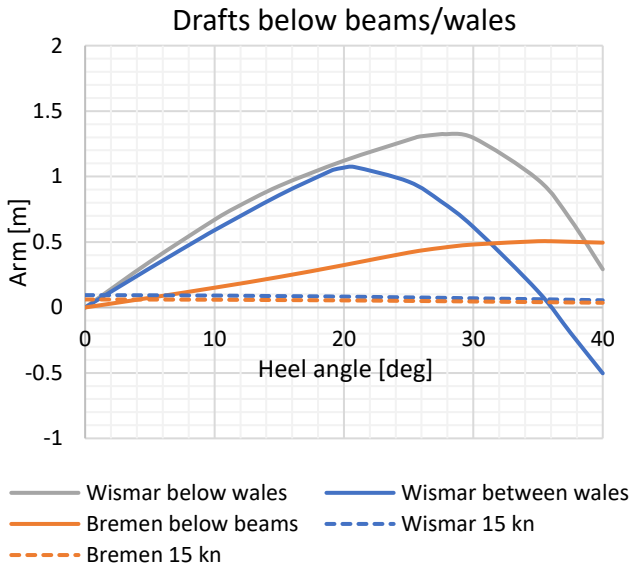

Figure 133 Stability curves for the Big Ship of Wismar and the Bremen cog in the draft below wales or protruding beams conditions, respectively.

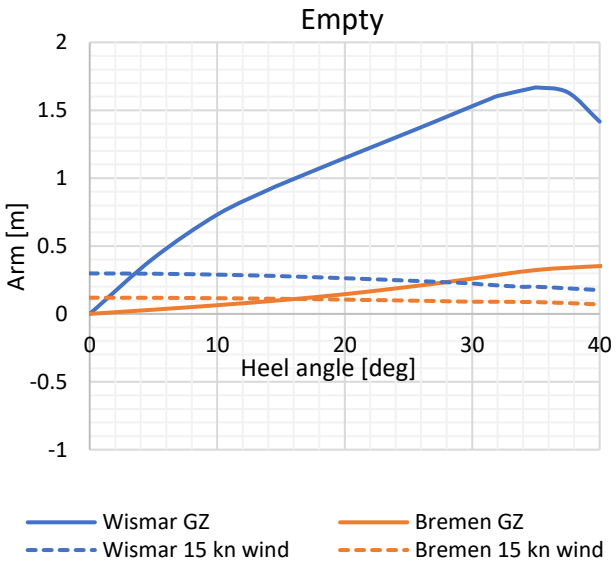

Figure 134 Stability curves for the Big Ship of Wismar and the Bremen cog in the empty or ballast conditions.

Overall, the Big Ship of Wismar has greater stability than the Bremen cog, being its only drawback the low freeboard and hence the low flooding angles, particularly in the Grågås condition. Between the conditions with the draft below or the 1m draft, the latter shows higher stability, especially since the flooding angle shifts from 19 to 26 degrees, see Figure 133 and Table 44.

The inherent low stability of the Bremen cog raises the question of whether this characteristic was common among cogs in general or if, conversely, the Bremen cog was simply a poorly designed vessel. Indeed, the Bremen cog sank shortly before its completion. If the Bremen cog was poorly designed, it would be misleading to regard it as the representative of the typical cog. However, the full-scale replicas of cogs and the calculations performed on the Ijsselcog also reveal a low stability and the necessity of employing substantial ballast to ensure the ship's stability. Performing complete stability calculations on other cogs would provide valuable insights into this matter.

The seakeeping calculations further indicate that the Big Ship of Wismar exhibits superior performance in waves. The Big Ship of Wismar demonstrates lower pitch motions in waves when compared to the Bremen cog. However, the most significant disparity lies in the roll behaviour of the two vessels. The metacentric height of the Big Ship of Wismar remains relatively unaffected by varying loading conditions, resulting in a consistent natural roll period regardless of cargo. This consistent roll behaviour means that the ship would have been more flexible in terms of the amount of transported cargo and that the roll behaviour would have been more predictable. On the other hand, the Bremen cog's metacentric height is highly sensitive to cargo weight and distribution,

leading to significant variations in the natural roll period between empty and fully loaded conditions. As a result, the Bremen cog's roll motions and stability would have been less predictable, requiring caution when handling and storing the cargo.
Furthermore, the natural roll period of the Bremen cog coincides with common wave peak periods in both the North Sea and the Baltic, making it prone to frequent roll resonant conditions, especially when the draft is below the beams, which is the condition that experiences the highest roll motions. In contrast, the Big Ship of Wismar has a very short roll period, making it less susceptible to excitation by waves typically encountered in the North Sea and the Baltic.
The calculations demonstrate that despite its higher freeboard and correspondingly higher flooding angle values, the Bremen cog's larger roll motions would cause the heeling angles to exceed the flooding angle more often and cause a greater likelihood of water embarkment due to waves than on the Big Ship of Wismar. Consequently, the Big Ship of Wismar can be regarded as more seaworthy in open seas than the Bremen cog.

Very limited information exists regarding the sailing capabilities of cogs based on written sources (Heinsius, 1956, p. 153). Most of the information on their performance comes from full-scale replicas, particularly from the Bremen's cog replica Kieler Hansekogge, for which model tests and sea trials have been performed (Brandt, Hoheisel, & Hochkirch, 1994). Results showed that the ship could sail with the wind blowing up to 105-113 degrees from the stern, but with a considerable leeway (Weski, 1999, p. 373). During the sea trials performed in summer 1992, with winds speeds not exceeding Force 7 or 15 m/s, the heel angle was about 15 degrees, which is in line with the results of the calculations done by Tanner (2018, p. 44) for the Bremen cog with a draft below the protruding beams in wind force 6. The sea trials also showed that even under moderate sea conditions, the ship experienced noticeable pitching and large roll motions (Weski, 1999, p. 374). This is in line with the results from the seakeeping calculations performed in this thesis which show large roll motions for the Bremen cog when sailing in stern quartering seas, especially for the condition with the draft below the beams. The optimal speeds of 8 to 9 knots measured during the sea trials with winds coming from 30 degrees from the aft are also in line with Tanner's (2018, p. 44) predictions for the Bremen cog with a draft below the beams and wind force 6. The average speed during the sea trials was 5 knots (Hoffmann & Hoffmann, 2009, pp. 289-290) and, in wind force 5 and 6, it was necessary to reef the sail or remove bonnets as the ship experienced excessive leeway (Brandt, Hoheisel, & Hochkirch, 1994, p. 65).

As described in section III.6, the Ubena von Bremen has also provided valuable information regarding the sailing performance of the Bremen cog. The Ubena von Bremen could withstand winds up to force 8, except when directly from the aft, where stability was compromised. Moreover, the

ship rolled heavily, causing seasickness among the crew. In winds up to force 4, it would drift without making any headway, while speeds of 5 knots were achievable with winds from the stern quarter in wind force 5 and 6. However, the ship struggled to sail against the wind and was unable to move away from the coast. The large windage area from the superstructure caused the ship to drift at speeds of 3 to 4 knots even without sails.

Considering these performance characteristics, the Bremen cog would have found itself in danger in winds blowing towards land due to the large leeway and inability to sail against the wind (Weski, 1999, p. 374).

As already mentioned, it remains questionable whether the performance of the Bremen cog can be deemed typical of all cogs. However, most of the cog wrecks found in Scandinavia and the Netherlands appear to have been driven to the shore by storms (Ellmers, 1994, p. 40). As Ellmers points out, the sailing experience with the full-scale cog replicas along the Hanseatic routes has shown that ships would have sailed along the coast, keeping the coast and the sheltered bays at sight in order to find refuge in case of storms. Sailors, as noted by Ellmers, would have preferred anchoring and waiting out unfavourable weather instead of sailing against the winds and away from the coast. The most dangerous scenario arose when a storm shifted direction and the wind started blowing into a previously sheltered bay, eliminating its protective qualities (Ellmers, 1994, p. 40) . Given this persistent danger, Weski (1999, p. 374) states that it is unsurprising that four ships dated 1294/1296 found in Scarborough were equipped with four anchors each.
Ships would have therefore sailed during daylight keeping the coast at a visible distance and anchored at night in sheltered bays (Crumlin-Pedersen, 1991, p. 70). Harbour entrance markers as the ones used in Scandinavia, which were tower-shaped wooden structures visible from afar, were introduced into the Hanseatic routes as an aid for navigation from around 1225 (Ellmers, 1994, p. 40). When open sea navigation was required for a specific route, Hanseatic sailors would wait for a clear night to navigate using the polar star as their guide. This navigation method was referred to as Nachtsprung by historian Adam von Bremen in the 11th century (Ellmers, 1994, p. 40).

The same sailing strategies seem to have been followed by the sailors of Nordic ships. Wrecks are also typically found in harbours and close to market settlements that were in use at that time (Crumlin-Pedersen, 1991, p. 70). As with the cogs, Nordic ships would have sailed by day along the coast and anchored in sheltered bays at night. In some circumstances, changes in winds due to storms would have pushed ships to the shore, where they sank in shallow waters. This is what would have occurred in Lynaes, where two 12th century ships have been found next to the local beach market site (Crumlin-Pedersen, 1979a). Written sources such as the travels by Ottar and Wulfstan,

reported to King Alfred in the late 9th century, show that ships travelled along the coast both in Norway and in Danish waters (Crumlin-Pedersen, 1985, pp. 91-92; Bruun, 1997, p. 1289). Likewise, a Danish taxation book from 1231 commissioned by King Valdemar II includes the description of a sailing route from Sweden to Estonia that follows the coastline and only makes the shortest possible open water crossings (Crumlin-Pedersen, 1985, p. 92). With the introduction of the compass, the navigation routes changed and, although still strongly reliant to the coastline, straight compass open water crossings became more common, as evinced by the 15th century 'Seebuch' descriptions of sailing directions (Crumlin-Pedersen, 1985, p. 92). As previously mentioned when discussing the sailing strategies of cogs, markers to aid navigation had been erected along the Scandinavian coast since the Viking Age. These markers, known as "tønder" or "varder" in Danish and Norwegian, can be found in place names such as Tønsberg and Vardø and later, after the introduction of Christianity, in names such as Korshavn and Korsø, as they took the form of crosses (Vikingeskibsmuseet, 2023e). Although sailing along the coast was the preferred strategy, Nordic ships also needed to keep a safe distance form it. Sailing experiments performed by Jarret (2023) in traditional Norwegian clinker-built square-rigged boats along routes known from written sources have shown that the presence of irregular and choppy seas, commonly found in narrow sounds or areas with sudden depth changes, poses a significant danger to these open boats. Jarret states that these conditions are more hazardous compared to strong yet consistent winds and the gentle swells of the open sea. Moreover, the risk is heightened by strong tidal currents and frequent reefs in coastal areas. Due to their light weight, shallow draught, and absence of a deep keel, these boats experience large beam leeway and are especially difficult to manoeuvre against the current and away from the rocks (Jarrett, 2023; Shaw, 2016, p. 18).

There is little knowledge about the navigational aids used by the Vikings in open seas. Most probably they relied on their senses, such as the observation of the waves, clouds, birds and other animals, the stars, and the position of the sun (Bruun, 1997, p. 1289; Jarrett, 2023). The sun's path and midday direction would have provided consistent orientation, while the stars were a reliable night-time reference, except during the bright Nordic summer nights when star observation was not possible (Vikingeskibsmuseet, 2023e). Night sailing would have been feasible along the Norwegian coast between May and July (Jarrett, 2023). A late 13th century manual of astronomical navigation for the North Atlantic confirms the practice of night sailing (Vinner, 1995, p. 296).

Like with cogs, full-scale replicas have provided valuable information on the sailing performance of Nordic cargo ships, especially the replicas of the Skuldelev ships. As discussed in section III.6, the Saga Siglar, a replica of Skuldelev 1, successfully navigated hurricane-force storms in the North Atlantic and between Greenland and Newfoundland (Vinner, 1995, pp. 303-304). It achieved speeds

of 9 knots in wind speeds of 10-15 m/s and even reached up to 10 knots in strong winds in the North Sea (Vinner, 1995, p. 292; Bruun, 1997, p. 1289). The replica of Skuldelev 3, known as the Roar Ege, reached speeds of up to 9 knots in crosswinds (Bruun, 1997, p. 1289). Experimental trials also showed that these replicas could sail against the wind at angles of up to 120 degrees from the stern, achieving speeds between 1.5 and 2 knots (Bruun, 1997, p. 1289).

Although it is difficult to compare the performance of Nordic cargo ships and cogs from the reported behaviour of the different replicas, Nordic ships appear to be able to reach higher speeds and withstand rougher weather than cogs. The results of the speed calculations performed as part of this thesis are in line with this observation and show that the Big Ship of Wismar had a higher speed potential than the Bremen cog despite its smaller sail. This is due to the much larger resistance of the Bremen cog caused by its larger draft, larger wetted surface, and fuller hull lines as indicated by the larger block, prismatic and waterplane coefficients, see Table 45.

The differences in resistance, or required power to overcome the resistance, are highest for the Grågås condition followed by the condition with intermediate draft, see Figure 135. When the two ships are compared at similar drafts, that is the Grågås condition for the Big Ship of Wismar at a draft of 1.6 m and the ballast condition for the Bremen cog at a draft of 1.5 m, the power required by both ships is similar. When compared at drafts with similar cargo capacities, i.e., the draft below beams for the Bremen cog at 2 m and the draft below wales for the Big Ship of Wismar at 1.3 m, the Bremen cog would need more than twice as much power as the Big Ship of Wismar.

Table 45
Wetted surface and geometry coefficients for the Bremen cog and the Big Ship of Wismar

Condition	Ship	Draft [m]	Wetted surface [m^2]	Block coefficient Cb [-]	Prismatic Coefficient Cp [-]	Waterplane Coefficient Cwp [-]
Grågås	Bremen	2.8	149.8	0.502	0.703	0.839
	Wismar	1.6	135.4	0.353	0.583	0.671
Draft below beams/wales	Bremen	2.0	117.0	0.476	0.681	0.806
	Wismar	1.3	118.4	0.318	0.568	0.660
	Wismar	1.0	99.7	0.269	0.544	0.638
Empty/ballast	Bremen	1.5	94.2	0.446	0.653	0.769
	Wismar	0.8	84.6	0.221	0.520	0.608

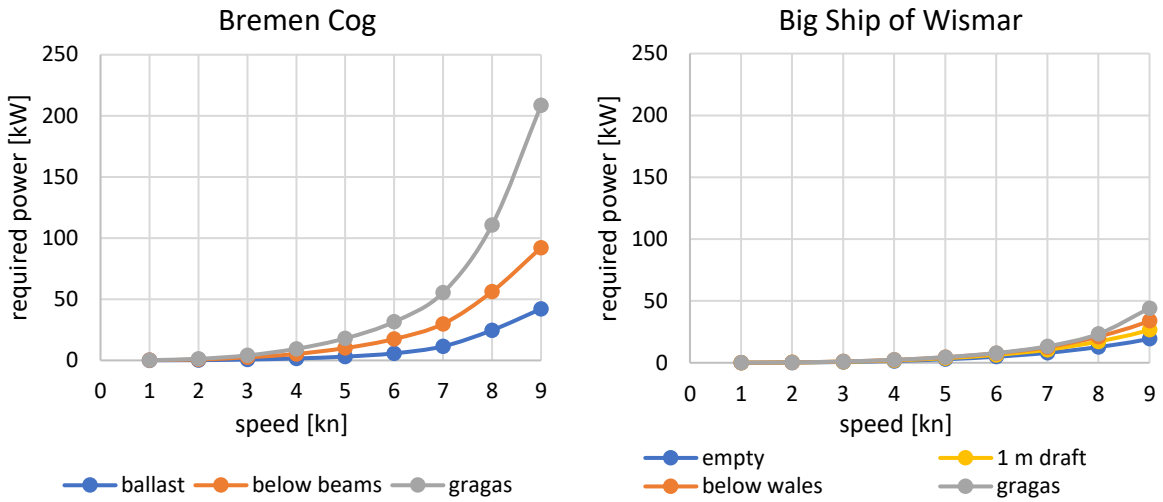

Figure 135 Required power to overcome the calm water resistance for the Bremen cog and the Big Ship of Wismar. (Hernandez Montfort).

The accuracy of the required power values obtained through the Holtrop & Mennen method may be limited since the method was developed based on modern ships that differ significantly from the Big Ship of Wismar and the Bremen cog. Nevertheless, it is evident that the Bremen cog experienced considerably higher resistance and required greater power to achieve similar speeds compared to the Big Ship of Wismar. To obtain more precise results, it would be necessary to conduct sea trials with full-scale replicas or employ more advanced computational fluid dynamics (CFD) calculations. CFD calculations could also provide valuable insights into the wave pattern along the hulls when advancing at forward speed. Specifically, they would help determine whether the hollow waterlines observed at the bow of cogs contributed to enhanced speed and were intentionally incorporated into their design, as suggested by Hocker & Ward (2004, pp. 73-75).

The method to compute the power generated by the sails that has been used in this thesis for the Big Ship of Wismar and by Tanner (2018) for the Bremen cog, is very basic since it only uses an average power per square meter of sail for different wind speeds without taking into account the actual proportions of the sail, nor the effects of the ship's speed on the apparent wind velocity acting on the sails. Therefore, the absolute values of the speeds should be taken with scepticism. Nonetheless, they seem to be in line with the speeds achieved with the full-scale replicas and the speed differences between the two vessels can still be considered as valid. Hence, the Big Ship of Wismar would have been able to sail faster than the Bremen cog in equivalent wind conditions. Although more advanced calculations could be done, it should be kept in mind that there is little knowledge about the exact proportions of the sails as no sails have even been found. Moreover, only very limited evidence of rigging has survived on wrecks. Most of the sail reconstructions have

therefore been based on the archaeological evidence preserved on the Skuldelev 3, which allowed to estimate the width of the sail based on the mast position and the position of rigging holes on its sides, and the sailing experiments performed with its full-scale replica the Roar Ege, which provided an indication of the height of the mast and sail. During these experiments, the square sail was designed to achieve a balanced relationship between the forces acting on the hull, sail, and rudder when sailing against the wind. As summarized by the Viking Ship Museum (Vikingeskibsmuseet, 2023f), when the sail was too wide in relation to the hull, the ship would veer away from the wind, making it unable to tack against the wind. On the other hand, when the sail was too narrow, the ship would turn into the wind without the rudder being able to compensate for it. These imbalances would render the ship unsafe and practically useless. Additionally, when the sail was too low, the ship sailed sluggishly and conversely, when the sail and mast were too high, the excessive loads would require reefing the sail prematurely. Through the conducted experiments, it was determined that the sails would have had approximately equal height and width, forming a right-angled square shape. The choice of right-angled square sails, as opposed to trapezoidal sails, is supported by the iconographic material on Viking Age and medieval ship graffiti, the 8th to 10th century Gotland stones, 10th century coins, and the 11th century Bayeux tapestry (Bischoff, 2017, pp. 12-15). Full-scale replicas of ships equipped with square sails, using a similar width definition as for the Skuldelev 3, have demonstrated excellent sailing performance in terms of handling, speed, and the ability to sail against the wind (Bischoff, 2017, p. 22).

These square sails do not however match the iconography found on rune stones, coins, and carvings, which show very large sails about twice as wide than tall, with yards extending from stem to stem and very high masts (Bischoff, 2017, p. 22; Shaw, 2016, p. 18). The depictions of ships are unlikely to provide an accurate representation of sail proportions, as they do not align with archaeological evidence and would fail to achieve the necessary balance for sailing against the wind. In addition, written sources mention rigging elements that not only provide valuable insights into the appropriate size of the sails but also suggest their ability to sail against the wind (Bischoff, 2017, p. 22). It remains debatable whether the sails on Nordic ships were similar to the square sails used on the Roar Ege or if they had a lower and broader rectangular shape. However, most sail and rigging reconstructions have been made by adhering to the sail proportions used on the Roar Ege, with the width of the sails scaled to the width of the ship.

The calculations conducted on the 3D model reconstructions of the Bremen cog and the Big Ship of Wismar, as well as the sailing performance of full-scale replicas, unequivocally demonstrate that Nordic ships outperformed the Bremen cog in terms of stability, speed, ship motions, and

seaworthiness. These findings refute the belief that cogs were technologically superior to contemporary Nordic cargo vessels and that their alleged superiority led then to eventually replace the Nordic vessels. While Christensen (1989, p. 20) had already reached a similar conclusion based on the larger size of Nordic cargo ships compared to contemporary cogs, the persisting idea of cog superiority, popularized by Heinsius' work, remains deeply ingrained in historical thinking today (Dhoop, 2016, p. 50). For instance, Rose (2007, pp. 77-78) states that “the quasi-monopoly which the Hanseatic cities were able to establish in the most important northern trades has been put down to the superiority of their ships, […] the cog, was larger and handled better than vessels of other designs”. The results of the calculations performed on the 3D model reconstructions of the Bremen cog and the Big Ship of Wismar presented here further reinforce Christensen's statement by directly comparing actual ship performance, providing compelling additional evidence against the notion of the cog’s superior sailing capabilities.

Other possible explanations for the disappearance of Nordic cargo vessels and the dominance of cogs have been presented in section II.3. These explanations primarily relate to societal changes that led to a more economic oriented approach to shipbuilding and maritime trade. Cogs were indeed structurally less complex and, since they did not require split planks from high quality timber like Nordic ships but used sawn planks instead, they required less timber and were less labour intensive than Nordic vessels (Hocker & Ward, 2004, p. 85; Ellmers, 1994, p. 39; Dokkedal, 1996, p. 62). Besides the purely economic considerations related to construction techniques, there may have been additional factors associated with the specific uses of the vessels that contributed to cogs being preferred over Nordic cargo vessels, despite their lower performance in terms of stability, seaworthiness, and speed.

According to Christensen (1989, p. 20; 2002, p. 92), the political and militaristic power of the Hanseatic League, coupled with their control over grain and salt trade, provides an explanation for the prevalence of cogs over Nordic ships. In that respect the characteristic high freeboard and superstructure present on cogs might indicate that these ships also had a militaristic purpose. Pictorial evidence indicates that sea battles followed a similar set-up as land warfare (Runyan, 1994, p. 52). While ships occasionally rammed each other, the primary tactic involved boarding and engaging in hand-to-hand combat on the decks (Waldus, Verweij, & van der Velde, 2019, p. 489). Prior to the use of gunpowder and guns, sinking the enemy's ship was indeed difficult and actually undesirable, as capturing a conquered vessel would have been more valuable (Bill, 2002, p. 49). Fighting also involved throwing projectiles such as arrows from elevated positions and so the ship’s superstructures or castles would have been extremely useful (Waldus, Verweij, & van der Velde, 2019, p. 489).

The earliest documented references to cogs can be traced back to AD 948 and 949 in Utrecht, where two tax documents mention the term "cogsculd", likely referring to a form of coastal defence involving small cogs (Englert, 2000, p. 46; Van de Moortel, 2011, p. 88). Likewise, documents from 1234 and 1239 indicate that the city of Lübeck used cogs in naval actions against the King of Denmark (Englert, 2000, p. 47). Moreover, written documents show that from 1394 Hanseatic towns used cogs as part of their fleets of warships, which were referred as “vredesschepen” and served as escorts for merchant ships sailing in convoys to protect them from pirates (Weststrate, 2008, p. 36; Lensen & Heitling, 1990, pp. 140-141, 145-148). Waldus, Verweij, & van der Velde (2019, p. 491) suggest that the large Ijsselcog might have been designed as a military vessel due to its size and freeboard height, while also serving a trading function as evidenced by the presence of cargo floors and shifting boards in its hold. The characteristic shape of cogs might thus be a result of trying to combine the functions of cargo and military vessels by maximising both their hold volume and freeboard height.

In contrast, written sources do not mention the involvement of genuine sailing Nordic vessels in warfare, suggesting that only ships that combined rowing and sailing were used in military conflicts (Englert, 2003, p. 274). Therefore, although the use of Nordic cargo vessels in military operations cannot be excluded, there seems to have been a clear distinction in purpose between the genuine sailing cargo vessels and the more specialized warships designed for both oar and wind propulsion.

As previously discussed in chapter two, the introduction of sailing vessels in the Nordic shipbuilding tradition occurred relatively late. The earliest archaeological evidence of genuine sailing Nordic vessels dates back to the period following the establishment of centralized royal power in Denmark during the late 10th century (Englert, 2003, p. 278). Following this period, Danish waters witnessed the emergence of a professional merchant seafaring network, which expanded gradually until achieving widespread coverage around 1200. This is supported by the increase in the number of towns with access to navigable waters and the distribution large cargo shipwrecks which indicate a direct connection between these vessels and the major ports and centres of secular and religious power and trade (Englert, 2003, p. 278). While during the Viking Age, trade between Scandinavia and western Europe primarily involved luxury items or small quantities of goods, which could easily be transported across the Haithabu isthmus connecting the Schlei inlet of the Baltic Sea and the North Sea, direct maritime traffic became necessary after 1000 when the urban growth in Western Europe created a large demand for natural resources and food (Weski, 1999, p. 365; Litwin, 1998, p. 93; Bill, 1995, p. 202). This shift marked a transition from the exchange of prestige goods among elites to the transportation of larger quantities of commodities such as dried fish, grain, salt, timber, beer, wine, tar, and wool to meet the demands of the urban communities (Ayers, 2013, p. 67).

The large cargo ships like Lynaes 1, the Big Ship of Wismar, the Big Ship of Bergen, and Karschau were definitely export ships built to carry heavy cargo and not luxury goods, but due to their building complexity and related costs they could have only been commissioned by the wealthiest elite members of the society, such as the nobility or the clergy (Englert, 2000, p. 144; Christensen, 2002, p. 91). The ship names containing the term "*buza*", which refers to cargo ships from Scandinavia, appearing in written sources from the late 12th century to the 14th century, such as the Icelandic Annales and the English toll roll, suggest that these vessels were owned by prominent members of society (Ditta & Auer, in press). For instance, the Qgvaldsnesbuza from the royal seat of Avaldsnes in Norway or the Lýsbúza from the Lysa monastery in Norway (Mundal, 2017, p. 44; Simek, 1979).

Over time, the growth of urban areas, the high demand for goods, and the Hanseatic League's control over the salt and grain trades would have shifted the shipbuilding and maritime trade activities from an elitist and prestige driven character to a simpler and more economically driven approach from the 13th century (Bill, 1997, p. 161). Written sources indicate that salt and grain were being transported in bulk (Wolf, 1986, pp. 26, 57, 65). This required large volumes of closed cargo space under a deck to protect the cargo from the weather. Remains of decks have been found on both the Bremen cog and the Ijsselcog (Weski, 1999, p. 373; Waldus, Verweij, & van der Velde, 2019, p. 483). The Nordic cargo vessels, which lacked a closed deck would not have been suitable for bulk transport.

Another potential benefit of cogs compared to Nordic cargo ships could have been their flat flush planking at the bottom, which is less susceptible to erosion and damage from grounding when sailing through shallow waters along the coast (Tanner, 2018, p. 42).

It can be concluded that despite Nordic cargo ships demonstrating superior performance in terms of speed, stability, and seaworthiness, cogs would have been superior in fulfilling the social needs of the time. These needs included the ability to transport large volumes of relatively light cargo in bulk over short distances along the coast between Hanseatic cities, serving both trading and militaristic purposes, and generating higher profits from maritime trade thanks to their reduced costs of production. As Tanner (2018, p. 55) points out, while the Bremen cog was not ideal for navigating the vast and exposed seas of the North Atlantic, it excelled in transporting cargo along coastal routes and relatively short sea crossings in the sheltered waters of northern Europe.

In the next concluding chapter, the findings and the implications discussed here are synthetized and their relevance to the research questions of the current thesis is highlighted.

VIII. Conclusions

The findings presented and discussed in this thesis have shed light on the potential and usefulness of employing modern naval architecture methods in combination with digital ship reconstruction models to assess ship performance in archaeological research. Moreover, they have provided valuable insights into the transformations observed in shipbuilding traditions throughout Northern Europe between the 12th and 14th centuries, which led to the disappearance of Nordic cargo ships and the dominance of Hanseatic cogs in the maritime trade. In this chapter the implications of these findings in relation to the research questions are addressed. I shall start by addressing the sub-questions first and conclude by addressing the main research question.

- What were the differences in sailing performance between Nordic cargo ships and cogs?

The findings from the calculations performed on the Big Ship of Wismar and the Bremen cog have shown substantial differences between them in all the aspects investigated in the current thesis. The first big difference is in their weight, which is essentially a direct consequence of the differences in building techniques and raw materials used in their construction. Although both ships have similar main dimensions, that is, same length and beam, the results show that the Bremen cog was twice as heavy as the Big Ship of Wismar. Moreover, the Big Ship of Wismar had a greater transverse stability than the Bremen cog, the latter requiring 15 tons of ballast to be stable. Related to the weight differences, the Bremen cog had a much larger draft than the Big Ship of Wismar. The latter would therefore have had access to shallow water harbours that would have been inaccessible for the Bremen cog. Regarding the cargo capacity, both ships had a similar capacity when sailing with a draft below the wales for the Big Ship of Wismar and a draft below the protruding beams for the Bremen cog. As discussed in the previous chapter, these were the most likely operational drafts. However, when considering a higher draft corresponding to the specifications in the Grågås codex, the Bremen cog had a much larger cargo capacity than the Big Ship of Wismar thanks to its high freeboard. Considering the stability of the ships and their inertia, which is defined by how the weights of the structural elements and the cargo are distributed, the results show that the stability and rolling behaviour of the Big Ship of Wismar would have been less affected by changes in the loading conditions than for the Bremen cog. Thus, the Big Ship of Wismar would have offered more flexibility and its behaviour would have been more predictable than the one on the Bremen cog, for which the crew would have needed to be more cautious when handling and storing cargo on board.
Regarding their speed potential, the results show that the Bremen cog experienced a much higher resistance than the Big Ship of Wismar due to its higher draft and fuller hull lines. Therefore, the Big

Ship of Wismar would have been able to sail at higher speeds than the Bremen cog in similar wind conditions, despite its smaller sail.
The seaworthiness of both vessels was evaluated by calculating their motions when subjected to sea state conditions typical for the Baltic Sea and the North Sea and by defining two safety criteria. The first being that the roll angle of the ships should remain below their flooding angle, and the second that the relative water elevation due to the waves and the ship motions should be lower than the freeboard of the ships. The results showed that the Big Ship of Wismar would have been able to withstand rougher conditions than the Bremen cog despite its lower freeboard thanks to its lower roll motions. Again, the behaviour of the Big Ship of Wismar was less affected by the differences in loading conditions while the Bremen cog was very sensitive.

Whether the results obtained for the Big Ship of Wismar and the Bremen cog can be generalized to represent all other Nordic cargo vessels and cogs remains questionable. However, the information provided by full scale replicas and calculations on other ships seem to confirm the results found in the current thesis. Sea trials with replicas of Nordic ships, including the replicas of the cargo ships Skuldelev 1 and 3, demonstrated exceptional performance in open seas, including the ability to withstand rough weather conditions and achieve high speeds. On the other hand, the replicas of cogs show more limitations in adverse weather and appear to have been more suitable for coastal and sheltered navigation. Moreover, the cog replicas and the stability calculations performed on other cogs such as the Ijsselcog, show that they required substantial ballast in their empty condition in order to be transversally stable, which is in line with the findings for the Bremen cog.

Performing similar calculations as those presented in this thesis on other Nordic cargo vessels and cogs would provide valuable insights into their performance characteristics, allowing for a comparison to be made with the observed differences between the Big Ship of Wismar and the Bremen cog. For example, the Ijsselcog has already undergone 3D model reconstruction and weight and initial stability calculations, making it possible to conduct a complete stability assessment, speed potential estimations, and seakeeping calculations like those performed in this thesis. Similarly, with hull reconstructions already completed for the Skuldelev ships and the Lynaes 1, generating complete 3D models and conducting weight and stability assessments, speed potential estimations, and seakeeping calculations should be feasible. Additionally, model scale tests or sea trials with full-scale replicas under comparable weather conditions would be highly valuable, although such endeavours are much more complex and costly than the computational work.

- Could these differences have played a role in the disappearance Nordic cargo ships and the dominance of cogs after 1300?

If we consider the differences in performance between Nordic cargo ships and cogs with regards to weight, stability, speed, and seaworthiness from a strictly technical point of view, it is clear that these cannot explain the changes in shipbuilding traditions that led to the disappearance of Nordic cargo ships. As discussed above, Nordic cargo ships exhibit superior performance compared to cogs. Thus, the results of the current research confirm the claim by Christensen (1989, p. 20), who stated that Hanseatic supremacy could not be explained by the technological superiority of their ships. He reached this conclusion based on the discovery of large cargo vessels built in the Nordic tradition, especially the Big Ship of Bergen, which disproved the previous belief that Nordic ships could not be built big enough to compete with cogs. Besides their size, a comparison of the ships' performance was however not done. Nevertheless, scholars shifted their focus towards socio-economic explanations to account for the disappearance of Nordic cargo ships and the dominance of cogs. The findings of the current research show that those socio-economic factors had such a big impact in shaping the transformations observed in shipbuilding traditions, that they outweighed ship performance considerations.

As presented earlier in the thesis, these socio-economic factors would have been related to the need of reducing shipbuilding costs and the political and militaristic power of the Hanseatic League together with its monopolistic trade organisation (Christensen, 1989, p. 20; Christensen, 2002, p. 92). Indeed, cogs could be built with swan planks of lesser quality timber and employed less labour-intensive construction techniques than Nordic ships. The transition from elaborate and costly shipbuilding techniques to more economical approaches appears to have been driven by factors such as rapid population growth and the increasing demand for efficient maritime transportation of goods (Bill, 1995, p. 202). Additionally, the establishment of the feudal system would have brought about social changes that, coupled to the demand for more cost-efficient ships, shifted the nature of shipbuilding and maritime trade from an elitist prestige-oriented mindset to a more pragmatic and business-driven approach (Bill, 1997, p. 161; Bill, 1995, p. 202).

It has been discussed in this thesis that a clear cut between the two shipbuilding traditions is unrealistic. Rather than a sharp shift from one to the other, the transformations occurred gradually with both traditions adopting features from each other and adapting to meet the evolving social needs.

- Which ship geometric characteristics impacting the sailing performance of Nordic cargo ships and cogs would have been favoured at that time, considering the intended use of the vessels?

As stated by Tanner (Tanner, 2018, p. 55), “there is no such thing as the ideal boat, it is not physically possible to design a vessel which is perfect for every task, sea state or weather condition”. Indeed, whether a ship performs well does not only depend on technological aspects such as the ability to reach higher speeds or being able to withstand higher wave heights and wind speeds, but also on the requirements needed for the task at hand. For instance, a slower, simpler ship might be considered to perform better than a faster and more technological advanced one if speed is not a relevant factor but construction and operational costs or cargo capacity are.

As discussed in the previous chapter, Nordic ships were lighter and had a smaller draft than cogs and thus this characteristic would have been favoured if trade in shallow waters was a critical factor. On the other hand, flat carvel-built bottoms such as the ones fond in cogs would have been more advantageous for ships prone to grounding because of their reduced sensitivity to erosion and damage and their lower repair costs. The hull shape of Nordic ships would have been preferred if speed and ability to sail in rough and open seas rather than along sheltered coastal routes would have been required.

The most relevant geometric characteristics of cogs that could explain their dominance are their high freeboard, the full hull lines, the presence of a closed deck, and the presence of a superstructure. The high freeboard of cogs and the full hull lines provided a large volume ideal for the transport of voluminous but light cargo, such as grain, in bulk. The presence of a closed deck further facilitated the transportation of bulk cargo by protecting it from adverse weather conditions. In contrast, Nordic vessels lacked a deck and had a low freeboard. This resulted in a limited cargo space that would have been more susceptible of getting wet by the effects of the weather, making the transport in bulk more challenging. The transport of cargo in bulk would have been required to fulfil the large demands of goods and food as a consequence of the fast population growth. Historical sources show indeed that salt and grain were being transported in bulk (Wolf, 1986, pp. 26, 57, 65).

The significant freeboard of cogs served a dual purpose, not only enabling the transportation of bulky cargo but also providing a defensive advantage against boarding during attacks at sea. In the face of rising piracy, ships would have needed to fulfil a defensive role besides their purely commercial one. Historical evidence suggests that cogs may have been involved in military operations as well. It is worth noting, as discussed in this thesis, that the direct correlation between

archaeological cogs and the term "cog" as described in historical sources can sometimes be misleading. Nonetheless, the presence of a deck on cogs would have been beneficial during maritime combat, as boarding and hand-to-hand combat were the main tactics employed during such engagements (Waldus, Verweij, & van der Velde, 2019, p. 489). The presence of the elevated superstructure would also have provided an efficient spot from which to throw projectiles to the enemies.

I have also discussed in this thesis that, without compasses, the sailing strategies would have consisted in sailing during the day along the coast and anchoring in sheltered places at night. Harbour entrance structures visible from afar were used both in Scandinavia since the Viking Ages and were introduced into the Hanseatic routes from around 1225 (Ellmers, 1994, p. 40). Open sea navigation would have been done only when strictly necessary and would have then been done at night using the polar star as a guide.

In conclusion, while Nordic cargo ships exhibited superior speed, stability, and seaworthiness, cogs were more suitable vessels to meet the social demands of that time.

- What are the benefits and limitations of applying modern naval architecture design methods to past shipbuilding traditions?

Modern naval architecture methods were of course not used in the past. Instead, shipbuilders must have relied on common sense, experience, and trial-and-error approaches to design their ships. Therefore, it is important to recognize that ancient ships were not built with the intention of meeting modern criteria. Even when ancient ships do not fulfil modern standards, it does not necessarily imply that they were poorly designed. Despite not conforming to modern safety standards, ancient ships might have been sailed successfully. Thus, while modern naval architecture methods offer valuable insights into ship performance, the evaluation of ancient ships should not be solely based on their deviation from modern standards but also on the understanding of the context in which they were built and operated.

Furthermore, it is crucial to acknowledge that modern naval architecture methods and standards were primarily developed for metal ships equipped with mechanical propulsion. As a result, these methods may not be directly applicable to ancient ships. For instance, some modern stability standards based on the GZ curves may not be suitable for open boats. This was the case for the GZ values required by the Bureau Veritas rules at high angles, which exceeded the flooding angles of the

Big Ship of Wismar. However, the fundamental principles of modern naval architecture, such as the theory behind the transverse stability of ships or the linear seakeeping theory, are principles rooted in physics. As a result, they can be applied to all ships or floating bodies, regardless of their hull shape or construction material. By employing modern naval architecture methods, even criteria and methods that may not directly apply to ancient ships, it becomes possible to systematically and objectively compare different ships in accordance with the scientific method. This enables the formulation and testing of hypotheses.

A notable issue that arises when using modern naval architecture methods on ancient ships is the potential for a misleading sense of accuracy. As emphasized in the thesis, archaeological remains of shipwrecks are often scarce and fragmented, resulting in the need for assumptions when reconstructing the original appearance of the ship. For some elements of ships, such as the rigging and sails, hardly any evidence has survived in the archaeological record and theoretical reconstructions are needed. Consequently, there exists a considerable amount of uncertainty in the process of reconstructing a ship. However, modern methods provide deterministic values for the aspects under study, which may be misleadingly perceived as accurate and indisputable answers.

To conclude, I finally address the main research question of this thesis:

- How can modern naval architecture methods be applied to the digital reconstruction models of ships, in particular a Nordic cargo ship and a Hanseatic cog, to assess and compare their sailing performance?

Besides their visual appeal, 3D reconstruction models of wrecks can serve as valuable tools for gaining insights into ship performance and for facilitating meaningful comparisons between vessels. However, it is important to acknowledge that different considerations come into play when developing a visualization model versus a model suitable for conducting calculations. While visualization models demand a high level of detail to achieve aesthetic realism, not every element needs to be modelled as a solid volume, especially those that remain visually hidden. On the contrary, weight and inertia calculations necessitate the precise modelling of each element as a closed volume, without any intersections between objects. Furthermore, for stability, speed, and seakeeping calculations, a smooth hull surface is used rather than an explicit representation each individual plank. By recognizing these distinct requirements, researchers can effectively harness the potential of 3D models to perform meaningful computational analyses.

It is however important to acknowledge that certain modern methods for the estimation of ship performance might not be applicable to ancient ships and thus results may not be accurate. For instance, the use of estimation methods based on geometric coefficients of modern ships, such as the Holtrop method for calm water resistance, may not yield accurate results when applied to ships such as the Big Ship of Wismar or the Bremen cog, which have very different hull shapes in comparison to modern ships.

Nevertheless, the relative differences between ships and the identification of patterns or changes over time can still offer valuable insights. These insights can help us understand the qualities that ancient shipbuilders would have deemed important and incorporated into their designs, the qualities that would have been considered as unimportant, and the characteristics would have been considered as disadvantageous and consequently abandoned. Regarding the differences between Nordic cargo ships and cogs, speed and seaworthiness in rough weather seem to have been less important qualities than cheaper construction costs, presence of a closed deck, and ample cargo space.

Another important consideration that needs to be kept in mind when modern naval architecture methods are applied to 3D model reconstructions is the inherent uncertainty of the reconstruction models. This uncertainty needs to be acknowledged when interpreting the results obtained from modern methods, which otherwise might imply a false sense of accuracy. For both the Bremen cog and the Big Ship of Wismar, rigging and sails were not preserved and their reconstruction is therefore just a theoretical one. Moreover, it has been shown that discrepancies in geometry exist between the reconstruction models of the Bremen cog depending on what material source is used and how it is interpreted. Thus, equally valid alternative reconstructions could in principle be made for each ship. Once this is acknowledged, modern naval architecture methods are a great approach for the systematic evaluation of possible alternatives. In the current thesis alternative calculations were performed for different water moisture content in timbers as well as for different possible operational drafts. However, conducting calculations on alternative hypothetical reconstructions of the Big Ship of Wismar and the Bremen cog would be of great value, particularly in relation to sail proportions and size, as well as to cargo weight distributions, which appeared to have a significant impact on the behavior of the Bremen cog.

Regarding the cargo densities and possible operational drafts, it would be useful to investigate the sailing routes of the vessels of that time, as well as the cargo that was being transported and the ways in which it was being stored in the holds. This would allow for a better estimate of the possible cargo weights and operational drafts, which could then be used in the calculations to assess the

ships' performance. However, this would primarily involve historical research, and caution must be exercised when applying it to the archaeological record. This is especially true for cogs, as the historical references to cogs do not necessarily correlate with the archaeological definition.

The current thesis has shown that modern naval architecture methods can successfully be applied to 3D model reconstructions of ancient ships to get a better understanding of their performance. Moreover, it has proved that by evaluating ship performance, we can gain a deeper understanding of broader research questions such as the assessment of the transformations in shipbuilding traditions and ship types over time. By doing so, we can infer the social changes that potentially influenced and drove these transformative processes.

Abstract

During the 13th and 14th centuries, the shipbuilding traditions in the Baltic Sea and North Sea regions underwent significant transformations. From 1000 to 1300, large cargo ships built in the Nordic shipbuilding tradition dominated the maritime trade. After 1300 the supremacy in the region's maritime trade shifted to German merchants and the Hanseatic League, leading to the disappearance of the Nordic shipbuilding tradition and the rise of cogs as the most common cargo vessels in Northern Europe. Initially, the shift from Nordic ships to cogs was attributed to the latter's perceived better performance, as it was believed that it was technically impossible to build large ships in the Nordic tradition. However, this assumption was challenged when large cargo vessels built in the Nordic tradition were discovered. As a result, scholars shifted their focus from technical explanations to socio-economic ones. These socio-economic narratives linked the dominance of cogs mainly to their lower shipbuilding costs, as well as the commercial, political, and military power of the Hanseatic League. Besides the differences in building techniques, Nordic cargo ships and cogs had very different hull shapes and therefore differences in performance are to be expected even when comparing ships of similar sizes. However, a comprehensive performance comparison between Nordic cargo ships and cogs has not been made since most shipwrecks are only partially preserved, and the evaluation of ship performance requires a complete hull. The 3D model reconstruction of shipwrecks provides thus an opportunity to evaluate the performance capabilities of ancient vessels. This thesis aims to apply modern naval engineering approaches, typically used for modern ships, to assess and compare the performance of Nordic cargo ships and cogs using 3D reconstruction models. The goal is to determine whether the socio-economic reasons for the shift from Nordic cargo ships to cogs went hand in hand with an improvement in ship performance. To this purpose weight and stability calculations, as well as speed estimations and seakeeping calculations are conducted on the 3D model reconstructions of the Big Ship of Wismar, a 12th century Nordic cargo ship, and the Bremen cog, a 14th century cog of similar size.

The results reveal significant differences between the Big Ship of Wismar and the Bremen cog in all the examined performance characteristics. Overall, the Big Ship of Wismar demonstrates superior transverse stability, speed, and seakeeping behaviour than the Bremen cog. These findings, together with the evidence from calculations on other ships and sea trials on full-scale replicas, indicate that the socio-economic factors had such a substantial impact on shaping the observed transformations in shipbuilding traditions, that they outweighed the reduction in ship performance. Additionally, cogs' key features, such as high freeboard, full hull lines, closed deck, and superstructure, appear to have played a crucial role in their supremacy. These characteristics not only allowed them to

transport cargo in bulk, but also provided a defensive advantage against attacks. While Nordic cargo ships exhibited superior speed, stability, and seaworthiness, cogs were more suitable for meeting the social demands of the time.

This thesis demonstrates that modern naval architecture methods can effectively be applied to 3D model reconstructions of ancient ships to enhance the understanding of ship performance in maritime archaeology. Additionally, it proves that evaluating ship performance can provide valuable insights on broader research questions, such as understanding the social changes that would have influenced and driven the transformative processes observed in shipbuilding traditions.

Bibliography

Andersen, B., & Andersen, E. (1989). *Rasejlet - Dragens vinge.* Roskilde: Vikingeskibshallen i Roskilde.

Andersen, E., Crumlin-Pedersen, O., Vadstrup, S., & Vinner, M. (1997). *Roar Ege: Skuldelev 3 skibet som arkaeologisk eksperiment.* Roskilde: Vikingeskibshallen i Roskilde.

Auer, J., & Ditta, M. (2019). *Bergung und Dokumentation des Bodendenkmals Wismar, Ostsee II, Fpl. 32 im Rahmen des Projektes "Seehafen Wismar, Fpl. 32" (3544-5504).* Landesamt für Kultur- und Denkmalpflege Mecklenburg-Vorpommern, Landesarchäologie. Schwerin: Landesamt für Kultur- und Denkmalpflege Mecklenburg-Vorpommern.

Ayers, B. (2013). Cities, cogs and commerce: archaeological approaches to the material culture of the North Sea World. In D. Bates, & R. Liddiard (Eds.), *East Anglia and its North Sea World in the Middle Ages* (pp. 63-81). Woodbridge: Boydell & Brewer.

Bill, J. (1994). Ship construction: tools and techniques. In R. Gardiner, & R. W. Unger (Eds.), *Cogs, caravels and galleons: the sailing ship 1000-1650* (pp. 29-46). Annapolis: Naval Institute Press.

Bill, J. (1995). Going into business. In O. Olsen, J. Madsen, & F. Rieck (Eds.), *Shipshape. Essays for Ole Crumlin-Pedersen* (pp. 195-202). Roskilde: Vikingeskibshallen i Roskilde.

Bill, J. (1997). *Small scale seafaring.* Copenhagen: University of Copenhagen.

Bill, J. (2002). Castles at sea. The warship of the High Middle Ages. In A. Nørgard Jørgensen, J. Pind, L. Jørgensen, & B. Clausen (Eds.), *Maritime warfare in Northern Europe. Technology, organisation, logistics and administration 500 BC-1500 AD. Papers from an international research seminar at the Danish National Museum, Copenhagen, 3–5 May 2000* (Vol. 6, pp. 47-56). Copenhagen: Publications from the National Museum Studies in Archaeology & History.

Bill, J. (2009). From Nordic to North European. Application of multiple correspondence analysis in the study of changes in Danish shipbuilding A.D. 900 to 1600. In R. Bockius (Ed.), *Between the seas. Tansfer and exchange in nautical technology. Proceedings of the eleventh international symposium on boat and ship archaeology. Mainz 2006* (pp. 429-437). Mainz: Verlag des Römisch-Germanischen Zentralmuseums.

Bill, J. (2013). Revisiting Gokstad. Interdisciplinary investigations of a find complex excavated in the 19th century. In S. Brather, & D. L. Krausse (Eds.), *Fundmassen. Innovative Strategien zur Auswertung frühmittelalterlicher Quellenbestände* (pp. 75-86). Darmstadt: Theiss.

Bischoff, V. (2017). Viking-Age sails: form and proportion. *Journal of Maritime Archaeology, 12*(1), pp. 1-24.

Bonde, N., & Daly, A. (1998). Dendrokronologiske undersøgelser fra arkæologiske udgravninger i Danmark 1997 Nationalmuseet. In *Arkæologiske udgravninger i Danmark 1997* (pp. 293-325). Copenhagen: Slots- og Kulturstyrelsen.

Bonde, N., & Daly, A. (2000). Dendrokronologiske undersøgelser 1999. In *Arkæologiske udgravninger i Danmark 1999* (pp. 326-339). Copenhagen: Slots- og Kulturstyrelsen.

Brandt, H., Hoheisel, W. d., & Hochkirch, K. (1994). *Experimentelle Ermittlung der Segelleistung von einem originalgetreuen Nachbau der Hansekogge von 1380.* Berlin: Technische Universitat Berlin & lnstitut fur Schiffs- und Meerestechnik.

Bremerhaven. (2023). *"Ubena von Bremen" - Hanseatic Cog*. Bremerhaven. https://www.bremerhaven.de/de/veranstaltungen/maritime-days-2022/ubena-von-bremen-hanseatic-cog.39567.html

Bruun, P. (1997). The Viking Ship. *Journal of Coastal Research, 13*(4), 1282-1289.

Bureau Veritas. (2022). *Rules for the classification of steel ships. NR467 - July 2022. Part B: hull and stability.* Paris: Bureau Veritas.

Christensen, A. E. (1985). Boat finds from Bryggen. In A. Herteig (Ed.), *The Bryggen papers, main series* (Vol. 1, pp. 47-278). Bergen, Oslo, Stavanger, Tromso: Universitetsforlaget AS.

Christensen, A. E. (1989). Hanseatic and Nordic ships in Medieval trade. Were the Cogs better vessels? In C. Villain-Gandossi, S. Busuttil, & P. Adam (Eds.), *Medieval ships and the birth of technological societies. Volume I: Northern Europe* (pp. 17-23). Valetta: European Coordination Centre for Research and Documentation in Social Sciences.

Christensen, A. E. (2002). The “Big Ship” of Bryggen in Bergen: What can it tell us? *Deutsches Schiffahrtsarchiv*, 87-95.

Ciortan, C., & Fonseca, N. (2011). Numerical simulations of the sails of a XVIth century Portuguese Nau. In L. Eca, E. Onate, J. Garcia, T. Kvamsdal, & P. Bergan (Eds.), *IV international conference on computational methods in marine engineering, MARINE 2011*, (pp. 278-289). Barcelona: International Center for Numerical Methods in Engineering (CIMNE).

Coates, J., McGrail, S., Brown, D., Gifford, E., Grainge, G., Greenhill, B., . . . Wright, E. (1995). Experimental boat and ship archaeology: principles and methods. *The International Journal of Nautical Archaeology, 24*(4), 293-301.

Crumlin-Pedersen, O. (1972). Skin or wood? A study of the origin of the Scandinavian plank boat. In O. Hasslof, H. Henningsen, & A. E. Christensen (Eds.), *Ship and shipyards, sailors and fishermen* (pp. 208-234). Copenhagen: Copenhagen University Press.

Crumlin-Pedersen, O. (1979a). Lynæsskibet og Roskilde søvej. In F. A. Birkebæk (Ed.), *13 bidrag til Roskilde by og omegn’s historie* (pp. 65-77). Roskilde: Vikingeskibshallen i Roskilde.

Crumlin-Pedersen, O. (1979b). Danish cog-finds. In S. McGrail (Ed.), *The archaeology of medieval ships and harbours in Northern Europe* (pp. 17-34). Oxford: BAR.

Crumlin-Pedersen, O. (1985). Cargo ships of Northern Europe AD 800-1300. In *Conference on waterfront archaeology in North European towns No.2* (pp. 83-99). Bergen: Historisk Museum Bergen.

Crumlin-Pedersen, O. (1991). Ship types and sizes AD 800-1400. In O. Crumlin-Pedersen (Ed.), *Aspects of maritime Scandinavia AD 200-1200. Proceedings of the Nordic seminar on maritime aspects of archeology, Roskilde, 13th-15th March 1989* (pp. 69-82). Roskilde: Vikingeskibsmuseet.

Crumlin-Pedersen, O. (1997). *Viking-Age ships and shipbuilding in Hedeby/Haithabu and Schleswig. Ships and boats of the North* (Vol. 2). Roskilde: Vikingeskibsmuseet.

Crumlin-Pedersen, O. (1999). Ships as indicators of trade in Northern Europe 600-1200. In J. Bill, & B. L. Clausen (Eds.), *Maritime topography and the medieval town. Papers from the 5th international conference on waterfront archaeology at the Danish National Museum, Copenhagen, 14-16 May 1998.* (pp. 11-20). Copenhagen: Danish National Museum.

Crumlin-Pedersen, O. (2000). To be or not to be a cog: the Bremen Cog in perspective. *The International Journal of Nautical Archaeology, 29*(2), 230-246.

Crumlin-Pedersen, O. (2003). Variations on a theme: 11th-century ship types of the north. In C. Beltrane (Ed.), *Boats, ships and shipyards: proceedings of the ninth international symposium on boat and ship archaeology, Venice 2000* (pp. 253-260). Oxford: Oxbow Books.

Daly, A. (2007). *Timber, trade and tree-rings. A dendrochronological Northern Europe, c. AD 1000 to c. AD 1650* [Unpublished PhD thesis]. Esbjerg: University of Southern Denmark.

Daly, A. (2008). *Lynæs J.nr. 2526.* Dendro.dk rapport 6. Brønshøj: Dendro.dk.

Daly, A. (2009). The chronology of cogs and their timber origin. In R. Bockius (Ed.), *Between the seas. Transfer and exchange in nautical technology. Eleventh international symposium on boat and ship archaeology, Mainz 2006*, (pp. 237-248). Mainz: Römisch-Germanisches Zentralmuseum.

Derret, C. R., & Barrass, B. (2001). *Ship stability for masters and mates* (5 ed.). Oxford: Butterworth-Heinemann.

Det Norske Veritas. (2010). *Recommended practice DNV-RP-C205. Environmental conditions and environmental loads.* Oslo: Det Norske Veritas.

Deutsches Schiffahrtsmuseum. (2023). *Bremen Cog can be visited again*. Deutsches Schiffahrtsmuseum. https://www.dsm.museum/en/press-area/bremen-cog-can-be-visited-again

Dhoop, T. (2016). Classifying and naming archaeological assemblages: some lessons from ship archaeology. *Terra Incognita, 8*, 47-66.

Ditta, M., & Auer, J. (2021). The 'Big Ship' of Wismar: a well-preserved 12 thcentury cargo vessel from the harbour of Wismar. In G. Boetto, P. Pomey, & P. Poveda (Eds.), *Open sea, closed sea. Local and inter-regional traditions in shipbuilding. Proceedings of the fifteenth international symposium on boat & ship archaeology Marseille 2018* (pp. 193-198). Paris: Archaeonautica.

Ditta, M., & Auer, J. (in press). Visualising a 'Big Ship'. The reconstruction of a 12th-century cargo vessel found in the harbour of Wismar. In *Sailing through history. Reading the past – imagining the future. Proceedings of the 16th international symposium on boat and ship archaeology, Zadar.*

Dokkedal, L. (1996). *Koggen i Nordeuropa fra 1150-1450 e. Kr. - Definition af skibstypen og diskussion af en mulig arsag til dens anvendelse i nordeuropaeisk skibsfart.* Copenhagen: Univeristy of Copenhagen. Institute of Archaeology and Ethnology.

Ejstrud, B., Cattrysse, A., Ditta, M., Nicolescu, D., Perissiou, D., Said, S., & Sherman, M. (2012). *Seven boats. Assessing the performance of ancient boats.* Esbjerg: Maritime Archaeology Programme, University of Southern Denmark.

Ellmers, D. (1994). The cog as a cargo carrier. In R. Gardiner, & R. W. Unger (Eds.), *Cogs, caravels and galleons: the sailing ship 1000-1650* (pp. 29-46). Annapolis: Naval Institute Press.

Ellmers, D. (1995). Crew structure on board Scandinavian vessels. In O. Olsen, J. S. Madsen, & F. Rieck (Eds.), *Shipshape. Essays for Ole Crumlin-Pedersen* (pp. 231-240). Roskilde: Vikingeskibshallen i Roskilde.

Engineering ToolBox. (2003). *Liquids - specific gravities*. Engineering ToolBox. https://www.engineeringtoolbox.com/specific-gravity-liquid-fluids-d_294.html

Engineering ToolBox. (2010). *Densities of common products*. Engineering ToolBox. https://www.engineeringtoolbox.com/density-materials-d_1652.html

Engineering ToolBox. (2012). *Food products - bulk densities*. Engineering ToolBox. https://www.engineeringtoolbox.com/foods-materials-bulk-density-d_1819.html

Englert, A. (2000). *Large cargo vessels in Danish waters.* Roskilde & Kiel: Christian-Albrechts-Universitat zu Kiel.

Englert, A. (2003). Large cargo vessels in Danish waters AD 1000-1250. Archaeological evidence for professional merchant seafaring before the Hanseatic period. In C. Beltrane (Ed.), *Boats, ships and shipyards: proceedings of the ninth international symposium on boat and ship archaeology, Venice 2000* (pp. 273-280). Oxford: Oxbow Books.

Englert, A. (2017). Transport with class. The large Nordic cargo ship from Karschau near Schleswig (Germany). In J. Gawronski, A. van Holk, & J. Schokkenbroek (Eds.), *Ships and maritime landscapes. Proceedings of the thirteenth international symposium on boat and ship archaeology, Amsterdam 2012* (pp. 273-279). Eelde: Barkhuis.

Feenstra, G. J. (2023, May 15). *Vaartocht zeevaartschool stc*. Kamper Kogge. https://kamperkogge.nl/vaartocht-zeevaartschool-stc/

Förderverein "Poeler Kogge" e.V. (2023). *Poeler Kogge "Wissemara"*. Poeler Kogge. https://www.poeler-kogge.de/kogge.html

Gerr, D. (1995). *The nature of boats. Insights and esoterica for the nautically obsessed.* Camden, Maine: International Marine McGraw-Hill.

Godal, J. B. (1995). The use of wood in boatbuilding. In O. Olsen, J. Madsen, & F. Rieck (Eds.), *Shipshape. Essays for Ole Crumlin-Pedersen* (pp. 271-282). Roskilde: Vikingeskibshallen i Rosekilde.

Gothche, M. (2006). The Roskilde ships. In L. Blue, F. M. Hocker, & A. Englert (Eds.), *Connected by the sea. Proceedings of the tenth international symposium on boat and ship archaeology, Roskilde 2003* (pp. 252-258). Oxford: Oxbow Books.

Haasum, S. (1995). Ship graffiti in the medieval churches of Gotland. In O. Olsen, J. S. Madsen, & F. Rieck (Eds.), *Shipshape. Essays for Ole Crumlin-Pedersen* (pp. 241-247). Roskilde: Vikingeskibshallen i Roskilde.

Hartemink, R. (2022, December 26). *Harderwijk*. Heraldy of the world. https://www.heraldry-wiki.com/heraldrywiki/index.php?title=Harderwijk

Hartemink, R. (2023, May 2). *Damme*. Heraldy of the World. https://www.heraldry-wiki.com/heraldrywiki/index.php?title=Damme

Haywood, J. (1991). *Dark Age of naval power. A reassessment of Frankish and Anglo-Saxon seafaring activity.* New York: Routledge, Chapman & Hall.

Heide, E. (2014). The early Viking ship types. In T.L. Nilsen, P. K. Sebak, & A. Thowsen (Eds.), *Sjøfartshistorisk Årbok 2012*, (pp. 81-153). Bergen: Stiftelsen Bergens sjøfartsmuseum.

Heinsius, P. (1956). *Das Schiff der hansischen Frühzeit. Quellen und Darstellungen zur hansischen Geschichte.* Weimar: H. Böhlaus Nachfolger.

Himeno, Y. (1981). *Prediction of ship roll damping - state of the art.* The University of Michigan. College of engineering, naval architecture and marine engineering. Ann Arbor: The University of Michigan.

Historischer Hafen Flensburg gGmbH. (2018). *Roland von Bremen*. Historischer Hafen Flensburg. https://historischer-hafen.de/schiff/roland-von-bremen/

Hocker, F. M., & Ward, C. A. (2004). *The philosophy of shipbuilding: conceptual approaches to the study of wooden ships.* College Station: Texas A&M University Press.

Hocker, F., & Daly, A. (2006). Early cogs, Jutland boatbuilders, and the connection between East and West before AD 1250. In L. Blue, F. M. Hocker, & A. Englert (Eds.), *Connected by the sea. Proceedings of the tenth international symposium on boat and ship archaeology, Roskilde 2003* (pp. 187-194). Oxford: Oxbow Books.

Hocker, F., & Vlierman, K. (1996). *Flevobericht 408: A small cog wrecked on the Zuiderzee in the early fifteenth century.* Lelystad: Rijkswaterstaat.

Hoffmann, G., & Hoffmann, P. (2009). Sailing the Bremen Cog. *International Journal of Nautical Archaeology, 38*(2), 281-296.

Hoheisel, W. D. (1994). A full-scale replica of the Hanse cog of 1380. In C. Westerdahl (Ed.), *Crossroads in ancient shipbuilding. Proceedings of the sixth international symposium on boat and ship archaeology (ISBSA 6). Oxbow monograph 40*, pp. 257-260. Oxford: Oxbow Books.

Holtrop, J., & Mennen, G. J. (1982). An approximate power prediction method. *International Shipbuilding Progress, 29*(335), 166-170.

Jackson, P., & Hawkins, P. (1998). The importance of Froude and Reynolds numbers in modelling downwind sails. In M. C. Thompson, & K. Hourigan (Eds.), *Proceedings of the 13th Australasian fluid mechanics conference* (pp. 515-518). Melbourne: Monash University Publishing.

Jarrett, G. (2023). *It's fine on a good day! Perceived risk and route choice among Viking Age seafarers. Potentials of digital mapping and experimental archaeology* [Unpublished manuscript]. Department of Archaeology and Ancient History, Lund University.

Jensen, K. (1999). *Documentation and analysis of ancient ships.* Copenhagen: Technical University of Denmark.

Kamper Kogge. (2023). *Feiten en weetjes*. Kamper Kogge. https://kamperkogge.nl/feiten-en-weetjes/

Kohrtz Andersen, P. (1983). *Kollerupkoggen.* Thisted: Museet for Thy og Vester Hanherred.

Lata, W. H., & Thiagarajan, K. P. (2007). Comparison of added mass coefficients for a floating tanker evaluated by comformal mapping and boundary element methods. In P. Jacobs (Ed.), *Proceedings of the 16th Australasian fluid mechanics conference* (pp. 1388-1391). Brisbane: The University of Queensland.

Lensen, L., & Heitling, W. H. (1990). *De geschiedenis van de Hanze. Bloeiperiode langs de IJssel.* Deventer: Arko uitgeverij Deventer.

Litwin, J. (1998). Medieval Baltic ships - traditions and constructional aspects. *L'innovation technique au Moyen Âge. Actes du VIe congrès international d'archéologie médiévale (1-5 Octobre 1996, Dijon - Mont Beuvray - Chenôve - Le Creusot - Montbard). 6*, pp. 88-97. Caen: Société d'Archéologie Médiévale.

Lloyd, A. R. (1989). *Seakeeping: ship behaviour in rough weather.* Chichester: Ellis Horwood Limited.

Maarleveld, T. (1995). Type or technique. Some thoughts on boat and ship finds as indicative of cultural traditions. *The International Journal of Nautical Archaeology, 24*, pp. 3-7.

Marchaj, C. A. (1964). *Sailing theory and practice.* London: Adlard Coles.

Marchaj, C. A. (1986). *Seaworthiness. The forgotten factor.* London: Adlard Coles.

McGrail, S. (1987). *Ancient boats in North-West Europe. The archaeology of water transport to AD 1500.* Abingdon: Routledge.

McGrail, S. (1988). Assessing the performance of an ancient boat—the Hasholme logboat. *Oxford Journal of Archaeology, 7*(1), pp. 35-46.

McGrail, S. (1995). Romano-Celtic boats and ships: characteristic features. *The International Journal of Nautical Archaeology, 24*(2), 139-145.

McGrail, S. (2006). *Ancient boats and ships* (Second ed.). Tarxien, Malta: Shire Archaelogy.

Morcken, R. (1980). *Langskip, knarr og kogge: nye synspunkter på sagatidens skipsbygging i Norge og Nordeuropa.* Bergen: self-publishing.

Morcken, R. (1988). Longships, knarrs and cogs. *Mariner's Mirror, 74*(4), 391-400.

Morton Nance, R. (1921). Killicks again. *The Mariner's Mirror, 7*(5), 135-141.

Mundal, E. (2017). Avaldsnes and Kormt in Old Norse written sources. In D. Skre (Ed.), *Avaldsnes. A Sea-Kings' manor in first millenium western Scandinavia* (pp. 35-52). Berlin: De Gruyter.

Myrhoj, H. M., & Gothche, M. (1997). The Roskilde ships. *Maritime Archaeology Newsletter from Roskilde*, 3-7.

Neves, M. S., Perez, N. A., & Valerio, L. (1999). Stability of small fishing vessels in longitudinal waves. *Ocean Engineering, 26*, 1389-1419.

Olliver, G. F., Dacunha, N. M., & Hogben, N. (1986). *Global wave statistics.* Old Woking: Unwin.

Orca3D. (2021). *Orca 3D user manual, version 2.0.* [Software user manual]. Orca 3D.

Pommernkogge Ucra. (2023). *Bildergalerie*. Pommernkogge Ucra. https://www.pommernkogge-ucra.de/?page_id=432#Kogge_07_web

Reinders, R. (1985). *Flevobericht 248: Cog Finds from the Ijsselmeerpolders.* Lelystad: Rijkwaterstaat.

Rose, S. (2007). *The medieval sea.* London: Bloomsbury Publishing.

Runyan, T. J. (1994). The cog as warship. In R. Gardiner, & R. W. Unger (Eds.), *Cogs, caravels and galleons: the sailing ship 1000-1650* (pp. 29-46). Annapolis: Naval Institute Press.

Santos, T. A., & Fonseca, N. (2007). Naval architecture applied to the reconstruction of an early XVII century Portuguese Nau. *Marine Technology, 44*(4), 254-267.

Shaw, D. W. (2016, Autumn). Secrets of the Viking ships. *Scandinavian Review*, 6-21.

Simek, R. (1979). Old Norse ship names and ship terms. *Northern Studies, 13*, 26-36.

Steen, S. (1934). Fartoier i Norden i middelalderen. In A. Schuck (Ed.), *Handel og samfardsel under Medeltiden* (pp. 282-300). Stockholm, Kobenhaven, Oslo: Bonnier.

Steffy, J. R. (1994). *Wooden shipbuilding and the interpretation of shipwrecks.* London: Texas A&M University Press.

Stein, M. (2023, 03 23). *Von 1380: Wieso liegt die Hansekogge in Kiel?* Kielerleben. https://www.kielerleben.de/news/1380-liegt-hansekogge-kiel-10026464.html

Tanner, P. (2013). *Newport medieval ship project. Specialist report: reconstructing the hull shape.* Newport city council. Cork: 3D Scanning Ireland.

Tanner, P. (2016). *The Bremen Kogge. Still a cog but not as we knew it.* German Maritime Museum. Bremerhaven: German Maritime Museum.

Tanner, P. (2018). *The Bremen Kogge. A seakeeping, stability and performance analysis.* Bremerhaven: German Maritime Museum.

Tanner, P. (2020). *The reconstruction and analysis of archaeological boats and ships.* Southampton: University of Southampton.

Tanner, P., & Belasus, M. (2021). The Bremen-Cog: reconstructed one more time. *Archaeonautica, 21*, 315-324.

Tempelman, R. (2003). *Stabiliteitsrapport Kamper Kogge.* Kamper Kogge. https://kamperkogge.nl/wp-content/uploads/2021/07/Stabiliteitsrapport_KamperKogge.pdf

Van Damme, T., Auer, J., Ditta, M., Grabowski, M., & Couwenberg, M. (2020). The 3D annotated scans method: a new approach to ship timber recording. *Heritage Science, 8*(75), 1-18.

Van de Moortel, A. (1991). *Flevobericht 331: a cog-like vessel fom the netherlands.* Lelystad: Rijkwaterstaat.

Van de Moortel, A. (2011). Medieval boats and ships of Germany, the Low Countries, and northeast France – archaeological evidence for shipbuilding traditions, shipbuilding resources, trade, and communication. In F. Bittmann, J. Ey, M. Karle, H. Jons, E. Strahl, & S. Wolters (Eds.), *Siedlungs- und Küstenforschung im südlichen Nordseegebiet* (Vol. 34, pp. 67-104). Wilhelmshaven: Niedersächsisches Institut für historische Küstenforschung.

Varenius, B. (1992). *Det nordiska skeppet. Teknologi och samhallsstrategi i vikingatid och mideltid.* Stockholm: Stockholm Univeristy.

Vikingeskibsmuseet. (2020, Sep 29). *Iron in the Viking ships - rivets and roves*. Vikingeskibsmuseet. https://www.vikingeskibsmuseet.dk/en/news/iron-in-the-viking-ships-rivets-and-roves

Vikingeskibsmuseet. (2023a). *Ottar*. Vikingeskibsmuseet: https://www.vikingeskibsmuseet.dk/en/professions/the-boat-collection/ottar

Vikingeskibsmuseet. (2023b). *Roar Ege*. Vikingeskibsmuseet. https://www.vikingeskibsmuseet.dk/en/professions/education/boats-storage/roar-ege

Vikingeskibsmuseet. (2023c). *The Viking Age crew*. Vikingeskibsmuseet. https://www.vikingeskibsmuseet.dk/en/professions/education/knowledge-of-sailing/the-ships-crew/crewmembers-in-the-viking-age

Vikingeskibsmuseet. (2023d). *The weaver*. Vikingeskibsmuseet. https://www.vikingeskibsmuseet.dk/en/professions/education/all-about-the-viking-ship/skibets-haandvaerkere/vaeveren

Vikingeskibsmuseet. (2023e). *Nature and sense navigation*. Vikingeskibsmuseet. https://www.vikingeskibsmuseet.dk/en/professions/education/knowledge-of-sailing/nature-and-sense-navigation

Vikingeskibsmuseet. (2023f). *The ship's sail*. Vikingeskibsmuseet. https://www.vikingeskibsmuseet.dk/en/professions/education/all-about-the-viking-ship/the-ships-sail

Vikingeskibsmuseet. (2023g). *The boat collection*. Vikingeskibsmuseet. https://www.vikingeskibsmuseet.dk/en/professions/the-boat-collection

Vinner, M. (1995). A Viking-ship off Cape Farewell 1984. In O. Olsen, J. S. Madsen, & F. Rieck (Eds.), *Shipshape. Essays for Ole Crumplin-Pedersen* (pp. 283-304). Roskilde: Vikingeskibshallen i Roskilde.

Waldus, W. B., Verweij, J. F., & van der Velde, H. M. (2019). The IJsselcog project: from excavation to 3D reconstruction. *The International Journal of Nautical Archaeology, 48*(2), 466-494.

Werenskiold, P. (2011). The most sophisticated and successful high-speed ships for their time. In T. J. Peltzer (Ed.), *Proceedings of the 11th international conference on fast sea transportation, FAST2011* (pp. 871-879). Alexandria: American Society of Naval Engineers.

Weski, T. (1999). The Ijsselmeer type: some thoughts on Hanseatic cogs. *The International Journal of Nautical Archaeology, 28*(4), 360-379.

Weski, T. (2003). Remarks on the identification of medieval ship types in Northern Europe. In C. Beltrane (Ed.), *Boats, ships and shipyards: proceedings of the ninth international symposium on boat and ship archaeology, Venice 2000* (pp. 281-288). Oxford: Oxbow Books.

Westerdahl, C. (1995). Traditional zones of transport geography in relation to ship types. In O. Olsen, J. S. Madsen, & F. Rieck (Eds.), *Shipshape. Essays for Ole Crumlin-Pedersen* (pp. 211-230). Roskilde: Vikingeskibshallen i Roskilde.

Weststrate, J. A. (2008). *In het kielzog van moderne markten. Handel en scheepvaart op de Rijn, Waal en IJssel ca. 1360-1560.* Hilversum: Uitgeverij Verloren B.V.

Wolf, T. (1986). *Tragfähigkeiten, Ladungen und Masse im Schiffsverkehr der Hanse : vornehmlich im Spiegel Revaler Quellen.* Köln: Böhlau.

Zwick, D. (2014). Conceptual evolution in ancient shipbuilding: an attempt to reinvigorate a shunned theoretical framework. In J. Adams, & J. Ronnby (Eds.), *Interpreting shipwrecks, maritime archaeological approaches. Southampton Archaeology Monographs New Series No. 4* (pp. 46-71). Southampton: Highfield Press.

Appendix A. Weight and inertia results

Table 46 Mass and inertia of the Big Ship of Wismar elements with homogeneous moisture content

Element	material	Density [kg/m3]	Volume [m3]	Mass [kg]	x [m]	y [m]	z [m]	Ix0 [kgm2]	Iy0 [kgm2]	Iz0 [kgm2]
hull planks above water	oak	848	1.89	1603	11.5	0.0	2.1	17350	99538	101336
hull planks wet	oak	848	3.8	3222	11.5	0.0	0.6	11609	73428	81807
keel wet	oak	800	0.45	360	11.2	0.0	0.1	48	13200	13160
keel	oak	800	0.14	112	12.0	0.0	2.9	1096	15480	14376
wales	pine	748	1.55	1159	12.0	0.0	1.8	15035	37176	44057
pine (except mast)	pine	700	9.53	6671	11.1	0.0	1.6	33530	280980	273910
oak elements	oak	800	9.67	7736	11.5	0.0	1.3	55200	256880	271384
windlass support	elm	720	0.16	115	3.8	0.0	2.3	1087	7373	7236
mast	pine	700	1.54	1078	12.3	0.1	9.1	112210	112210	4172
sail	wool	350	0.43	151	14.2	1.3	8.7	14312	14788	3220
anchors	stone	1600	0.07	112	21.0	0.0	2.7	800	10448	9712
ropes & other equipment				900	11.5	0.0	2.0	3600	3600	0
crew (10 men)			1.97	1000	11.5	0.0	3.0	25305	60350	53071
cargo, T=1.6m		925	83.65	77352	11.6	0.0	1.3	380018	736141	845432
cargo, T=1.3m		552	83.65	46181	11.6	0.0	1.3	226879	439493	504742
cargo, T=1m		217	84.65	18372	11.6	0.0	1.3	89192	172775	198426

Note. The moments of inertia are given at the centreline, baseline and amidships (11.54 m from the origin coordinate system).

Table 47 Mass and inertia of the Big Ship of Wismar elements with heterogeneous moisture content

Element	material	Density [kg/m^3]	Volume [m^3]	Mass [kg]	x [m]	y [m]	z [m]	Ix_0 [kgm^2]	Iy_0 [kgm^2]	Iz_0 [kgm^2]
hull planks above water	oak	898	1.89	1697	11.5	0.0	2.1	18373	105407	107311
hull planks wet	oak	1047	3.8	3979	11.5	0.0	0.6	14333	90660	101004
keel wet	oak	1000	0.45	450	11.2	0.0	0.1	60	16500	16450
keel	oak	850	0.14	119	12.0	0.0	2.9	1165	16448	15275
wales	pine	788	1.55	1221	12.0	0.0	1.8	15839	39164	46413
pine (except mast)	pine	740	9.53	7052	11.1	0.0	1.6	35446	297036	289562
oak elements	oak	850	9.67	8220	11.5	0.0	1.3	58650	272935	288346
windlass support	elm	763	0.16	122	3.8	0.0	2.3	1152	7813	7668
mast	pine	740	1.54	1140	12.3	0.1	9.1	118622	118622	4410
sail	wool	350	0.43	151	14.2	1.3	8.7	14312	14788	3220
anchors	stone	1600	0.07	112	21.0	0.0	2.7	800	10448	9712
ropes & other equipment				900	11.5	0.0	2.0	3600	3600	0
crew (10 men)		508	1.97	1000	11.5	0.0	3.0	25305	60350	53071
cargo, T=1.6m		901	83.65	75409	11.6	0.0	1.3	370473	717651	824197
cargo, T=1.3m		529	83.65	44238	11.6	0.0	1.3	217334	421003	483507
cargo, T=1m		194	84.65	16429	11.6	0.0	1.3	79759	154503	177442

Note. The moments of inertia are given at the centreline, baseline and amidships (11.54 m from the origin coordinate system).

Table 48 Mass and inertia of the Bremen cog elements

Element	material	Density [kg/m^3]	Volume [m^3]	Mass [kg]	x [m]	y [m]	z [m]	Ix_0 [kgm^2]	Iy_0 [kgm^2]	Iz_0 [kgm^2]
Layer: Bolts	Iron	7850	0,003	22,8	17,61	0,03	3,40	298	7425	7120
Layer: Stem	Oak	800	0,939	751,2	18,03	0,01	4,03	14928	260256	245344
Layer: Keel	Oak	800	0,814	651,0	8,05	0,01	0,10	25	57181	57174
Layer: Sternpost	Oak	800	0,278	222,3	-0,66	0,01	2,19	1407	1619	214
Layer: Strake 4	Oak	800	0,786	628,9	8,55	0,00	0,64	1739	60248	61176
Layer: Strake 3	Oak	800	0,615	491,8	8,49	0,00	0,48	788	46712	47122
Layer: Strake 2	Oak	800	0,599	478,8	8,38	0,00	0,31	373	43474	43699
Layer: Strake 1	Oak	800	0,632	505,4	8,07	0,00	0,15	110	41672	41748
Layer: Scanned Frames	Oak	800	2,344	1875,1	7,90	0,01	0,33	1808	145722	146870
Layer: Strake 8	Oak	800	0,751	601,1	8,17	-0,72	2,19	6262	67536	67536
Layer: Strake 8 New	Oak	800	0,192	153,3	7,70	2,82	1,70	1663	10599	11368
Layer: Strake 7	Oak	800	0,781	624,6	8,67	-0,13	1,73	5109	69275	70134
Layer: Strake 7 New	Oak	800	0,042	33,7	4,08	2,46	1,38	269	646	786
Layer: Strake 6	Oak	800	0,801	641,0	8,21	0,00	1,40	3943	65485	66395
Layer: Strake 5	Oak	800	0,941	752,6	8,48	0,00	1,06	3300	77618	78654
Layer: TreeNails	Oak	800	0,045	36,4	6,30	-0,47	2,34	384	2035	1952
Layer: Keelson		800	0,726	580,7	9,03	0,00	0,35	81	51142	51075
Layer: 1st Futtock - Copy	Oak	800	3,302	2641,2	8,38	-0,25	1,58	19245	277522	279356
Layer: Deck Beam 5 - Frame 35 - Copy	Oak	800	0,434	347,4	1,46	0,00	2,38	2878	2719	1643
Layer: Cross Beam frame 26 - Copy	Oak	800	0,449	359,3	5,34	0,00	2,05	2662	11760	11410
Layer: MidShip Beam Frame 20 - Copy	Oak	800	0,523	418,3	8,87	-0,11	2,14	3307	34870	34324
Layer: Cross Beam Frame 10 - Copy	Oak	800	0,431	345,0	14,12	0,00	2,41	2993	70762	69738
Layer: Missing Frames	Oak	800	1,824	1459,0	7,57	2,99	3,25	29794	142824	139936
Layer: Transom Beams - Copy	Oak	800	0,528	422,1	-1,12	0,00	4,93	5846	5976	1112
Layer: 2nd Futtock - Copy	Oak	800	1,610	1287,8	9,52	-2,77	3,27	26011	166758	163976
Layer: Strake 9	Oak	800	0,552	441,8	9,67	-1,71	2,65	5960	62360	61774
Layer: Strake 9 New	Oak	800	0,359	287,5	6,08	2,62	2,39	3816	19248	19656
Layer: WashBoard Strake New	Oak	800	0,392	313,8	7,11	-3,45	4,07	9006	29184	27752
Layer: Washboard Strake	Oak	800	0,392	313,8	7,11	3,46	4,07	9006	29182	27755
Layer: Strake 12 New	Oak	800	0,548	438,5	8,43	3,07	3,76	10579	53901	51952
Layer: Strake 12	Oak	800	0,548	438,5	8,43	-3,07	3,76	10579	53901	51954
Layer: Strake 11	Oak	800	0,562	449,6	8,38	-2,73	3,37	8908	55056	53489
Layer: Strake 11 New	Oak	800	0,562	449,6	8,38	2,73	3,37	8908	55056	53489
Layer: Strake 10	Oak	800	0,460	368,3	8,75	-2,54	2,99	6075	46558	45755
Layer: Strake 10 New	Oak	800	0,460	368,3	8,75	2,54	2,99	6075	46558	45755
Layer: CrossBeam Frame 6	Oak	800	0,727	581,8	15,86	-0,37	3,62	9630	153968	148272
Layer: 3rd Futtock - Copy	Oak	800	0,108	86,5	2,56	-3,28	3,85	2245	1966	1590
Layer: ForeBit - Copy	Oak	800	0,069	55,2	18,20	0,12	4,76	1298	19576	18352
Layer: New	Oak	785	11,070	8684,4	8,90	0,36	2,56	109485	934787	911275
Layer: Aft Stringer - Copy	Oak	800	0,160	127,6	1,79	-2,78	3,46	2524	2141	1614

Note. The moments of inertia are given at the origin coordinate system. Continues next two pages.

Continuation of Table 48

Element	material	Density [kg/m³]	Volume [m³]	Mass [kg]	x [m]	y [m]	z [m]	Ix_0 [kgm²]	Iy_0 [kgm²]	Iz_0 [kgm²]
Layer: 2016 Stringers – Copy	Oak	800	0,892	713,7	2,42	-2,22	2,36	8578	11205	10500
Layer: F 0 - Copy	Oak	800	0,114	91,3	17,84	0,03	4,47	1952	30858	29155
Layer: Lower Fore Stringer - Copy	Oak	800	0,326	260,8	15,45	0,00	3,66	5218	66114	64318
Layer: Upper Fore Stringer - Copy	Oak	800	0,130	104,2	15,06	-3,00	4,19	2789	25656	24774
Layer: MidShip Beam Frame 20	Oak	800	0,523	418,0	8,91	-0,44	2,74	4978	36398	35023
Layer: Deck Beam 5 - Frame 35	Oak	800	0,555	443,6	1,47	-0,48	2,92	5140	4803	2268
Layer: Cross Beam frame 26	Oak	800	0,579	463,1	5,39	-0,47	2,64	4901	16742	15072
Layer: Cross Beam Frame 10	Oak	800	0,164	131,1	14,11	1,57	2,81	1454	27133	26514
Layer: Breasthook - Copy	Oak	800	0,394	315,0	17,87	0,00	4,73	7632	107704	101184
Layer: MastStep Reinforcement - Copy	Oak	800	0,069	55,1	9,31	0,00	0,39	60	4792	4836
Layer: Stanchion	Oak	800	0,039	31,3	9,04	-0,02	1,31	60	2614	2554
Layer: DeckBeams - Copy	Oak	800	1,584	1266,8	8,43	0,00	3,02	12607	132784	122232
Layer: Channel Wale	Oak	800	0,211	168,6	8,77	-3,66	3,63	4482	16192	16240
Layer: Side Stem Timbers - Copy	Oak	800	0,509	407,0	16,63	-0,04	3,19	5150	117928	113277
Layer: Deck Boards - Copy	Oak	800	0,189	151,4	7,23	-1,69	3,27	2254	14966	13948
Layer: Aft Stanchion	Oak	800	0,330	264,0	-1,69	0,00	5,03	1733	1518	484
Layer: Castle CrossBeam 2	Oak	800	0,422	337,3	-0,93	0,00	4,86	9458	8347	1695
Layer: Castle CrossBeam 1	Oak	800	0,192	153,3	1,47	-0,03	5,17	4685	4425	924
Layer: Castle Deck Supports	Oak	800	0,340	271,6	3,89	-0,28	3,70	5106	8448	5256
Layer: Protective covering	Oak	800	0,168	134,2	6,43	0,00	4,55	4730	8412	7485
Layer: Crosspieces	Oak	800	0,079	63,4	6,32	0,00	4,87	2396	4076	3434
Layer: Channel Stanchions	Oak	800	0,221	176,5	6,35	-0,01	4,65	6256	11058	9575
Layer: Inner Stanchions	Oak	800	0,708	566,6	4,66	0,00	4,57	18390	26664	20744
Layer: Windlass	Oak	800	1,105	884,0	1,70	0,07	3,51	12468	13748	3854
Layer: Castle Wall	Oak	800	0,143	114,0	3,04	0,00	4,47	3706	3559	2704
Layer: Castle Roof	Oak	800	0,217	173,9	2,47	0,00	5,09	6623	6101	3723
Layer: Bulkheads	Oak	800	0,481	385,0	2,88	-0,28	4,15	8470	12078	7044
Layer: HandRail	Oak	800	0,748	598,1	0,19	-0,02	5,92	26464	25814	10082
Layer: Capstan Base	Oak	800	0,245	195,9	-0,28	-0,08	5,42	5772	5894	135
Layer: Working Platform	Oak	800	0,057	45,8	6,84	0,01	4,97	1589	3312	2638
Layer: Castle Deck Planks	Oak	800	1,220	976,3	1,56	0,06	5,34	33173	37752	15240
Layer: Castle Deck Beams	Oak	800	0,564	450,9	0,73	0,00	5,31	14568	15104	4290
Layer: Castle Outer Stringers	Oak	800	0,301	241,1	1,91	0,00	4,56	7981	6939	4842
Layer: Castle Outer Deck Beam	Oak	800	0,122	97,2	1,85	-0,01	5,25	3800	3344	1792
Layer: Rudder	Oak	800	0,376	300,9	-1,49	0,00	2,95	3386	4210	825
Layer: Rudder	Iron	7850	0,009	74,5	-1,32	0,00	2,63	652	816	157
Layer: Castle Ceiling	Oak	800	0,174	139,0	2,72	0,00	4,10	3877	3752	2946
Layer: Capstan - Copy	Oak	800	0,297	237,4	-0,53	-0,07	6,04	8726	8792	79
Layer: Toilet	Oak	800	0,025	20,0	-1,28	-2,84	4,58	581	452	195

Continuation of Table 48

Element	material	Density [kg/m³]	Volume [m³]	Mass [kg]	x [m]	y [m]	z [m]	Ix_0 [kgm²]	Iy_0 [kgm²]	Iz_0 [kgm²]
Layer: DrainBoard	Oak	800	0,051	41,0	1,67	-2,43	4,01	912	775	367
Layer: DrainBox	Oak	800	0,064	51,2	1,46	2,46	4,12	1194	984	432
Layer: Door	Oak	800	0,051	40,4	4,13	-1,77	4,20	857	1425	822
Layer: Hatch	Oak	800	0,064	51,0	10,84	-0,01	3,23	538	6544	6016
Layer: LadderRailings	Oak	800	0,442	353,5	5,58	-0,01	4,66	9630	20011	13657
Layer: Iron Nails	Iron			700	8,16	0,00	2,45			
Layer: Ladder	Oak	800	0,173	138,0	11,18	0,00	1,79	551	17831	17312
Layer: Yard	Hemp	940	0,028	26,7	9,56	0,21	18,15	8846	11261	2529
Layer: Yard	Spruce	450	0,924	415,6	9,57	0,20	18,10	140360	177156	45155
Layer: Mast	Spruce	450	5,186	2333,7	9,26	0,00	10,19	335016	534933	200007
Layer: SailArea	Sail canvas	153	0,585	89,5	12,20	2,47	12,68	17067	29521	15799
Layer: Sheets	Hemp	940	0,044	41,5	4,76	-0,19	8,44	4274	6245	3358
Layer: Brail_Lines	Hemp	940	0,109	102,8	7,20	0,86	11,29	15679	22532	8648
Layer: Halyard	Hemp	940	0,075	70,9	7,20	0,09	15,74	20387	24466	4783
Layer: Blocks	Lignum Vitae	1170	0,006	7,0	9,07	0,04	19,24	2647	3203	659
Layer: Main Shrouds	Hemp	940	0,164	154,6	7,89	0,00	10,99	24327	33577	11299
Layer: Flag		500	0,012	6,0	10,97	2,29	23,49	3450	4155	7945
Layer: Anchors	Mixed	2540	0,236	599,2	17,75	0,01	4,70	15286	202842	191196
Layer: Min Ballast	Stones	1531	9,431	14400	7,50	0,00	0,51	16661	958528	966992
Layer: BeamEnds Cargo		430	100,880	43345	7,77	0,00	1,55	203246	3354201	3330205
Layer: Gragas Cargo		896	120,530	108003	7,75	0,00	1,69	791202	11617922	11473636

Appendix B. Big Ship of Wismar, ORCA 3D stability calculations results

Empty condition

Stability Criteria - Bureau Veritas_Empty, Intact Stability

Name	Angle 1	Angle 2	Required	Actual	Pass / Fail
GM At FreeEquil >= 0.15 meters	0		0,15	4,622	Pass
GZ At 30 >= 0.2 meters	30		0,2	1,4471	Pass
Angle At GZmax >= 25 deg	33,7397		25	33,7397	Pass
Area Between FreeEquil and 30 >= 3.151 meters-deg	0	30	3,151	25,5778	Pass
Area Between 30 and 40 >= 1.1719 meters-deg	30	40	1,1719	14,5265	Pass
Area Between FreeEquil and 40 >= 5.157 meters-deg	0	40	5,157	40,1044	Pass
Area Between FreeEquil and Flood >= 5.157 meters-deg	0	31,2183	5,157	27,3662	Pass
Area Between 30 and Flood >= 1.1719 meters-deg	30	31,2183	1,1719	1,7884	Pass

Stability Criteria - Bureau Veritas_Empty, Weather criteria, 5 kt _empty

Name	Angle 1	Angle 2	Required	Actual	Pass / Fail
Angle At SteadyEquil <= 16 deg	0,3795		16	0,3795	Pass
Angle At SteadyEquil <= DeckImm*0.8 deg	0,3795		24,6196	0,3795	Pass
Angle At SteadyEquil < Flood deg	0,3795		31,2183	0,3795	Pass
ResRatio Between SteadyEquil-21 deg and Flood > 1	-20,6205	31,2183	1	1,8748	Pass
FloodHt At SteadyEquil > 0.5 meters	0,3795		0,5	1,6975	Pass
Angle At SteadyEquil+21 deg < Flood deg	21,3795		31,2183	21,3795	Pass

Stability Criteria - Bureau Veritas_Empty, Weather criteria, 10 kt_empty

Name	Angle 1	Angle 2	Required	Actual	Pass / Fail
Angle At SteadyEquil <= 16 deg	1,5201		16	1,5201	Pass
Angle At SteadyEquil <= DeckImm*0.8 deg	1,5201		24,6196	1,5201	Pass
Angle At SteadyEquil < Flood deg	1,5201		31,2183	1,5201	Pass
ResRatio Between SteadyEquil-21 deg and Flood > 1	-19,4799	31,2183	1	1,6372	Pass
FloodHt At SteadyEquil > 0.5 meters	1,5201		0,5	1,6218	Pass
Angle At SteadyEquil+21 deg < Flood deg	22,5201		31,2183	22,5201	Pass

Stability Criteria - Bureau Veritas_Empty, Weather criteria, 15 kt_empty

Name	Angle 1	Angle 2	Required	Actual	Pass / Fail
Angle At SteadyEquil <= 16 deg	3,4499		16	3,4499	Pass
Angle At SteadyEquil <= DeckImm*0.8 deg	3,4499		24,6196	3,4499	Pass
Angle At SteadyEquil < Flood deg	3,4499		31,2183	3,4499	Pass
ResRatio Between SteadyEquil-21 deg and Flood > 1	-17,5501	31,2183	1	1,3016	Pass
FloodHt At SteadyEquil > 0.5 meters	3,4499		0,5	1,4938	Pass
Angle At SteadyEquil+21 deg < Flood deg	24,4499		31,2183	24,4499	Pass

Stability Criteria - Bureau Veritas_Empty, Weather criteria, 20kt_empty

Name	Angle 1	Angle 2	Required	Actual	Pass / Fail
Angle At SteadyEquil <= 16 deg	6,301		16	6,301	Pass
Angle At SteadyEquil <= DeckImm*0.8 deg	6,301		24,6196	6,301	Pass
Angle At SteadyEquil < Flood deg	6,301		31,2183	6,301	Pass
ResRatio Between SteadyEquil-21 deg and Flood > 1	-14,699	31,2183	1	0,9365	Fail
FloodHt At SteadyEquil > 0.5 meters	6,301		0,5	1,311	Pass
Angle At SteadyEquil+21 deg < Flood deg	27,301		31,2183	27,301	Pass

Stability Criteria - Bureau Veritas_Empty, Weather criteria, 5 kt + gust_empty

Name	Angle 1	Angle 2	Required	Actual	Pass / Fail
Angle At SteadyEquil <= 16 deg	0,854		16	0,854	Pass
Angle At SteadyEquil <= DeckImm*0.8 deg	0,854		24,6196	0,854	Pass
Angle At SteadyEquil < Flood deg	0,854		31,2183	0,854	Pass
ResRatio Between SteadyEquil-21 deg and Flood > 1	-20,146	31,2183	1	1,7722	Pass
FloodHt At SteadyEquil > 0.5 meters	0,854		0,5	1,666	Pass
Angle At SteadyEquil+21 deg < Flood deg	21,854		31,2183	21,854	Pass

Stability Criteria - Bureau Veritas_Empty, Weather criteria, 10 kt + gust_empty

Name	Angle 1	Angle 2	Required	Actual	Pass / Fail
Angle At SteadyEquil <= 16 deg	3,4499		16	3,4499	Pass
Angle At SteadyEquil <= DeckImm*0.8 deg	3,4499		24,6196	3,4499	Pass
Angle At SteadyEquil < Flood deg	3,4499		31,2183	3,4499	Pass
ResRatio Between SteadyEquil-21 deg and Flood > 1	-17,5501	31,2183	1	1,3016	Pass
FloodHt At SteadyEquil > 0.5 meters	3,4499		0,5	1,4938	Pass
Angle At SteadyEquil+21 deg < Flood deg	24,4499		31,2183	24,4499	Pass

Stability Criteria - Bureau Veritas_Empty, Weather criteria, 15 kt + gust_empty

Name	Angle 1	Angle 2	Required	Actual	Pass / Fail
Angle At SteadyEquil <= 16 deg	8,2196		16	8,2196	Pass
Angle At SteadyEquil <= DeckImm*0.8 deg	8,2196		24,6196	8,2196	Pass
Angle At SteadyEquil < Flood deg	8,2196		31,2183	8,2196	Pass
ResRatio Between SteadyEquil-21 deg and Flood > 1	-12,7804	31,2183	1	0,7653	Fail
FloodHt At SteadyEquil > 0.5 meters	8,2196		0,5	1,1932	Pass
Angle At SteadyEquil+21 deg < Flood deg	29,2196		31,2183	29,2196	Pass

Stability Criteria - Bureau Veritas_Empty, Weather criteria, 20 kt + gust_empty

Name	Angle 1	Angle 2	Required	Actual	Pass / Fail
Angle At SteadyEquil <= 16 deg	17,2674		16	17,2674	Fail
Angle At SteadyEquil <= DeckImm*0.8 deg	17,2674		24,6196	17,2674	Pass
Angle At SteadyEquil < Flood deg	17,2674		31,2183	17,2674	Pass
ResRatio Between SteadyEquil-21 deg and Flood > 1	-3,7326	31,2183	1	0,3566	Fail
FloodHt At SteadyEquil > 0.5 meters	17,2674		0,5	0,6848	Pass
Angle At SteadyEquil+21 deg < Flood deg	38,2674		31,2183	38,2674	Fail

1 m draft condition

Stability Criteria - Bureau Veritas_T=1m, Intact stability					
Name	Angle 1	Angle 2	Required	Actual	Pass / Fail
GM At FreeEquil >= 0.15 meters	0		0,15	4,044	Pass
GZ At 30 >= 0.2 meters	30		0,2	1,2958	Pass
Angle At GZmax >= 25 deg	27,7525		25	27,7525	Pass
Area Between FreeEquil and 30 >= 3.151 meters-deg	0	30	3,151	25,0923	Pass
Area Between 30 and 40 >= 1.1719 meters-deg	30	40	1,1719	8,9483	Pass
Area Between FreeEquil and 40 >= 5.157 meters-deg	0	40	5,157	34,0406	Pass
Area Between FreeEquil and Flood >= 5.157 meters-deg	0	25,8495	5,157	19,6429	Pass
Area Between 30 and Flood >= 1.1719 meters-deg	30	25,8495	1,1719	-5,3994	Fail
Angle At GZmax >= 15 deg	27,7525		15	27,7525	Pass
Area Between FreeEquil and GZmax >= 180/3.14*(0.055+0.001*(30-GZmax)) meters-deg	0	27,7525	3,2817	22,148	Pass

Stability Criteria - Bureau Veritas_T=1m, Weather criteria, 5kt_T=1m					
Name	Angle 1	Angle 2	Required	Actual	Pass / Fail
Angle At SteadyEquil <= 16 deg	0,2575		16	0,2575	Pass
Angle At SteadyEquil <= DeckImm*0.8 deg	0,2575		20,4084	0,2575	Pass
Angle At SteadyEquil < Flood deg	0,2575		25,8495	0,2575	Pass
ResRatio Between SteadyEquil-18 deg and Flood > 1	-17,7425	25,8495	1	1,8454	Pass
FloodHt At SteadyEquil > 0.5 meters	0,2575		0,5	1,4993	Pass
Angle At SteadyEquil+18 deg < Flood deg	18,2575		25,8495	18,2575	Pass

Stability Criteria - Bureau Veritas_T=1m, Weather criteria, 10kt_T=1m					
Name	Angle 1	Angle 2	Required	Actual	Pass / Fail
Angle At SteadyEquil <= 16 deg	1,03		16	1,03	Pass
Angle At SteadyEquil <= DeckImm*0.8 deg	1,03		20,4084	1,03	Pass
Angle At SteadyEquil < Flood deg	1,03		25,8495	1,03	Pass
ResRatio Between SteadyEquil-18 deg and Flood > 1	-16,97	25,8495	1	1,7008	Pass
FloodHt At SteadyEquil > 0.5 meters	1,03		0,5	1,4476	Pass
Angle At SteadyEquil+18 deg < Flood deg	19,03		25,8495	19,03	Pass

Stability Criteria - Bureau Veritas_T=1m, Weather criteria, 15kt_T=1m

Name	Angle 1	Angle 2	Required	Actual	Pass / Fail
Angle At SteadyEquil <= 16 deg	2,3192		16	2,3192	Pass
Angle At SteadyEquil <= DeckImm*0.8 deg	2,3192		20,4084	2,3192	Pass
Angle At SteadyEquil < Flood deg	2,3192		25,8495	2,3192	Pass
ResRatio Between SteadyEquil-18 deg and Flood > 1	-15,6808	25,8495	1	1,4804	Pass
FloodHt At SteadyEquil > 0.5 meters	2,3192		0,5	1,3612	Pass
Angle At SteadyEquil+18 deg < Flood deg	20,3192		25,8495	20,3192	Pass

Stability Criteria - Bureau Veritas_T=1m, Weather criteria, 20kt_T=1m

Name	Angle 1	Angle 2	Required	Actual	Pass / Fail
Angle At SteadyEquil <= 16 deg	4,1313		16	4,1313	Pass
Angle At SteadyEquil <= DeckImm*0.8 deg	4,1313		20,4084	4,1313	Pass
Angle At SteadyEquil < Flood deg	4,1313		25,8495	4,1313	Pass
ResRatio Between SteadyEquil-18 deg and Flood > 1	-13,8687	25,8495	1	1,2099	Pass
FloodHt At SteadyEquil > 0.5 meters	4,1313		0,5	1,2399	Pass
Angle At SteadyEquil+18 deg < Flood deg	22,1313		25,8495	22,1313	Pass

Stability Criteria - Bureau Veritas_T=1m, Weather criteria, 5 kt + gust_T=1m

Name	Angle 1	Angle 2	Required	Actual	Pass / Fail
Angle At SteadyEquil <= 16 deg	0,5794		16	0,5794	Pass
Angle At SteadyEquil <= DeckImm*0.8 deg	0,5794		20,4084	0,5794	Pass
Angle At SteadyEquil < Flood deg	0,5794		25,8495	0,5794	Pass
ResRatio Between SteadyEquil-18 deg and Flood > 1	-17,4206	25,8495	1	1,7839	Pass
FloodHt At SteadyEquil > 0.5 meters	0,5794		0,5	1,4778	Pass
Angle At SteadyEquil+18 deg < Flood deg	18,5794		25,8495	18,5794	Pass

Stability Criteria - Bureau Veritas_T=1m, Weather criteria, 10 kt + gust_T=1m

Name	Angle 1	Angle 2	Required	Actual	Pass / Fail
Angle At SteadyEquil <= 16 deg	2,3192		16	2,3192	Pass
Angle At SteadyEquil <= DeckImm*0.8 deg	2,3192		20,4084	2,3192	Pass
Angle At SteadyEquil < Flood deg	2,3192		25,8495	2,3192	Pass
ResRatio Between SteadyEquil-18 deg and Flood > 1	-15,6808	25,8495	1	1,4804	Pass
FloodHt At SteadyEquil > 0.5 meters	2,3192		0,5	1,3612	Pass
Angle At SteadyEquil+18 deg < Flood deg	20,3192		25,8495	20,3192	Pass

Stability Criteria - Bureau Veritas_T=1m, Weather criteria, 15 kt + gust_T=1m

Name	Angle 1	Angle 2	Required	Actual	Pass / Fail
Angle At SteadyEquil <= 16 deg	5,2384		16	5,2384	Pass
Angle At SteadyEquil <= DeckImm*0.8 deg	5,2384		20,4084	5,2384	Pass
Angle At SteadyEquil < Flood deg	5,2384		25,8495	5,2384	Pass
ResRatio Between SteadyEquil-18 deg and Flood > 1	-12,7616	25,8495	1	1,0635	Pass
FloodHt At SteadyEquil > 0.5 meters	5,2384		0,5	1,1665	Pass
Angle At SteadyEquil+18 deg < Flood deg	23,2384		25,8495	23,2384	Pass

Stability Criteria - Bureau Veritas_T=1m, Weather criteria, 20 kt + gust_T=1m

Name	Angle 1	Angle 2	Required	Actual	Pass / Fail
Angle At SteadyEquil <= 16 deg	9,4454		16	9,4454	Pass
Angle At SteadyEquil <= DeckImm*0.8 deg	9,4454		20,4084	9,4454	Pass
Angle At SteadyEquil < Flood deg	9,4454		25,8495	9,4454	Pass
ResRatio Between SteadyEquil-18 deg and Flood > 1	-8,5546	25,8495	1	0,6229	Fail
FloodHt At SteadyEquil > 0.5 meters	9,4454		0,5	0,8982	Pass
Angle At SteadyEquil+18 deg < Flood deg	27,4454		25,8495	27,4454	Fail

Water below wales condition

Stability Criteria - Bureau Veritas_T=1.3m, Intact Stability					
Name	Angle 1	Angle 2	Required	Actual	Pass / Fail
GM At FreeEquil >= 0.15 meters	0		0,15	3,456	Pass
GZ At 30 >= 0.2 meters	30		0,2	0,6146	Pass
Angle At GZmax >= 25 deg	20,8048		25	20,8048	Fail
Area Between FreeEquil and 30 >= 3.151 meters-deg	0	30	3,151	20,577	Pass
Area Between 30 and 40 >= 1.1719 meters-deg	30	40	1,1719	0,8901	Fail
Area Between FreeEquil and 40 >= 5.157 meters-deg	0	40	5,157	21,4671	Pass
Area Between FreeEquil and Flood >= 5.157 meters-deg	0	19,1872	5,157	10,595	Pass
Area Between 30 and Flood >= 1.1719 meters-deg	30	19,1872	1,1719	-9,0076	Fail
Angle At GZmax >= 15 deg	20,8048		15	20,8048	Pass
Area Between FreeEquil and GZmax >= 180/3.14*(0.055+0.001*(30-GZmax)) meters-deg	0	20,8048	3,68	12,3181	Pass

Stability Criteria - Bureau Veritas_T=1.3m, Weather criteria, 5kt_T=1.3m					
Name	Angle 1	Angle 2	Required	Actual	Pass / Fail
Angle At SteadyEquil <= 16 deg	0,1732		16	0,1732	Pass
Angle At SteadyEquil <= DeckImm*0.8 deg	0,1732		15,1725	0,1732	Pass
Angle At SteadyEquil < Flood deg	0,1732		19,1872	0,1732	Pass
ResRatio Between SteadyEquil-15 deg and Flood > 1	-14,8268	19,1872	1	1,5772	Pass
FloodHt At SteadyEquil > 0.5 meters	0,1732		0,5	1,2044	Pass
Angle At SteadyEquil+15 deg < Flood deg	15,1732		19,1872	15,1732	Pass

Stability Criteria - Bureau Veritas_T=1.3m, Weather criteria, 10kt_T=1.3m					
Name	Angle 1	Angle 2	Required	Actual	Pass / Fail
Angle At SteadyEquil <= 16 deg	0,6896		16	0,6896	Pass
Angle At SteadyEquil <= DeckImm*0.8 deg	0,6896		15,1725	0,6896	Pass
Angle At SteadyEquil < Flood deg	0,6896		19,1872	0,6896	Pass
ResRatio Between SteadyEquil-15 deg and Flood > 1	-14,3104	19,1872	1	1,4888	Pass
FloodHt At SteadyEquil > 0.5 meters	0,6896		0,5	1,1697	Pass
Angle At SteadyEquil+15 deg < Flood deg	15,6896		19,1872	15,6896	Pass

Stability Criteria - Bureau Veritas_T=1.3m, Weather criteria, 15kt_T=1.3m

Name	Angle 1	Angle 2	Required	Actual	Pass / Fail
Angle At SteadyEquil <= 16 deg	1,5511		16	1,5511	Pass
Angle At SteadyEquil <= DeckImm*0.8 deg	1,5511		15,1725	1,5511	Pass
Angle At SteadyEquil < Flood deg	1,5511		19,1872	1,5511	Pass
ResRatio Between SteadyEquil-15 deg and Flood > 1	-13,4489	19,1872	1	1,3477	Pass
FloodHt At SteadyEquil > 0.5 meters	1,5511		0,5	1,1117	Pass
Angle At SteadyEquil+15 deg < Flood deg	16,5511		19,1872	16,5511	Pass

Stability Criteria - Bureau Veritas_T=1.3m, Weather criteria, 20kt_T=1.3m

Name	Angle 1	Angle 2	Required	Actual	Pass / Fail
Angle At SteadyEquil <= 16 deg	2,7562		16	2,7562	Pass
Angle At SteadyEquil <= DeckImm*0.8 deg	2,7562		15,1725	2,7562	Pass
Angle At SteadyEquil < Flood deg	2,7562		19,1872	2,7562	Pass
ResRatio Between SteadyEquil-15 deg and Flood > 1	-12,2438	19,1872	1	1,1633	Pass
FloodHt At SteadyEquil > 0.5 meters	2,7562		0,5	1,0305	Pass
Angle At SteadyEquil+15 deg < Flood deg	17,7562		19,1872	17,7562	Pass

Stability Criteria - Bureau Veritas_T=1.3m, Weather criteria, 5 kt + gust_T=1.3m

Name	Angle 1	Angle 2	Required	Actual	Pass / Fail
Angle At SteadyEquil <= 16 deg	0,388		16	0,388	Pass
Angle At SteadyEquil <= DeckImm*0.8 deg	0,388		15,1725	0,388	Pass
Angle At SteadyEquil < Flood deg	0,388		19,1872	0,388	Pass
ResRatio Between SteadyEquil-15 deg and Flood > 1	-14,612	19,1872	1	1,5399	Pass
FloodHt At SteadyEquil > 0.5 meters	0,388		0,5	1,19	Pass
Angle At SteadyEquil+15 deg < Flood deg	15,388		19,1872	15,388	Pass

Stability Criteria - Bureau Veritas_T=1.3m, Weather criteria, 10 kt + gust_T=1.3m

Name	Angle 1	Angle 2	Required	Actual	Pass / Fail
Angle At SteadyEquil <= 16 deg	1,5511		16	1,5511	Pass
Angle At SteadyEquil <= DeckImm*0.8 deg	1,5511		15,1725	1,5511	Pass
Angle At SteadyEquil < Flood deg	1,5511		19,1872	1,5511	Pass
ResRatio Between SteadyEquil-15 deg and Flood > 1	-13,4489	19,1872	1	1,3477	Pass
FloodHt At SteadyEquil > 0.5 meters	1,5511		0,5	1,1117	Pass
Angle At SteadyEquil+15 deg < Flood deg	16,5511		19,1872	16,5511	Pass

Stability Criteria - Bureau Veritas_T=1.3m, Weather criteria, 15 kt + gust_T=1.3m

Name	Angle 1	Angle 2	Required	Actual	Pass / Fail
Angle At SteadyEquil <= 16 deg	3,4868		16	3,4868	Pass
Angle At SteadyEquil <= DeckImm*0.8 deg	3,4868		15,1725	3,4868	Pass
Angle At SteadyEquil < Flood deg	3,4868		19,1872	3,4868	Pass
ResRatio Between SteadyEquil-15 deg and Flood > 1	-11,5132	19,1872	1	1,0587	Pass
FloodHt At SteadyEquil > 0.5 meters	3,4868		0,5	0,9814	Pass
Angle At SteadyEquil+15 deg < Flood deg	18,4868		19,1872	18,4868	Pass

Stability Criteria - Bureau Veritas_T=1.3m, Weather criteria, 20 kt + gust_T=1.3m

Name	Angle 1	Angle 2	Required	Actual	Pass / Fail
Angle At SteadyEquil <= 16 deg	6,1834		16	6,1834	Pass
Angle At SteadyEquil <= DeckImm*0.8 deg	6,1834		15,1725	6,1834	Pass
Angle At SteadyEquil < Flood deg	6,1834		19,1872	6,1834	Pass
ResRatio Between SteadyEquil-15 deg and Flood > 1	-8,8166	19,1872	1	0,7181	Fail
FloodHt At SteadyEquil > 0.5 meters	6,1834		0,5	0,8022	Pass
Angle At SteadyEquil+15 deg < Flood deg	21,1834		19,1872	21,1834	Fail

Grågås condition

Stability Criteria - Bueau Veritas_T=1.6m, Intact Stability					
Name	Angle 1	Angle 2	Required	Actual	Pass / Fail
GM At FreeEquil >= 0.15 meters	0		0,15	4,4916	Pass
GZ At 30 >= 0.2 meters	30		0,2	0,0074	Fail
Angle At GZmax >= 25 deg	15,8757		25	15,8757	Fail
Area Between FreeEquil and 30 >= 3.151 meters-deg	0	30	3,151	13,0367	Pass
Area Between 30 and 40 >= 1.1719 meters-deg	30	40	1,1719	-3,78	Fail
Area Between FreeEquil and 40 >= 5.157 meters-deg	0	40	5,157	9,2567	Pass
Area Between FreeEquil and Flood >= 5.157 meters-deg	0	13,9432	5,157	5,1688	Pass
Area Between 30 and Flood >= 1.1719 meters-deg	30	13,9432	1,1719	-5,9356	Fail
Angle At GZmax >= 15 deg	15,8757		15	15,8757	Pass
Area Between FreeEquil and GZmax >= 180/3.14*(0.055+0.001*(30-GZmax)) meters-deg	0	15,8757	3,9625	6,6178	Pass

Stability Criteria - Bueau Veritas_T=1.6m, Weather criteria, 5kt_T=1.6m					
Name	Angle 1	Angle 2	Required	Actual	Pass / Fail
Angle At SteadyEquil <= 16 deg	0,1272		16	0,1272	Pass
Angle At SteadyEquil <= DeckImm*0.8 deg	0,1272		11,0421	0,1272	Pass
Angle At SteadyEquil < Flood deg	0,1272		13,9432	0,1272	Pass
ResRatio Between SteadyEquil-14 deg and Flood > 1	-13,8728	13,9432	1	0,9832	Fail
FloodHt At SteadyEquil > 0.5 meters	0,1272		0,5	0,9068	Pass
Angle At SteadyEquil+14 deg < Flood deg	14,1272		13,9432	14,1272	Fail

Stability Criteria - Bueau Veritas_T=1.6m, Weather criteria, 10kt_T=1.6m					
Name	Angle 1	Angle 2	Required	Actual	Pass / Fail
Angle At SteadyEquil <= 16 deg	0,5086		16	0,5086	Pass
Angle At SteadyEquil <= DeckImm*0.8 deg	0,5086		11,0421	0,5086	Pass
Angle At SteadyEquil < Flood deg	0,5086		13,9432	0,5086	Pass
ResRatio Between SteadyEquil-14 deg and Flood > 1	-13,4914	13,9432	1	0,9284	Fail
FloodHt At SteadyEquil > 0.5 meters	0,5086		0,5	0,881	Pass
Angle At SteadyEquil+14 deg < Flood deg	14,5086		13,9432	14,5086	Fail

Stability Criteria - Bueau Veritas_T=1.6m, Weather criteria, 15kt_T=1.6m

Name	Angle 1	Angle 2	Required	Actual	Pass / Fail
Angle At SteadyEquil <= 16 deg	1,1412		16	1,1412	Pass
Angle At SteadyEquil <= DeckImm*0.8 deg	1,1412		11,0421	1,1412	Pass
Angle At SteadyEquil < Flood deg	1,1412		13,9432	1,1412	Pass
ResRatio Between SteadyEquil-14 deg and Flood > 1	-12,8588	13,9432	1	0,8407	Fail
FloodHt At SteadyEquil > 0.5 meters	1,1412		0,5	0,8384	Pass
Angle At SteadyEquil+14 deg < Flood deg	15,1412		13,9432	15,1412	Fail

Stability Criteria - Bueau Veritas_T=1.6m, Weather criteria, 20kt_T=1.6m

Name	Angle 1	Angle 2	Required	Actual	Pass / Fail
Angle At SteadyEquil <= 16 deg	2,0277		16	2,0277	Pass
Angle At SteadyEquil <= DeckImm*0.8 deg	2,0277		11,0421	2,0277	Pass
Angle At SteadyEquil < Flood deg	2,0277		13,9432	2,0277	Pass
ResRatio Between SteadyEquil-14 deg and Flood > 1	-11,9723	13,9432	1	0,7263	Fail
FloodHt At SteadyEquil > 0.5 meters	2,0277		0,5	0,7785	Pass
Angle At SteadyEquil+14 deg < Flood deg	16,0277		13,9432	16,0277	Fail

Stability Criteria - Bueau Veritas_T=1.6m, Weather criteria, 5 kt + gust_T=1.6m

Name	Angle 1	Angle 2	Required	Actual	Pass / Fail
Angle At SteadyEquil <= 16 deg	0,2862		16	0,2862	Pass
Angle At SteadyEquil <= DeckImm*0.8 deg	0,2862		11,0421	0,2862	Pass
Angle At SteadyEquil < Flood deg	0,2862		13,9432	0,2862	Pass
ResRatio Between SteadyEquil-14 deg and Flood > 1	-13,7138	13,9432	1	0,9601	Fail
FloodHt At SteadyEquil > 0.5 meters	0,2862		0,5	0,896	Pass
Angle At SteadyEquil+14 deg < Flood deg	14,2862		13,9432	14,2862	Fail

Stability Criteria - Bueau Veritas_T=1.6m, Weather criteria, 10 kt + gust_T=1.6m

Name	Angle 1	Angle 2	Required	Actual	Pass / Fail
Angle At SteadyEquil <= 16 deg	1,1412		16	1,1412	Pass
Angle At SteadyEquil <= DeckImm*0.8 deg	1,1412		11,0421	1,1412	Pass
Angle At SteadyEquil < Flood deg	1,1412		13,9432	1,1412	Pass
ResRatio Between SteadyEquil-14 deg and Flood > 1	-12,8588	13,9432	1	0,8407	Fail
FloodHt At SteadyEquil > 0.5 meters	1,1412		0,5	0,8384	Pass
Angle At SteadyEquil+14 deg < Flood deg	15,1412		13,9432	15,1412	Fail

Stability Criteria - Bueau Veritas_T=1.6m, Weather criteria, 15 kt + gust_T=1.6m

Name	Angle 1	Angle 2	Required	Actual	Pass / Fail
Angle At SteadyEquil <= 16 deg	2,5668		16	2,5668	Pass
Angle At SteadyEquil <= DeckImm*0.8 deg	2,5668		11,0421	2,5668	Pass
Angle At SteadyEquil < Flood deg	2,5668		13,9432	2,5668	Pass
ResRatio Between SteadyEquil-14 deg and Flood > 1	-11,4332	13,9432	1	0,6617	Fail
FloodHt At SteadyEquil > 0.5 meters	2,5668		0,5	0,7422	Pass
Angle At SteadyEquil+14 deg < Flood deg	16,5668		13,9432	16,5668	Fail

Stability Criteria - Bueau Veritas_T=1.6m, Weather criteria, 20 kt + gust_T=1.6m

Name	Angle 1	Angle 2	Required	Actual	Pass / Fail
Angle At SteadyEquil <= 16 deg	4,5494		16	4,5494	Pass
Angle At SteadyEquil <= DeckImm*0.8 deg	4,5494		11,0421	4,5494	Pass
Angle At SteadyEquil < Flood deg	4,5494		13,9432	4,5494	Pass
ResRatio Between SteadyEquil-14 deg and Flood > 1	-9,4506	13,9432	1	0,4503	Fail
FloodHt At SteadyEquil > 0.5 meters	4,5494		0,5	0,6084	Pass
Angle At SteadyEquil+14 deg < Flood deg	18,5494		13,9432	18,5494	Fail

Appendix C. Seakeeping calculations results

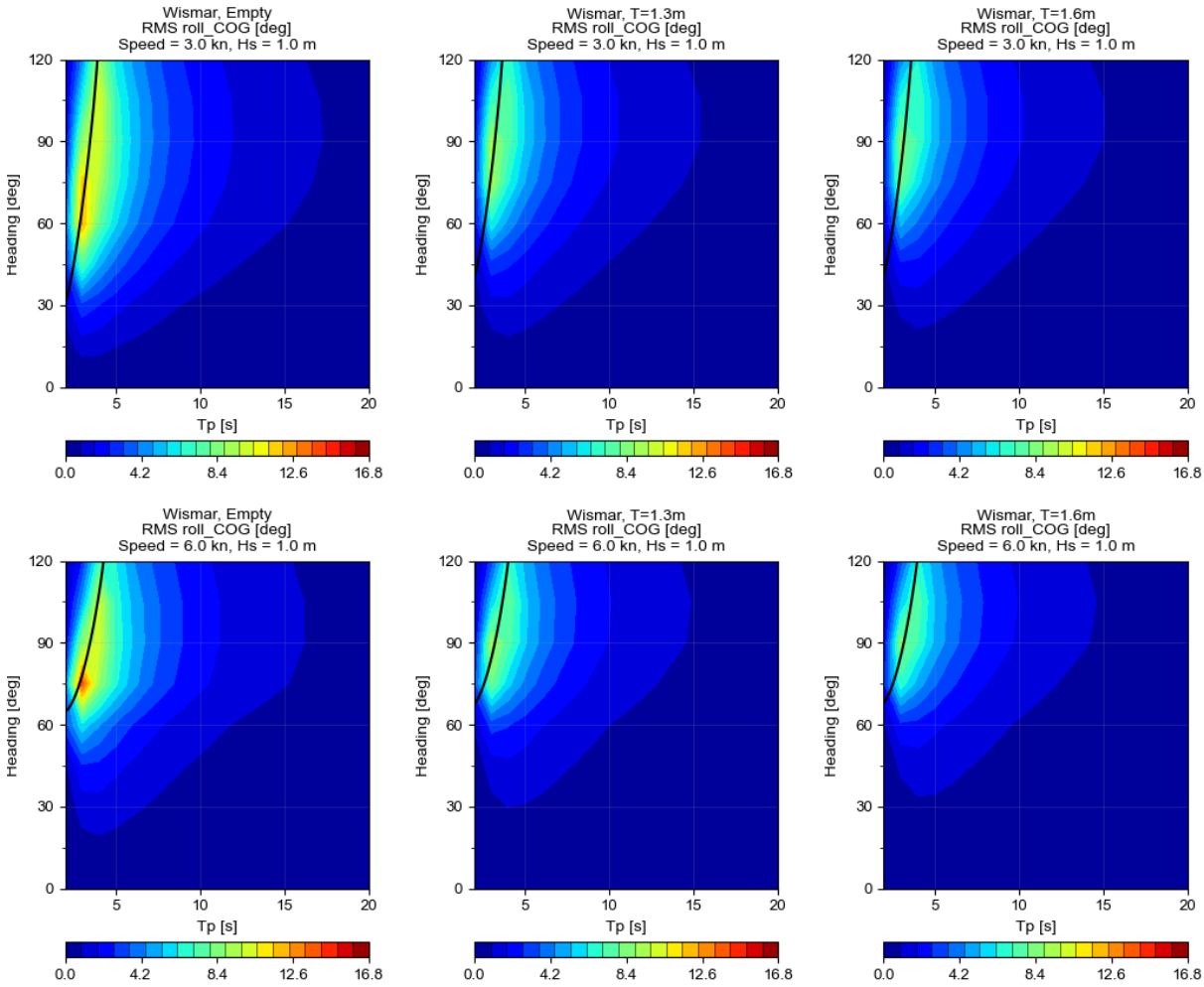

Figure 136 RMS roll for the Big Ship of Wismar in 1 m significant wave height as a function of the wave peak period and the wave heading, for 3 knots (top) and 6 knots (bottom). The black line indicates the conditions where wave peak period matches the natural roll period. (Hernandez Montfort).

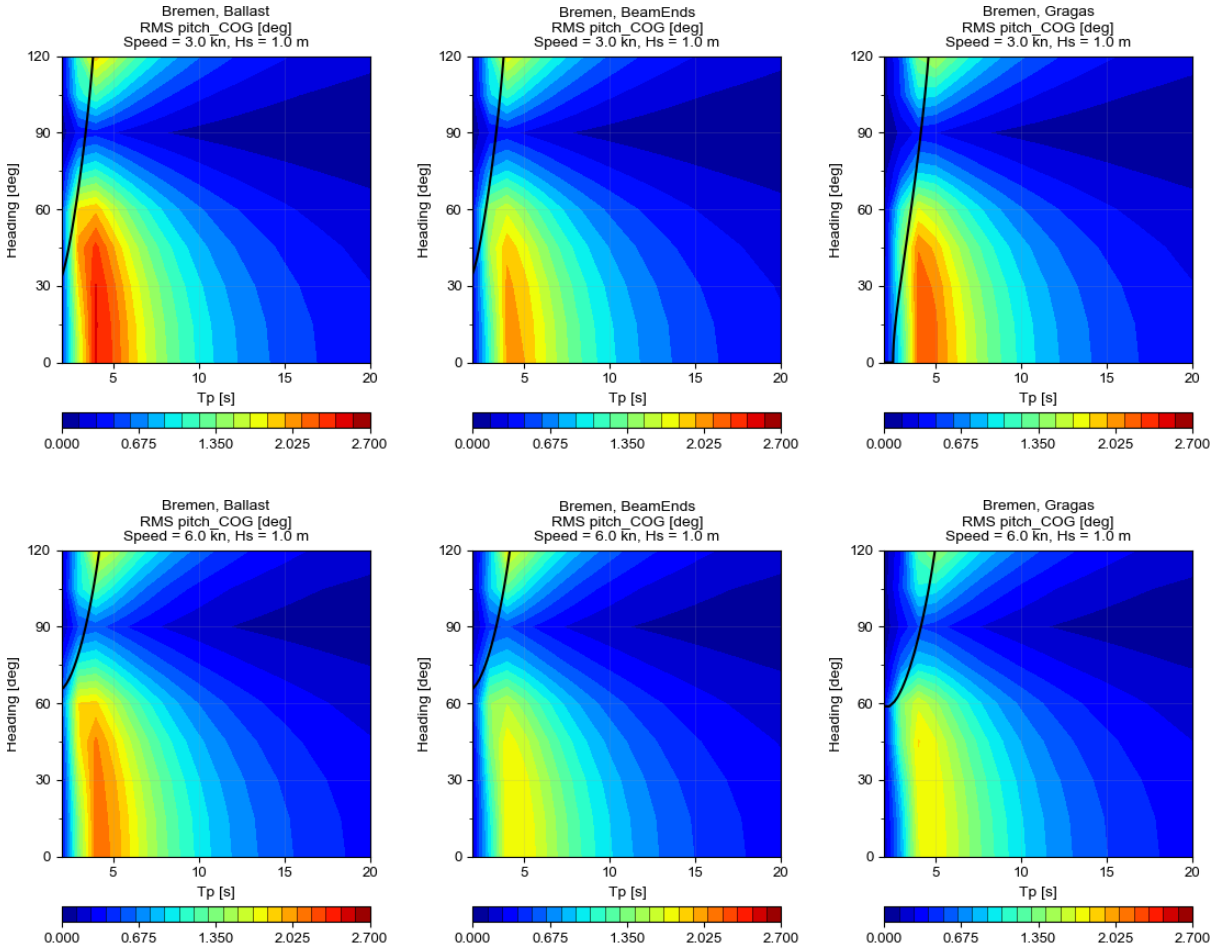

Figure 137 RMS pitch for the Bremen cog in 1 m significant wave height as a function of the wave peak period and the wave heading, for 3 knots (top) and 6 knots (bottom). The black line indicates the conditions where wave peak period matches the natural pitch period. (Hernandez Montfort).

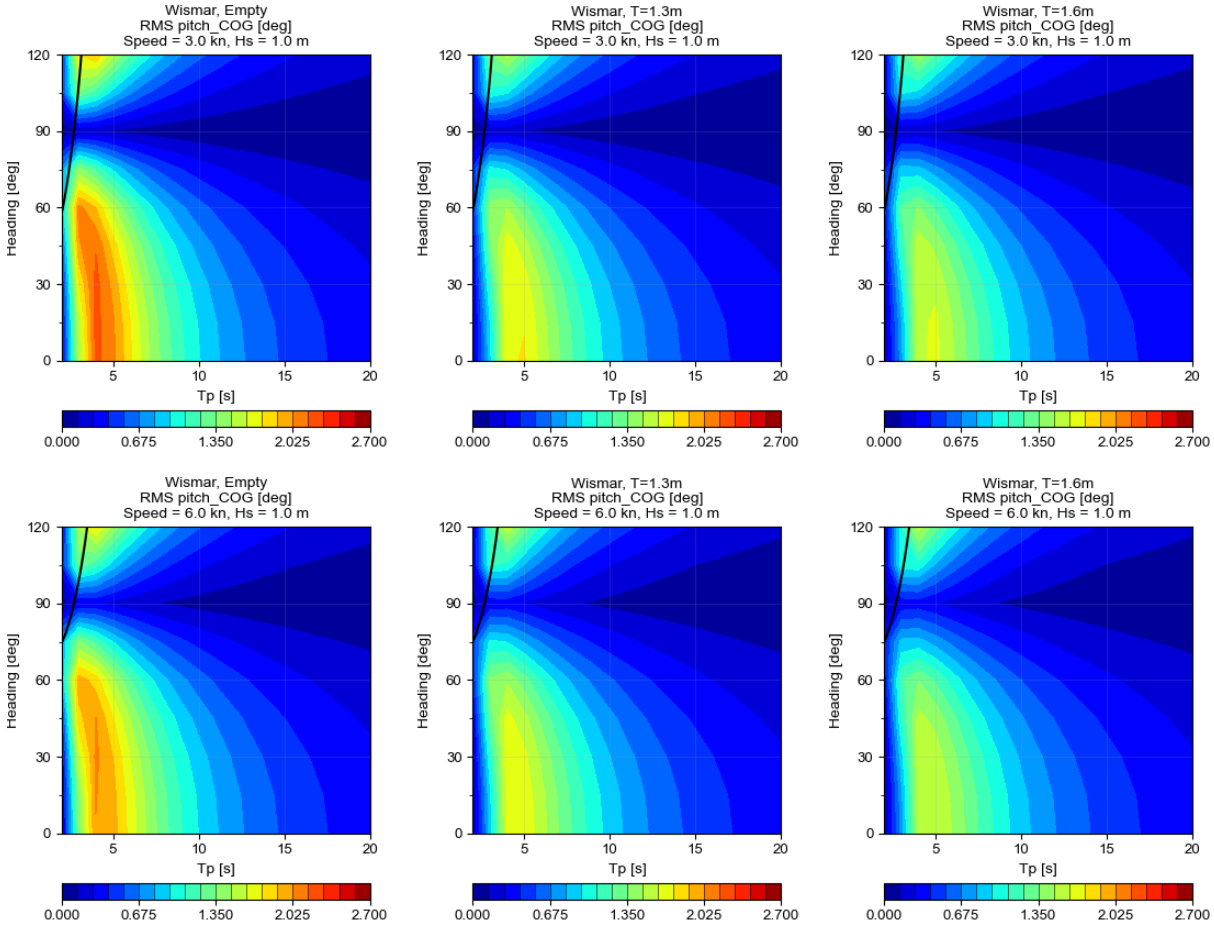

Figure 138 RMS pitch for the Big Ship of Wismar in 1 m significant wave height as a function of the wave peak period and the wave heading, for 3 knots (top) and 6 knots (bottom). The black line indicates the conditions where wave peak period matches the natural pitch period. (Hernandez Montfort).

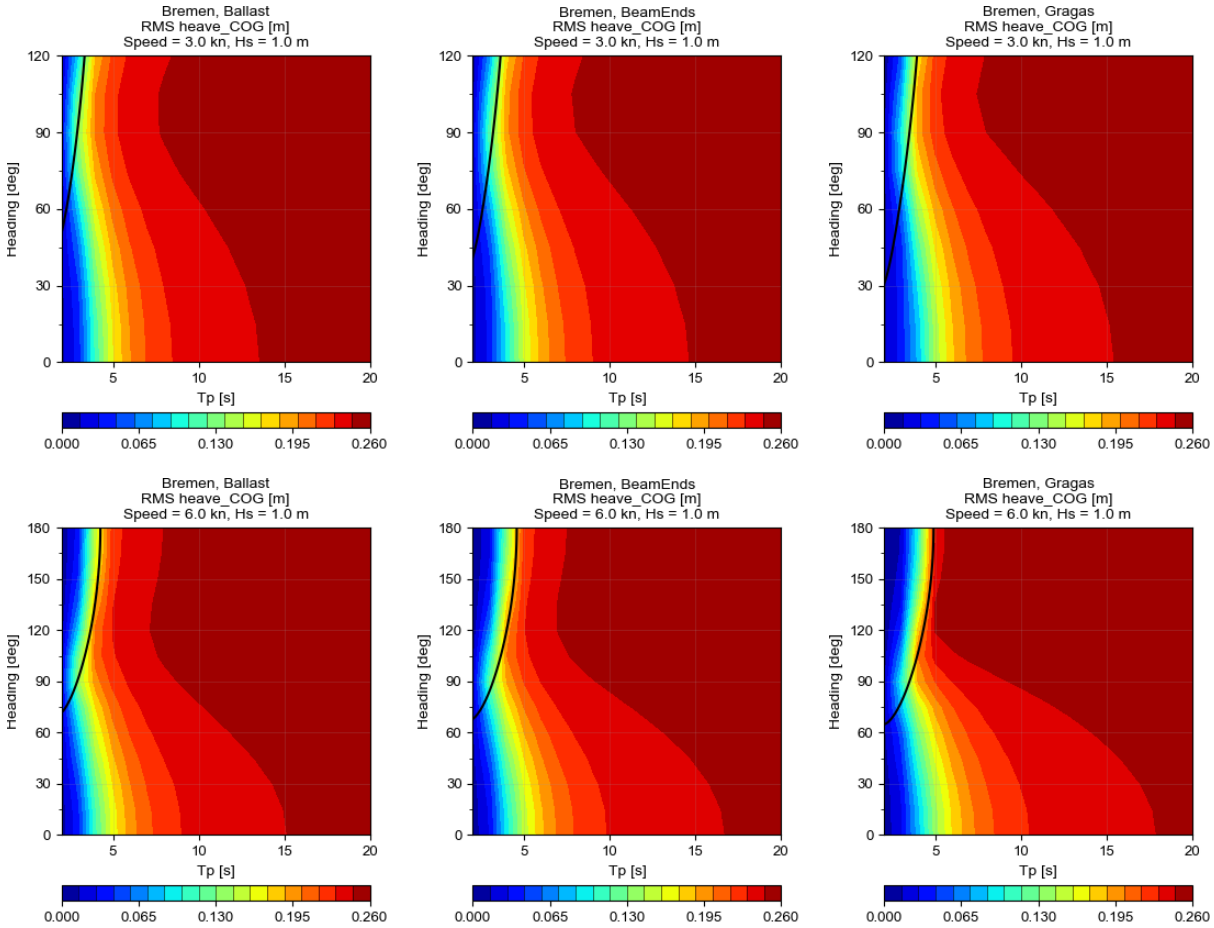

Figure 139 RMS heave for the Bremen cog in 1 m significant wave height as a function of the wave peak period and the wave heading, for 3 knots (top) and 6 knots (bottom). The black line indicates the conditions where wave peak period matches the natural heave period. (Hernandez Montfort).

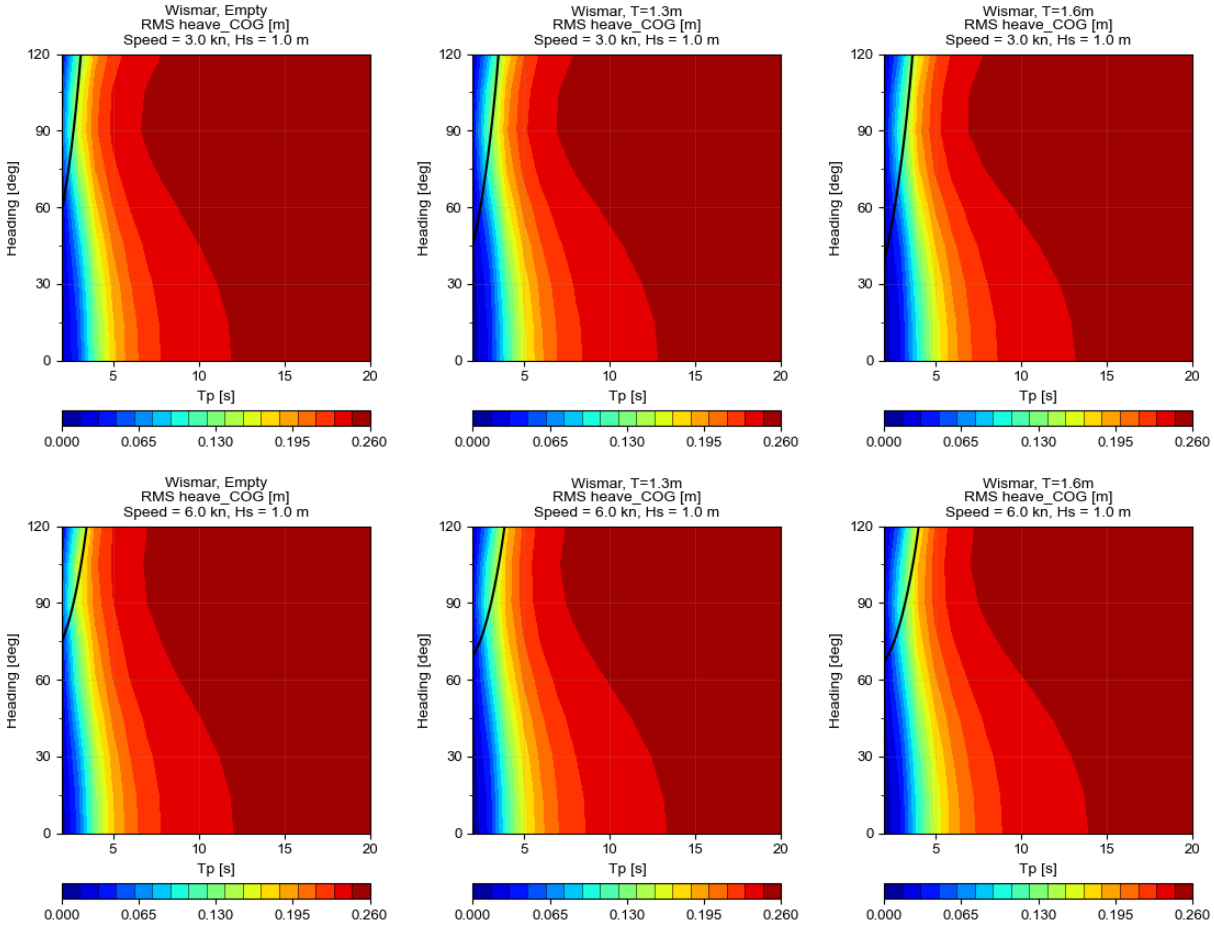

Figure 140 RMS heave for the Big Ship of Wismar in 1 m significant wave height as a function of the wave peak period and the wave heading, for 3 knots (top) and 6 knots (bottom). The black line indicates the conditions where wave peak period matches the natural heave period. (Hernandez Montfort).

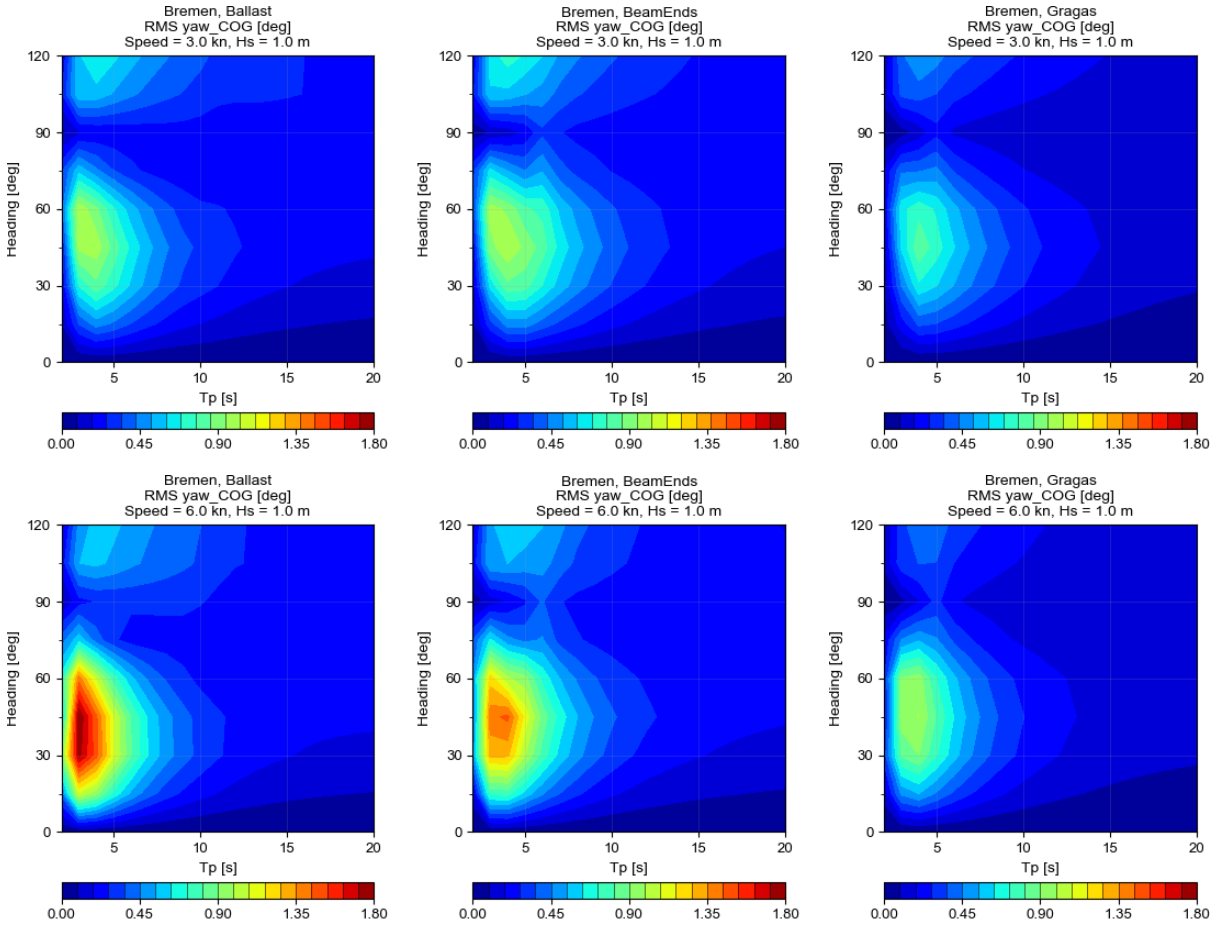

Figure 141 RMS yaw for the Bremen cog in 1 m significant wave height as a function of the wave peak period and the wave heading, for 3 knots (top) and 6 knots (bottom). (Hernandez Montfort).

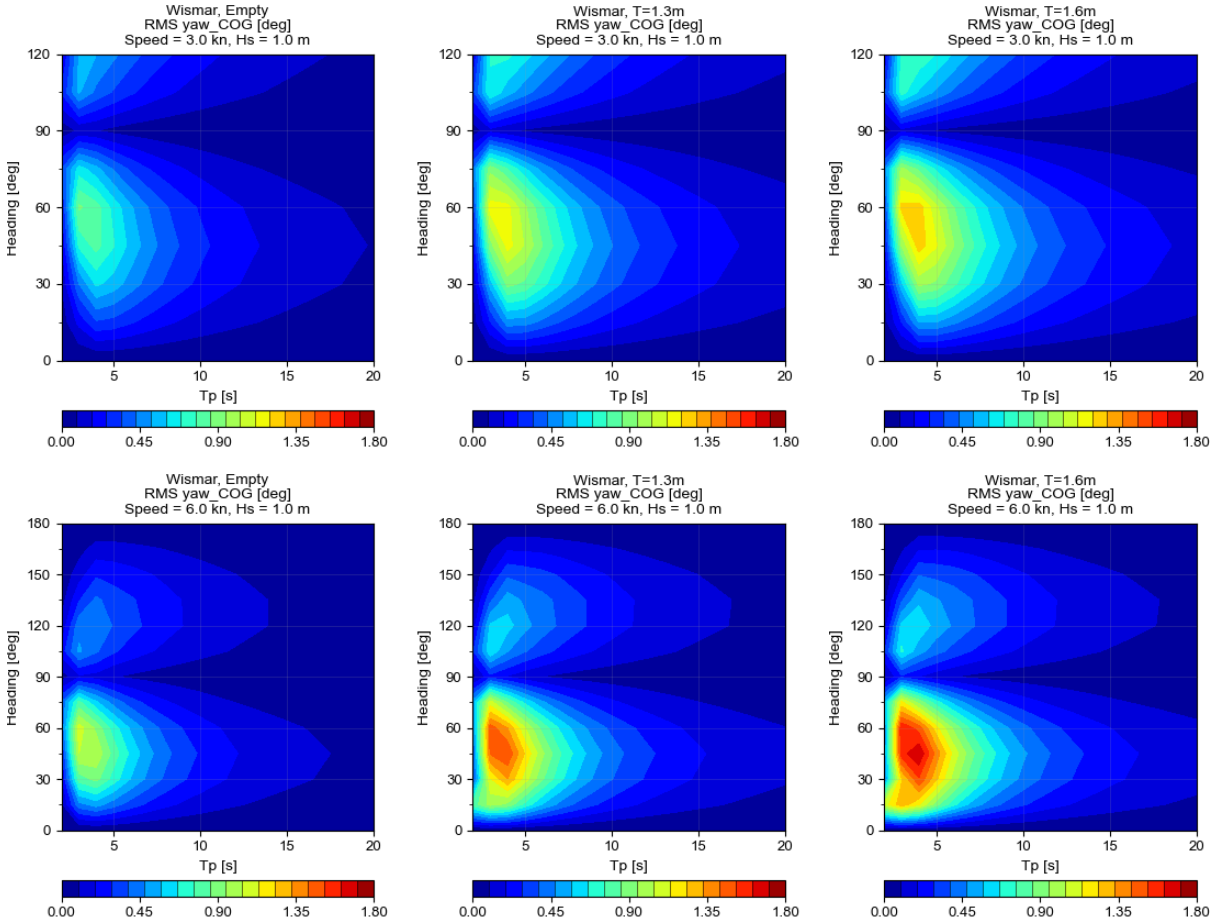

Figure 142 RMS yaw for the Big Ship of Wismar in 1 m significant wave height as a function of the wave peak period and the wave heading, for 3 knots (top) and 6 knots (bottom). (Hernandez Montfort).

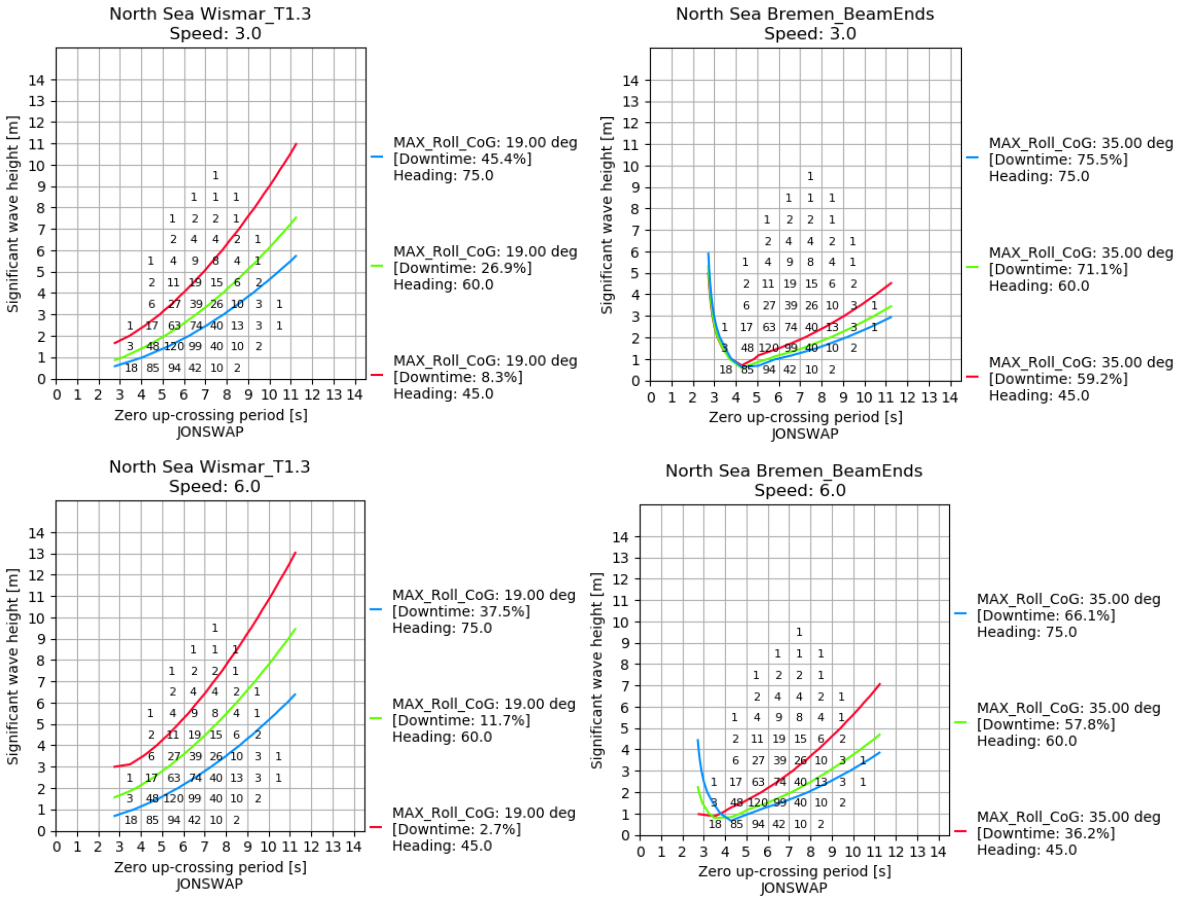

Figure 143 Downtime in the North Sea for an MPM of roll equal to the flooding angle for the Big Ship of Wismar in the draft below wales condition (left) and the Bremen cog in the draft below beams condition (right), for 3 knots (top) and 6 knots (bottom). Each colour represents one wave heading. (Hernandez Montfort).

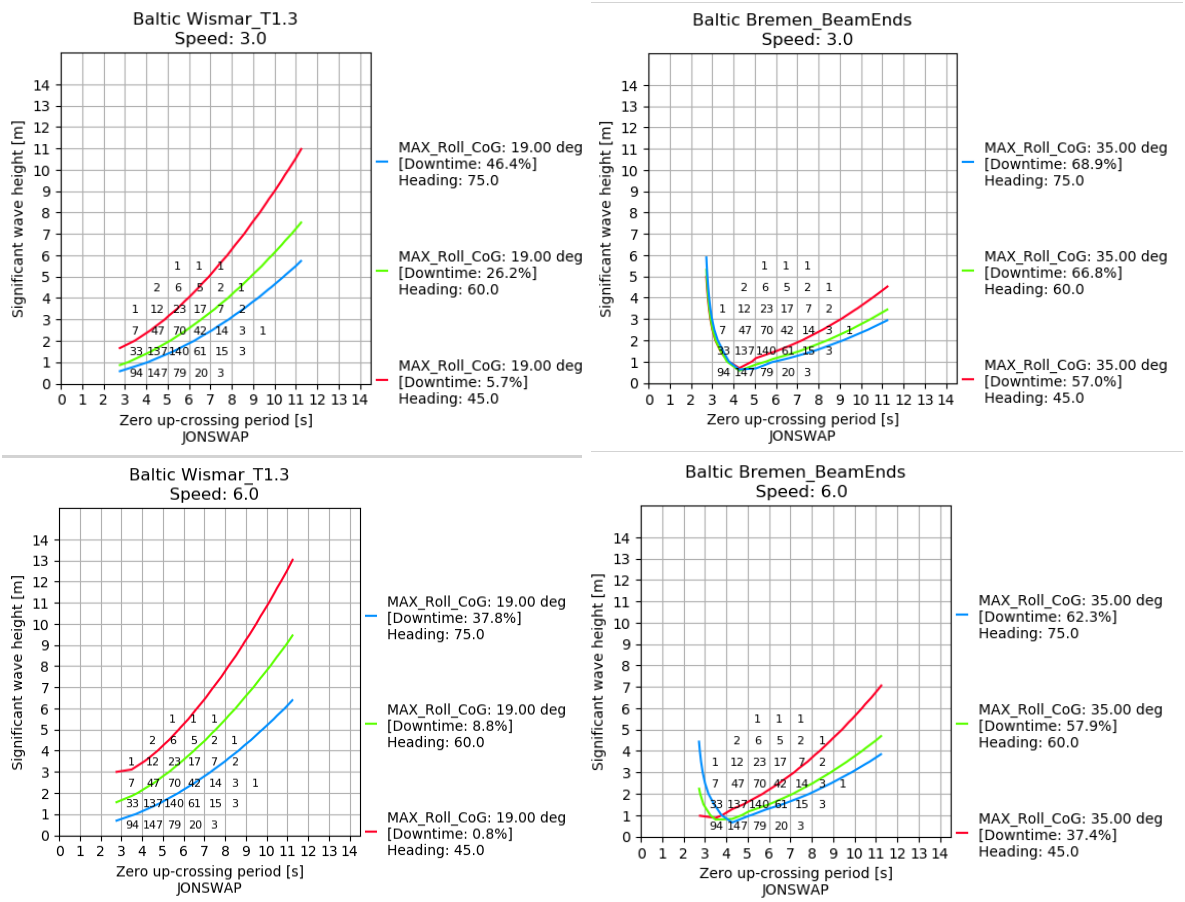

Figure 144 Downtime in the Baltic Sea for an MPM of roll equal to the flooding angle for the Big Ship of Wismar in the draft below wales condition (left) and the Bremen cog in the draft below beams condition (right), for 3 knots (top) and 6 knots (bottom). Each colour represents one wave heading. (Hernandez Montfort).

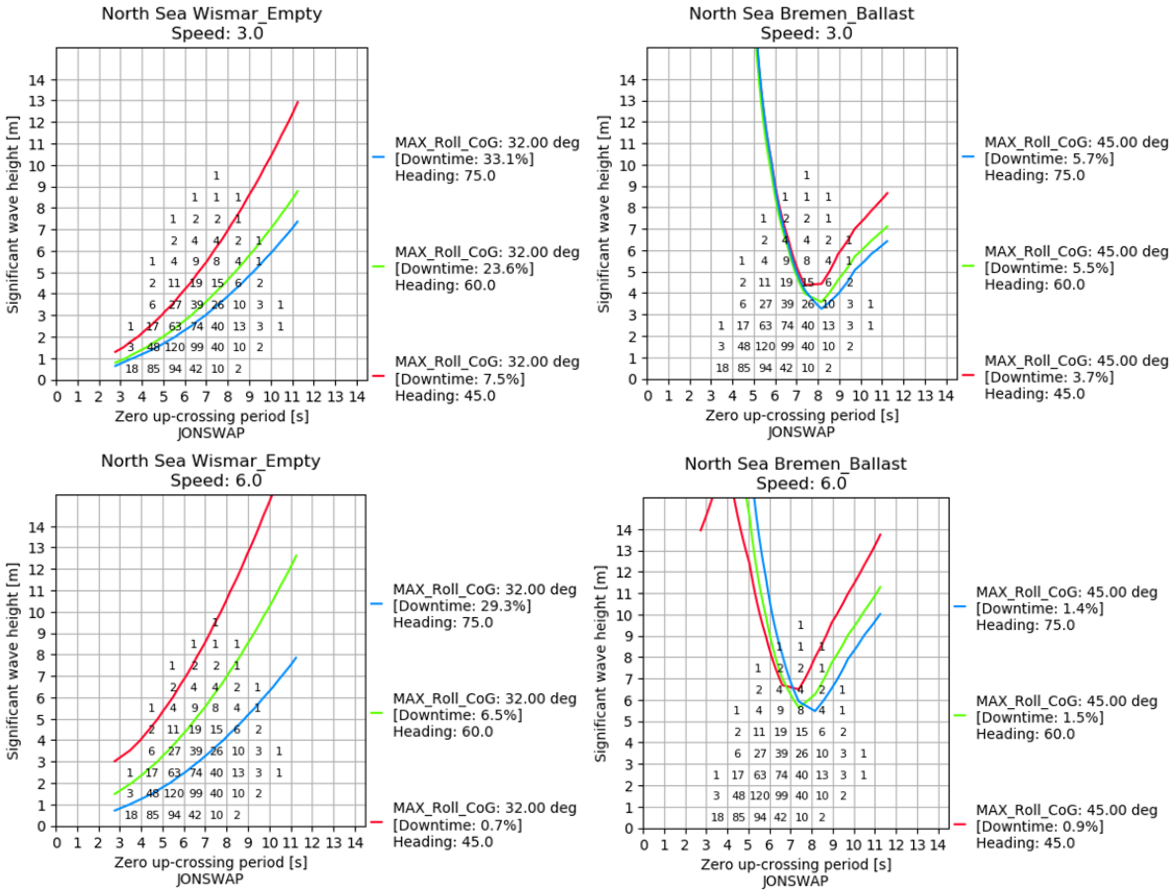

Figure 145 Downtime in the North Sea for an MPM of roll equal to the flooding angle for the Big Ship of Wismar in the empty condition (left) and the Bremen cog in the ballast condition (right), for 3 knots (top) and 6 knots (bottom). Each colour represents one wave heading. (Hernandez Montfort).

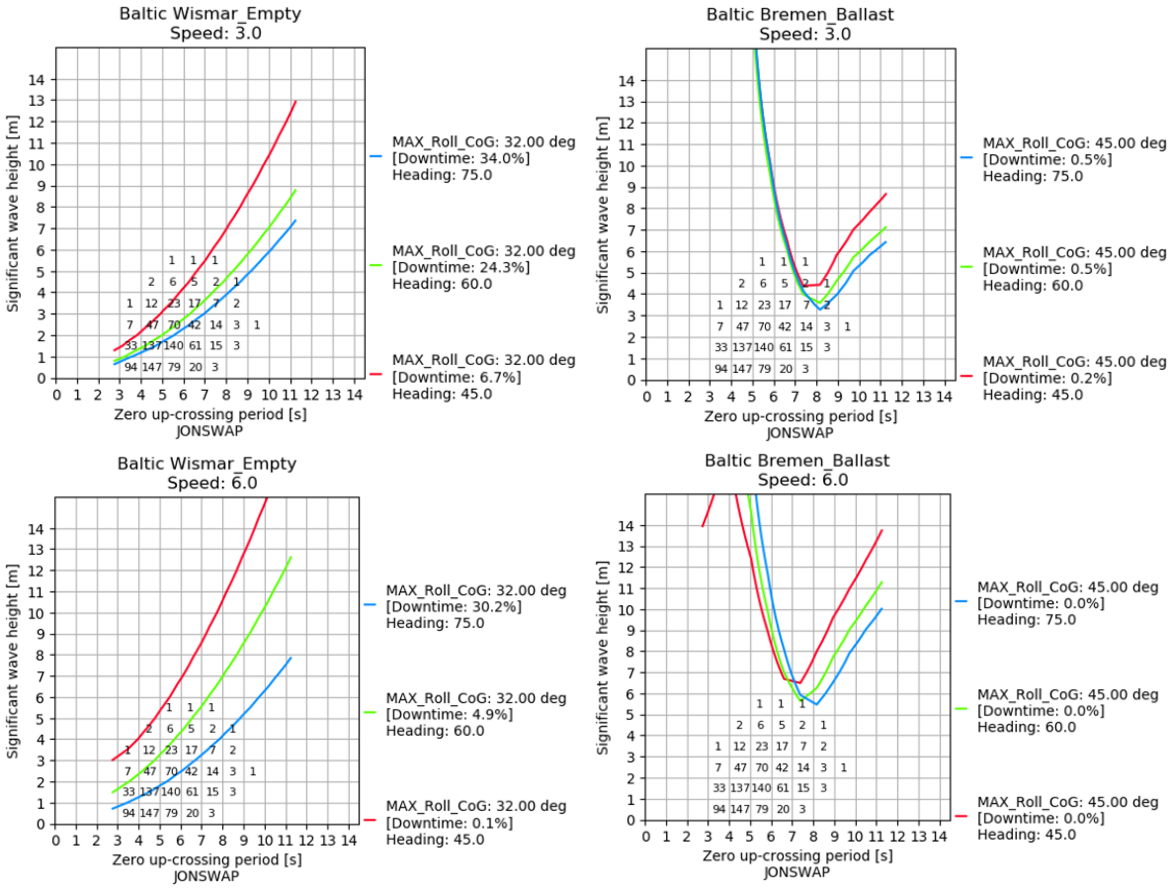

Figure 146 Downtime in the Baltic Sea for an MPM of roll equal to the flooding angle for the Big Ship of Wismar in the empty condition (left) and the Bremen cog in the ballast condition (right), for 3 knots (top) and 6 knots (bottom). Each colour represents one wave heading. (Hernandez Montfort).

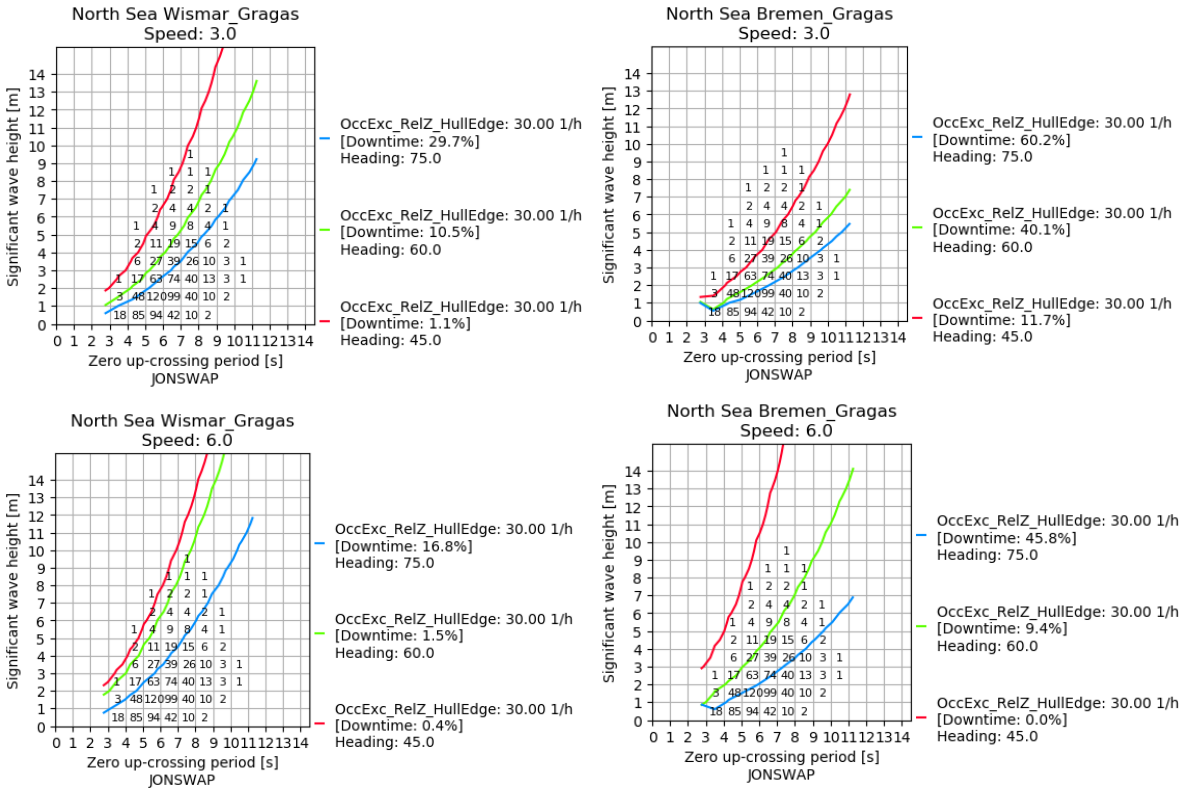

Figure 147 Downtime in the North Sea for the criterion on water elevation exceeding the edge of the hull for the Big Ship of Wismar (left) and the Bremen cog (right) in the Grågås condition, for 3 knots (top) and 6 knots (bottom). Each colour represents one wave heading. (Hernandez Montfort).

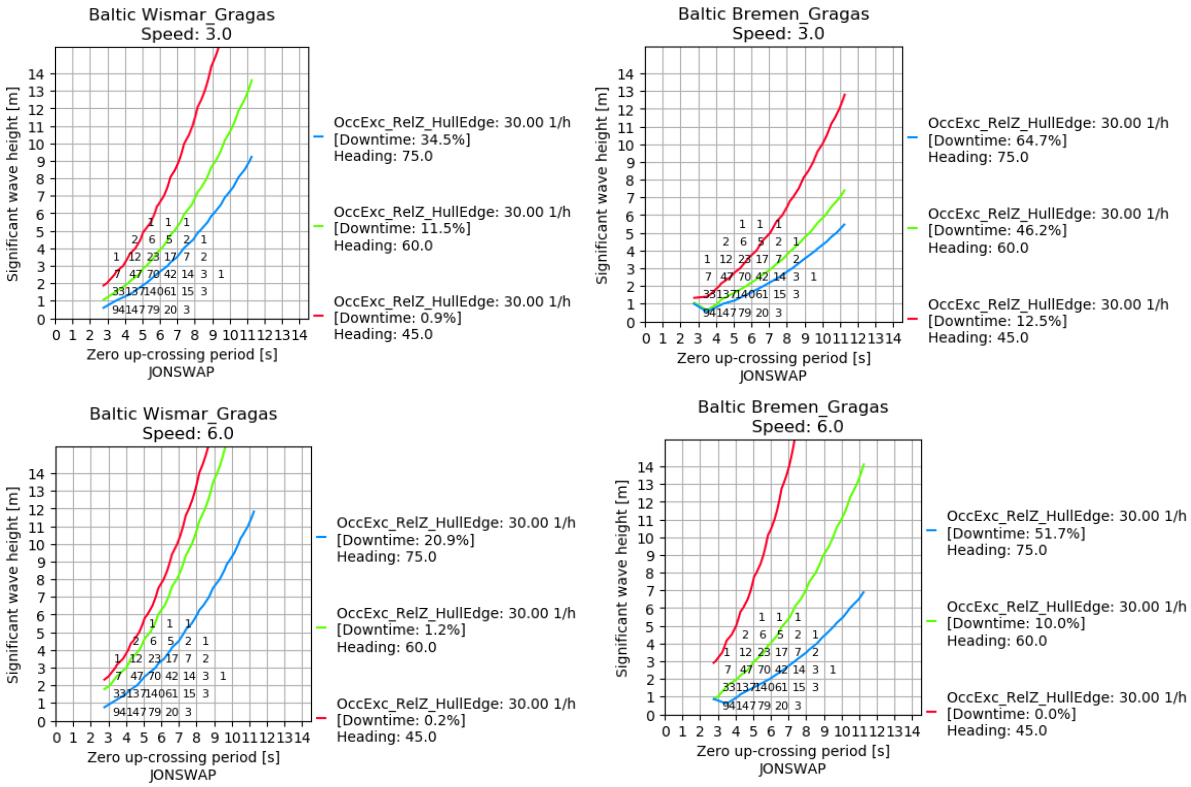

Figure 148 Downtime in the Baltic Sea for the criterion on water elevation exceeding the edge of the hull for the Big Ship of Wismar (left) and the Bremen cog (right) in the Grågås condition, for 3 knots (top) and 6 knots (bottom). Each colour represents one wave heading. (Hernandez Montfort).

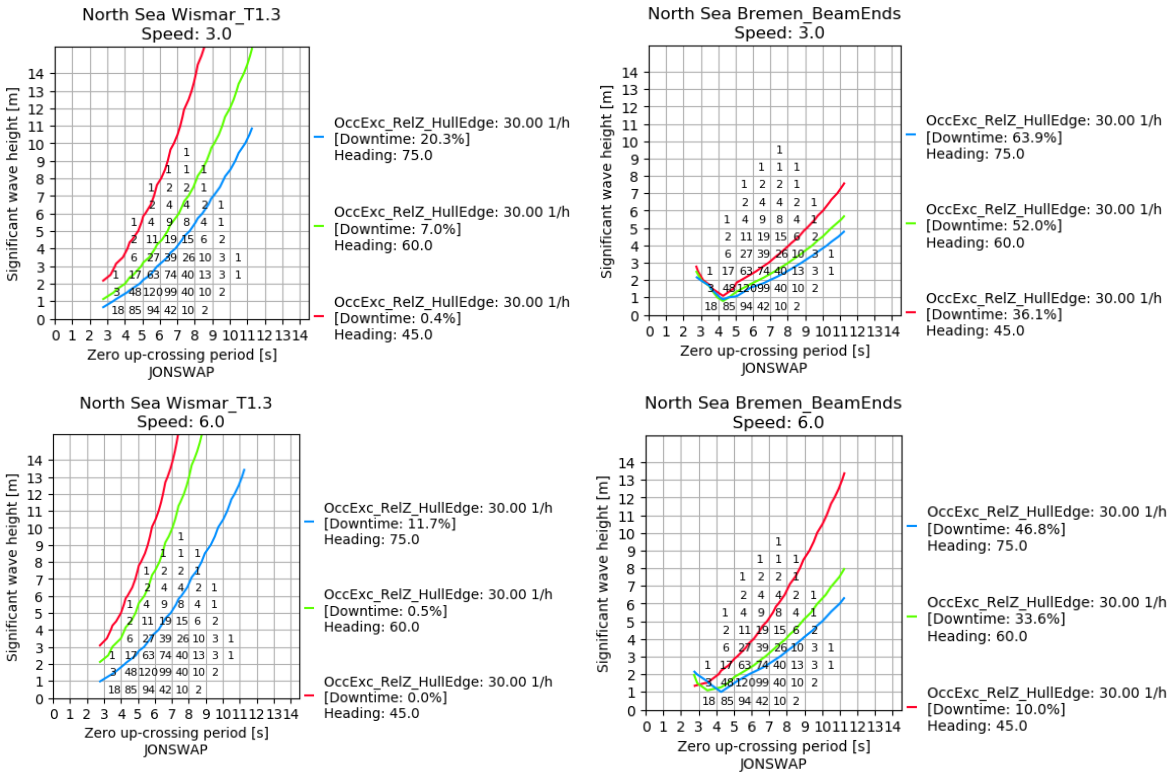

Figure 149 Downtime in the North Sea for the criterion on water elevation exceeding the edge of the hull for the Big Ship of Wismar in the water below wales condition (left) and the Bremen cog in the water below beams condition (right), for 3 knots (top) and 6 knots (bottom). Each colour represents one wave heading. (Hernandez Montfort).

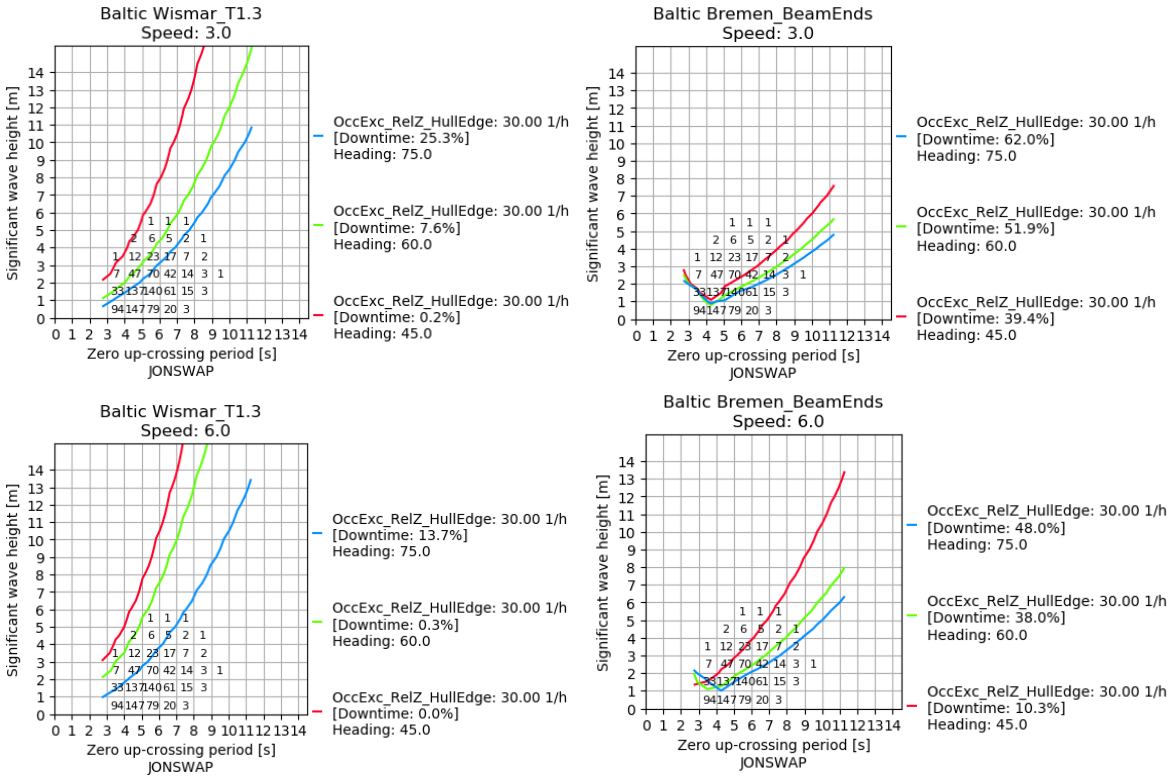

Figure 150 Downtime in the Baltic Sea for the criterion on water elevation exceeding the edge of the hull for the Big Ship of Wismar in the water below wales condition (left) and the Bremen cog in the water below beams condition (right), for 3 knots (top) and 6 knots (bottom). Each colour represents one wave heading. (Hernandez Montfort).

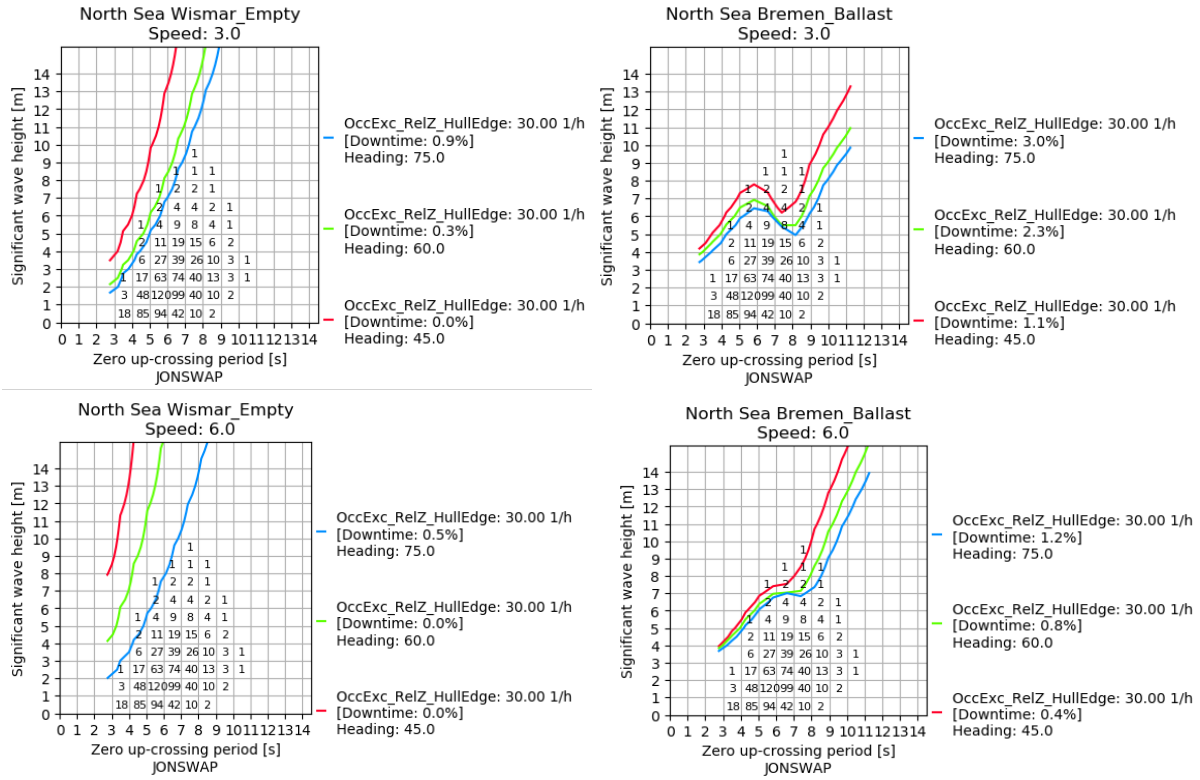

Figure 151 Downtime in the North Sea for the criterion on water elevation exceeding the edge of the hull for the Big Ship of Wismar in the empty condition (left) and the Bremen cog in the ballast condition (right), for 3 knots (top) and 6 knots (bottom). Each colour represents one wave heading. (Hernandez Montfort).

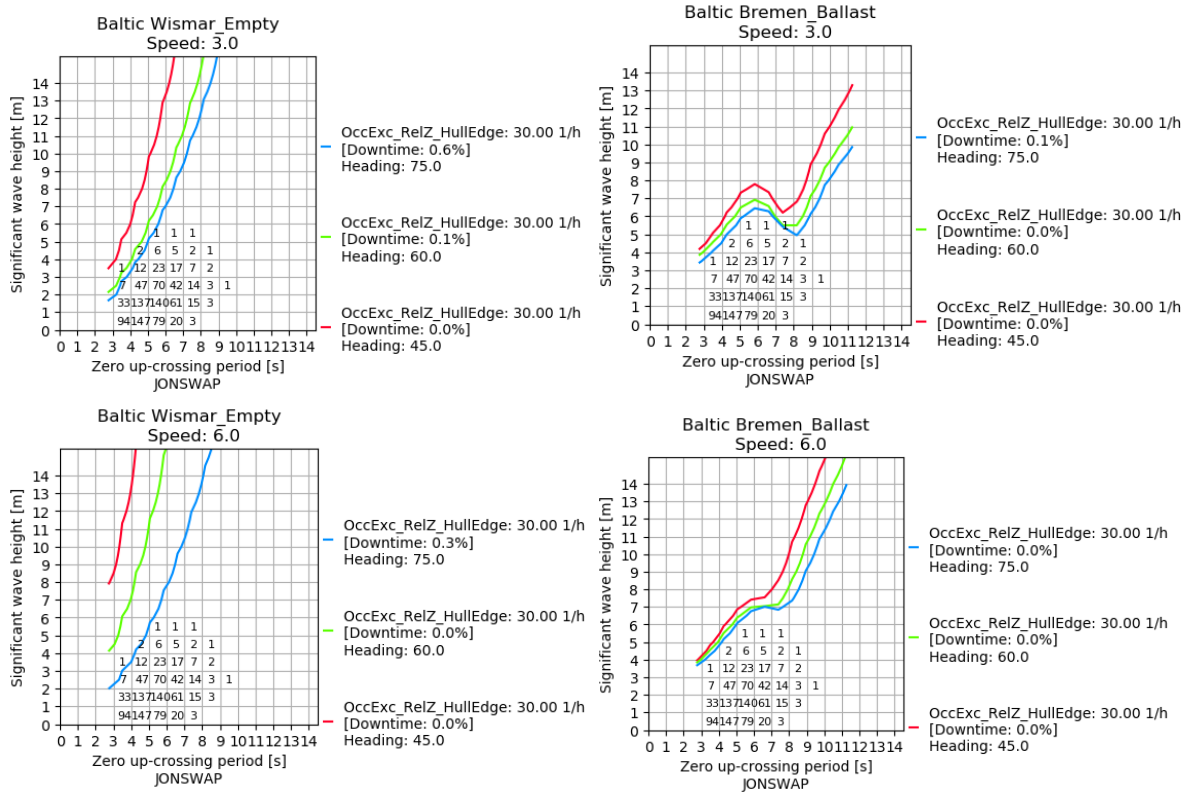

Figure 152 Downtime in the Baltic Sea for the criterion on water elevation exceeding the edge of the hull for the Big Ship of Wismar in the empty condition (left) and the Bremen cog in the ballast condition (right), for 3 knots (top) and 6 knots (bottom). Each colour represents one wave heading. (Hernandez Montfort).

SHIPMO

Fast seakeeping calculations: behaviour of a ship in a seaway

At MARIN the program SHIPMO is available for the calculation of the behaviour of a ship in a seaway. The program is based on the well-known 'strip theory'.

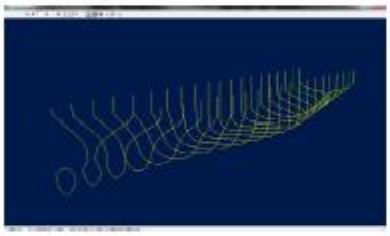

The added resistance in waves can be calculated by four approximation methods: Gerritsma/Beukelman, Boese, Salvesen and a combination of these methods. The program also accommodates multihulls such as catamarans and trimarans.

Computational approach

The potential theory underlying SHIPMO assumes slenderness of the ship's hull and linearity of the hydrodynamic forces. The assumption of slenderness opens up the opportunity for a 2-D 'strip-wise' solution of the hydrodynamic forces in waves. The assumption of linearity implies that in principle the results are valid for relatively small motions only and that the ship is supposed to have vertical sides. The program is actually split up into two parts. In the first part the hydrodynamic forces are calculated. In the second part the equations of motion are solved.

The hull form is approximated by an arbitrary number (usually 20-40) of frames or sections. Each section shape is approximated by a number of line elements. It is assumed that there is no direct hydrodynamic interaction between the sections. The ship-wave interaction problem is described as the superposition of two smaller problems: a fixed ship in incoming and diffracted waves (the diffraction problem) and a moving ship in radiated waves (the radiation problem). For each section, the fundamental radiation-diffraction problem is solved and the corresponding hydrodynamic forces are calculated.

After evaluation of the wave excitation forces and the reaction forces on the individual sections, the global forces are obtained by integration over the ship length. The integration can also be carried out for a segment of the ship. The wave excitation forces are composed of the incoming (or Froude-Krylov) wave forces and the diffraction wave forces. The reaction forces are expressed in terms of added mass and damping coefficients.

In the second part of the program the equations of motion are solved. Several options exist to include the nonlinear effects of:

- viscous roll damping due to the generation of eddies around the bilge, skin friction damping, lift damping
- flow around bilge keels and skegs
- fin and rudder stabilisers, both passive and active
- anti-roll tanks

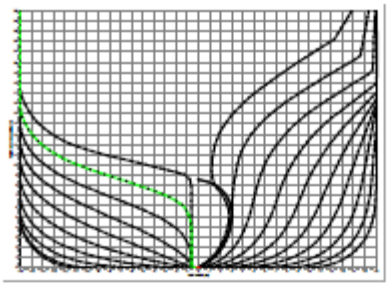

Strip-wise geometry description of container ship

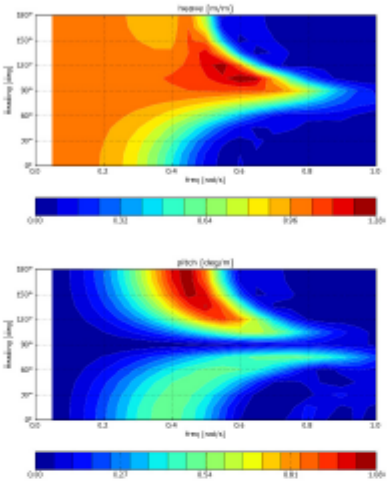

Heave (top) and pitch (bottom) motion of container ship in regular waves

Input

- body plan
- draft at aft and fore perpendiculars, transverse metacentric height
- mass distribution, radii of gyration
- appendages: bilge keels, skegs, fins, rudders
- ship speeds
- regular waves: wave directions, wave frequencies, water depth
- irregular waves: significant wave height and wave period

Output

- motions: surge, sway, heave, roll, pitch and yaw
- response in reference points:
  - relative vertical motion and velocity
  - absolute motions, velocities and accelerations
- internal loads at transverse cuts:
  - transverse and vertical shear forces and bending moments, torsional moment
- added resistance in waves

All results are available in the form of Response Amplitude Operators (RAOs) in the frequency domain. To obtain a meaningful interpretation of the motion characteristics the results have to be combined with wave climate and motion criteria. An interface with the program WASCO was developed to facilitate an efficient handling at this part of the analysis.

Applications

Despite the theoretical limits of linear strip-theory the program is used for a wide range of applications and hull forms. The most important applications are:

- prediction of seakeeping behaviour in initial design
- comparison of hull forms
- evaluation of the performance of roll stabilisers
- optimization of experimental programs; e.g. by a rational selection of heading, speed, wave height and period

The use of SHIPMO has yielded a large volume of valuable information. In general it can be concluded that the over-all motions of various ship types in waves of limited height are predicted with fair accuracy. The main limitations are the prediction of:

- the roll response
- the relative wave elevation in the ship's sides due to 3-dimensional effects
- the added resistance in short waves or in beam and stern quartering waves
- the behaviour in extreme conditions

For more information contact the MARIN Software Group
T + 31 317 49 32 37
E msg@marin.nl